NOTICE

The quality of this microform is heavily dependent upon the quality of the original thesis submitted for microfilming. Every effort has been made to ensure the highest quality of reproduction possible.

If pages are missing, contact the university which granted the degree.

Some pages may have indistinct print especially if the original pages were typed with a poor typewriter ribbon or if the university sent us an inferior photocopy.

AVIS

La qualité de cette microforme dépend grandement de la qualité de la thèse soumise au microfilmage. Nous avons tout fait pour assurer une qualité supérieure de reproduction.

S'il manque des pages, veuillez communiquer avec l'université qui a conféré le grade.

La qualité d'impression de certaines pages peut laisser à désirer, surtout si les pages originales ont été dactylographiées à l'aide d'un ruban usé ou si l'université nous a fait parvenir une photocopie de qualité inférieure.

NL-339 (r. 88/04) c

Canada

A CRITICAL REVIEW OF THE SYMMETRIC PUNCHING SHEAR OF REINFORCED CONCRETE FLAT SLABS

by

Mongi Grira

A Thesis
presented to the University of Ottawa
in partial fulfillment of the
requirements for the degree of
Master of Applied Science
in
Civil Engineering

DEPARTMENT OF CIVIL ENGINEERING
UNIVERSITY OF OTTAWA
OTTAWA, ONTARIO
October, 1990

ISBN 0-315-68088-1

UNIVERSITÉ D'OTTAWA
UNIVERSITY OF OTTAWA

Abstract

The problem of symmetric punching shear arises most often in relation to interior column-flat plate connections , and is associated with the high concentrations of shear at the column peripheries. Many experimental programs were undertaken by previous researchers. The test results, methods of analysis and suggested design equations of previous published experimental research are reviewed.

An experimental investigation on model slabs and on a 1/3 scale composite bridge deck showed that the ultimate punching shear load depends on the shape of the loaded area, the compressive strength of concrete, the flexural reinforcement ratio and on the arrangement of steel bars. Punching failure follows the formation of an inclined failure surface from the edge of the loaded area to the opposite slab face running through the effective depth at a mean angle of 22 to 30 degrees.

One theoretical approach is to treat punching shear by means of ordinary flexure theory. A study of the application of the yield line theory proves that this theory alone is not recommended to treat local failure because of the violent and non-ductile nature of punching shear failure. Punching shear can be modeled also by ties and struts. Even though this approach explains the distribution of the forces in any direction and it is easy to understand and little success has been achieved by previous researchers to develop it. An explanation of the application of the strut and tie model to symmetric punching shear is given to provide a base for future experimental programs and the development of this approach.

The mechanism of symmetric punching of slabs without shear reinforcement is described based on observations from tests. An empirical equation to determine the ultimate punching load of flat slabs is proposed. This equation provides infor-

mation on the effect of different parameters on punching shear. North American and British codes are discussed and compared to the proposed equation.

Some researchers have tried to rationally model the punching shear of flat slabs. Four rational models are selected for discussion and compared to the proposed equation. The upper bound solution model which is based on the plastic approach focuses upon the translational displacement rates in the failure surface, neglecting any slab rotation. A major weakness of this approach is that the effect of flexural reinforcement is neglected. Pralong's model uses a lower bound approach involving the tensile strength of concrete. This model fails to predict punching shear failure loads of under-reinforced or heavily reinforced slabs. Even though the approach of applying ties and struts models to the punching of flat slabs offers the brightest prospects of providing a rational and generally applicable description of the phenomenon, the application of the proposed truss model by Alexander and Simmonds [4] is in doubt. The contribution of the steel is questionable. A notable mechanical model proposed by Kinnunen and Nylander [37]is considered as the most complete one to date. It involves the rigid rotation of slab portions separated by radial cracks. The calculation is rather complicated but it is suitable for computer use.

It is concluded that the proposed equation can predict the ultimate punching shear loads of flat slabs with confidence similar to Kinnunen and Nylander's model. The existing rational models can be improved, but in the short term it is well to remember that an honest empirical approach with a defined range of applicability is preferable to misleading models. Present North American codes should be updated to express the state of present day knowledge, particularly with the inclusion of the influence of the flexural reinforcement.

Acknowledgements

The author expresses his appreciation to his supervisor Professor N. J. Gardner for his constant encouragement, sustained guidance and support throughout this investigation. The financial support from the Tunisian Government is gratefully acknowledged.

A sincere gratitude is expressed to the technical staff of the structure laboratory of the University of Ottawa for their assistance and recommendations in the fabrication and testing of the slab models.

Many thanks to all graduate students and friends who contributed their help and support.

To my fiancée *ILHEM*

Contents

List of Tables

List of Figures

Notations

a_v	=	Half distance between two supports
A_c	=	Area of failure surface
A_b	=	Cross-section area of steel
A_s	=	Area of steel in chosen section of slab
A_{slab}	=	Area of a slab
A_{sp}	=	Area of prestressed reinforcement
A_{sr}	=	Area of ordinary reinforcement in prestressed concrete
A_v	=	Total cross-sectional area of shear reinforcement
b	=	Side dimension of a square column
B	=	Side length of a square slab
B	=	Width of the slab area contributing to punching strength
c	=	Diameter of a circular column
C	=	Diameter of circular a slab
C_0	=	Diameter of circular shear crack after failure
d	=	Effective depth of a slab
d	=	Cover of reinforcing mat
d_a	=	Maximum aggregate size
d_r	=	Effective depth of ordinary reinforced concrete
d_p	=	Effective depth of prestressed concrete
e	=	Eccentricity of a column
jd	=	Lever arm of the interior resisting moment of a slab.
f_{cc}	=	Cylindrical compressive strength of concrete
f_{ce}	=	Average effective concrete prestress immediately after postensioning
f_{ct}	=	Tensile strength of concrete
f_{ct}	=	Effective strength of concrete

f_{co} = Maximum compressive stress of concrete

f_{cu} = Cube Compressive strength of concrete

f'_{cu} = Effective cube compressive strength of concrete

f_{sp} = Split cylindrical tensile strength of concrete

f_y = Yield stress of non prestressed reinforcing bars

$f_{0.2}$ = 0.2% proof stress of prestressed reinforcement

h = Overall thickness of the slab

K = Dimensionless parameter

K_a = Coefficient depends on the type of concrete

K_{sc} = Coefficient depends on the geometry of the column

K_y = Dimensionless parameter

m = Ratio effective compression strength to effective tensile strength.

M = Applied Moment

M_u = Ultimate resisting moment of a slab

$mf1$ = Positive ultimate flexural load

$my1$ = Positive yield moment

L_s = Shear span length

P1 = Theoretical load calculated from equation

P2 = Theoretical load calculated from equation

P_{test} = Ultimate failure load measured during test

P_u = Theoretical ultimate shear load

P_{ue} = Ultimate capacity load at an eccentricity e

P_{ol} = Decompression load of a prestressed slab in the longitudinal direction

P_{ot} = Decompression load of a prestressed slab in the transverse direction

P_{ul} = longitudinal component of P_u

P_{ut} = Transverse component of P_u

P_y = Yield load

Q = Dimensionless parameter

R = Radius of yield fan

R1	=	Resultant if tangential forces in the reinforcement
R2	=	Resultant of radial forces in the reinforcement
r_3	=	Maximum distance from which the shear reinforcement should be placed
r_s	=	Radius of the slab area in which the yield point stress f_y is reached in the reinforcement over a column
Ru	=	Punch radius at the bottom of the slab
S	=	Effective tributary width of reinforcing bar
u	=	Length of control perimeter
u_0	=	Perimeter of a column
U_0	=	Perimeter of a slab
U_p	=	Perimeter of the punch surface at the bottom of a slab
v_u	=	Ultimate shear stress
V	=	Shear force
y	=	Depth of shear crack
w_{ws}	=	$\rho \frac{fy}{fco}$
w	=	Reinforcing index
α	=	Angle of failure surface with respect to horizontal
ϕ	=	Friction angle of concrete
Φ	=	Partial safety factor for resistances
ϕ_u	=	Ratio of the ultimate shearing capacity of the slab to its ultimate flexural capacity
ρ_x, ρ_y	=	Reinforcement ratio in x and y direction respectively
ρ_{ws}	=	Shear reinforcement ratio
λ	=	Parameter depends upon ϕ
μ	=	Parameter depending upon ϕ
γ	=	Partial safety factor for resistances or materials
σ_t	=	Stress in the conical shell
ψ	=	Angle of rotation
ϵ_{ctr}	=	Characteristic value of the circumferential concrete strain at failure

Chapter 1

Introduction

1.1 General

One of the features in design of modern day reinforced concrete buildings is the use of a flat plate cast monolithically with supporting columns. A flat plate is, by definition, a two-way slab structure with a uniform thickness, without beams, drop panels or column capitals. Flat plate structures have properties that are demanded for many types of construction such as underground parking, commercial towers and industrial buildings. In fact, it has a number of advantages over other forms of reinforced concrete slab construction namely:

- The labor costs is low due to the simplified formwork that speeds up construction.
- The overall height of a building can be reduced when beams, drop panels or capitals are not used.

- The installation of electrical and mechanical services in commercial and industrial buildings is easy.
- Economy of repetitive use of formwork.

One of the practical problems for flat plate construction system is how to avoid punching shear failure at the columns. Punching shear is generally associated with high concentrations of shear forces and bending moments at the column peripheries. In the case of symmetric punching, the ultimate limit state is characterized by the formation of a frustrum of a cone having generatrices inclined with respect to the plane of the slab by an angle α, usually between 22 and 30 degrees.

The subject of concentrated loads acting on reinforced concrete slabs has interested many investigators in the past. Many experiments have been conducted and empirical and semi-empirical formulas devised in an attempt to relate apparent shearing stresses in the slab, caused by concentrated loads, to the concrete strength. Much of the knowledge upon which the formulas are based has been taken from information and techniques related to reinforced concrete beams. The current methods used by North American codes have been criticized for not properly accounting for all the variables involved. This emphasizes the need for better analytical models and more reliable design equations.

The essential parameters needed to determine the punching shear resistance of a slab-column connection are the effective depth of the slab, the reinforcement steel ratio and the strength of concrete. In the literature most of the researchers just reported results of tests conducted on model slabs. The researchers were divided in two groups: those who believed that the punching shear failure is determined by the failure of the concrete in tension and those who believed that it is caused by

the compression failure of concrete. The first group suggested empirical equations for the design of slab-column connections. They were agreed that once the applied load exceeds the capacity of the connection, shear reinforcement may be used like in beams. The second group explained the failure phenomenon and because of the difficulties in modeling the phenomenon, they also proposed empirical equations to determine punching shear resistance of a slab column connection.

While reasonably accurate empirical procedures have been developed for the prediction of symmetric punching strengths, efforts to develop rational behavioural models have met with limited success. A design procedure based on a simple convincing rational model would give the designer a clear indication of the effects of each parameter. Code design procedures usually favour a simplified empirical approach. These procedures are reliable only over the limited range of data for which they were calibrated and they cannot be extrapolated with confidence. Moreover design procedures used by the codes tend to be extremely conservative with the result that designers may opt for beams, drop panels, capitals or some form of shear reinforcement, thereby foregoing the advantages of the flat plates.

While the American design approach is usually to develop equations or specifications suitable for codification, the European approach is often to develop a model providing a reasonable facsimile of the actual behavior of slab-column connection. These models can supply a realistic conceptual picture of the mechanism of failure and of the transitions where shear governs to those in which flexural effects govern. A notable model is that proposed by Kinnunen and Nylander [37] and subsequently modified by Kinnunen [38].

In this project attention is confined to the problem of the punching shear strength of thin and medium-thickness concrete slabs. An explanation of the behavior of interior column-slab connections is presented to serve as a background to develop

a reliable model for predicting the ultimate behavior of connections without shear reinforcement.

1.2 Objectives

The objectives of the present project are:

1. Explain better the behavior of the slabs under punching loads at cracking.
2. Develop a simple empirical equation for punching shear resistance of slabs and compare its predictions to code equations and published results.
3. Study existing rational models and compare their predictions of the punching shear resistance of slabs with the developed equation.

1.3 Scope

1. Review of the previous researches on symmetric punching shear and summarize their test results and recommendations.
2. Conduct experimental investigations on model slabs having different arrangements of steel and subjected to different area loadings and on the deck of a composite concrete slab steel girder bridge.
3. Apply the yield line theory and the strut and tie models to the slab-column connections.
4. Statistical analysis of the present experimental data from this investigation and published data.

5. Comparison of the code predictions with the experimental results.

6. Study existing rational models and comparison of their predictions with the experimental results.

1.4 Outline

The thesis first presents a literature review on the symmetric punching shear in Chapter 2. A detailed description of the experimental program is given in Chapter 3. Chapter 4 outlines the theories of the yield line method and the strut and tie models, with their application to reinforced concrete flat slabs. An empirical study with discussion of the codes' models is shown in Chapter 5. A detailed study of some rational models for punching shear is presented in Chapter 6. The conclusions and recommendations from this study are presented in Chapter 7.

Chapter 2

Literature Review

In 1948, Richart [15] performed a systematic study of the resistance of foundation footings to shear failure. The principal parameters studied were:

- The effect of the amount of steel and the geometry of the mat.
- The anchorage of steel bars.
- Concrete strength.
- The effective location of the critical section.

Most of the footings tested failed in punching shear. Richart observed that the shear failure was accompanied by the high tensile stresses in the reinforcement and extensive cracking of concrete. Richart reported that the shear stress v computed at a section taken at a distance equal to the effective depth of the slab d from the column faces, varied between two limiting values. These values were expressed as a function of the compressive strength of concrete f_{cc} with calculated shear stress v varying between $0.05 f_{cc}$ and $0.09 f_{cc}$.

The results of these tests have been applied to slab shear design procedures even though the footing slabs tested were very thick. For this reason, extrapolation of the results was questioned by many researchers.

In 1953, Hognestad [21] recognized the influence of flexural strength of the reinforced concrete slabs, on the ultimate shearing stress. Hognestad re-evaluated the tests of column footings done by Richart using the following equation:

$$v_u = \frac{P_u}{4(b+2d)jd} \tag{2.1}$$

where:

v_u : Shear stress.

P_u : Ultimate shear failure load.

b : Side dimension of square column.

d : Effective depth of the slab.

jd : Lever arm of the interior resisting moment of the slab.

Hognestad showed that the equation (2.1) did not give a consistent factor of safety with respect to shearing failures. He suggested that the ultimate shear strength of slabs is mainly dependent on three variables:

- Material properties used in the slab (quality of concrete as expressed by the cylinder strength f_{cc}, the amount , type and quantity of flexural reinforcement).
- Shape and size of the loaded area as compared to the slab thickness.
- Span, support conditions and edge restraints of the slab.

Hognestad believed that the failure of slabs in punching shear takes place at the compression zone directly around the loaded area. For this reason he used the

control perimeter u to be the perimeter of the loaded area u_o. To determine the ultimate shearing stress of a variety of slabs, the following empirical equation was proposed:

$$v_u = \left(0.035 + \frac{0.07}{\phi_u}\right) f_{cc} + 130 \qquad (psi) \tag{2.2}$$

Where ϕ_u is the ratio of the ultimate shearing capacity of the slab to the ultimate flexural capacity of the slab if it had not failed in shear. The ultimate flexural capacity was calculated using yield line theory and was dependent on the properties of the slab and the size and position of the loaded area. Equation (2.2) is valid only for slabs dimension and concrete strengths in the range tested by Richart. .

In 1956, Elstner and Hognestad [21] carried out shear tests of 39 reinforced concrete flat slabs in order to extend the ranges of slab variables of previous test programs. They reported that their test results confirmed the finding of the re-evaluation of Richart's footing investigation by Hognestad. But they showed that the equation (2.2) gave unsafe estimates of the ultimate shear strength of slabs of high strength concrete. The following equation was proposed for slabs without shear reinforcement:

$$v_u = \frac{0.046}{\phi_u} f_{cc} + 333 \qquad (psi) \tag{2.3}$$

It was also reported that a concentration of tensile reinforcement directly beneath the loaded area or the presence of compression reinforcement had a negligible effect on the ultimate shear strength of the tested slabs.

In 1957, Whitney [61] reviewed the tests reported by Elstner and Hognestad and noted that the proposed equation (2.3) was not valid because it was assumed that the shear strength is a simple function of the concrete compressive strength and does not depend on the flexural reinforcement. He found that, in calculating the

shear stress, the most consistent values for all slab thickness were obtained by assuming the critical section for shear to be at a distance of $\frac{d}{2}$ from the column faces. Whitney assumed that the shear strength is primarily a function of the ultimate resistance moment M_u, of the slab per unit width inside the "Pyramid of Rupture"(The frustrum of a cone with surfaces sloping out in all directions from the loaded area at an angle of 45 degrees). Then he selected all the tests of Richart and Elstner and Hognestad which were considered to have failed in pure shear for analysis. Excellent agreement with the test results was achieved using the following equation:

$$v_u = 100 + 0.75\frac{M_u}{d^2}\sqrt{\frac{d}{L_s}} \qquad (psi) \qquad (2.4)$$

where L_s is the distance from the face of the column to the line of support (Shear span).

According to equation (2.4), the moment M_u can be raised by concentrating the flexural reinforcement inside the pyramid of rupture. Therefore the shear strength of a slab will be raised. This finding contradicted Elstner and Hognestad [21]. Whitney suggested that this discrepancy could have been the result of bond failures in the Elstner and Hognestad tests.

In 1960, Kinnunen and Nylander [37] presented a rational mechanical model for analysis of the slab-column connections subjected to concentric loading. This model was developed on the basis of 61 tests involving circular slabs on circular column. The slabs were loaded at the free edges. The model focused on slab segments separated by radial cracks which bear on a conical shell of concrete at the apex of the inclined crack. Equilibrium for each successive rotation of the slab about this apex is maintained by the vertical and horizontal components of the reinforcement and of the compressive forces in the concrete. Failure of the model is assumed to occur when the tangential strain in the conical shell reaches a

characteristic value which is a function of the column diameter to effective depth ratio $\frac{c}{d}$, and is based on the test data. This approach attempts to account for the triaxial compressive stress and the resultant increase in strength and stiffness of the concrete. When the concrete is incapable of resisting additional stress failure occurs. In order to apply this model, a depth for the inclined crack must be assumed and two independent equations must be solved by iteration. Kinnunen and Nylander found their test specimens failed at a load about 10% higher than the predicted value and concluded that this was a result of the contribution of dowel action. More discussion of this model and its equations is given in Chapter 6.

In 1961, Moe [44] carried out tests in order to study the punching failure mechanism. The testing program involved 43 square slabs, ($1.8m \times 1.8m \times 150mm$) of which 15 possessed holes through various locations of the slab. 8 were designed to study the effect of varying the concentration of reinforcement through the pyramid of rupture, 6 were used to study the influence of shear reinforcement, 2 were utilized for an investigation into extreme column loads. Moe reported that for the case of pure punching, it was the triaxial stresses in the non-cracked compression zone which led to the ultimate failure and punching through the slab. However, the distribution of stresses and the actual mechanism of failure was considered too complex to analyze. The contribution to shear resistance by membrane and dowel action was recognized to be approximately 10%.

Moe suggested that the critical section to compute the nominal shearing stresses should be taken along the perimeter of loaded area. After a statistical analysis of tests of Richart, Elstner and Hognestad and his tests, Moe proposed the following equation for shear stress:

$$v_u = \left(15\left(1 - 0.075\frac{b}{d}\right) - 5.25\phi_u\right)\sqrt{f_{cc}} \qquad (psi) \qquad (2.5)$$

His selection of the shear stress to be proportional to the square root of concrete strength was based on the assumption that a shear failure very often is a splitting type failure, similar to the type of failure observed in specimens under tension, and the tensile strength is generally assumed to be proportional to $\sqrt{f_{cc}}$.

Among Moe's conclusions was that the shear strength of slabs is, to some extent, dependent upon the flexural strength but concentration of the flexural reinforcing steel in a narrow band across the column does not increase the shear strength. Also, the case where an unbalanced moment is transferred to the column was studied. Moe assumed the variation of shear stresses around the column perimeter to be linear and that the maximum shear stress would be the same as for the case where no unbalanced moment is transferred. He suggested that only a fraction K of the moment KM (K=0.33) should be considered acting around the column perimeter.

In 1963, Kinnunen [38] re-examined the accuracy of his earlier theory as applied to slabs with two-way reinforcement and modified the theory slightly to take into account the effect of dowel and of tensile membrane action both of which were evident in the slabs tested. The calculation process involved is lengthy and more time-consuming compared to the first theory.

In 1964, Hognestad, Elstner and Hanson [63] studied the shear strength of reinforced structural lightweight aggregate concrete slabs. They revised equation(2.5) to be :

$$v_u = \left(2.24\left(1 - 0.075\frac{c}{d}\right) - 0.784\phi_u\right) f_{sp} \qquad (psi) \qquad (2.6)$$

where f_{sp} is the split cylinder tensile strength of concrete.

In 1965, Taylor and Hayes [61] reported the results of tests of 22 plain and reinforced concrete slabs failing in punching shear. The specimens were simply

supported 900 mm square slabs and 75 mm thick. The reinforcing steel ratio varied between 0 and 2.0% in compression and between 0.77% and 1.54% in tension. They checked their results with the recommendations of the British code CP 114 and found the code equation gave an adequate safety margin against punching shear failure. Also it was reported that the restraint of the edges clearly affected subsequent behavior but the crack widths of restrained slabs are similar to those of the simply supported slabs. Taylor and Hayes reported that restraint of the edges of the slabs from outward movement generally increased their punching shear strength. This increase was 24 to 60% when the corresponding simply supported slabs were near to flexural failure at collapse (low reinforcement), but only 0 to 16% when the corresponding simply supported slabs were not close to flexural failure at collapse (high reinforcement). This influence was explained as being caused by the extent of flexural cracking. For a highly reinforced slab, the width and depth of crack will greatly reduce the area of concrete in compression and hence the area of concrete available to resist shear. Slab confinement will reduce this cracking for the highly reinforced slab but this effect would be less for a slab with a high quantity of reinforcement since cracking has already been minimized.

The punching failure mechanism was explained to be due to rupture on diagonal planes. The inclined failure surface for punching shear does not develop from main flexural cracks. The region at the top of the inclined failure surface comes under the influence of the stresses beneath the load plate which means the eventual failure will be by rupture of the compression zone. The widening and the extension of the cracks reduces the compression zone to a size which is not capable of resisting the shearing stresses.

In 1966, Mowrer and Vanderbilt [48] described the shear strength of 57 lightweight aggregate reinforced concrete flat slabs; 26 of these slabs were reinforced in compression. Their analysis showed that none of the empirical shear strength equations in existence served consistently to predict the strength of lightweight aggregate concrete specimens. On the basis of their tests, equation(2.5) was revised to read:

$$v_u = \left(9.7\left(1+\frac{c}{d}\right) - 5.25\phi_u\right)\sqrt{f_{cc}} \qquad (psi) \qquad (2.7)$$

Their use of the compressive strength (equation 2.7) gave better agreement between computed and measured strengths than did the splitting strength (equation 2.6). They poorly discussed the failure mechanism of the slabs and the effect of the compression reinforcement on the punching shear resistance.

During the same year Yitzhaki [65] tested 16 circular slabs for punching under circular, square and rectangular load areas, and 12 slabs with diagonal reinforcement. He explained the punching of slabs subjected to concentric loading as being primarily a function of the flexural strength of the slab. The punching resistance is the result of friction in the compression zone with the vertical component of the inclined resultant carrying the shear. By adding flexural reinforcement, the compression force on this zone increases, hence adding to the frictional resistance to shear.

After reviewing the test results of Elstner and Hognestad, Moe, Kinnunen and Nylander, Yitzhaki proposed the following equation:

$$P_u = 8(1-\frac{w}{2})d^2(149.3+0.164\rho f_y)(1+0.5\frac{c}{d}) \qquad (Lbs) \qquad (2.8)$$

where w is the reinforcing index ($\rho\frac{f_y}{f_{cc}}$). This equation permits the calculation of punching strength of a slab without reference to a fictitious shear stress. He suggested that this equation was just as accurate, over a wide range of concrete

strengths and percentages of reinforcement, as that proposed by Moe. It was shown also that yield line theory is capable of closely predicting the punching strength of many of the tests reported in the literature, with slightly higher test strength, the result of strain hardening of the reinforcement.

Yitzhaki also noted that if the strength of a slab-column connection is increased by increased tension reinforcement, then punching failure is governed by some critical value for the slope of the resultant force on the compression zone. Bending up a part of the flexural reinforcement in a specified manner was found to be useful and economical. Tests involving this form of shear reinforcement indicated the strength could be increased by 50%.

In 1967, Long and Bond [40] presented a method for determining the punching load which was based on elastic thin plate theory. Development of the technique began with circular, simply supported slabs and with a square column replaced by an equivalent circular column having the same area as the original one. The elastic thin plate analysis resulted in tangential moments which are greater than the radial moments. This is in agreement with the experimental results of Kinnunen and Nylander. For the case where the concrete fails before the steel yields, an interpolation factor was used to express the actual degree of fixity, and is solved by iteration. This involves the assumption that a single circumferential crack forms around the load perimeter and its width, and hence the slab slope, was determined from equations developed for the prediction of cracks in beams. For the stresses in the concrete, a linear distribution of bending stress was assumed which gives a parabolic distribution of shearing stress, which is maximum at the neutral plane. The stresses caused by the dispersion of the column load play a significant role in the failure of the connection. A correction factor of 1.3 was applied to all calculated failure loads, to take account of the dowel and tensile

membrane action.

During the same year, Grow and Vanderbilt [32] reported on tests to failure of 10 post-tensioned lightweight aggregate concrete flat slabs. They studied the effect of variation of the effective prestress on punching strength of slabs. They pointed out that there is a linear increase in shear strength with an increase in their either effective initial prestress or ultimate cable force. Comparisons of test results with predicted strengths using equations (2.5), (2.6) and (2.8) were all reasonably good. Based on data of their study, they developed equations relating strength of a slab to cable force.

$$v_u = 360 + 0.30 f_{ce} \qquad (psi) \tag{2.9}$$

where v_u is the ultimate shear stress of a slab and f_{ce} is average effective concrete prestress immediately after post-tensioning.

Apparently, any equation developed on the basis of tests of simply supported slabs could be used with fair accuracy in computing the strength of prestressed flat slabs, but Grow and Vanderbilt reported that the tested specimens failed to represent real structures in a number of important respects. The shapes of the real lines of contraflexure around the columns did not match any of the selected shapes, the edge shears and deflections of the specimens were quite different from those of the structures, and in-plane forces that may be developed in real structures were generally lacking in test specimens. Therefore, the true factor of safety of the design procedures for flat plate floors, based on tests done, is problematical. They suggested that in order to have a better understanding of the shear strength of both reinforced and prestressed concrete flat slabs, it would be necessary to test models which more closely simulate real structures than simply supported plates of previous investigations.

In 1968, Corley and Hawkins [16] tested 21 concentrically loaded slab-column specimens containing either lightweight or normal weight aggregate concrete and shear head reinforcement made from structural shapes. Based on their tests, they proposed a design procedure for shear heads at interior supports. The tests showed that up to 75% higher shear capacity was reached in specimens with shear heads compared to specimens without shear heads. Also the tests indicated that even larger increases may be possible.

In 1970, Zaghlool, dePaiva and Glockner [68] studied the behavior and the strength of the column-slab connections in the presence of axial and biaxial bending. They tested four specimens each of which was a full size, square, single panel flat structure cast monolithically with a square column at each corner. For an interior square column and slab connection subjected to combined bending moment M and a vertical shear force V, the ultimate vertical shear stress was given as:

$$v_u = \frac{V}{u_o d} + \frac{KMb}{2I_c} \tag{2.10}$$

in which u_0 is the perimeter of the column, I_c is the moment of inertia, b width of a square column and K is a moment reduction factor. In the above equation a linear stress acting along a critical perimeter was assumed. The authors showed that the method proposed by Moe was conservative for corner columns. A value of K which would result in reasonable predictions of strength was found to be 0.4 instead of the value 0.33 determined by Moe for interior columns. They proposed a simplified method to determine the punching strength of corner columns. They assumed that the inclination angle α of the diagonal cracks to the horizontal equal to 45 degrees. Dowel action and aggregate interlock are negligible, and the compression zone carried no shear. Based on the assumption that failure will take place when the principal tensile stresses produced by the shearing forces

exceed the tensile strength of the concrete, they proposed the following equation:

$$v_u = \left(5.6 + \left(\frac{4d}{b}\right)\right)\sqrt{f_{cc}} \tag{2.11}$$

This equation showed a good correlation with their tests.

In 1973, Zaghlool and dePaiva [69] reported on tests of corner elements with the discontinuous edges supported and the column subjected to biaxial moment. The slabs were 1.10 m square and 150 mm thick. The variables studied were the column width to the effective slab depth ratio b/d, the reinforcement ratio ρ, and the ratio between unbalanced moment to shear transfer M/V. It was found that it was the inner corner which first punched through the slab and that with increasing reinforcement, the slope of the punching surface becomes steeper and the shear stress increased. The punching failure observed was attributed to be a result of failure of the compression zone resisting the combined action of flexure and shear. It was noted that the ultimate nominal shear stress v_u decreased as the ratio M/V increased. Also as b/d ratio was increased v_u remained practically constant unlike the decrease observed by Moe for interior column. In developing an analytical technique for the analysis of the corner column-slab connections, they used an approach which attempted to satisfy both equilibrium and compatibility and which assumed the concrete in compression zone above the head of the failure crack has to reach some critical stress condition.

In 1974, Smith and Burns [60] tested three post-tensioned flat plate specimens with a single column stub in the center and reinforced with various amounts of bonded reinforcement. They analyzed the shear capacity and flexural strength of the specimens and the results were compared to previous design equations. They pointed out that as the amounts of bonded reinforcement increased, the behavior of the specimens improved. Also the equation developed by Grow and Vanderbilt was not conservative for their tests.

During the same year, Masterson and Long [44] adopted a flexural approach using finite elements to describe four basic stages in the punching failure of an interior column:

- Flexural and shear cracks form in the tension zone of the slab near the face of the column.
- Slab tension steel close to the column yields.
- Flexural and shear cracks extend into what was the compression zone of the concrete.
- Failure occurs before yielding extends beyond the vicinity of the column.

They assumed punching was caused by a rupture of the reduced compression zone.

In 1975, Long [42] derived empirical formulas for predicting the punching capacity of slabs at interior columns by simplifying previously reported analytical procedures, which take into consideration the interaction of flexural and shear effects. He recommended that the punching load for a slab is taken to be the lesser of the two values calculated from the following equations.

$$P_u = \frac{0.8\rho f_y d^2(1 - 0.59\rho\frac{f_y}{f_{cc}})}{(0.2 - 0.9\frac{b}{L_s})} \qquad (Lbs) \qquad (2.12)$$

or

$$P_u = \frac{16(b+d)d(100\rho)^{0.25}\sqrt{f_{cc}}}{0.75 + 4\frac{b}{L_s}} \qquad (Lbs) \qquad (2.13)$$

where L_s is the span length between two columns. Equation (2.12) was derived on the basis that steel reinforcement yields before failure. whereas in equation (2.13), the failure takes place before the steel reaches the yield point. Also Long

studied the case of combined shear and transfer moment loading and proposed that the lesser of the two values predicted by equations (2.12) and (2.13) should be multiplied by the lesser of the following two factors:

$$K_1 = \frac{1}{1 + 15\frac{e}{L_s}} \tag{2.14}$$

$$K_2 = \frac{1}{1 + 0.9\frac{e}{b}} \tag{2.15}$$

where e is the eccentricity with respect to column center line. It should be noted that the above expressions are based on isotropically reinforced square slabs which are supported on square columns with equal spans. Application to relevant test results reported by previous investigators indicated that the proposed formula represented a significant improvement over previous ones. For design, it was recommended that the punching capacity formulas be reduced by a factor of 0.8 to ensure that the predicted strength is always conservative.

During the same year, Hewitt and Batchelor [34] developed a model of punching failure for calculating the punching load of a slab with known boundary restraints. The model involved incorporation of boundary restraining forces and moments into the idealized model of failure proposed by Kinnunen and Nylander for simply supported slabs. Assumptions were similar to those of Kinnunen and Nylander, taking the largest circle that could be inscribed in the slab as theoretical circular specimen and assuming loaded area with the same perimeter as the test column. Before the model was extended to deal with restrained slabs, it was tested for accuracy using 165 tests of simply supported slabs reported by previous investigators. Using this model, it was concluded that the punching load is enhanced by 20% due to dowel effects. Then, the authors investigated the actual restraint factor F_r in existing bridges. The investigation consisted of running a computer program with measured data and varying F_r until a reasonable match between observed and calculated deflections was reached. Lower bound values

were found to be F_r =0.25 and 0.50 for composite and non-composite bridge decks respectively.

In 1976, Langohr, Ghali and Dilger [38] reported that punching failure is usually brittle and takes place by widening of an inclined crack which first extends to the top tensile fiber near the column perimeter and propagates to the bottom (compression) surface of the slab. They suggested that punching failure in concrete flat slabs can be prevented with shear reinforcement consisting of individual vertical bars provided with mechanical anchorage at their two ends. Based on their tests of slabs reinforced for shear, it was proposed to use the following equation for design.

$$P_u = 4\sqrt{f_{cc}}ud + \beta_v A_v f_y \qquad (Lbs) \tag{2.16}$$

where A_v is the total cross-sectional area of shear reinforcement. The critical section was taken at a distance $\frac{d}{2}$ from the column faces. The coefficient β_v (< 1.0) is a reduction factor to account for the fact that the average stress level in the shear reinforcement at the flexural failure load is less than f_y. It was recommended that the value of β_v be taken as 0.6 for design.

If equation (2.16) predicts a value of P_u greater than the flexural strength of the slab determined by the yield line theory then the latter theory should be considered for design.

In the same year Ghali, Elmasri and Dilger [19] reported on tests of six full scale simply supported slabs subjected to a constant vertical load and with unbalanced moment applied both statically and dynamically. It was found that the lower the flexural reinforcement ratio ρ, the more ductile the failure became. The angle α between the failure crack and the horizontal increased with smaller amounts of flexural reinforcement. For a ρ of 0.5% , it was found that a number of the

reinforcing bars had yielded before punching occurred. Increasing the flexural strength by increasing ρ to 1.0% and 1.5% resulted in smaller increases in ultimate moment being transferred; this was attributed to failure in shear occurring before the flexural strength could be fully mobilized

In 1977, Breastrup, Nielson et al [55] derived an upper-bound solution for axisymmetric punching of a plain or conventionally reinforced slab by assuming concrete to be a rigid-perfectly-plastic material. A modified Coulomb failure criterion was used as the required yield condition. The theory gives the optimal failure surface as a combination of a conical surface and a catenary of revolution; under special circumstances, the failure surface may reduce to a truncated cone or a complete catenary of revolution. According to the method, the punch radius, R, at the bottom of the slab as given by :

$$R_u = c\cosh\left(\frac{h}{k_2}\right) + k_1 \sinh\left(\frac{h}{k_2}\right) \tag{2.17}$$

where h is the thickness of the slab. R_u is chosen to minimize the load in which the constants k_1 and k_2 must satisfy :

$$c_0{}^2 = k_1{}^2 + k_2{}^2 \tag{2.18}$$

The upper bound to the failure load is given by:

$$P_u = 0.5\pi f_{cu}^{'}\left(\lambda\left(k_2 h + R_u\sqrt{R_u^2 + k_2{}^2} - c_0 k_1\right) - \mu(R_u{}^2 - c_0{}^2)\right) \qquad (N) \tag{2.19}$$

where λ and μ depend upon the angle of internal friction of the concrete ϕ (taken as 37 degrees), and upon the ratio of its tensile to its compressive strength, the recommended value of which is 1/400. With these assumptions, $\lambda = 0.992$ and $\mu = 0.987$. The effective compressive strength of concrete $f_{cu}^{'}$, has been determined empirically on the basis of test data on conventional reinforced concrete slabs, and the recommended value in terms of uniaxial compressive strength, $f_{cu}^{'}$, is $3.77\sqrt{f_{cu}^{'}}$ (MPa).

In 1981, Regan [53] proposed a method for calculating the shear strength of slab-column connections. This method was incorporated in the British code (BS 8110-1985). At an interior columns free from any unbalanced moment, the following expression for ultimate shear force was proposed.

$$P_u = K_a K_{sc} \left(\frac{300}{d}\right)^{0.25} (100\rho f_{cu})^{\frac{1}{3}}\, 2.69(u_o + 7.85d) \qquad (N) \qquad (2.20)$$

where: K_a =0.13 for normal dense concrete and 0.105 for lightweight aggregate and $K_{sc} = 1.15\sqrt{4\pi \times column\quad area/(column\quad perimeter)^2}$. The prediction by this equation was compared to the test data taken from his work and references. It was found that equation (2.20) is practically a lower bound to the test results and can be taken as an expression of characteristic strength. A method for calculating the shear strength of slabs which are also subjected to unbalanced moment was also given. It was assumed that the unbalanced moment was transferred to the column by shear stresses acting along the line of contraflexure about the column. For a square column the ultimate load capacity with an eccentricity e is given as a function of the ultimate concentric load capacity P_u;

$$P_{ue} = \frac{P_u}{1 + \frac{1.5e}{b+2d}} \qquad (2.21)$$

In 1982, Pralong [52] proposed an alternative lower bound approach involving the tensile strength of the concrete, for the calculation of the punching resistance of a column slab connection. He modelled the shear resistance of an isotropically reinforced slab subjected to a load applied uniformly around a circle of radius c by that of a series of beams radiating from the circle. The radial beams are viewed as sandwich structures with tension and compression zones separated by a core subjected to shear. Pralong predicted the punching shear resistance of a slab with isotropic reinforcement to be proportional to the cubic root of the concrete strength. This model also, once shear reinforcement is present, can provide the

vertical tensile resistance supplied by concrete. It was assumed that failure was due to yielding of the shear and part of the flexural reinforcements. More details of this model are given in Chapter 6.

In 1985, Ong and Mansur [51] conducted an experimental program on simply supported, two-way epoxy-bonded steel concrete open sandwich slabs under a central patch load. Beside the method of surface preparation for the steel plate, they studied the effect of the size of patch load, grade of concrete and thickness of concrete topping on punching shear resistance. They found that flexural stiffness and ultimate strength of the slabs increased with increasing size of patch load, concrete grade and thickness of the concrete topping. At low reinforcement ratios, an open sandwich slab fails by flexure rather than punching shear. The authors reported that both CP 110 and the ACI-ASCE recommendations, and the plastic theory underestimates the punching shear strength of open sandwich slabs. On the basis of their test data, they suggested a modification of the plastic theory. For open sandwich slab, the effective compressive strength of concrete should be taken as:

$$\acute{f}_{cu} = 5.47\sqrt{f_{cu}} \qquad (MPa) \tag{2.22}$$

In the same year, Regan [56] tested 15 reinforced concrete slabs which were post-tensioned in one direction. He used his results to develop an extension of the recommendations for punching shear in the draft revision of CP 110-72, that is an extension to allow for prestress. The approach employs the idea of a decompression load in a way analogous to that currently used for prestressed beams. A design equation was proposed for the punching strength of a prestressed slab:

$$P_{up} = P_u + P_{ol}\left(\frac{P_{ul}}{P_u}\right) + P_{ot}\left(\frac{P_{ut}}{P_u}\right) \qquad (N) \tag{2.23}$$

where P_u is the punching strength of geometrically similar reinforced concrete slab, P_{ol} and P_{ot} are the decompression loads of the prestressed slab in the longitudinal and transverse directions respectively, and P_{ul} and P_{ut} are the longitudinal and transverse component of P_u. The critical section was taken 1.5d from the column faces and the nominal shear stress was expressed as:

$$v_u = 0.27(100\rho f_{cu})^{\frac{1}{3}}\left(\frac{500}{d}\right)^{0.25} \qquad (MPa) \tag{2.24}$$

The effective slab depth and the combined steel ratio are defined as:

$$d = \frac{A_{sr}d_r + A_{sp}f_{0.2}d_p}{A_{sr}f_y + A_{sp}f_{0.2}} \tag{2.25}$$

$$\rho = \frac{A_{sr} + A_{sp}}{bd} \tag{2.26}$$

where:

d_r : effective depth of ordinary reinforced concrete

d : effective depth of prestressed concrete

A_{sr} : steel area of ordinary reinforced concrete

A_{sp} : steel area of prestressed concrete

f_y : yield stress of non-prestressed reinforcement bars

$f_{0.2}$: 0.2% proof stress of prestressed reinforcement.

The proposed equation showed a very good agreement with the test results.

In 1986, Jiang and Shen [35] reported that the expression for the punching strength in the upper bound Breastrup-Nielson solution is lengthy and not attractive to practicing engineers. They derived a design formula for punching shear strength using the theory of plasticity. The problem was treated as three-dimensional axisymmetrial one, and the material was assumed to be rigid-plastic. They suggested a failure criterion for concrete, in which a second-degree parabola

was used for the Coulomb-Mohr yield envelope. For practical use, it was suggested that the ultimate strength of a concrete slab in punching shear could be calculated using the following equation:

$$P_u = 0.233(c + h)hf_{cc} \qquad (MPa) \tag{2.27}$$

More details of this theoretical solution are given in Chapter 6.

In 1987, Alexander and Simmonds [4] used a truss analogy to model the flow of forces between flat slabs and columns under combined shear and moment. Using this three-dimensional truss model, the ultimate strength of slab-column connections can be determined. The authors used the model to predict only the failure conditions of edge column-flat slab connections without shear reinforcement of 43 tests reported by previous investigators, but also it can be used to obtain a complete shear-moment interaction diagram of ultimate capacities for a slab column connection. The failure mechanism was assumed due to concrete cover failing to contain the out-of-plane component of force between the reinforcement and the concrete compression struts. It was assumed that the concrete tensile strength capacity is related to the square root of the concrete cylindrical strength. A full discussion of this model is presented in Chapter 6.

During the same year, Bazant and Cao [8] performed punching shear tests on nine geometrically similar reinforced concrete slabs of different sizes. They pointed out that since the punching shear failure of slabs without stirrups is brittle, the size-effect law for brittle failure could be applied. The tests showed that the nominal shear stress at failure is not constant, as assumed in the current design formulas, but decreases as the size increases. Thus, the punching shear behavior of thin slabs is closer to linear elastic fracture mechanics. Using the size-effect law for brittle failures due to distributed cracking, the authors proposed a design

equation for punching shear resistance of concrete based on their tests:

$$P_u = 0.085\pi c h f_{cc} \frac{(1 + 0.6\frac{h}{c})}{\sqrt{1 + \frac{h}{25d_a}}} \qquad (N) \qquad (2.28)$$

where d_a is the maximum aggregate size. Previous test data by various investigators were analyzed by the authors using the above equation, but the results neither contradicted nor validated the proposed formula. It should be noted that the specimens tested by Bazant and Cao were too small to allow a pure punching shear failure to develop and were very heavily reinforced.

In the same year (1987), Walker and Regan [65] investigated the behavior of corner bays of a flat plates in 11 tests of slabs on four columns. A modification of the equivalent frame method of ACI 318-83 was proposed. The authors compared the test data with the proposed equation and reported that the ACI code gave reasonable prediction of column moment near failure, although it did tend to overestimate the moment before cracking occurs.

Among their findings they listed:

- The ACI method provided satisfactory estimates of column moments.
- Reinforcement details have some influence on column moment resistance and a diagonal arrangement of top steel increases stiffness of the members for corner regions.
- The top steel of the slab must cross and be anchored beyond the critical crack. In a floor slab, this crack passes through the inner corner of the column and is normally inclined at 45 degrees to the slab edges.

In 1987, Elgabry and Ghali [20] reported results of tests done on five full-scale reinforced concrete flat plate interior column connections subjected to shear-

moment transfer. Four specimens contained various arrangements of stud-shear reinforcement which are vertical rods mechanically anchored at their top and bottom. The fifth specimen had no shear reinforcement. The main purpose of the test prog ram was to study the effectiveness of this type of shear reinforcement on the punching resistance of a slab-column connection, and to verify proposed code provisions. They suggested that the ultimate shear strength at a critical section of $\frac{d}{2}$ from the column faces, within the shear reinforcement zone can be computed using the following equation:

$$v_u = 2\sqrt{f_{cc}}\left(1+\frac{1}{\beta}\right)+\frac{A_v f_{yv}}{uS} \qquad (psi) \tag{2.29}$$

where β is the ratio of long to short side of column cross-section and should not be smaller than 2, A_v is the cross-sectional area of one row of shear studs distributed over a perimeter u, f_{yv} is the specified yield strength of shear studs and S distance between the shear studs elements. In a case where an unbalanced moment is present, the ACI code equation was used for the analysis of their test data.

$$v_u = \frac{V}{A_c}+\frac{KMC_{AB}}{I_c} \tag{2.30}$$

where A_c and I_c are the area of concrete and polar moment of inertia of the assumed critical section respectively. C_{AB} is the length of the side AB of the column. Their test results proved the effectiveness of well-anchored stud-shear reinforcement in increasing the shear strength and ductility of corner slab-column connections. In addition to verification of the validity of their proposed design equation, they suggested minimum requirements for the dimensions of top anchor heads and bottom anchor strips.

In 1988, Gonzalez-Vidosa, Kotsovos and Pavlovic [31] did an analytical investigation based on Nonlinear Finite Element Modeling to predict the symmetrical punching shear of reinforced concrete slabs with and without shear reinforcement.

For their investigation they took data for nine slabs tested by previous investigators. They did the correlation between predicted and experimental values based on the maximum load-carrying capacity of the slab, the crack pattern and the load deflection curves from zero to ultimate load. They found that slabs loaded through circular areas have up to 40 % higher strength than similar slabs loaded through square areas of the same loaded area perimeter. In addition, circular slabs are stiffer than square slabs of the same span. They pointed out that a triaxial compressive state of stress exists in the vicinity of the column face. They classified the slab-column behavior into two types: ductile and brittle. In the ductile-type behavior, the concrete cracks at approximately 25 % of the ultimate load and all the steel near the column faces yields with strain values of 6 to 8 %. The flexural failure is accompanied by an increase in the depth of the radial cracks up to $\frac{5}{6}$ of the slab effective depth. In a brittle type behavior, failure occurs before the flexural reinforcement reaches its yield stress. Circumferential cracks increase in depth up to two thirds of the slab effective depth. The failure is caused by the decrease of the compression zone with consequence compression failure of the concrete.

In 1989, Fenwick and Dickson [22] reported on tests on three one-way reinforced concrete slabs under concentrated load. The first slab was simply supported, the second was flexurally restrained , and the third was fully fixed at the ends. Their findings showed that the fully fixed slab resisted punching shear 75 % more than the simply supported slab. However the resistance increased only by about 30 % when the slab is flexurally restrained. In addition, the mid-deflection of the fully restrained slab and flexurally restrained slabs were only 81 % and 62 % respectively of the simply supported slab. Moreover, the behavior of the simply supported slab was more ductile compared to the restrained ones. The authors measured the strain in the reinforcing steel and reported that for the

simply supported slab, all the steel bars yielded. However only half of the bars yielded for the case of flexurally restrained slab. For the fully fixed slab only 2 of 32 bars yielded and the compression strains in the concrete were much higher than in the other two. Their results were compared with the response predicted from standard thin plate theory and the ACI code predictions. The significant differences between the theoretical predictions and the experimental results were explained by the presence of membrane action and the tensile resistance of the concrete at a cracked section.

During the same year, Gardner [26] reviewed Regan, Bazant and Cao, and the Code equations on punching shear capacity of reinforced concrete slabs and its relation to concrete strength and steel ratio. He discussed his experimental investigations and concluded that the shear capacity is proportional to the cube root of concrete strength and steel ratio, and that the ACI-CSA code equations are too conservative. He endorsed an equation similar to that of BSS110:19S5 code.

$$v_u = 0.99\,(\rho f_{cc})^{\frac{1}{3}} \left(\frac{400}{d}\right)^{\frac{1}{4}} \qquad (MPa) \tag{2.31}$$

Gardner showed that the BS S110-S5 requirement for the shear perimeter which should be rectangular at distance 1.5 times the effective slab depth outside the column faces regardless of whether the columns are rectangular or circular in section was appropriate.

Chapter 3

Experimental Investigation

3.1 Introduction

One of the simplest way to model an interior column-slab connection is to apply a concentric load to a simply supported model slab. Even though this method fails to model boundary effects on the strength of a connection, it gives a clear idea about the failure mechanism. Previous researchers [34], [62] proved that the effect of the boundary restraint does not affect the failure mechanism of a column-slab connection, but it increases the punching resistance of the slab. An experimental program carried out in the structural laboratory at the University of Otrawa involved testing of 19 simply supported slabs in order to determine how the punching shear resistance of interior column-slab connections may be affected by the variation of the concrete cover, the load area and support perimeter, reinforcement ratio, effective spacing and cross-sectional shape of steel bars. A second experimental program involved punching through the deck slabs of an existing bridge before it was thrown away. Hence failure mechanism and the

ultimate punching shear load of bridge slab decks could be compared to those of simply supported slabs. The experimental data will be added to previous data from chosen literature in order to verify the validity of some existing theories and models and to develop a suitable empirical equation for punching shear resistance.

3.2 Slab Specimens

The laboratory tests were designed to use a 1500 kN Tinius Olsen Universal testing machine. This limited the diameter of the slabs tested to 800 mm. The size of the loading plates were designed to ensure that a shear failure could occur and such that the failure surface does not coincide with the support edges. The distance from the edges of a plate to the support is varying from 2.55d to 3.4d where d is the effective depth of a slab.

3.2.1 Layout of Slabs

Three series of slabs were tested in the structural laboratory of the University of Ottawa. Series A consisted of three identical circular slabs of diameter of 800 mm, an overall thickness h of 100 mm and a clear cover of 13 mm. The effective spacing of the #10M reinforcing bars in both directions was 83 mm. The objective of this series was to determine at what fraction of the ultimate load internal cracks occurred in the thickness of the slabs.

Series B consisted of three slabs similar to that of series A. Slab B1 was exactly identical to those of the series A. However the slab B2 had both tension and compression flexural reinforcement with covers of 13 mm. The slab B3 had the

same effective depth as B1, but with an overall thickness of 150 mm, that is a cover of 63 mm. A further objective of the test series was to determine wether punching strength is proportional to control perimeter.

The series C consisted of thirteen slabs, ten square slabs and three circular slabs. All the slabs were 100 mm thick and had 13 mm clear concrete cover. Slabs C1 to C6 were reinforced in transverse and longitudinal directions with #10M steel bars. The effective spacing of the reinforcement in both directions was 83 mm. Slab C7 was reinforced also with #10M bars with double spacing (165 mm). However slab C8 had a steel bar spacing of 165 mm but the reinforcement used was two #10M tied together to give a reinforcement ratio equal to that of the first six slabs (C1,C2,...,C6). Slab C9 was similar to C8, but #15M bars were used instead of two tied #10M bars. The steel bars used in slab C10 were #15M with an effective spacing in both directions of 83 mm. The last three circular slabs in the series are reinforced with #10M bars spaced 83 mm in both directions. A summary of the characteristics of each slab is given in Table 3.1.

3.2.2 Material Properties

Reinforcing Steel

The reinforcement used in all the slabs are either #10M or #15M deformed steel bars. These bars were manufactured to conform to the CSA Standard G30.12. The stress-strain relationship of the steel as determined from tension tests is shown in Figure 3.1. During tests, the yield and the ultimate stresses were found respectively to be 480 MPa and 685 MPa for #10M, and 380 MPa and 825 MPa for #15M bars.

Concrete

For the first two series of slabs, the concrete was mixed in the structural laboratory at the University of Ottawa. The concrete mix design for each batch was specified to be 20 Kg of Type 10 Portland cement, 46 Kg of sand, 38 Kg of fine aggregate (10 mm) and 38 Kg of coarse aggregate (20 mm). The water-cement ratios were measured to be 0.55 and 0.52 for Series A and Series B respectively. Six control concrete cylinders (150 mm × 300 mm) were taken from each series to be tested at the same day as the slabs were tested. The average cylindrical compressive strengths based on standard cylinder tests were 21 MPa and 29.8 MPa for Series A and B respectively.

For the third Series of slabs, ready-mixed concrete was delivered by a local supplier. A normal weight concrete with a 28-day compressive strength of 30 MPa, a 100 mm slump, zero entrained air, and a 20 mm maximum size aggregate were specified. The concrete had a water cement ratio of 0.47. The mix proportions for a cubic meter consisted of 330 Kg of Normal Type 10 Canada cement, 1130 Kg of coarse limestone aggregates, 790 Kg of sand and 155 Kg of water. Sixteen concrete control cylinders (150 mm × 300 mm) were taken for the whole 13 slabs in order to determine the compressive strength during each testing day. The values of f_{cc} are shown in Table 3.2.

3.2.3 Test System

A "Super L UTM " machine supplied by Tinius Olsen Testing Machine Co., Inc. was used to test the slabs. The machine was hydraulically powered with a load capacity varying from 50 kN to 1500 kN. In operation, the load was applied by

the upward friction-free motion of a piston. Testing speeds were variable from 0 to 75 mm per minute. The readings of loads were indicated in Newtons. During the test, the failure load was recorded automatically. Figure 3.2 shows a general view of the testing machine.

The deflections of the slabs under the applied loads were measured by two dial gauges placed symmetrically at the opposite corners of the testing machine. The load was applied through seven different bearing plates each 25 mm thick: two circular plates having diameters of 100 and 150 mm, two square plates having sides 100 and 150 mm long, and two isosceles triangle plates having side lengths of 100 and 200 mm. The seventh plate had the shape of "L" with 150 and 100 mm of exterior and interior side lengths. Slabs were simply supported on continuous supports: two circular ones with a diameter of 530 and 686 mm and one square with 686 mm of length sides.

3.2.4 Fabrication and Curing

The circular moulds for series A and B were made of steel and the square ones for series C were made of plywood. The reinforcing bars were securely wired together and carefully placed in the forms so that correct distances were maintained. An orthogonal reinforcing mesh was placed at the bottom of each slab. Each mesh was located on concrete spacers to get a concrete cover of 13 mm. Concrete for slabs and control cylinders was vibrated using an poker vibrator. All specimens were cured in the laboratory under a temperature of 22 C for 7 to 12 days.

3.2.5 Testing Procedures

The sequence of events followed in the testing of each specimen consisted of placing, positioning the test specimen, instrumenting, and applying load in increments until the specimen collapsed.

Series A

The three slabs and the control cylinders were tested on the same day. All the slabs were simply supported on a 530 mm diameter circular ring and were loaded through a 100 mm circular plate. The objective of this series of tests was to determine at what fraction of the ultimate did internal diagonal cracks occur. The first specimen was loaded to failure and the other two slabs to 75 and 55 percent of the A1 failure load respectively. The second and the third half slabs were sawed in half to observe if diagonal cracks had occured.

Series B

The slabs of this series were designed to study the effect of the compression reinforcement and the thickness of the concrete cover on the punching shear capacity. Slab B1 was a control. All the slabs were loaded to failure. The load was applied through a circulate plate of 100 mm in diameter. The slabs were simply supported on the 530 mm circular ring. The deflection was measured up to failure load. Deflection readings are taken at load intervals of 30 kN. The average loading rate was 50 kN/min. In order to determine the specified compressive strength of concrete, five control cylinders were tested under compression load during the day of test.

Series C

This series of slabs were designed to study the effect of the following parameters on the punching shear resistance:

- Loading area shape (circular, square, triangle and "L" shape).
- Cyclic loading.
- Support shape (circular and rectangular).
- Loading area and support sizes.
- Steel reinforcement ratio.
- Effective steel reinforcement spacing.
- Steel reinforcement shape.

The first four slabs in this series (C1,C2,C3,C4) were simply supported on a 686 mm circular ring and were loaded to failure through different platens, the 150 mm circular plate, the 200 mm length side triangle plate, the 150 mm square and the "L" shape plates respectively. Slab C5 was tested under cyclic load using the 150 mm circular plate. It was also simply supported on the 686 mm diameter circular ring. Slab C6 was loaded to failure under 150 mm diameter circular plate. It was simply supported on the 686 mm square ring. Slabs C7,C8,C9,and C10 were simply supported on the 686 mm diameter ring and they were loaded to failure through the 150 mm diameter circular plate. The last three slabs (C11,C12,C13) were simply supported on the 530 mm ring and were loaded respectively under 100 mm circular, 100 mm square through 100 mm side length triangular plates.

The average rate of loading was set to about 50 kN/min. Deflection readings were taken at intervals of 20 kN using dial gauges. The loading was taken up to failure, then it stopped automatically and the maximum resistance load carried by the slab until punching failure was recorded by the testing machine. The slabs of this series (C) were tested on three different days. To determine the compressive strength of concrete, five control cylinders were tested each day. A summary of the description of the slabs and the tests purposes is given in Table 3.1.

3.2.6 Test Results and Structural Behaviour

The ultimate loads at which slabs failed are recorded as P_{test} in Table 3.2. Also the measured perimeter U_p of the punched-out area of each slab was reported in this table. A detail description of each slab behavior is reported in the following sections.

Series A

Slab A1 failed in punching shear. Extensive cracks developed at the bottom surface of the slab. They propagated from the center of the specimen to the support. These cracks widened as the load increased. The crack pattern of slab A1 is shown in Figure 3.3. In order to determine at what load the concrete started cracking diagonally, slabs A2 and A3 which were both loaded up to 55 and 75 percent respectively of the failure load of slab A1, were loaded and then cut in half. No cracks were observed inside the slabs which indicates that concrete does not crack at loads less than 75 percent of the ultimate load. The measured linear relationship between the applied load and the central deflection of the slabs is

shown in Figure 3.4.

Series B

Control slab B1 failed in punching shear. The crack patterns shown in Figure 3.5 are similar to that of slab A1. Slab B2 failed in punching shear at a deflection slightly higher than that of the control slab B1, and at an ultimate load 6 percent less than that of slab B1. This was not expected, since the slab was reinforced in compression. After failure, it was found that shear crack around the periphery of the loaded area, on the compression face, developed vertically until it reached the compression steel reinforcement. From there the shear crack changed direction to be inclined. Hence placement of compression steel was harmful that it decreased the depth of the concrete between the top steel mat and the bottom one. This may have an effect on the effective depth considered in design. Therefore, the punching shear capacity was decreased since it depends on the effective depth as will be explained in the next Chapter.

When the concrete cover in slab B3 was five times that of slab B1 the failure mode was completely changed from punching shear to flexural failure. There was no final punching through and loading was stopped after many radial cracks reached the edges of the slab. The crack patterns at the bottom of slab B3 is shown in Figure 3.5. The load-deflection curve of this slab series is shown in Figure 3.6. It can be seen that the deflection is linearly proportional to the applied load at the beginning of the load stages. The ductility of slab B3 is greater than that of the other slabs.

Series C

All the specimens of this series failed in punching shear. The shear failures were characterized by a sudden punching through the load platen with little or no warning. The behavior of the slabs will be described based on the different purposes of the test:

• Loading Area Shape:

Figure 3.7 shows a neat circular hole and a nearly circular base of a pushed through frustrum of a cone at the top and the bottom faces of the slab C1 after the test. The effect of the punching through the other plates can be seen in Figure 3.8, 3.9 and 3.10. Neat triangular and square holes with round edges were left on the top faces of slabs C2 and C3 after being tested. The shear crack at the bottom face of slabs C2 and C3 indicate that pushed-through solids were respectively frustrums of triangular and square pyramids with round corners. However, the punching of slab C4 through an "L" shape plate left on the top face a hole having a trapezoidal shape. The shape of the shear crack at the bottom face of slab C4 can be seen in Figure 3.10. The concentration of high stresses was at the corner of the "L" shape. Nevertheless the "L" shape load area may have the same physical effect as the trapezoidal one.

The load deflection curves for the first four slabs are shown in Figure 3.11. It can be seen that slabs C1 and C2 which were loaded through a circular and a triangular plates failed at the same values of deflections. Slabs C3 and C4 failed also at the same deflection values but lesser than at which the other two specimens failed.

In order to study in more detail the effect of the load area shape on punching shear

resistance, the perimeter and the area of the loading plates can be considered as parameters. The 150 mm diameter plate was taken as a control. Table 3.3 shows the ratios of the perimeters and the areas of the bearing plates used to test slabs C2, C3 and C4, to the perimeter and the area of the circular plate respectively. Also, the ratio of the failure loads of slabs C2, C3 and C4 to the slab C1 test load is given in the same table. The surface area of the triangular plate is the same as the circular one and the slab C2 failed at the same load as slab C1. Whereas the square and the "L" shape plates have an area 27 percent higher and 29 percent less than the circular plate respectively. Slabs C3 and C4 failed at loads 6 percent more and 7 percent less than that of C1 respectively. Even though the triangular and the square plates have perimeters 27 percent greater than the control plate (150 mm circular plate), slabs C2 and C3 failed at load equal and 6 percent high than the C1 slab failure load respectively; whereas the "L" shape plate has a perimeter 6 percent higher than the control plate, but slab C4 failed at a load 7 percent less than that of slab C1. Thus, a slab loaded through a circular area can resist more load than a similar slab loaded through an area with sharp edges.

• Effect of cyclic load:

Slab C5 was tested under cyclic load. Its behaviour was compared to that of C1. Figure 3.12 shows that the cyclic load seems does not have an effect on the crack pattern which were much the same as those under monotic loading up to failure. loading. Cracks widened and spread as the number of cycles increased but were always confined within the supported boundaries. The punched-out area was larger and less symmetrical than that resulting from monotic loading. The punching shear resistance of the slab decreased by 19 percent. Hence the fatigue effect on the shear resistance of a slab can be seen in Figure 3.13 which shows also the inelasticity of the concrete.

• Effect of support shape:

Slab C6 was supported on the 686 mm square ring and was loaded to failure through the 150 mm circular plate. Figure 3.13 also shows the crack pattern at the bottom face of slab C6. More flexural cracks were developed compared to slab C1. These cracks give an idea of the yield lines radiating from the center of the slab to the corners of the square supports. The cracks near the corners of the square supports indicate that the slab had been rotated around an axis a-a during the test (See Figure 3.12). In fact when more load was applied after the failure, the whole slab was lifted. This behaviour was not observed for the case of a circular support. Furthermore, slab C6 failed at a load 13.5 percent higher than the failure load of the slab C1 (see Figure 3.14). This is not reflected by the difference in the compressive strength only, (f_{cc} of C6 is 6 percent higher than that of C1) but also by the perimeter of the support. The square ring has a perimeter 27 percent greater than that of the circular ring. As a conclusion, under the same area load a square slab can resist more load than a circular slab.

• Effect of reinforcement ratio:

Slabs C7 and C10 have half and twice the reinforcement respectively of slab C1 and were tested under the same conditions as slab C1. Figure 3.15 shows the crack patterns at the bottom faces of slab C7 and C10 after failure. The effect of the flexural reinforcement in punching shear resistance is shown in Figure 3.16. It can be seen from this figure that the reinforcement ratio is critical in punching shear resistance. The slab C1 is again taken as a control. Decreasing the reinforcement ratio by 50 % resulted in a 33 % decrease of the punching shear strength (without taking the difference in f_{cc}). However when the reinforcement ratio was doubled the strength was increased by only 10 percent. Furthermore, slabs C1 and C7 failed at almost the same slab deflections. In contrast slab C10

failed at deflection value 24 percent less than the other. Hence the concentration of flexural reinforcement at a column-slab connection can considerably increase its stiffness but not its punching resistance.

• Effect of the reinforcing spacing:

Slab C9 was reinforced with #15 bars spaced at 165 mm, to give the same reinforcement ratio as slab C1 (with #10 bars spaced at 83 mm). The comparison between slab C9 and slab C1 is shown in Figure 3.17. The effective reinforcement spacing keeping the same steel ratio had no effect in the punching shear resistance. The result was expected since the area of steel crossing the failure surface of the specimen (C9) is the same as that of slab C1.

• Effect of steel bar shapes:

Slab C8 was reinforced with two #10M tied steel bars, whereas slab C9 was reinforced with #15M. Both slabs have the same reinforcement ratio and effective bar spacing. They were tested under the same conditions. Figure 3.18 shows the crack patterns of slabs C8 and C9 after punching shear failure test. The effect of cross-section shape of the reinforcement steel on the ultimate resistance load can be seen in Figure 3.19. With the same reinforcement ratio and different shapes of bars, slab C8 and C9 failed at the same value of deflection but under different loads. In fact, when the tied #10 bars were used, the shear strength of slab C8 was 16.5 percent lower compared to slab C1 and C9. If the difference in results is considered to be purely due to experimental scatter, then the difference in the stiffness of the steel bars used in the specimens (C8, C9) had not effected the punching shear resistance.

• Scale effect:

Slabs C11, C12, C13 were tested to study the scale effect. They were simply supported on a circular ring of 533 mm diameter and loaded through plates having side dimensions of 100 mm. Figures 3.20 and 3.21 show the physical behavior of these slabs under symmetric punching load. A comparison between the effect of different area shapes on punching shear resistance is shown in Figure 3.22. Even though, the areas and the support length used for slabs C11, C12 and C13 are smaller than the others slabs of this series, the effect of the loaded area shape is the same as was reported for the first four slabs. It is important to note that there was almost no difference in the unit shear stress between these small slabs and the first three slabs (C1, C2, and C3). In addition, the failure mechanism of the last three slabs is the same as that of all the other slabs of this series.

3.3 Bridge Test

3.3.1 Description of the Bridge

The bridge had been constructed in the University of Ottawa structural laboratory for testing under thermal loads in the late seventies. It was a reduced scale model of a highway composite bridge that spans the Red River near Ste-Agathe, Manitoba. The model shown in Figure 3.23, was made to (1/3) scale which reduced the overall size to approximately 16.2 meters long and 3.22 meters wide. The model composite bridge consisted of four W15x10 steel beams with steel diaphragms and a cast-in-place concrete deck of thickness of 62.5 mm. The four girders were spaced at each 900 mm, and connected transversely by ten C-beams

acting as diaphragms. Three diaphragms were located at each support, and two of them were equally spaced at each span. The bridge model had span lengths of 4.86 m, 6.47m, and 4.86 m. The structural action of the slab is essentially one-way. Figure 3.24 shows the reinforcement layout and the steel ratios. The tension steel ratio varies from 0.0198 to 0.0314 and the compressive steel ratio from 0.0071 to 0.0316.

The girders of the bridge model were simply supported at one end. At that end, there was no longitudinal movement but only rotation. At all other support piers, the girders were supported to permit both rotation and longitudinal displacement. More information about the structural properties of this model bridge can be found in Reference [61].

3.3.2 Material Properties

The slab was reinforced with two different sizes of steel bar. The (#3) deformed billet bars had a 414 MPa specified minimum yield point and a minimum tensile strength of 620 MPa. The 1/4 in (#2) hot-drawn plain bars had a yield point of 400 MPa and ultimate tensile strength of 488 MPa.

The slab deck was cast into five stages. The average ultimate cylinder strength of each section shown in Figure 3.25 from right to left is 48.2, 51.7, 44.7, 50.3 and 47.5 MPa respectively. (Reference 61)

3.3.3 Loading device and testing procedure

The loading device included a hydraulic jack, a load cell and two circular load bearing plates with a diameters of 4 and 6 inches. Central deflections were measured by dial gauges. The bridge was tested at four different longitudinal line positions (see Figure 3.25). Along each position line, the punching was done on the middle, left and right decks. During the tests, the bridge was punched along the line 1 using the 100 mm diameter plate, then the equipment was moved to the line 2, and the punching was done using the 150 mm diameter one. Along the position line 3, the test carried out with the same plate (150 mm diameter) in order to determine the effect of the lateral bracing on the punching shear resistance. The middle deck was loaded up to 50 percent of the ultimate load and then released. Also, the left and the right ones were loaded up to about 60 percent of ultimate punching load, and then released . After 24 hours, the load was reapplied until punching failure occurred.

At the last stage, the bridge decks were loaded through the 150 mm diameter plate. The right deck was not loaded. The left one was loaded to failure. The middle deck was loaded in several stages as follows: the load was applied up to 70 percent of the ultimate load and the deck was left under this load for 24 hours. Then the load was released and reapplied up to 80 percent of the ultimate load. The load was left for five hours and then released. After that, the load was reapplied again increased by about five percent, then released and reapplied again until the bridge deck failed in punching shear. During the above process deflection measurements were taken. The load stress increments were decreased from 25 kN in the beginning of the tests to 10 kN when the concrete was believed to be cracked (after 60 percent of the ultimate load).

3.3.4 Observations from the Bridge Test

The bridge test results are shown in Table 3.4. The first cracks opened up on the bottom surface of the bridge deck in the form of tangential flexural cracks at a distance from the deck center approximately equal to the radius of the loaded area. These cracks were believed to take place when the sound of the concrete crushing was heard. The first crack was approximately at 50 percent of the ultimate load. Immediately after the load exceeds the cracking load, radial cracks developed starting at the tangential crack along the circumference of the loaded area. As the radial cracks extended, more tangential cracks developed outside the circumference of the loaded area. Then a final tangential crack occurred coinciding with, or located outside, the tangential crack which was observed before failure at the greatest distance from the circumference of the loaded area. Although accelerated creep of concrete usually gave some warning, failure was always explosive but damage was confined to the panel tested. The failure usually left a neat circular hole in the top of the deck bridge and pushed-through frustum of a cone with a nearly circular base. The perimeter of this base was measured to be at 3d from the periphery of the loaded area. It should be noted that the diaphragms contributed to the lateral stiffness of the bridge. In fact, the failure load was increased by about 30 percent. (see Table 3.3). Even though the bridge was reinforced in compression (top side), it is believed this did not affect the punching shear capacity of the deck since the compression forces were taken by the concrete not the steel.

The relation between the applied load and the central deflection along the position line 2 for the left and the right decks is shown in Figure 3.26. The relation is linear in the beginning and becomes parabolic when the load approaches the ultimate state. Figure 3.27 shows the relationship between the applied load and

the deflection of the middle deck of the model bridge. During the unloading phases, the reading of the deflection was not taken because of the limitation of the instruments. In fact, when the hydraulic jack was released, it was very hard to control the load during the unloading process. When the middle deck of the bridge underwent cyclic loading, it was observed that the stiffness decreased as the number of cycles increased. Hence, when the deck was unloaded and reloaded again, without any modification of the instruments, the deflection reading was much higher than that of the previous loads.

3.3.5 Calculation

The characteristic parameters of the bridge, the calculated and the test values of the punching shear loads are shown in Table 3.5. The ultimate punching load was calculated using Kinnunen and Nylander model and taking into account a 10 percent dowel effect. In the calculation, the effect of the compressive steel was neglected because it is believed that the compressive force is taken by the concrete only. The effective depth was taken from the center of top steel mat to the center of the bottom one. From Table 3.5, it can be seen that there is a slight difference between the values of ultimate punching load predicted by the model and the test results. This difference is caused by the effect of the lateral restraints of the decks. Also, this difference increased to about 10 percent at the presence of diaphragms. Therefore, the model predictions of the punching shear load of restrained one way slabs is very good.

3.4 Summary

The first slab series (A) showed that there is no exact value for the concrete cracking load. However, before punching shear takes place, a slab undergoes extensive flexural cracking on the tension side. Series B showed that compression steel reinforcement may not beneficial and a thick concrete cover can change the failure mode from brittle to ductile. Series C tests showed that the shape of the loaded area can have an effect on the strength of a slab-column connection. Hence columns with sharp edges resist less load compared to column with round edges. Also cyclic loading can affect the punching resistance of a slab. In addition, the reinforcement, the effective spacing of the bars compared to the effective depth d and the side length of the load area and the cross-sectional area of the flexural steel are sometimes critical.

The bridge tests showed that the boundary restraint may increase the punching resistance of a slab. There was no difference in the failure mechanism between the slabs and the bridge.

Table 3.1: Description of the slabs

Slab Numb.	H (mm)	d (mm)	c * (mm)	Punch Shape	C * (mm)	Support Shape	ρ	Bar size	Test Purpose
A1	100.0	78.0	100.0	Circular	533.0	Circular	0.0147	#10M	Control
A2	100.0	78.0	100.0	"	533.0	"	0.0147	"	Load 75% P_u
A3	100.0	78.0	100.0	"	533.0	"	0.0147	"	Load 55% P_u
B1	100.0	78.0	100.0	Circular	533.0	"	0.0147	#10M	Control
B2	100.0	78.0	100.0	"	533.0	"	0.0147	"	Double Reinf.
B3	150.0	78.0	100.0	"	533.0	"	0.0147	"	Thick cover
C1	100.0	78.0	150.0	Circular	686.0	"	0.0147	#10M	Control
C2	100.0	78.0	200.0	Triangular	686.0	"	0.0147	"	Load shape
C3	100.0	78.0	150.0	Square	686.0	"	0.0147	"	"
C4	100.0	78.0	150.0	L shape	686.0	"	0.0147	"	"
C5	100.0	78.0	150.0	Circular	686.0	"	0.0147	"	Cyclic load
C6	100.0	78.0	150.0	"	686.0	Square	0.0147	"	Support shape
C7	100.0	78.0	150.0	"	686.0	Circular	0.0074	"	Half Reinf.
C8	100.0	78.0	150.0	"	686.0	"	0.0147	"	Two tied bars
C9	100.0	78.0	150.0	"	686.0	"	0.0147	#15M	Double Spac.
C10	100.0	73.0	150.0	"	686.0	"	0.0294	#15M	Double Reinf.
C11	100.0	78.0	100.0	"	533.0	"	0.0147	#10M	Control
C12	100.0	78.0	100.0	Triangular	533.0	"	0.0147	"	Load shape
C13	100.0	78.0	100.0	Square	533.0	"	0.0147	"	"

* Here. c and C are the side lengths of loaded areas and the support respectively

Table 3.2: Test results of the slabs

Slab Numb.	f_{cc} (MPa)	U_p (mm)	P_{test} (kN)	P_u(Eq. 5.6) (kN)	P_{test}/P_u	Comment
A1	21.0	1300	176.8	142.4	1.23	Control
A2	21.0	-	-	142.4	-	Load 75%P_u
A3	21.0	-	-	142.4	-	Load 55%P_u
B1	29.8	1300	160.6	160.0	1.00	Control
B2	29.8	1150	150.4	160.0	0.94	
B3	29.8	-	203.2	160.0	1.27	Flexure
C1	29.6	1600	200.0	190.8	1.04	Control
C2	29.6	2200	221.2	190.8	1.15	
C3	29.6	1600	211.5	202.9	1.04	
C4	29.6	1600	185.1	178.3	1.02	
C5	33.4	1700	163.5	198.6	0.91	
C6	33.4	1600	227.5	198.6	1.14	
C7	29.6	1600	133.4	160.7	0.83	
C8	30.6	1600	167.0	192.9	0.86	
C9	30.6	1600	200.4	192.9	1.03	
C10	33.4	1700	220.8	218.6	1.01	
C11	29.6	1300	170.0	159.6	1.06	
C12	29.6	1200	160.0	144.0	1.11	
C13	29.6	1600	190.0	159.6	1.13	

Table 3.3: Characteristics of the plates used during tests

Slabs	C1	C2	C3	C4
Plate Type	Circular	Triangle	Square	"L" shape
$\frac{PlatePerimeter}{C1PlatePerimeter}$	1.00	1.27	1.27	1.06
$\frac{PlateArea}{C1PlateArea}$	1.00	0.98	1.27	0.71
$\frac{P_{test}}{P_{test(C1)}}$	1.00	1.00	1.06	0.93

Table 3.4: Bridge test results

position	P_{test} (kN)			Remarks
	Left Deck	Mid-Deck	Right Deck	
1	-	63.6	-	
2	90.0	106.2	90	
3	(61.5)*	(67.1)*	(61.5)*	Punching on the
	101.2	139.8	120.3	top of a diaphragm
4	67	(78.3)*	-	
	-	(83.9)**	-	
	-	(89.5)***	-	
	-	106.2	-	

* The bridge was left under this load for 24 hours.

** The bridge was left under this load for 5 hours.

*** The bridge was unloaded when reached this load and loaded again to failure.

Table 3.5: Bridge characteristics and test results

Position	d (mm)	c (mm)	ρ	f_{cc} (MPa)	P_{test} (kN)	P_u K&N model (kN)	P_{test}/P_u
Left Deck							
2	48	150	0.016	48.2	90.0	93.4	0.96
3	48	150	0.016	51.7	102.2	95.0	1.12
4	48	150	0.016	44.7	87.0	91.7	0.95
Mid-Deck							
1	49	100	0.0258	48.2	63.6	86.4	0.74
2	49	150	0.0258	48.2	106.2	122.8	0.86
3	49	150	0.0258	51.7	139.8	126.2	1.11
4	49	150	0.0258	44.7	106.2	119.3	0.89
Left Deck							
2	48	150	0.016	48.2	90.0	93.4	0.96
3	48	150	0.016	51.7	120.3	95.0	1.27

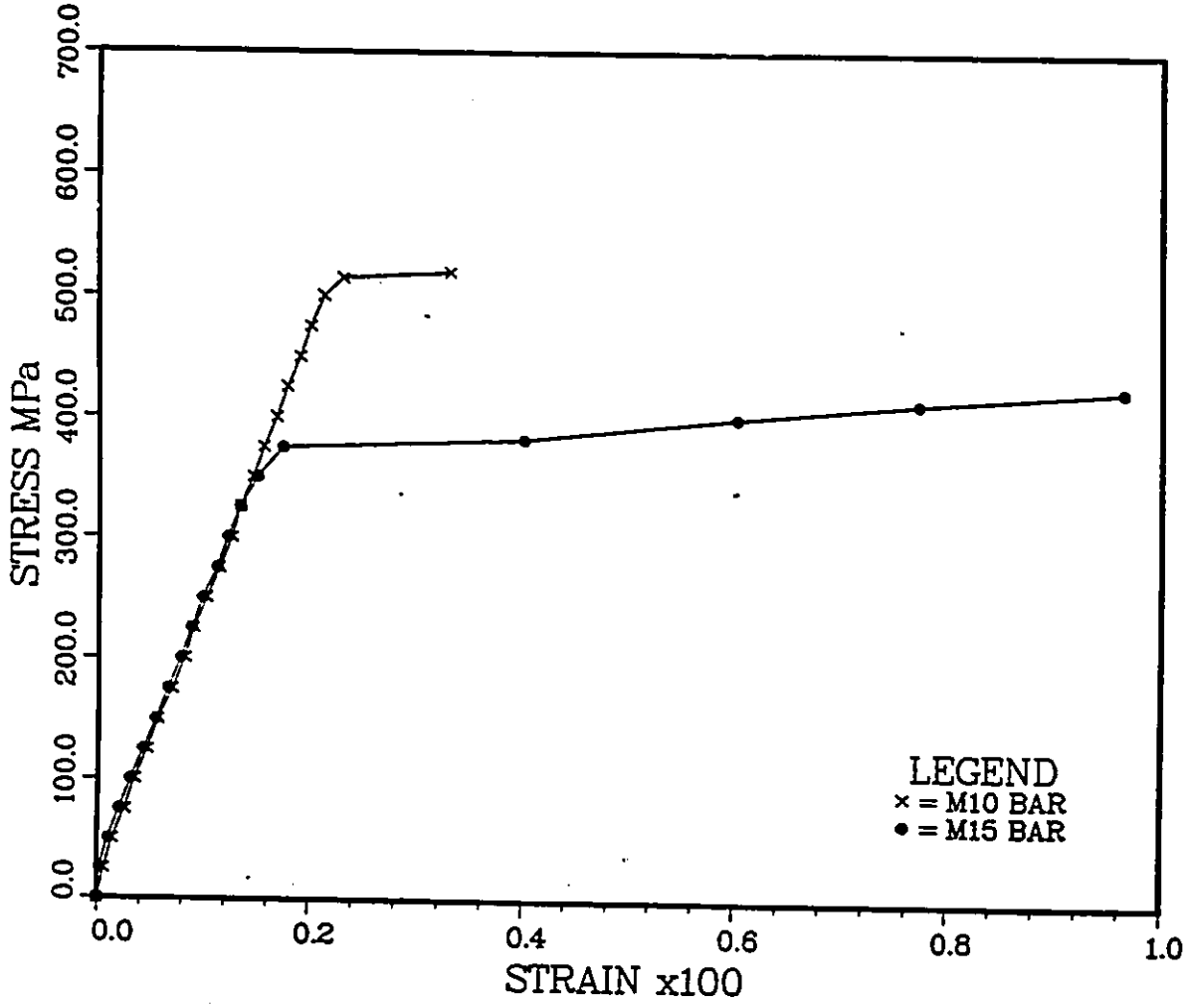

Figure 3.1: Strain-Stress relationship of the steel used in the slabs

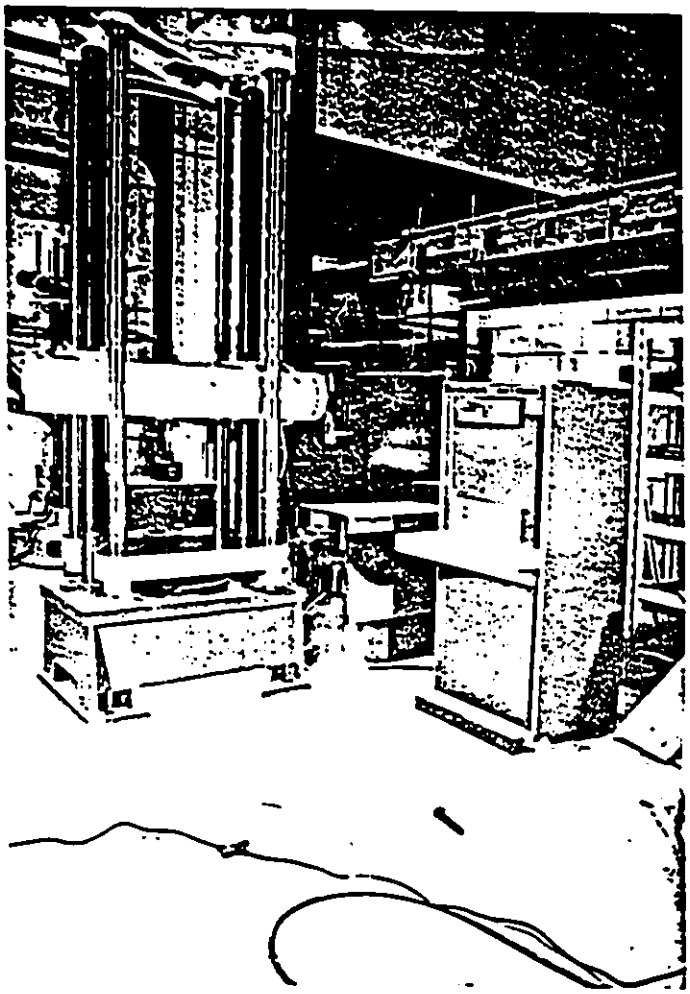

Figure 3.2: The Super L UTM machine used during the tests

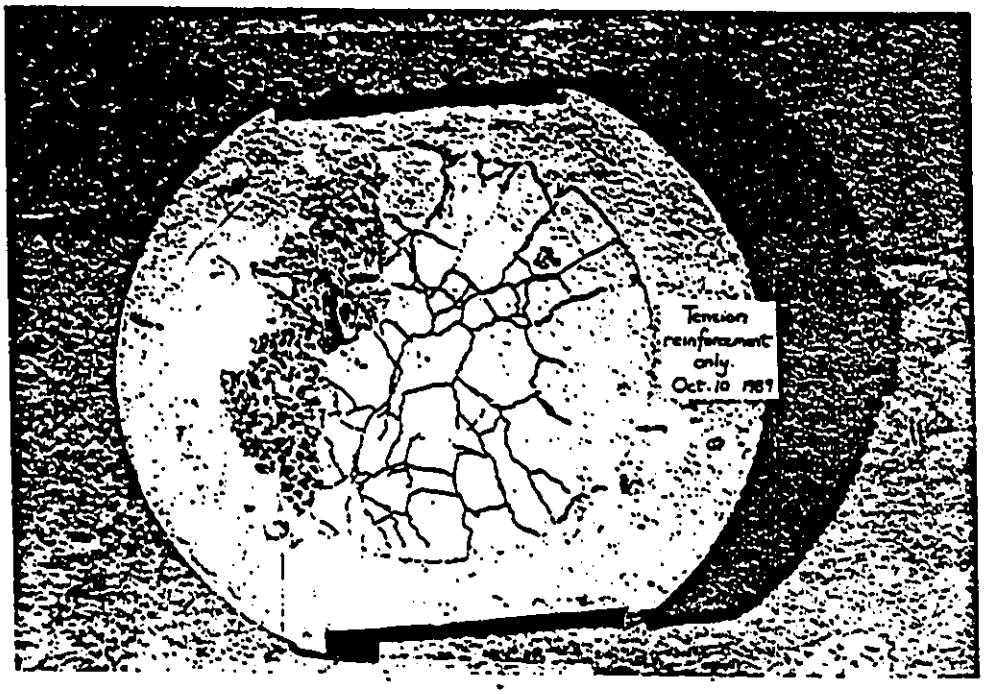

Figure 3.3: The Crack patterns at the tension side of slab A1

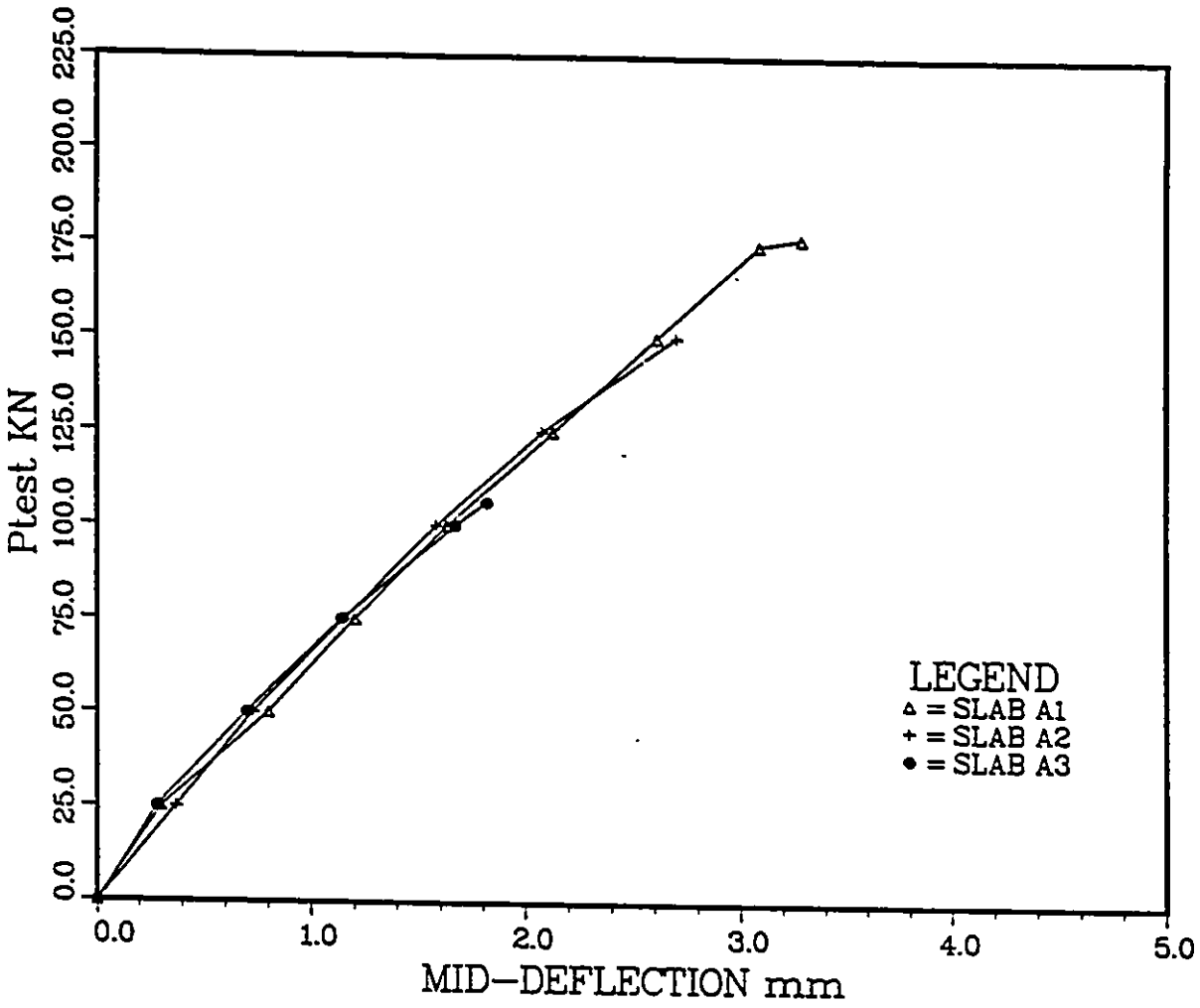

Figure 3.4: Relationship between the applied load and the mid- deflection of series A slabs

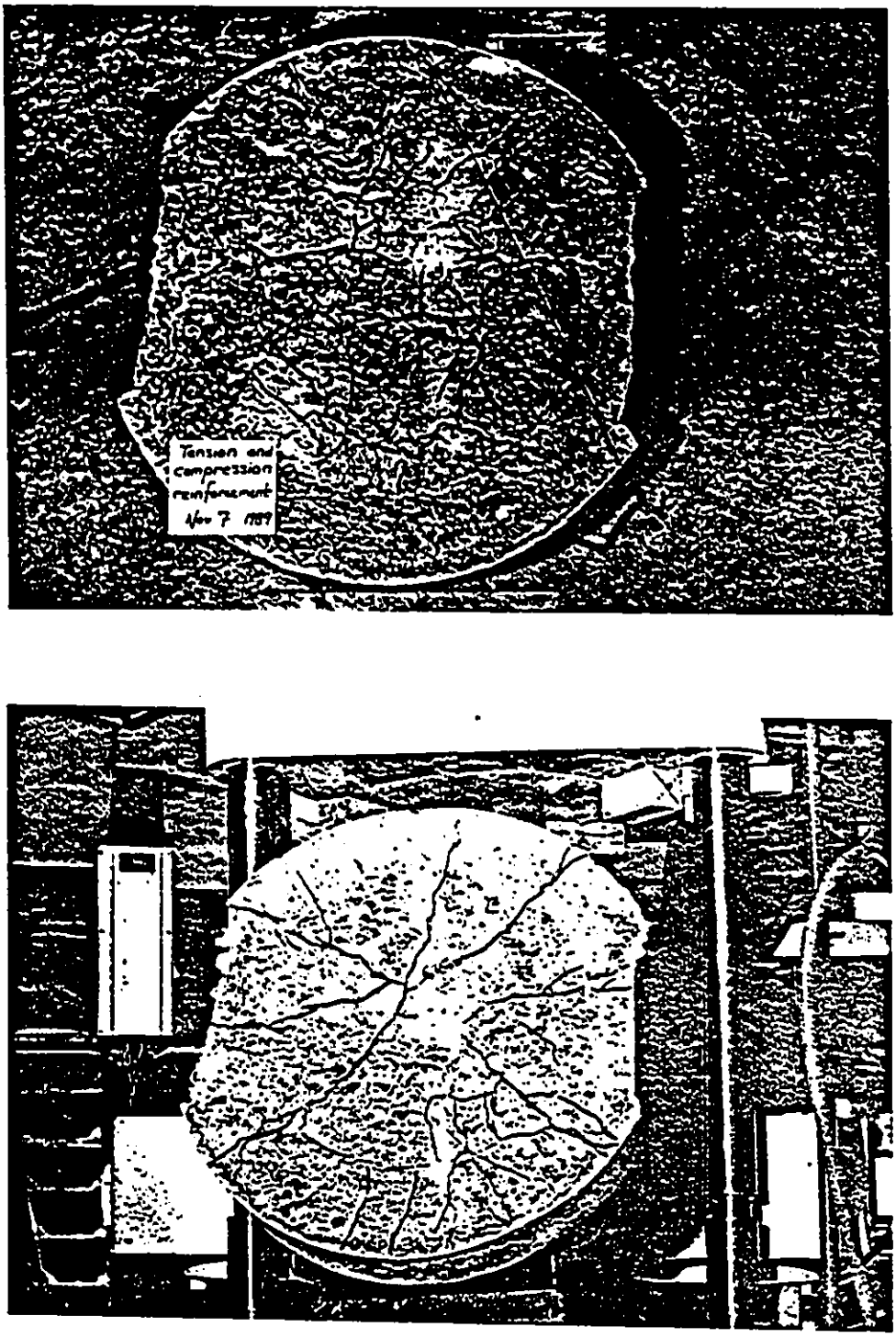

Figure 3.5: The Crack patterns at the tension sides of slab B1 and B3

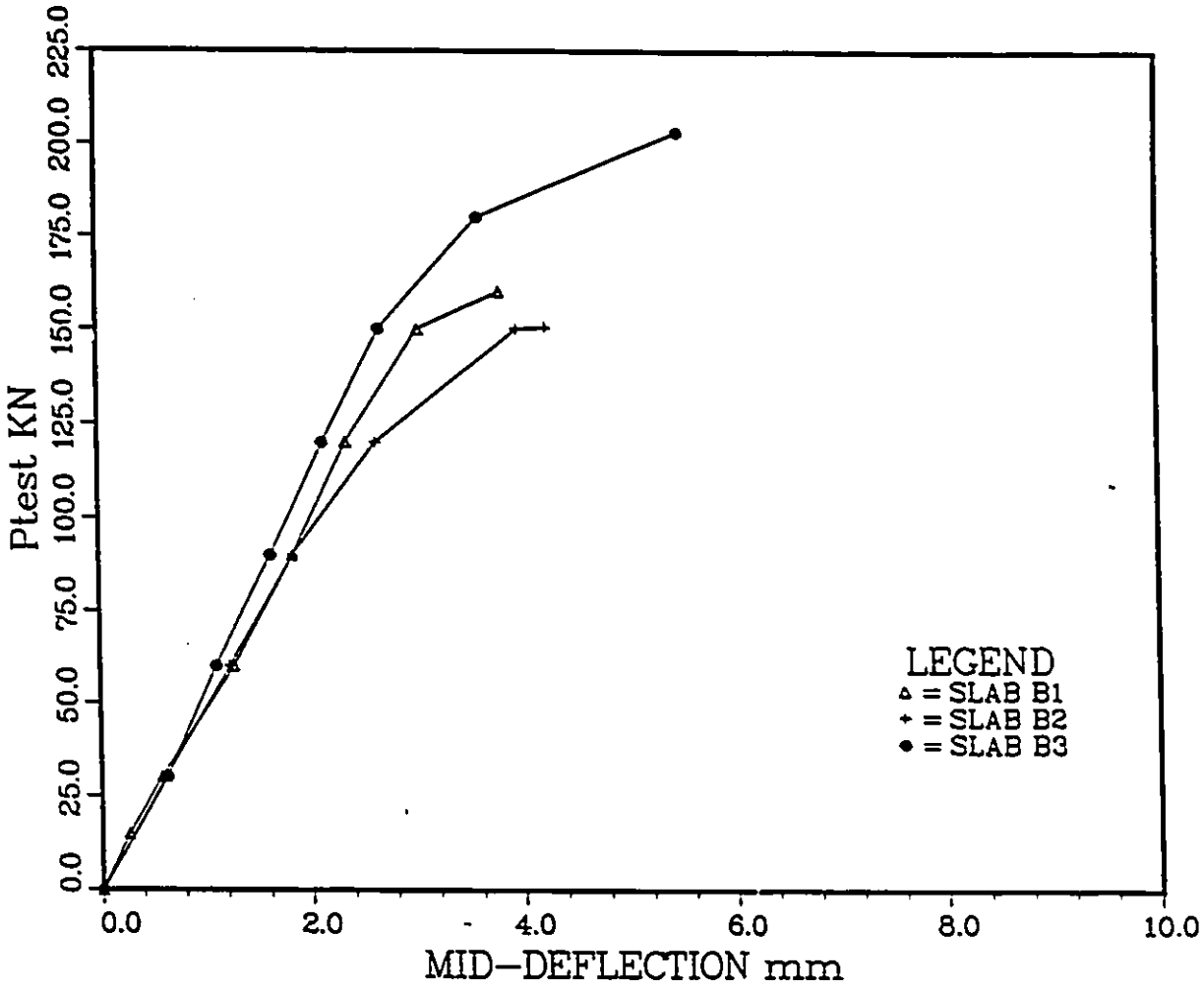

Figure 3.6: Relationship between the applied load and the mid- deflection of series B slabs

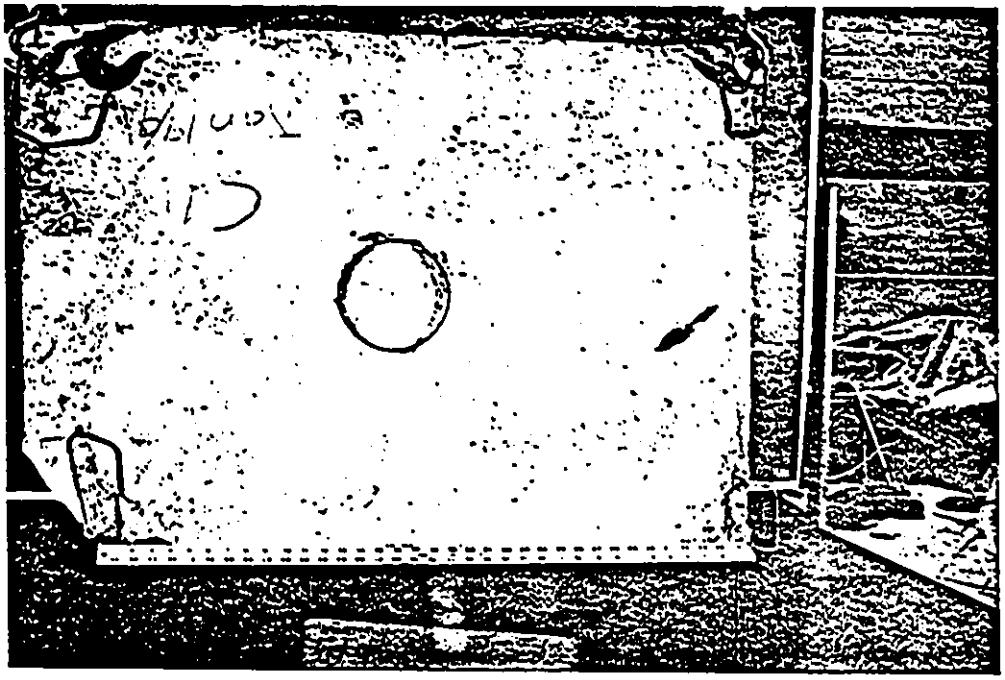

Figure 3.7: Crack patterns at the top face of slab C1

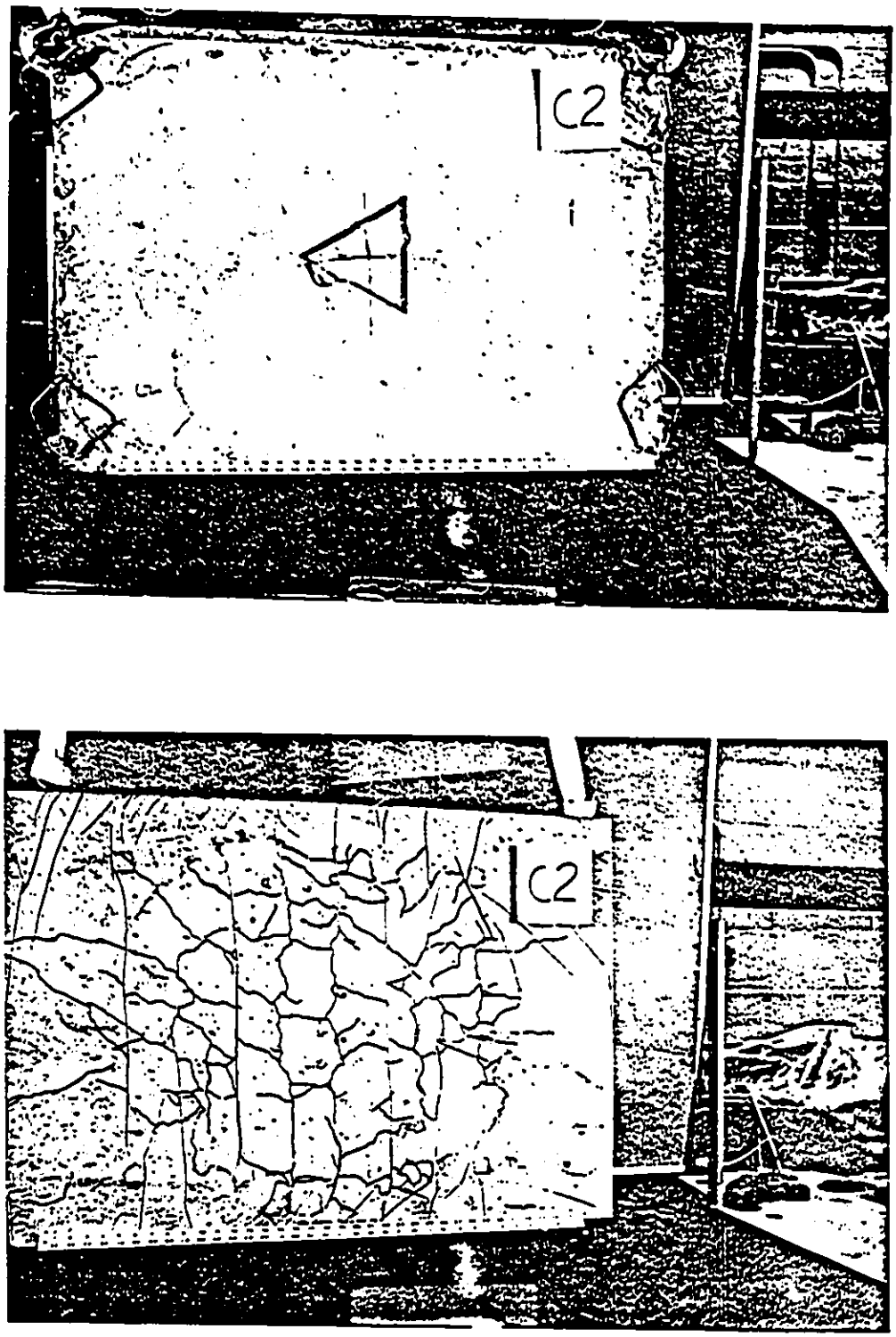

Figure 3.8: Crack patterns at the top and bottom faces of slab C2

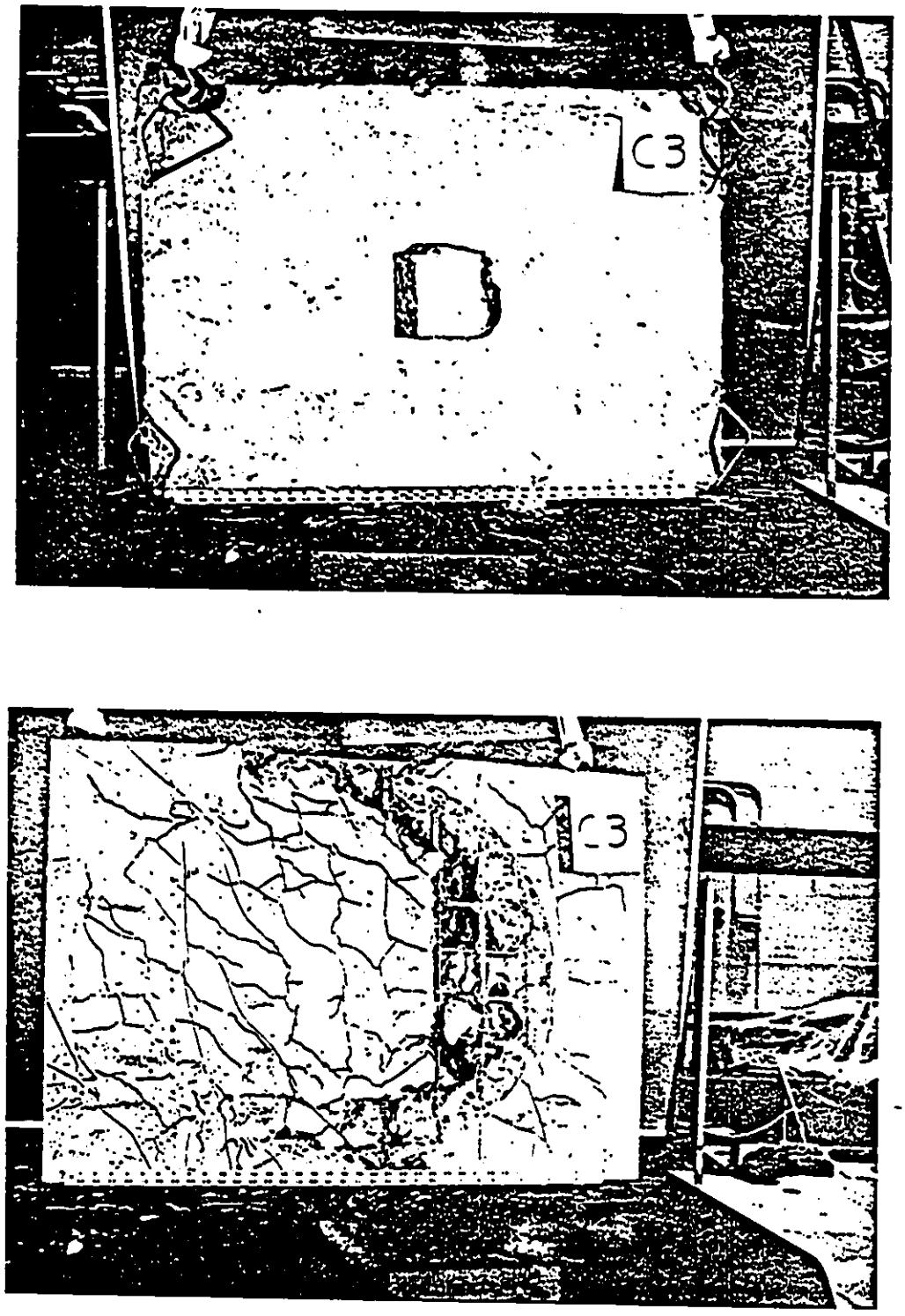

Figure 3.9: Crack patterns at the top and bottom faces of slab C3

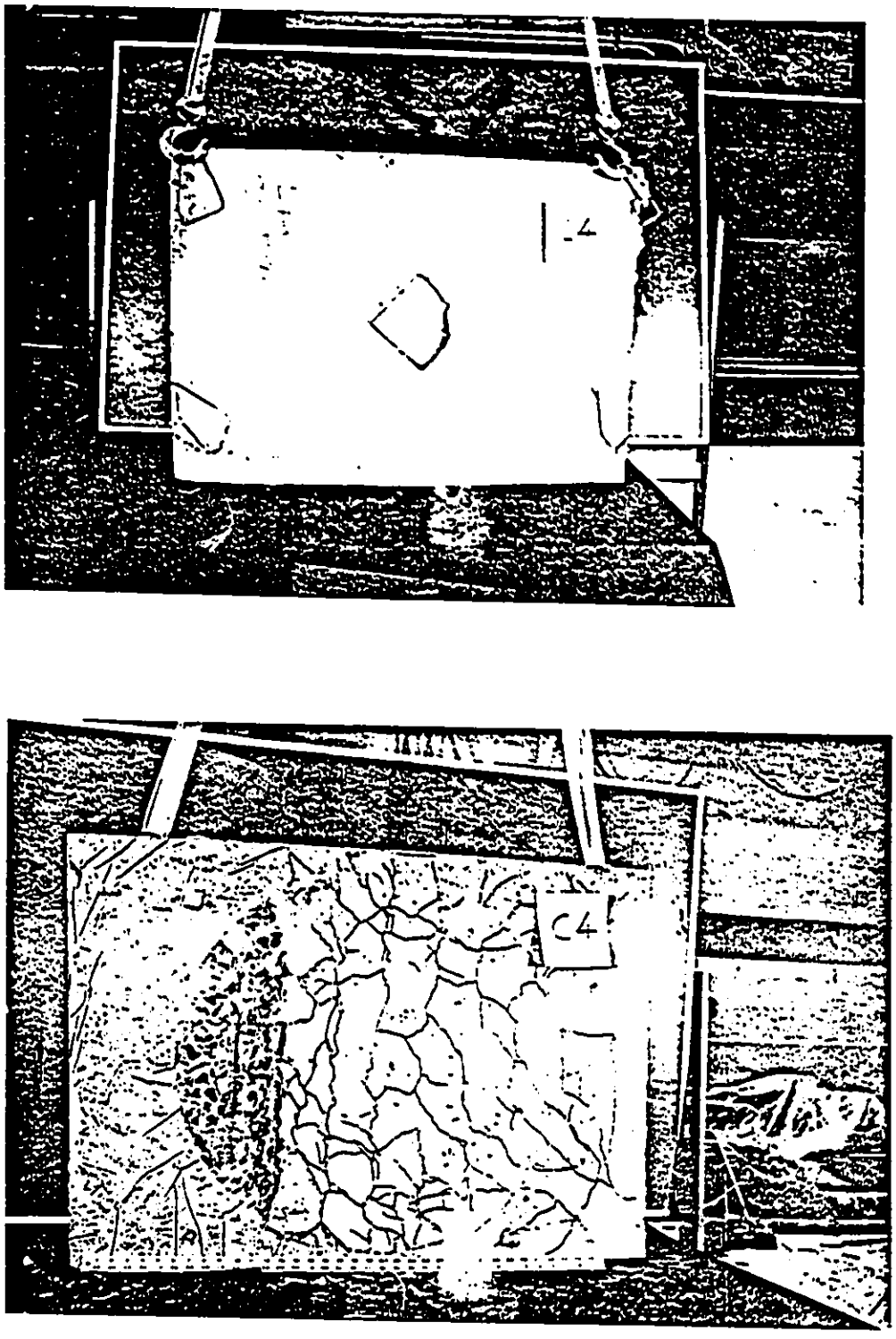

Figure 3.10: Crack patterns at the top and bottom faces of slab C4

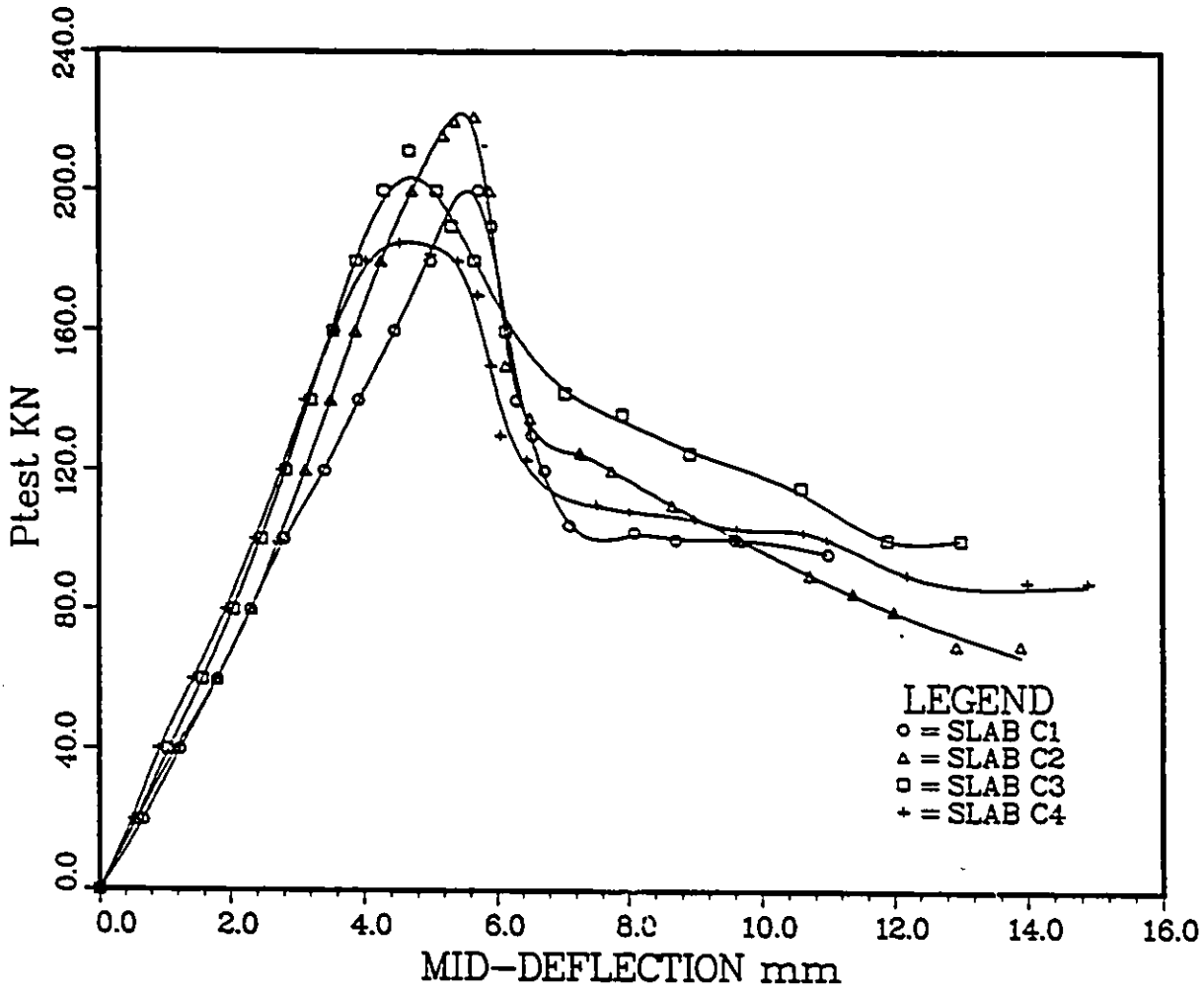

Figure 3.11: Effect of area shape on punching shear capacity

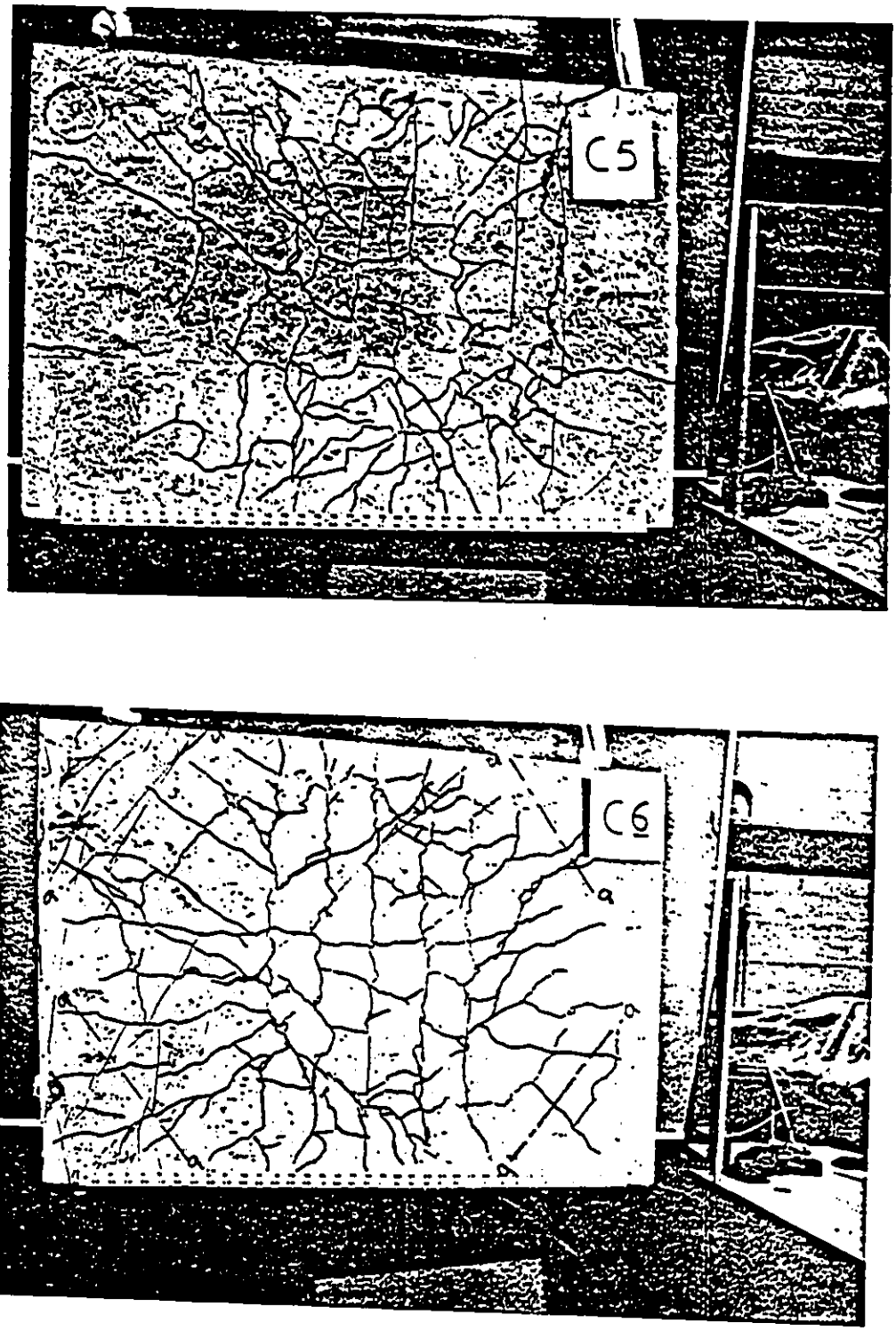

Figure 3.12: Crack patterns at the tension sides of slabs C5 and C6

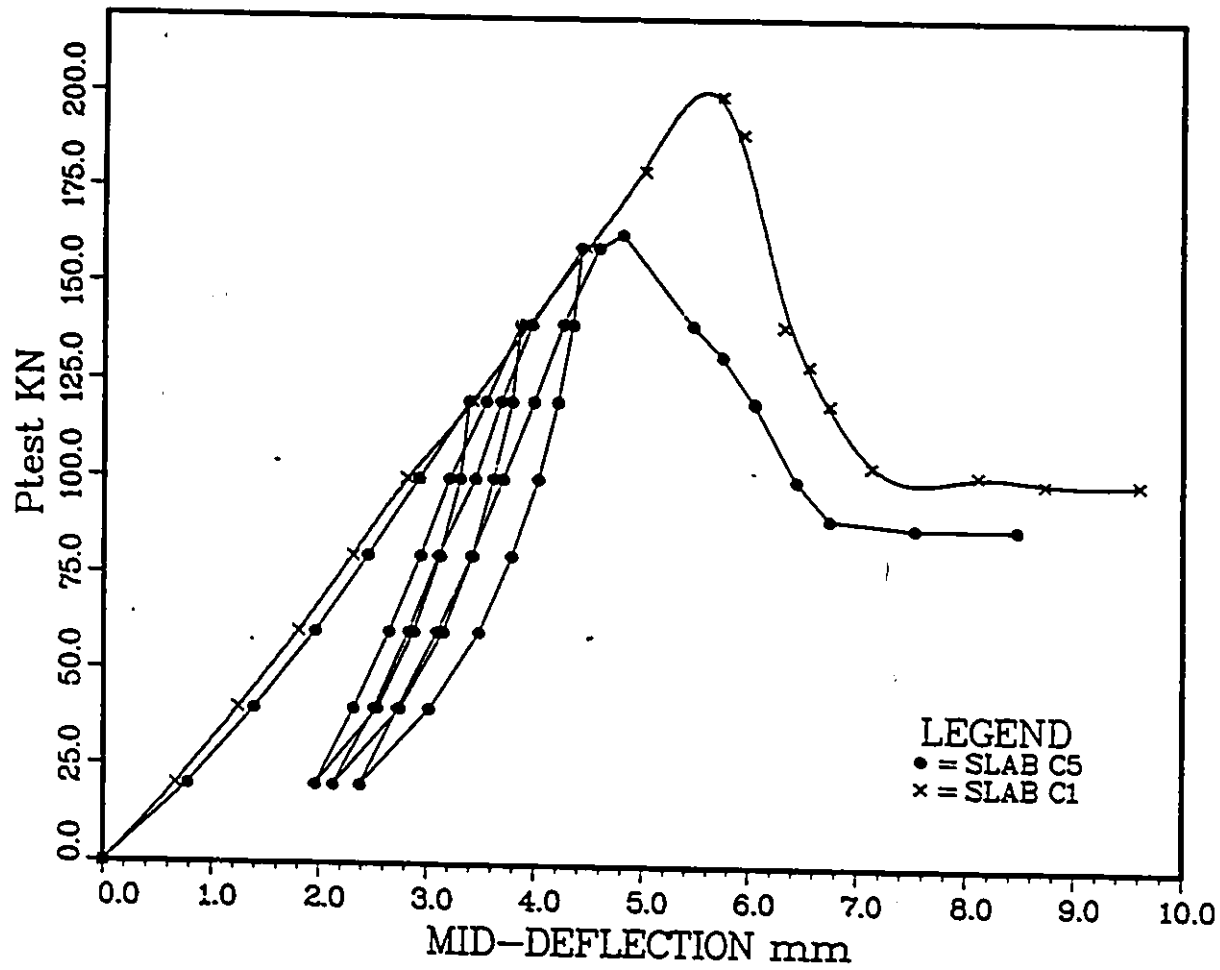

Figure 3.13: Effect of cycling load on punching shear capacity

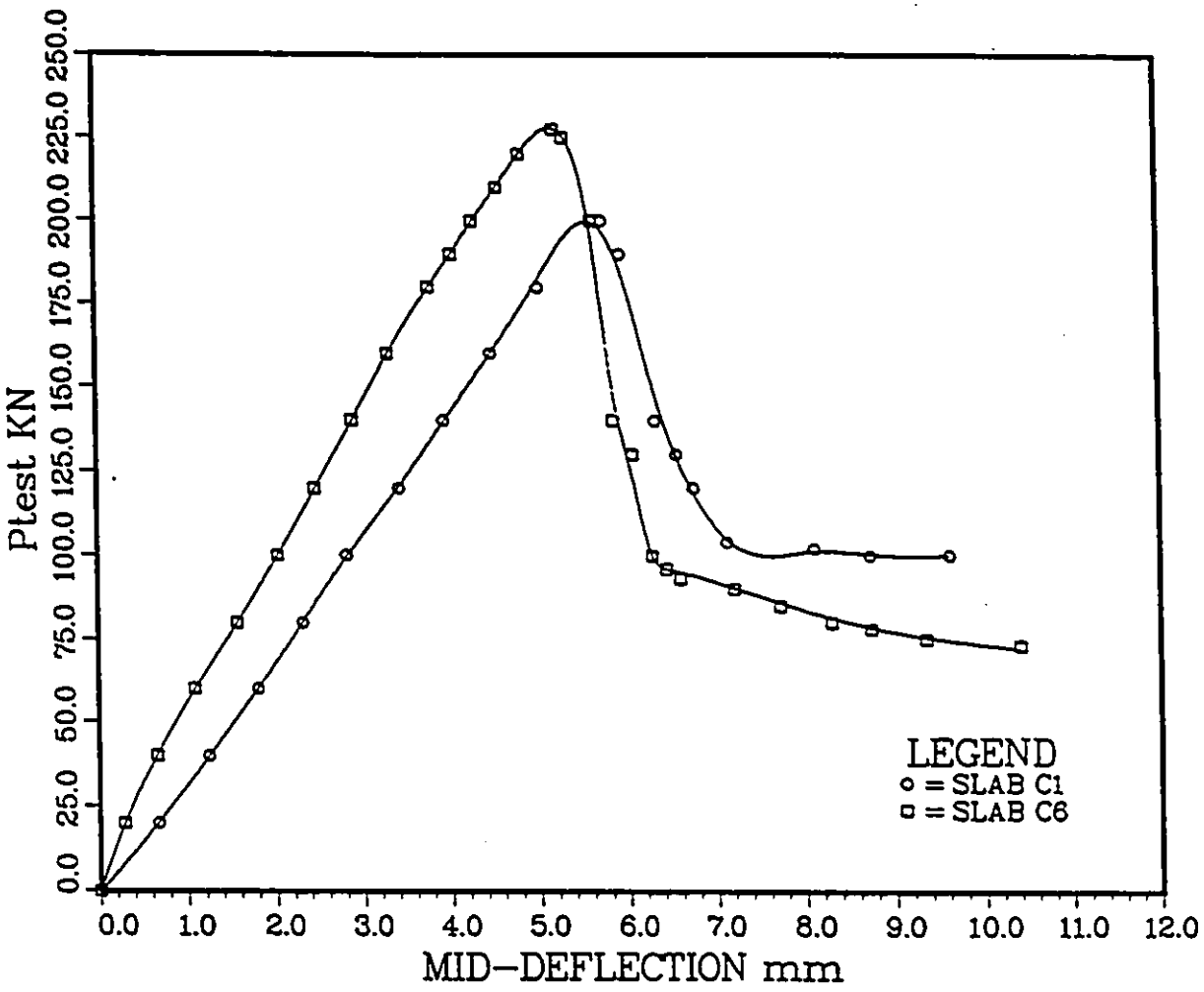

Figure 3.14: Effect of the shape of support on the punching shear capacity

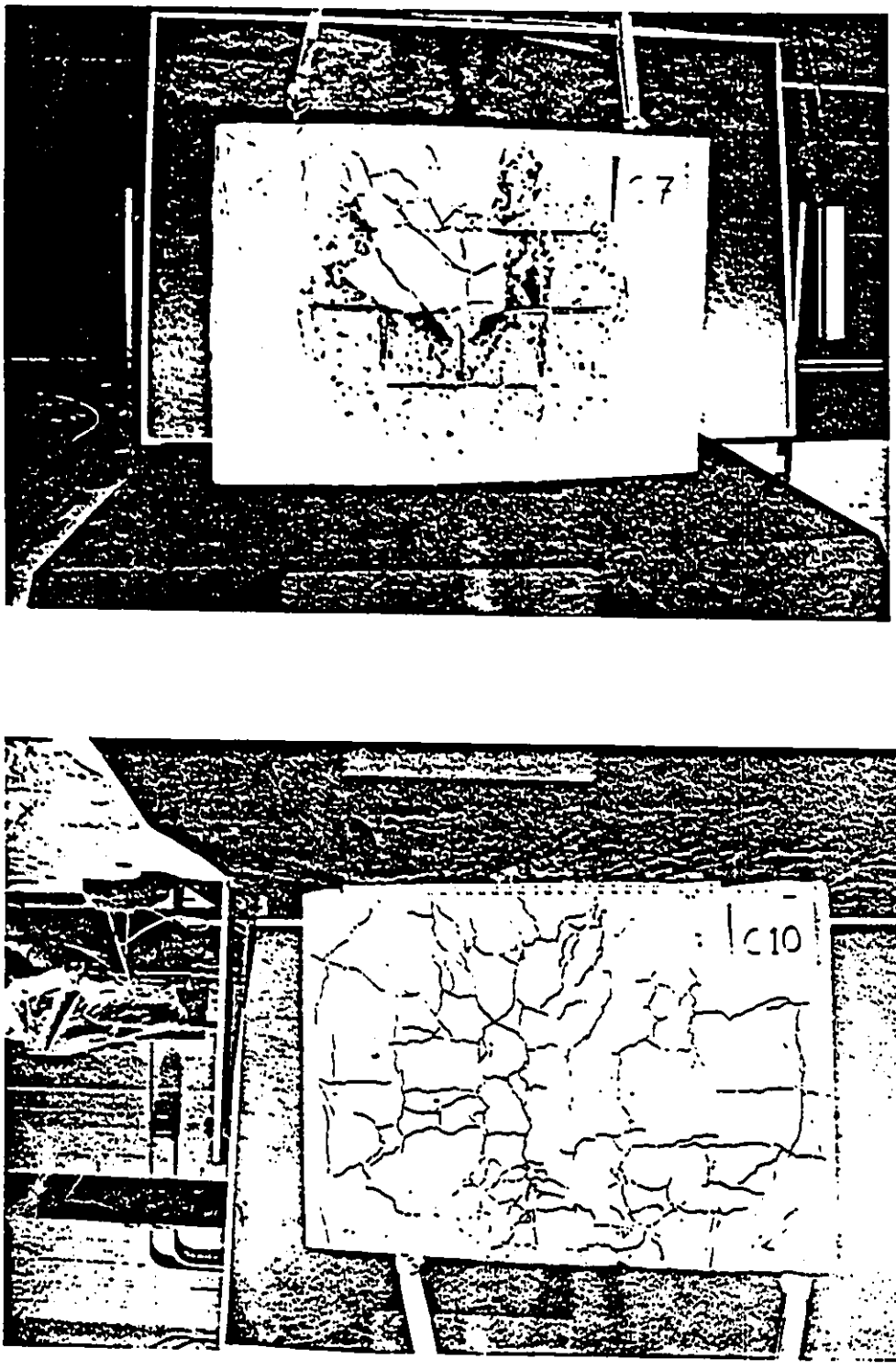

Figure 3.15: Crack patterns at the tension sides of slabs C7 and C10

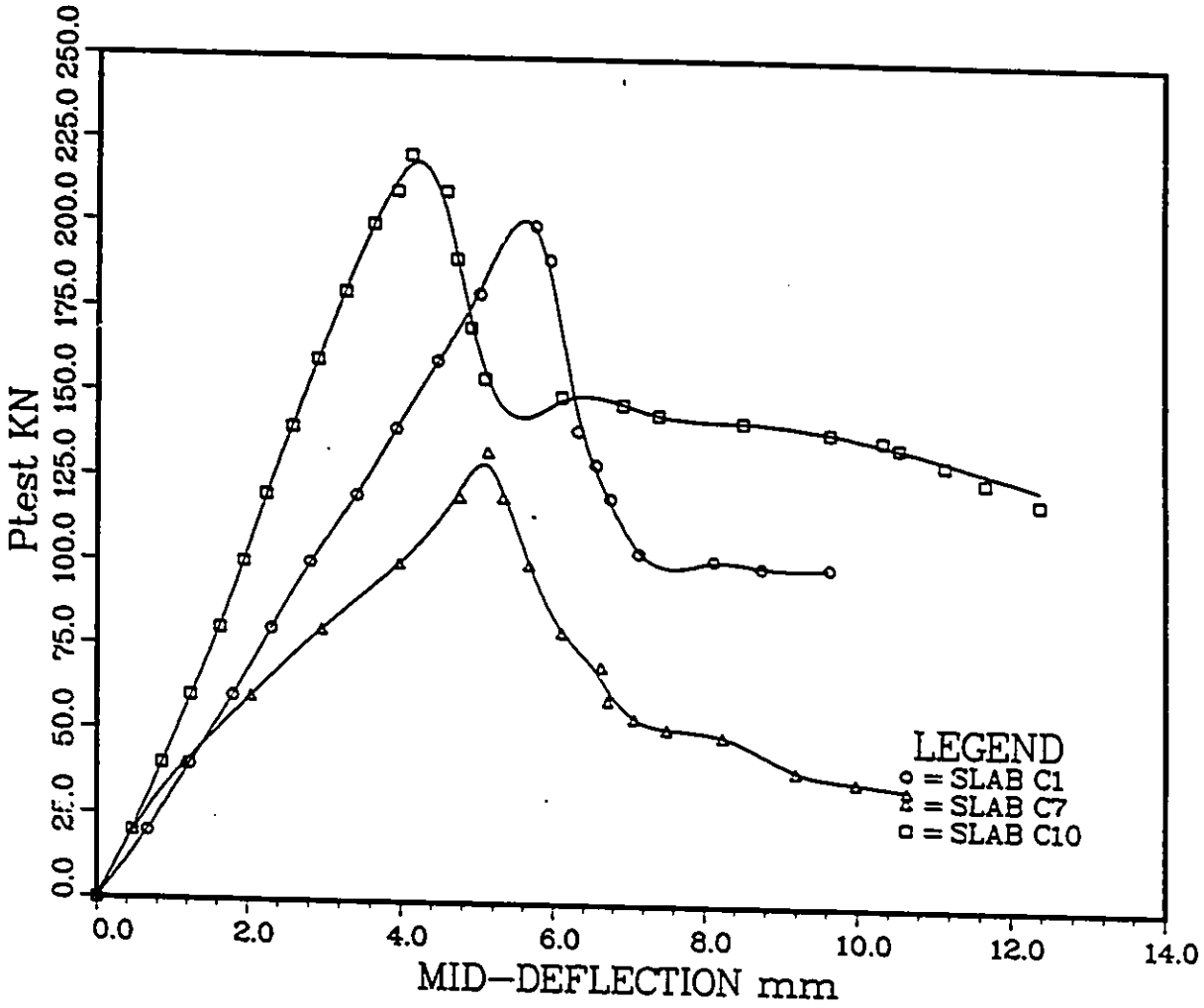

Figure 3.16: Effect of the reinforcement ratio on punching shear capacity

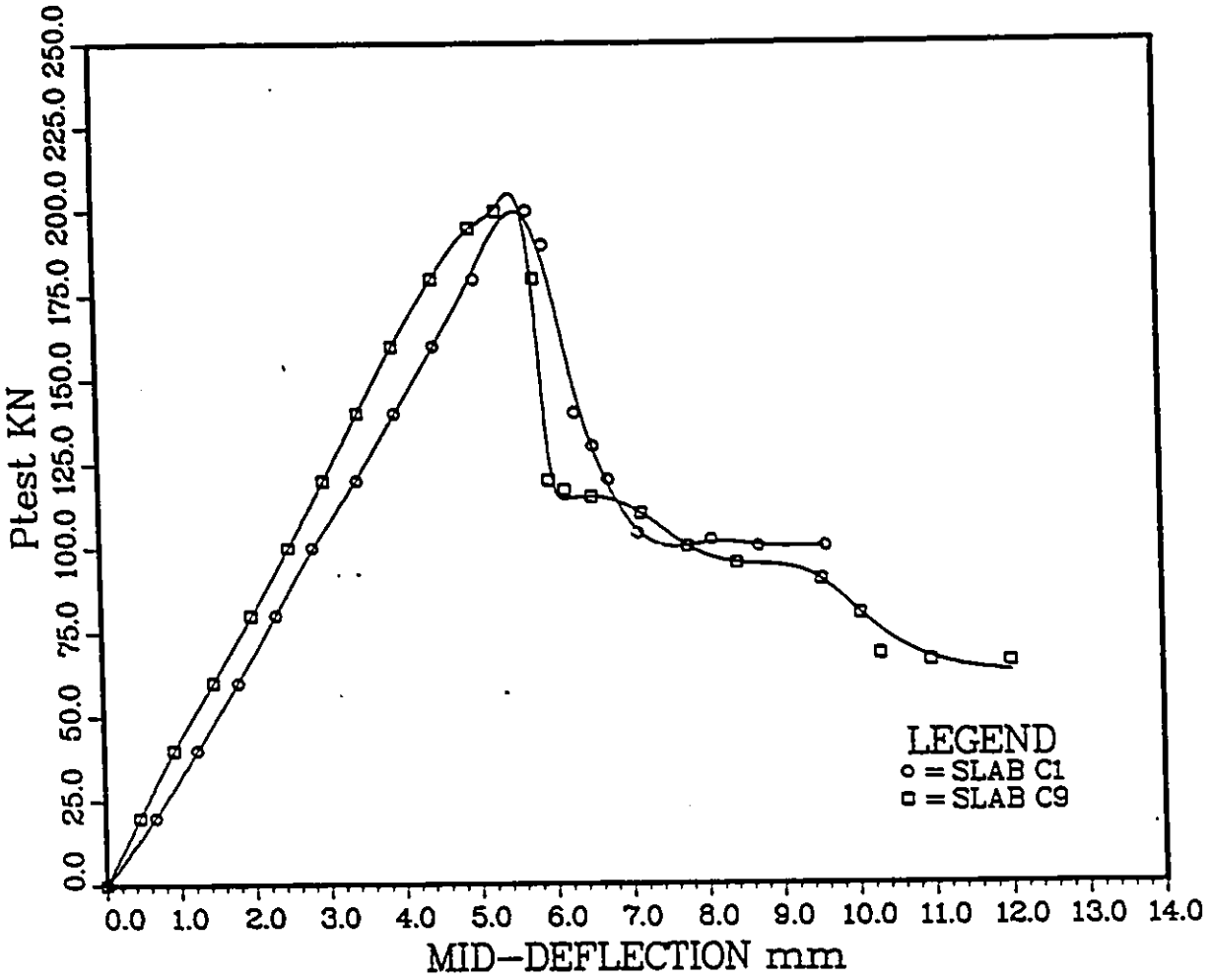

Figure 3.17: Effect of the reinforcement spacing on punching shear capacity

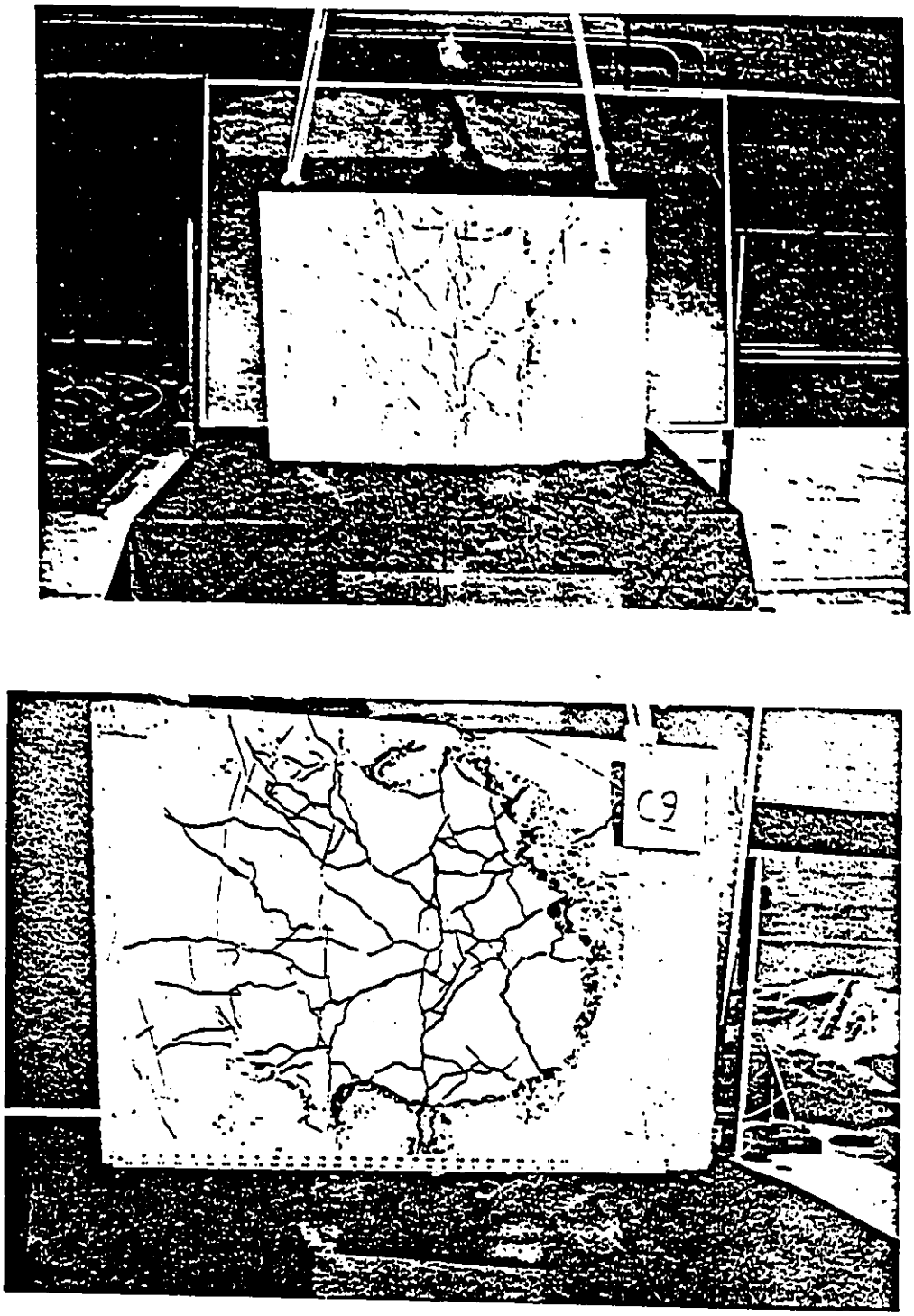

Figure 3.18: Crack patterns at the tension sides of slabs C8 and C9

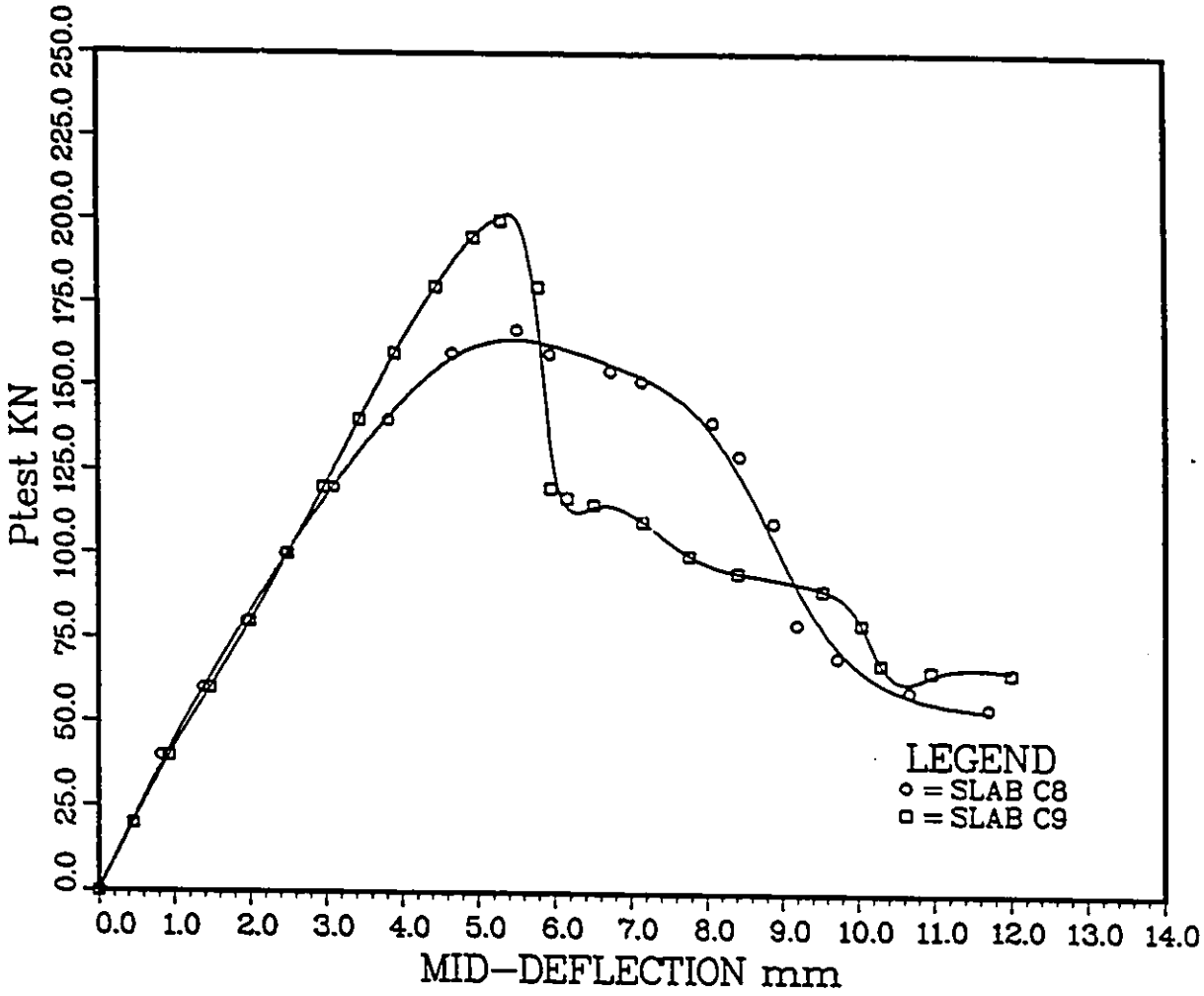

Figure 3.19: Effect of the shape of the cross-section of the reinforcing bars on punching shear capacity

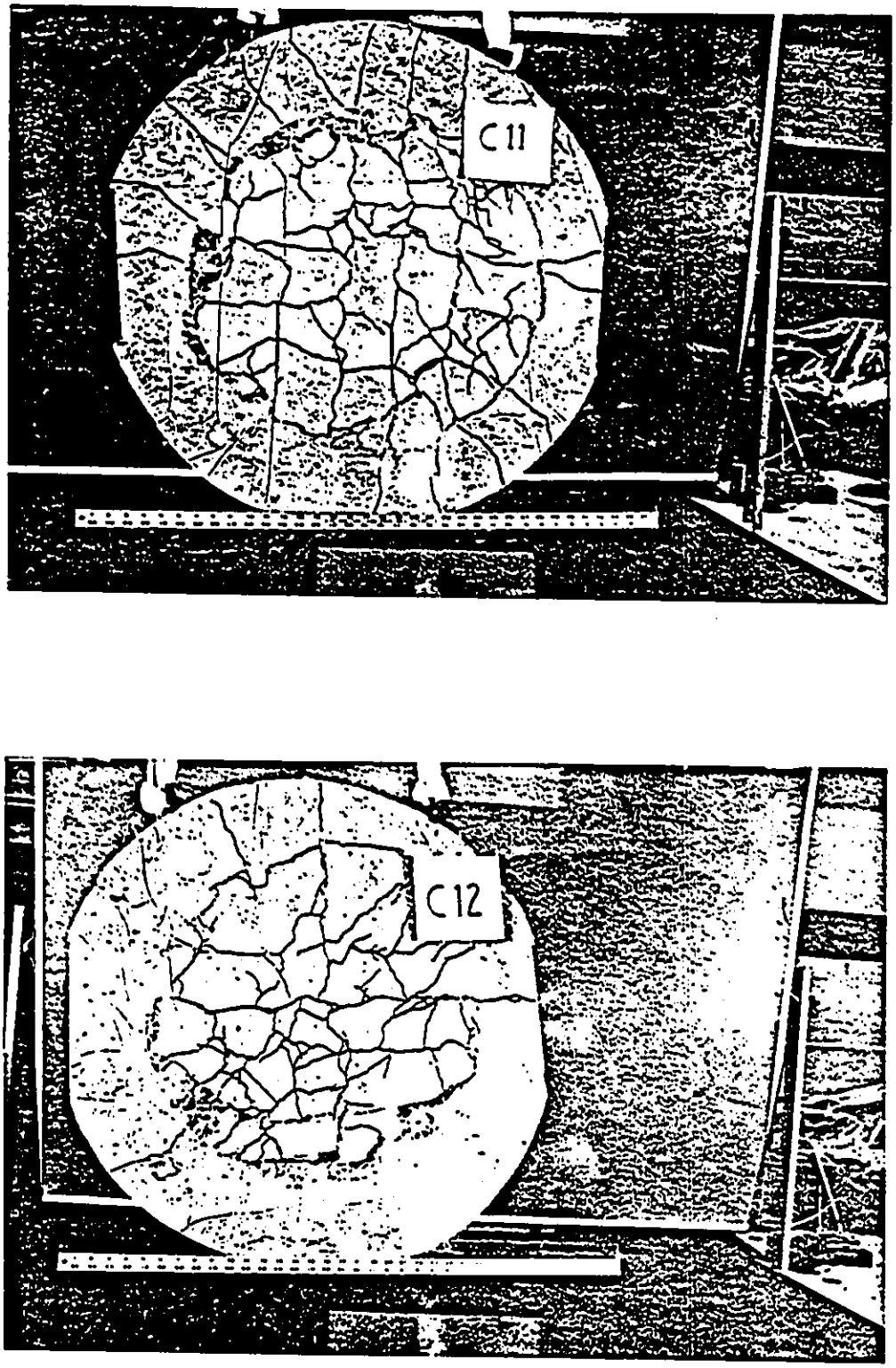

Figure 3.20: Crack patterns at the tension sides of slabs C11and C12

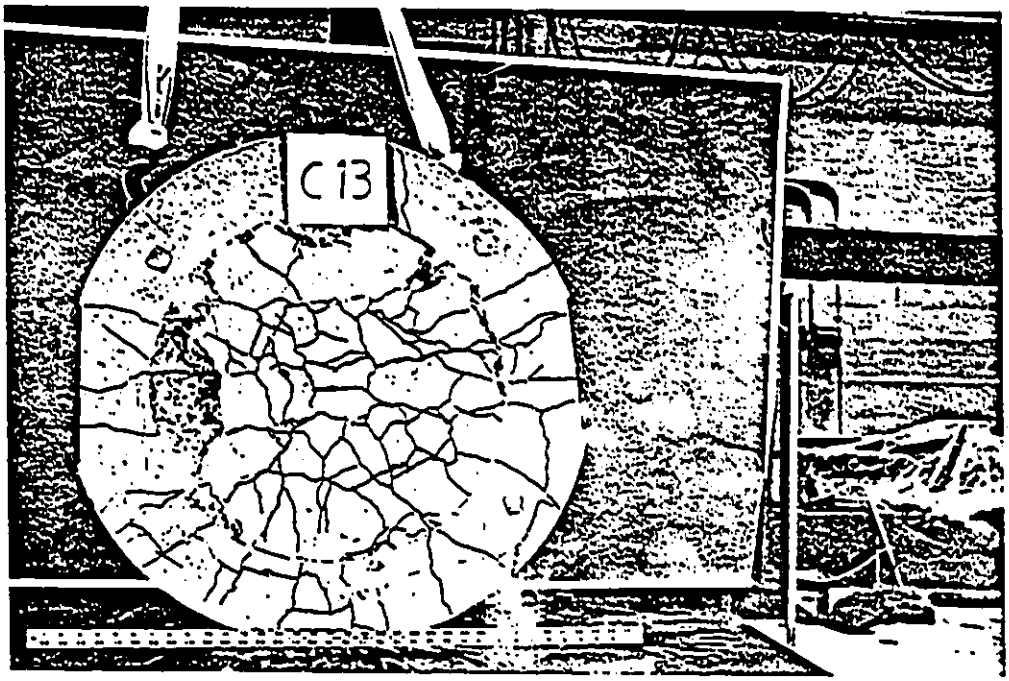

Figure 3.21: Crack patterns at the top and bottom faces of slab C13

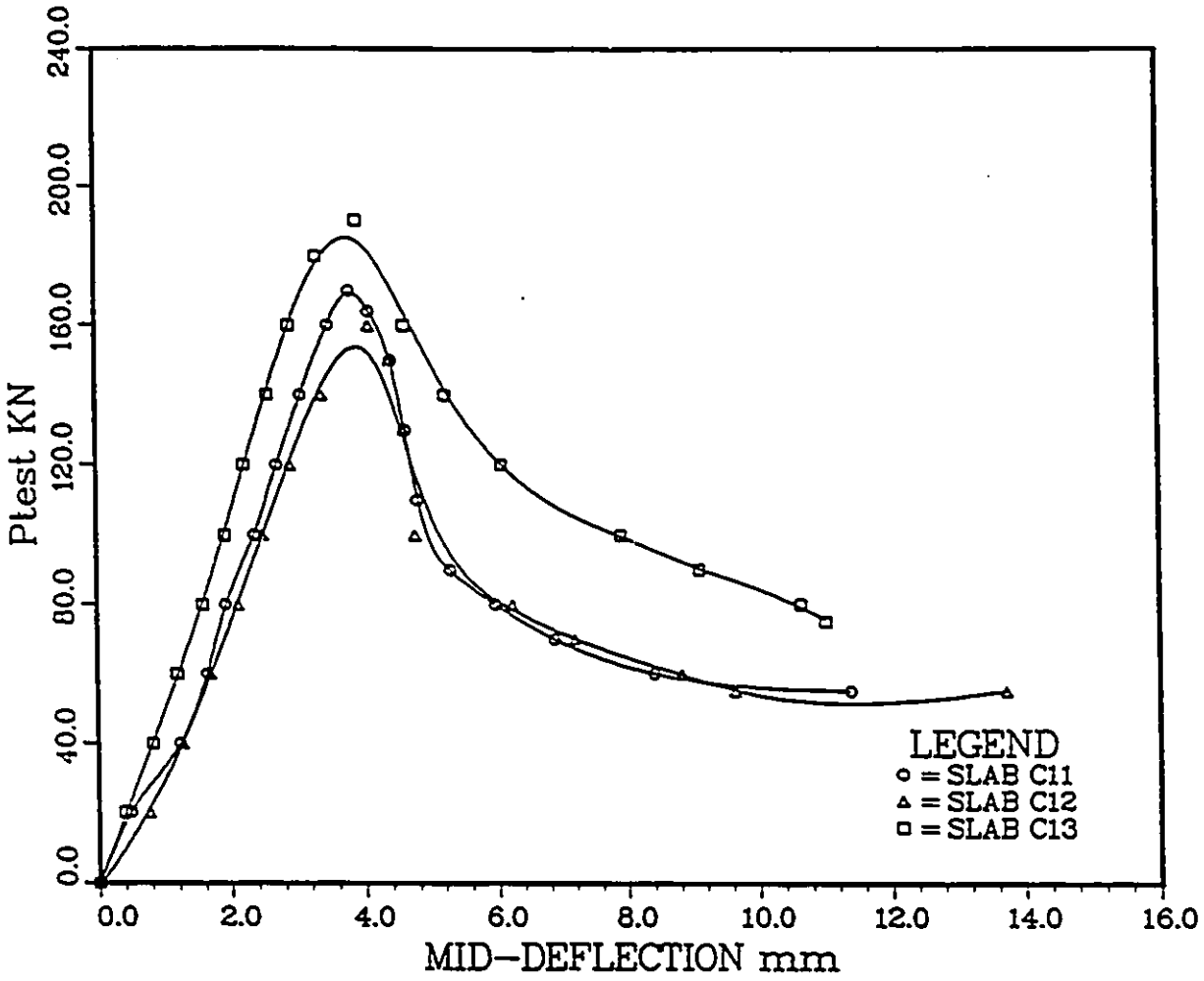

Figure 3.22: Load-Deflection relationship of slabs (Scale effect)

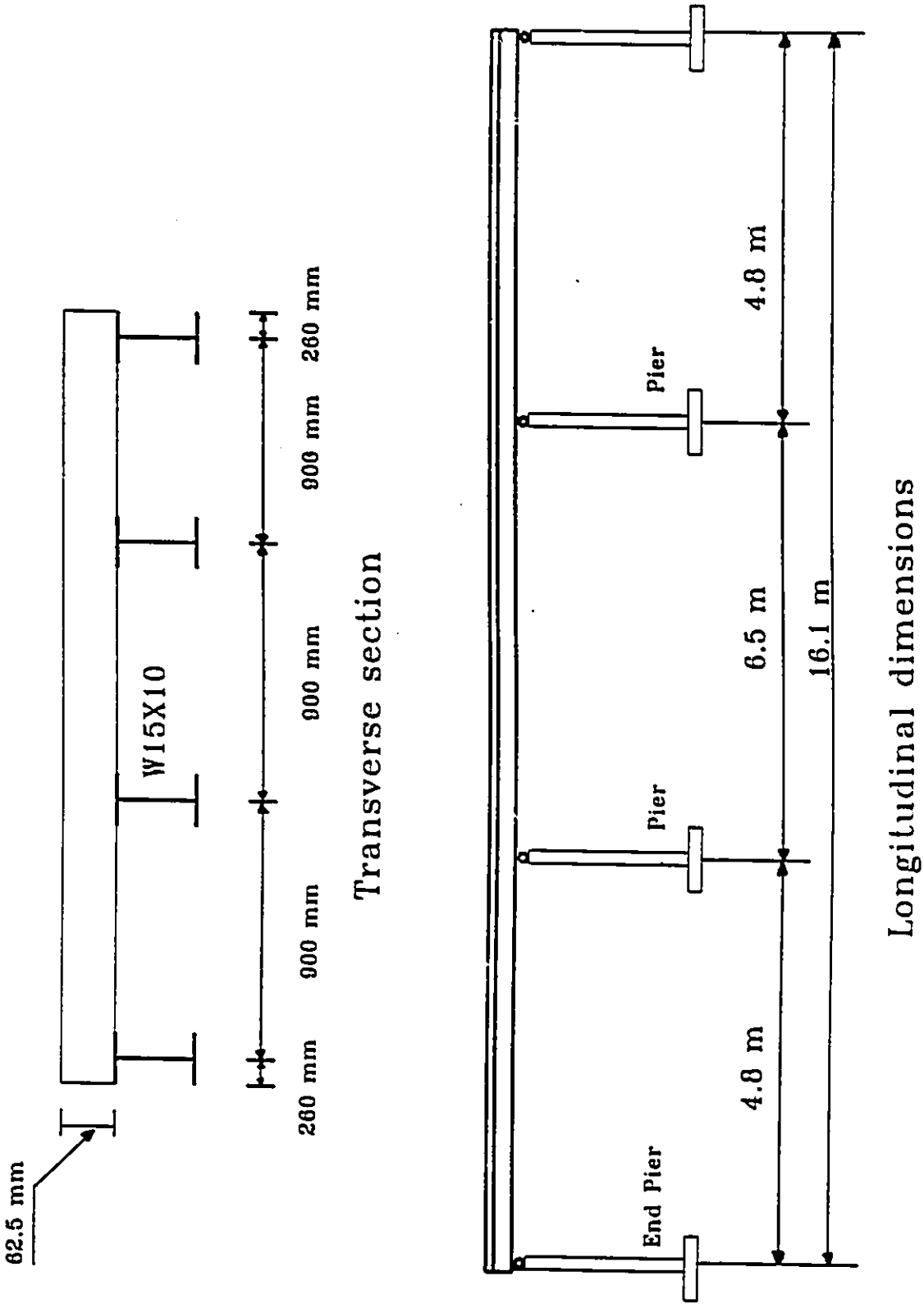

Figure 3.23: The 1/3-scale model bridge

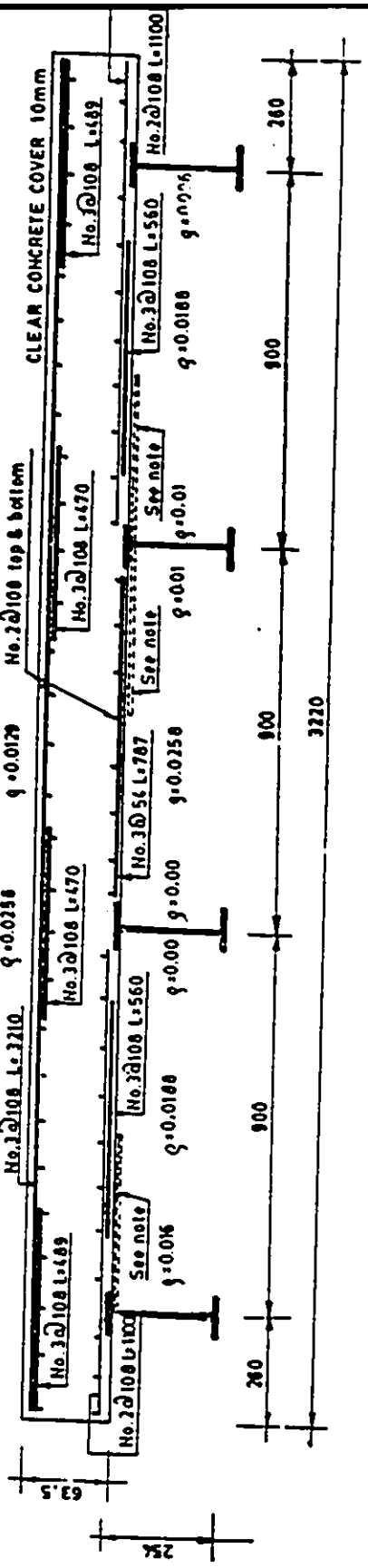

Figure 3.24: Reinforcement layout of the model bridge

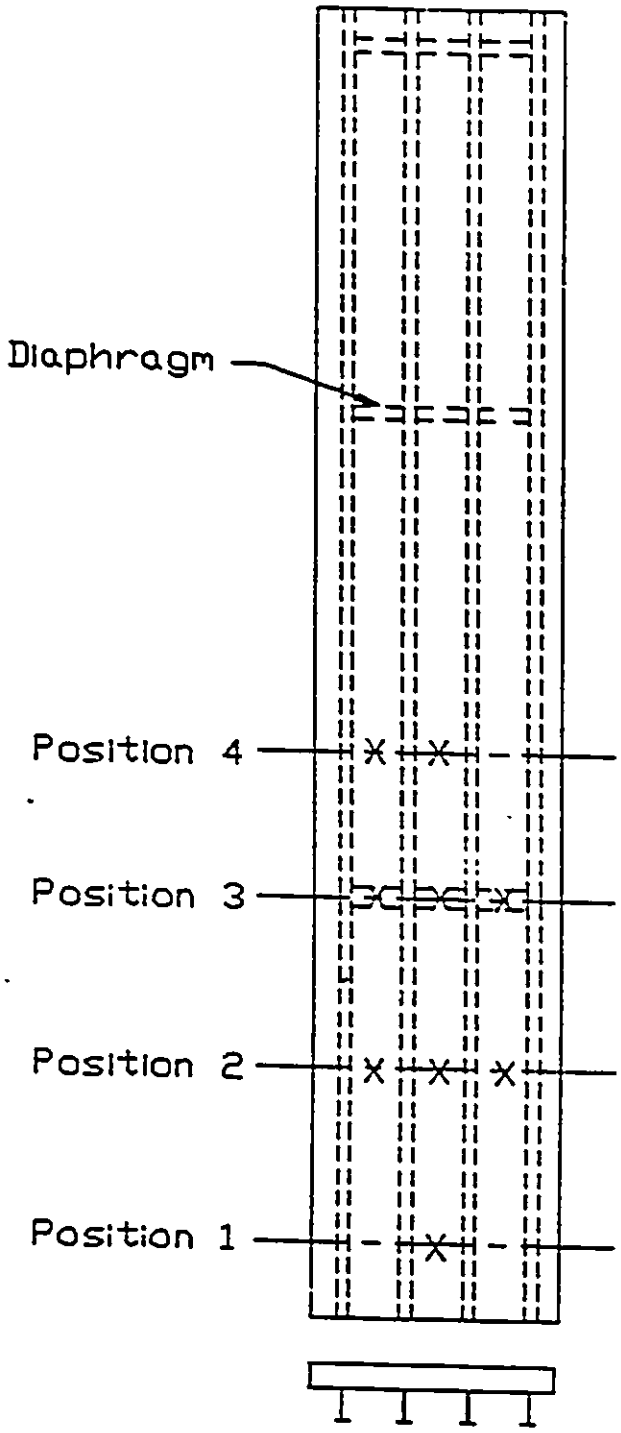

Figure 3.25: Loading positions on the bridge decks

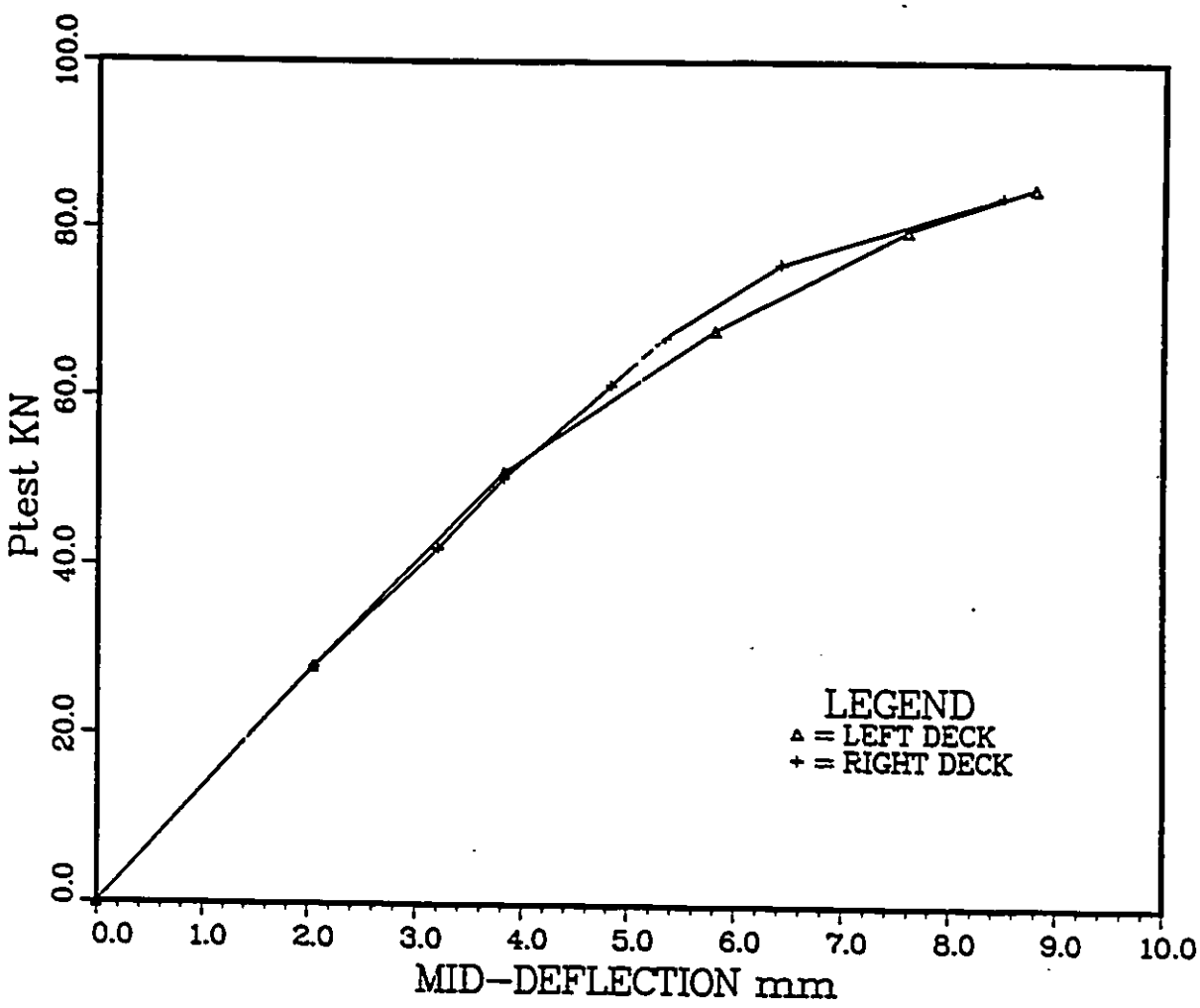

Figure 3.26: Load-Deflection relationship of the left and the right decks of the bridge (position line 2)

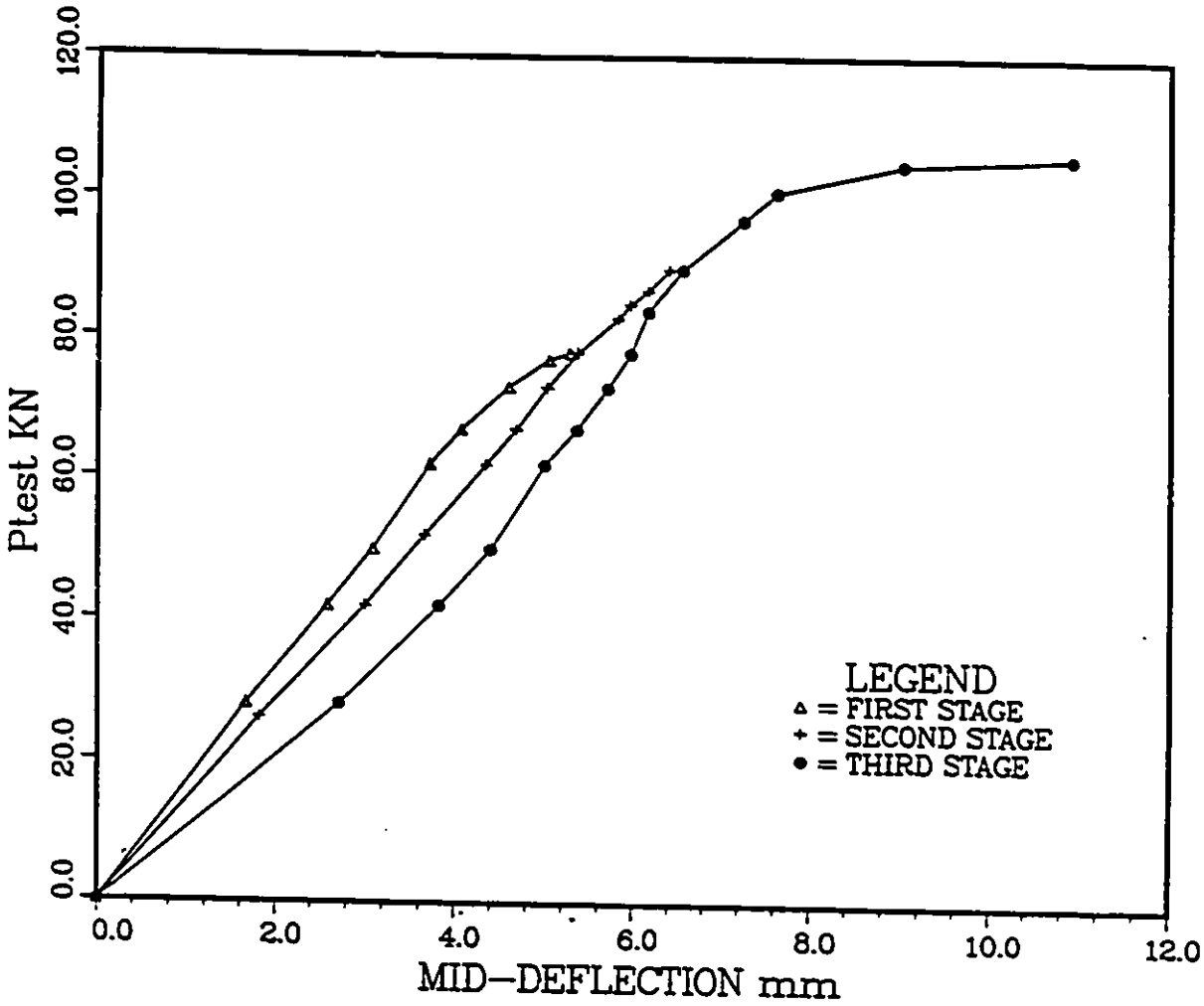

Figure 3.27: Load-Deflection relationship of the middle deck of the bridge (position line 2)

Chapter 4

Theoretical Investigation

4.1 Introduction

The intersections of flat slabs or plates with their supporting columns have been analyzed in a variety of ways. Beside empirical and semi-empirical analysis, many investigators tried to model the punching shear phenomenon rationally to give a better theoretical explanation of the analysis. One of the most popular methods to analyze flat slabs is the yield line theory. Even though, it was originally developed for flexural analysis of slabs, some investigators tried to make it useful for punching shear analysis. A second theoretical method that has been developed and used with great success for beams is the truss method. This theory has been applied to model edge column-slab connections by Alexander and Simmonds with limited success. Because of the popularity and the simplicity of these two methods, which are easy understood by engineers, it is of interest to present and discuss them in this Chapter. In the case of the yield line method, only the ultimate punching shear load equations will be presented for some different

column-slab connections but not the derivation. However, for the case of the strut and tie models only a basic theoretical explanation is given because up to day no successful method has been proposed.

4.2 Yield Line Theory

4.2.1 General

As it was reported in the literature review (Chapter 2), many investigators recognized that the flexural strength of a slab has a strong influence on the punching resistance. For instance, as early as 1943, Johansen [27] believed that punching shear is a secondary phenomenon and analyzed some test slabs according to yield line theory. Other attempts to link punching shear and flexural strength were made by Hognestad [21], Whitney [61], and Moe [44] who included a term P_{flex} in their empirical shear equations. This term was defined as the ultimate flexural capacity that the slab would have if it had not failed in shear. The yield line method of analysis gives an lower bound to the ultimate load capacity of a reinforced concrete slab by a study of assumed mechanisms of collapse. The yield line theory is based on plastic behavior occurring along a pattern of yielding lines, the location of which depends on the loading and boundary conditions. By considering a number of likely yield line patterns, the correct failure pattern, i.e., that providing the least collapse load, can usually be identified. A relationship between the applied force and the resisting moment can be established by equating the work done by the external force to the energy required for internal deformation along the yield lines. If a mechanism requires values of positional parameters defining the locations of junctions of yield lines in a mechanism to be

determined first, the loading is expressed as a function of these positional parameters. The minimum value of the collapse loading for the proposed mechanism can be then found by differentiating the function with respect to each positional parameter in turn and equating the resulting expressions to zero.

4.2.2 Observations from Tests

Figure 4.1 shows two fan cracking patterns developed in the bottom of two circular slabs loaded to failure under circular and square loads respectively. The slabs are simply supported. It can be seen that both fan patterns are indistinguishable, except that the cracks on the tension side, around the periphery of the loaded area have a slightly different shape. However the cracks in the case of square columns are roughly circular. Thus, no significant difference is expected between the two theoretical equations for the two cases. For simplicity the square column can be treated as a circular one with a radius of the largest circle which could be inscribed in the loaded area. The physical equivalent of this is to assume that the corners of the loading surface exert little or no pressure on the slab.

When a slab is supported on a circular column stub casted monolithically with it and loaded through its periphery, only few cracks may develop above the loaded area. However, in the case when the column is larger, these cracks diminish and other cracks around the column may form. To model the behavior of slab-column connections, these observations must be taken into account beside other conditions such as the amount of flexural reinforcement in the slab. The punching shear test slabs were simply supported along the edges, that is the corners of the specimens were free to lift. Thus there was no negative yield moment.

4.2.3 Yield Line Equations

A column may be located in the interior of a structure, near a slab boundary, at the slab boundary and near or in corners. Also the shape of the load, the support and the load conditions differ from one structure to an other. In this study, only simply supported slabs subjected to symmetric concentric loading will be considered with. When he developed the yield line theory, Johansen [27] assumed that yielding of the tension reinforcement is concentrated across certain lines in the slab plane, the yield lines. In order to simplify, as much as possible, the rather long equations, a very simple yield condition will be used. The slab reinforcement is considered to be isotopic. The tension slab reinforcement will be assumed to provide a yield moment of m_{y1} per unit length of slab in two mutually perpendicular directions. It is assumed that shear does not affect the yield line theory solutions, and that punching failure of the slabs, at the column under consideration, will be the first failure. Only yield patterns which model many of the punching test specimens and results reported in the literatures will be presented. (More details can be found in References [27], [28], [29], [30] and [42].

Circular Slabs

For this case, the square loaded area is replaced by a circle with same perimeter (so that the average shear stress at the column edge remains invariant). Figure 4.2 shows a circular slabs with a diameter C loaded through a circular plate of diameter c. The slab is simply supported and the reinforcement is assumed to be isotropic. The conventional theory for the ultimate design of reinforced concrete stipulates the following equation for evaluating the positive yield moment (the

only one which will be dealt with in this study) and the positive ultimate flexural moment which are respectively:

$$m_{y1} = \frac{7}{8}\rho f_y d^2 \tag{4.1}$$

$$m_{f1} = \rho f_y d^2 \left(1 - 0.5\rho \frac{f_y}{f_{cc}}\right) \tag{4.2}$$

As it has been reported in the literature, the shape of the fan yield line patterns are similar to Figure 4.2. Applying the principle of virtual work and equating the energy input to a unit of displacement of the load to the energy simultaneously absorbed in the yield line hinges, the yield load can be expressed as:

$$P_u = \int_0^{2\pi} \frac{m_{y1} C d\gamma}{C - c} \tag{4.3}$$

where $d\gamma$ is defined in Figure 4.2. Solving this equation leads to:

$$P_u = \frac{2\pi m_{y1}}{1 - \frac{c}{C}} \tag{4.4}$$

The derivation of the above equation was based on the assumptions that the fan spreads to the boundaries of the slab and no cracks have developed in the slab beneath the load. If the last assumption is not correct and the yield lines continue under the load, and Gesund [28] showed that:

$$P_u = \frac{2\pi m_{y1}}{1 - \frac{2c}{3C}} \tag{4.5}$$

Square Slabs

For this case, any loaded area shape will replaced by a square with the same perimeter. The simply supported slab shown in Figure 4.3 has a positive moment capacity m_{y1}. The yield lines will form along the diagonals which are lines of maximum moment. Corner levers will form permitting the slab corners to rotate

about the axis a-a. Assuming a deflection of unity at the column, the principle of virtual work enables the calculation of the deflections of the loading and the rotations of the yield lines. The work done by the load is then equated to the dissipation of energy in the yield lines to give the value of the loading to cause collapse.

$$P_u = 4m_{y1}(B-2x)\frac{2}{B-b} + 4m_{y1}x\sqrt{2}\frac{\sqrt{2}}{B-b-x} \tag{4.6}$$

where B is the side length of the square slab and x is as defined in Figure 4.3.

A yield-line pattern will develop corresponding to the value of x giving a minimum value of P_u in the above equation:

$$\frac{\partial P_u}{\partial x} = 0; \qquad gives \quad x = (1-0.5\sqrt{2})(B-r) \tag{4.7}$$

which substituted into equation (3.6) gives:

$$P_u = 8m_{y1}\left(\frac{1}{1-\frac{b}{B}} - 3 + 2\sqrt{2}\right) \tag{4.8}$$

If the corners are tied down, the yield lines must go through the corners, that is, $x = 0$, and

$$P_u = 8m_{y1}\left(\frac{1}{1-\frac{b}{B}}\right) \tag{4.9}$$

Square Slab Supported Along Two Opposite Edges

This type of slab is shown in Figure 4.4. Loading is applied through a square column stub at the center. Reinforcement is isotopic and the positive yield moment is m_{y1}. With a unit deflection at the column, the flexural load can be obtained by virtual work:

$$P_u = 4m_{y1}\left(\frac{1}{1-\frac{b}{B}}\right) \tag{4.10}$$

Circular and Square Footing

The formations of yield fans for square or circular footing are shown in Figure 4.5. This kind of structure can be treated as a large slab of an area A_{slab} and supported on a circular column, of radius c located at its center. The slab is loaded with a uniformly distributed load W per unit area. This loading produces an axial force P in the column. It is assumed that the slab will not crack above the column. The formation of the yield fan shown in Figure 4.5 will permit the entire slab outside the fan to drop the same distance when failure occurs. Gesund developed the equation for the ultimate punching load at yield to be:

$$P_u = \frac{2\pi m_{yl}}{(1-\frac{c}{R})(1-\frac{\pi R^2}{3A_{slab}}(1+\frac{c}{R}+\frac{c^2}{R^2}))} \tag{4.11}$$

where R is the radius of the fan and it was defined as:

$$R = c\left(\frac{3}{2}\frac{A_{slab}}{\pi c^2} - \frac{1}{2}\right)^{\frac{1}{3}} \tag{4.12}$$

4.2.4 Calculation Results

The punching resistance loads of the bridge decks and the author's tested slabs were predicted by the yield line theory. The predicted ultimate loads and the failure test loads are denoted by P_{yield} and P_{test} respectively in the tables and the Figures in this Chapter. A comparison between the predicted and the test results of the author's experiment is shown in Figure 4.6 where the ratio $\frac{P_{test}}{P_{yield}}$ is plotted against P_{test} . From this Figure, it can be seen that only few points which represent the predictions for the bridge decks, are inside the interval of tolerance (+ 15%). In contrast, only two points representing the slabs results are inside this interval.

Also, 77 more specimens of slabs supported along their edges and subjected to punching loads, reported in the literature were analyzed. The calculation results are presented in Figure 4.7 which indicates that the yield line theory may not predict the punching shear capacity of a slab, but it can determine its ultimate flexural capacity.

4.2.5 Discussion

One of the main assumptions in the yield line method is that the slab section along a yield line possesses the capacity for rotation which will permit moment distribution from points of high stress concentration to other parts of the slab. This type of behavior is possible only in under-reinforced slabs that possess sufficient ductility and which do not fail prematurely in shear. It is necessary to consider a number of different possible collapse mechanisms to determine the minimum value of the collapse loading of a slab. A major disadvantage of the yield line method is that an engineer may miss the critical mechanism. The yield line theory only predicts collapse due to formation of a mechanism. Therefore, the reinforcement in the most highly stressed regions of a slab reaches the yield point prior the collapse. When the value of $\frac{P_{yield}}{P_{test}}$ is less than one it is an indication that the failure is flexure rather than shear. However to distinguish between flexural and shear failure modes, a certain function depending on the geometry and the strength of the slab should be established. Gesund and Kanshik (28) defined a dimensionless parameter Q_0 to determine when shear failure can be calculated from the yield line theory.

$$Q_0 = \frac{\rho^2 f_y d^2}{\sqrt{f_{cc}} u_0 U_0} \tag{4.13}$$

where u_0 and U_0 are the perimeter of the column and slab respectively. The above equation is a combination of two relationships that the authors established. The

first one is the relative strengths (bending and shear) which is a function of $\frac{\rho f_y d^2}{f_{cc} u_0 d}$. and the second one is the relationship by the loadings. The authors assumed that the flexural load is related to the shear one through $\frac{\rho d}{U_0}$

It was suggested that punching shear failure takes place and could be predicted by yield line theory only when the parameter Q_0 is greater than 4. However, if one looks to the Figure 4.8, it can be noted that around only 40 percent of the all points are in this range, and around two thirds of them are above the unity line. This indicates that the yield lines theory can not predict the punching resistance of a concrete structure with good accuracy even within the suggested limit. Three main assumption were adopted to derive the above parameter Q_0.

- The tensile resistance of concrete is proportional to the square root of f_{cc}.
- The shear resistance of a concrete slab is independent of the flexural reinforcement.
- The critical failure section is the column faces.

These three assumptions were not justified by Gesund and Kanshik and they lead to a very conservative results. The first two assumption are similar to the ACI code. As it will be discussed in Chapter 5, the tensile strength of concrete is proportional to the cube root of f_{cc} not as assumed in the above theory. Also, the neglect of the effect of the flexural reinforcement is unrealistic to model a slab-column connection in the shear failure mode. Moreover, the third assumption means that the shape of the failure surface is not a cone frustum, which is a contradiction to what was observed during tests.

In order to simplify the parameter Q_0 and make it more reasonable, it is better to assume that the shear stress in concrete is proportional to the cubic root of

f_{cc}. This assumption is adopted by most European codes and it is appreciated by Gardner. In addition, the equivalent diameters of a column and a slab (c and C respectively) regardless of their shape, can be used instead of using the perimeters u_0 and U_0 in the above equation, since the perimeter is directly proportional to the diameter. Therefore equation (4.13) can be rewritten as:

$$Q = \frac{\rho f_y d^2}{(f_{cc})^{\frac{1}{3}} cC} \tag{4.14}$$

If one regards the unity line in Figure 4.9 as the dividing line between primarily shear and primarily flexural failure, then it is apparent when Q is less than 3.5 the specimen might have failed in flexure. However, when Q is between 3.5 and 9, approximately half the specimens probably failed in bending and the other half in shear, while for Q greater than 9, most specimens might have failed in punching shear. Therefore, the suggested parameter does not help too much in distinguishing between failure modes.

4.2.6 Summary

The yield line theory is a powerful tool to check the flexural strength of a slab-column connection but not to determine its punching resistance. Therefore, after designing a column-slab connection to resist punching shear, flexural resistance should be checked. If the ultimate design punching shear resistance load is greater than the that predicted by the yield line theory, then the mode of failure is likely to be flexural. This is true only when the slab is under-reinforced.

4.3 Strut and Tie Model Theory

4.3.1 Introduction

While the elastic analysis can accurately model the flow of the stresses prior to cracking, it can not predict the redistribution of stresses that will occur after cracking of the concrete. Inelastic finite element models are capable of predicting the stress flows in a slab-column connection for all levels of loading up to failure. However these models are too time-consuming for use in every day design. Therefore a more convenient method should be developed in order to simplify the punching shear problem.

Cracked reinforced concrete carries load principally by compressive stresses in the concrete and tensile stresses in the reinforcement. After significant cracking has occurred, the principal compressive stress trajectories in the concrete tend towards straight lines, and hence can be approximated by straight compressive struts. The tension ties used to model the principal reinforcement meet with concrete struts at nodal zones. Thus, the internal flow of forces can be modeled using concrete compressive struts, tension ties and nodal zones. This concept can be referred as a truss model.

4.3.2 Observation from Tests

Figure 4.10 shows a reinforced concrete corbel after failure tested by Cook. The author reported that the failure occurred in the specimen by concrete crushing under the bearing plate after large strains were recorded in the main tie and after the occurrence of severe spalling of the concrete cover surrounding the bearing

plate. In this case it was believed that the failure was caused by excess yielding of the flexural steel reinforcement. Slab C1 was cut in half to show the failure cracks in concrete. Figure 4.11 shows a transversal section of slabs C1. It can be easily seen that the cracks run along an inclined straight line similar to that in corbels. The opening of the cracks is wider in the tension side than those in the compression side.

4.3.3 Truss Model

One of the characteristics of truss models is their ability to closely predict the inclination of the cracks in concrete structures. These cracks form perpendicular to the direction of principal tension in concrete . The principal compression stresses flow in the regions between and parallel to these cracks.

The symmetric punching of reinforced concrete slabs can be compared to a double-side corbel. Figure 4.12 shows the predicted principal stresses and strains of a corbel by non-linear finite element analysis. As it can be seen, the predicted flow of concrete compressive stresses concentrates around inclined straight lines. The high stresses concentrate under the load point of application and around the column faces at the bottom of the corbel. The flow of stresses can be modeled as shown in Figure 4.13a. The forces are modeled in a truss shape shown in Figure 4.13b. With the geometry of the truss model determined, the forces in the struts and the ties can be found from statics.

Figure 4.14 shows an interior column-slab connection with no unbalanced moment acting. The cracks are essentially radial, indicating the compression forces flow toward the column from all directions. While the surface cracks do not provide complete information on the force flow in the concrete, they do give an indication

of the horizontal directions of the compressive concrete forces. Evidence for the vertical directions may be observed from the final failure mechanism. That is, the vertical component of the acting forces is dependent of the inclination of the failure surface and the arrangement of flexural reinforcement. The inclination of the failure surface is determined by the longitudinal crack running some distance away and around the column faces. This crack will be referred later as a shear crack.

4.3.4 Model Components

The interior slab-column connection may be viewed as three dimensional space truss, with the struts being compressive concrete pieces bound together by flexural reinforcement ties. To formulate the truss model, the actual dimensions of the compressive struts and tension ties should be determined first. The importance of these dimensions has been pointed out by Marti [43]. Simmonds and Alexander proposed two types of struts, which are:

- In-plane struts that are parallel to the plane of the slab.
- Out-of-plane or shear struts that are at some angle α to the plane of the slab.

In-Plane Struts

The directions of the in-plane struts are shown in Figure 4.15. These struts meet the column faces at corners. For the case of a square column, the radial cracks usually start at the corners because of the high concentration of stress. Because

of the symmetry of the cross-section of the column, equilibrium is satisfied by summing the in-plane forces in both directions. Once the applied stress exceeds the resistance stress of these struts on the tension side, flexural cracks start opening and increase in depth. Once the cracks openings reach the position of the flexural reinforcement, the in-plane struts become ineffective and the reinforcing steel will resist the in-plane forces.

Out-of-Plane Struts

As it can be seen in Figure 4.16, the compressive struts on the column faces are inclined and form a fan pattern allowing forces to enter this face from portions of the slab outside of the width of the column faces. Beside the radial cracks, tangential cracks will be also developed at some distance from the faces column. The depth of this crack will increase with an increase of load, therefore the depth y of the compressive zone decreases. Hence the resistance stress of the " out of plane " struts depends on y. Since it is difficult to predict y, the forces in the struts should be determined as function of the compressive strength of the cracked concrete. Figure 4.16 shows a plan view of the distribution of the force of square column-slab connection.

4.3.5 Ultimate Failure Load

Criteria should be established for determining the ultimate resistance of the interior column connection. For equilibrium, the sum of the vertical components of the fan struts must equal to the shear force, and the horizontal components of the fan-struts must equal to the sum of the forces in the flexural reinforcement. Therefore, two failure mode are possible, namely the failure of the tension

steel tie or the compression strut. The concrete in the region of the column and, especially in the compression zone, is confined by the concentration of the compressive forces, so that failure of the concrete struts at the column face can be expected to occur at a stress higher than f_{cc}.

Flexural Reinforcement Failure

This mode of failure was rarely observed by previous researchers. It occurs when the reinforcing steel has a very low yield streugth, and a rupture of the mat takes place when the opening of the longitudinal crack was significantly wide. Such types of failure can be avoided by placing enough steel on the tension side of the slab-column connection. In the development of their truss model, Alexander and Simmonds assumed that the flexural steel will always reach yield at failure. Therefore a failure of the slab-column connection takes place as soon as the steels reach the yield point. As it will discussed in Chapter 6, this assumption is not realistic. Kinnunen and Nylander [36] reported in their tests, steel started yielding at approximately 40 percent of the ultimate load. However other investigators such as Regan reported that slabs tested for punching shear failed before the steel reach its yield stress.

Concrete Compression Failure

Most of the previous investigators reported that slabs tested for punching shear, failed by compression failure of the concrete. An analytical solution to the punching failure problem should be based on the determination of the failure stress at which the concrete struts fail at the column faces. The failure stress should not exceed the crushing strength of the cracked concrete. This stress varies around

the column and with the connection design properties. The estimation of failure stress depends on strut inclinations and the widths of the areas at the side faces of column on which the struts bear.

4.3.6 Relation Between α and the Failure Load

To determine the geometry of the forces of the truss model shown in Figure 4.12b, three quantities are of significant importance to consider. These are the failure angle α, the magnitude of the tensile force in the steel tie and the magnitude of resistance capacity of the concrete strut. With equilibrium satisfie in the vertical direction, the ultimate failure load can be determined by knowing any of the above two parameters. In the case of the corbel shown in Figure (4.13), α is predetermined because the loading points coincide with the conjunction of the steel tie and the concrete strut forces.

During the tests conducted in the structural laboratory of the University of Ottawa, the punch perimeter U_p at the bottom of slab of each specimen was measured. Therefore the angle α can be expressed as :

$$\alpha = \tan^{-1}\left(\frac{2\pi d}{U_p - u_o}\right) \qquad Circular \ \ slabs \tag{4.15}$$

or

$$\alpha = \tan^{-1}\left(\frac{8d}{U_p - u_o}\right) \qquad Square \ \ slabs \tag{4.16}$$

Other shapes of load area or slabs should be analyzed by means of equivalent circular or square areas.

The failure surface angle with respect to the horizontal plane depends on the geometry of the slab-column connection, the material properties and the applied load. This dependence is shown in Figure 4.18 where the test results of the

present work were used. An exponential curve was drawn to fit the experimental data. The suggested equation to determine theoretically the angle α is:

$$\tan\alpha = 0.73 - e^{(-K_p^{0.25})} \tag{4.17}$$

where

$$K_p = \frac{P_u}{\rho c d} \tag{4.18}$$

The above relation indicates that the angle α depends on ultimate punching resistance load P_u which in turn depends on the slab-column connections and the material properties. Also, it should be noted that as the effective depth of the slab increases, the failure surface angle and the ultimate load increase but not proportionally. The choice of the exponential function was based on the fact that maximum value of α is 36 degrees and α decreases as the ratio $\frac{P_u}{\rho c d}$ decreases but not linearly. Theoretically K_p is equal to zero only when P_u is zero, but in practice K_p will never reach zero and could be small only when the load is very small and the side dimension of the loaded area is big. However, most K_p values may be greater than 0.8. It should be noted also that the above equation is not valid for the case of a point load. Furthermore, equation (4.17) was determined from on the present experimental work. The ultimate punching resistance load can not determined theoretically based on equation (4.17) because it has two unknowns. Therefore another function relating P_u to f_{cc} is needed. This relation can be determined experimentally by measuring the strain of concrete at failure.

4.3.7 Summary

The tie and struts model is a powerful tool that can be used by structural engineers nowadays to model a slab-column connection. It explains the distribution

of the forces in any direction. The major difficulty in the model is determination of the failure surface angle. To date, no researcher has successfully used this rational model to explain the complicated failure mode of a slab- column connection. The only way to overcome the problem is to determine the critical stress at which the concrete struts at the column face can be expected to fail. Knowing this and the geometric dimensions of the slab-column connection, a relation between the surface failure angle and the applied load can determined experimentally.

4.4 Conclusion

Both theories presented above are important for background knowledge. The yield line theory gives an idea of the flexural behavior of a slab-column connection but it can not predict its ultimate punching shear load. However, in the case of under- reinforced slabs, punching shear failure of a slab can be governed by the yielding of the steel. Hence the punching shear failure load may be predicted by the yield line theory. Even though the truss model is considered to be an easy rational model that can be understood by most engineers, little success has been achieved to developed it. More experimental work on various slab-column connections with different geometry, and theoretical explanation is needed in future.

Table 4.1: Yield line theory predictions of the slabs test results

Slab Numb.	P_{test} (kN)	P_{yield} (kN)	$\frac{P_{test}}{P_{yield}}$
A1	176.S	290.4	0.61
B1	160.6	290.4	0.55
B2	150.4	139.2	1.07
B3	203.2	290.4	0.70
C1	200.0	301.9	0.66
C2	221.2	329.6	0.67
C3	211.5	329.6	0.67
C4	1S5.1	329.6	0.56
C5	163.5	301.9	0.54
C6	227.5	279.2	0.S1
C7	133.4	151.9	0.SS
CS	167.0	301.9	0.55
C9	200.4	301.9	0.66
C10	220.S	52S.9	0.42
C11	170.0	290.4	0.5S
C12	160.0	290.4	0.55
C13	190.0	312.0	0.61
Mean			0.65
Coefficient of variation			10.20

Table 4.2: Yield line theory predictions of the bridge test results

Position Line	P_{test} (kN)	P_{yield} (kN)	$\frac{P_{test}}{P_{yield}}$
Left deck			
2	90.0	91.2	0.99
3	101.2	91.2	1.11
4	87.0	91.2	0.95
Mid-deck			
1	63.6	147.0	0.43
2	106.2	153.2	0.69
3	139.8	153.2	0.91
4	106.2	153.2	0.70
Right-deck			
2	90.0	91.2	0.99
3	120.3	91.3	1.32

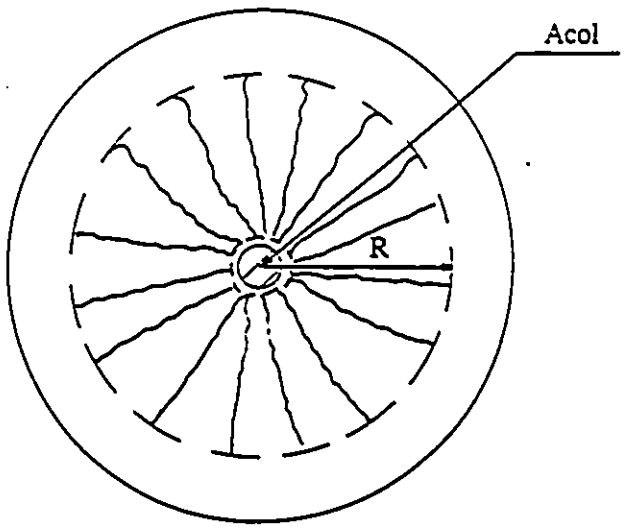

a- Circular Column

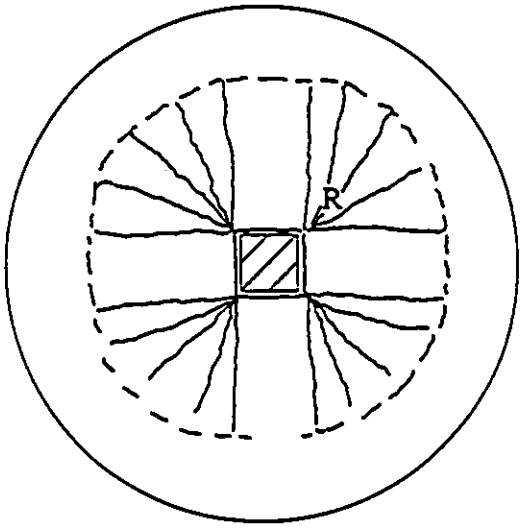

b- Square Column

Figure 4.1: Yield line pattern for symmetric punching

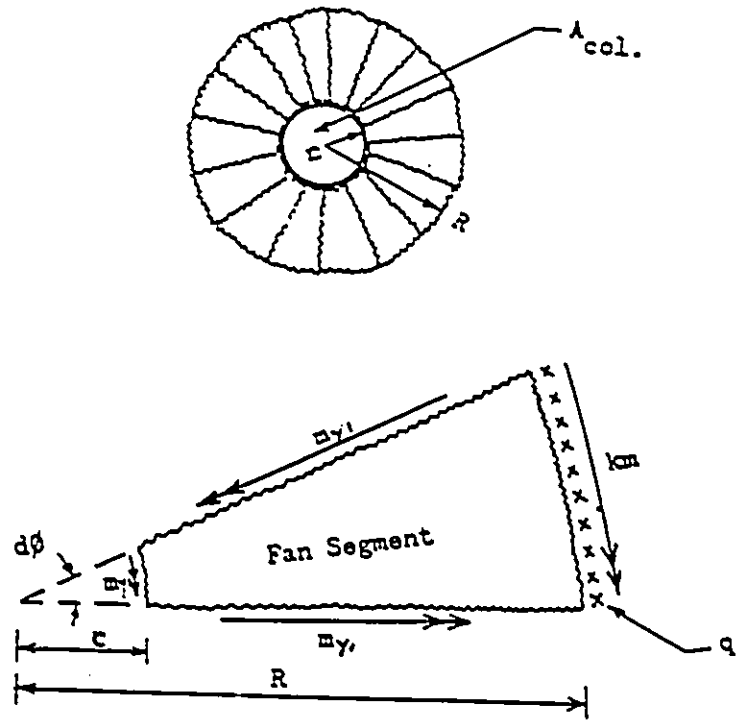

Figure 4.2: Yield line pattern for circular slabs

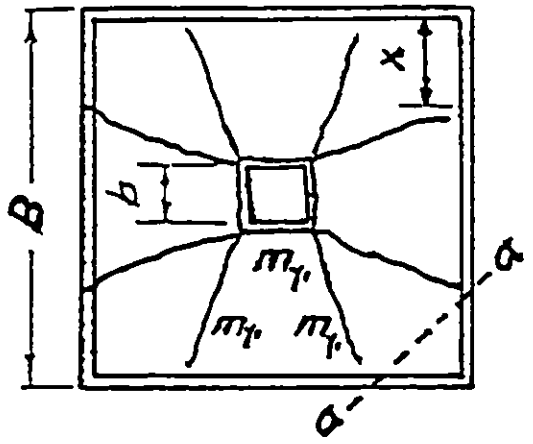

Figure 4.3: Yield line pattern for square slabs

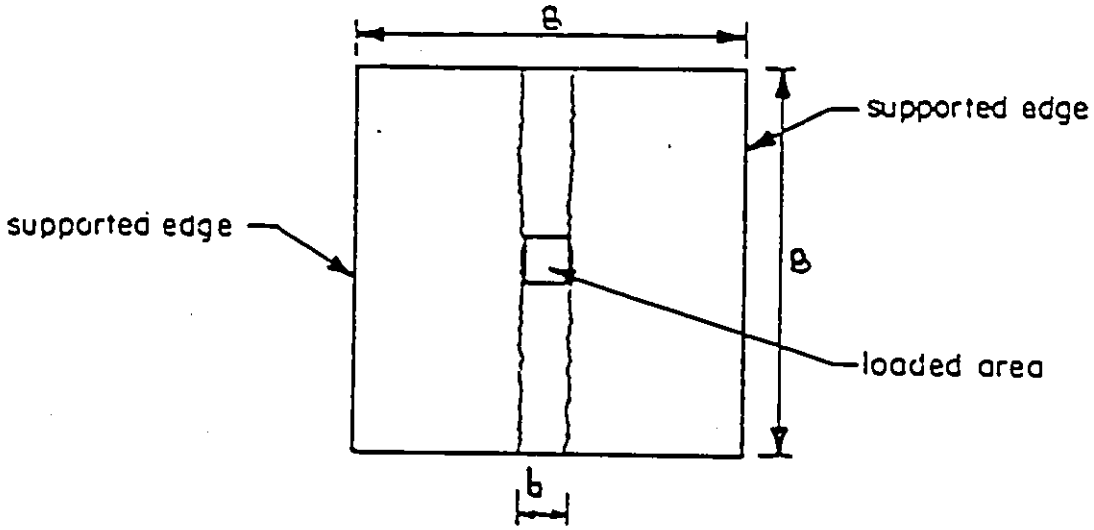

Figure 4.4: Yield line pattern for square slabs supported along their opposite edges

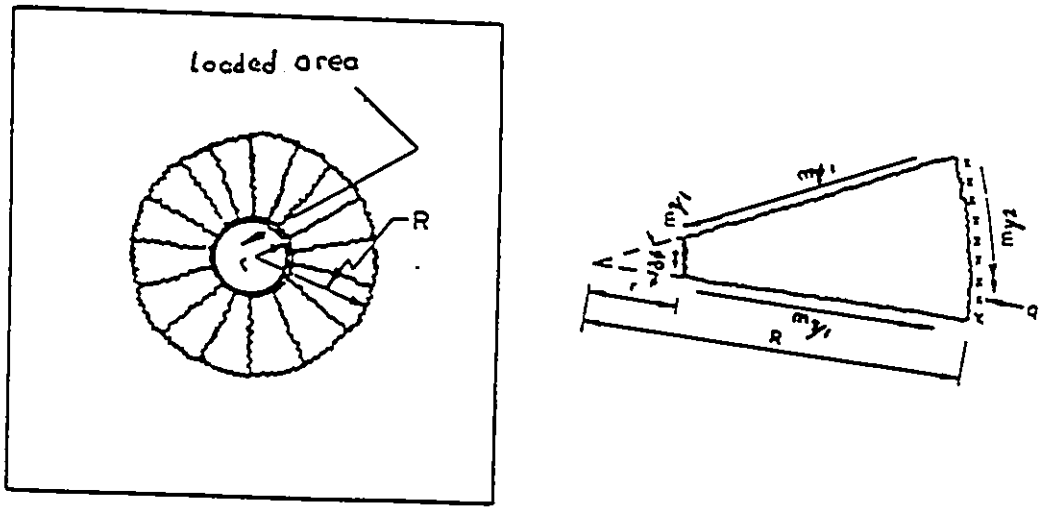

Figure 4.5: Yield line pattern for square and circular footing

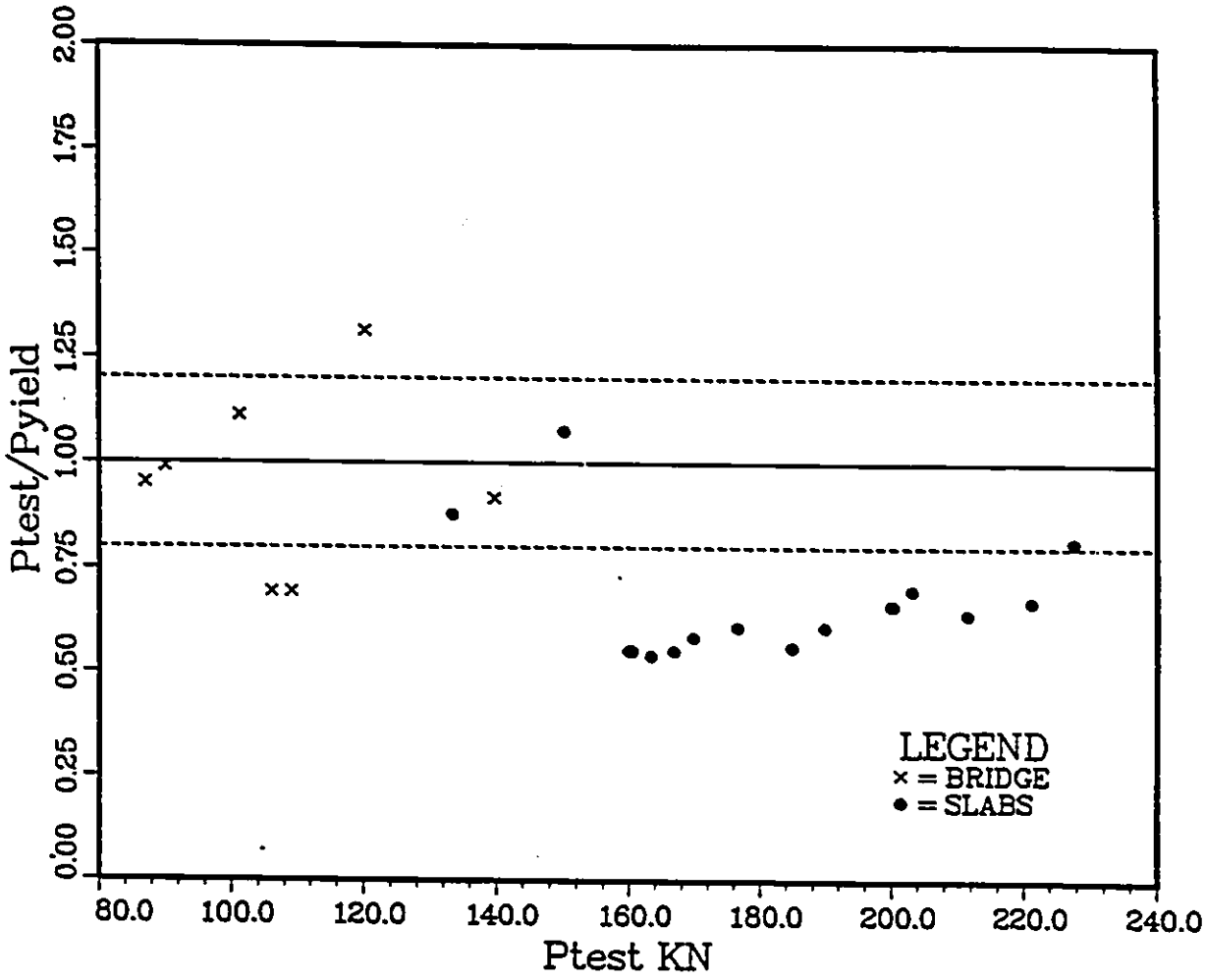

Figure 4.6: Yield line theory predictions of ultimate capacity of the bridge decks and the tested slabs

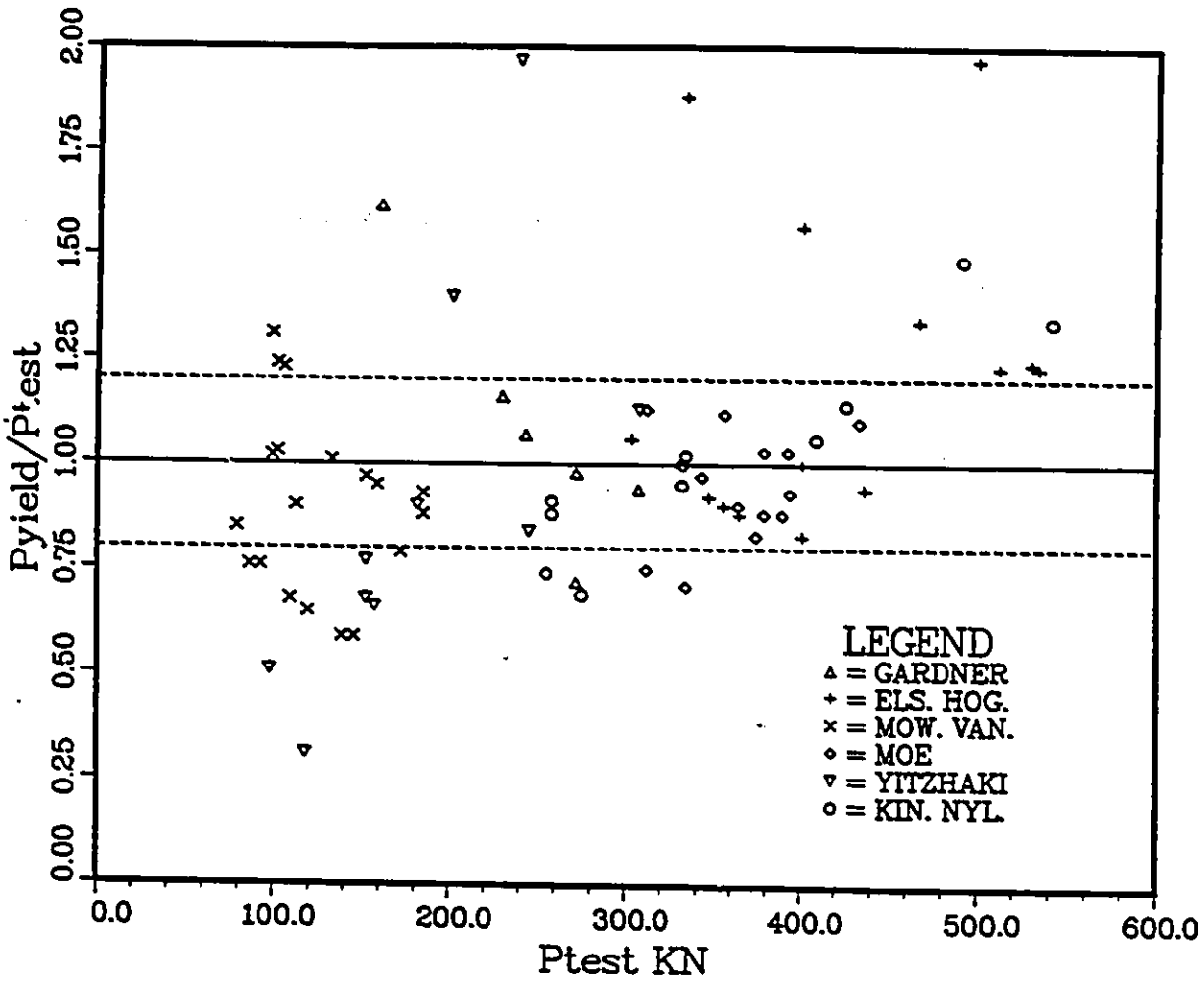

Figure 4.7: Correlation between the predicted values P_{yield} and the test results

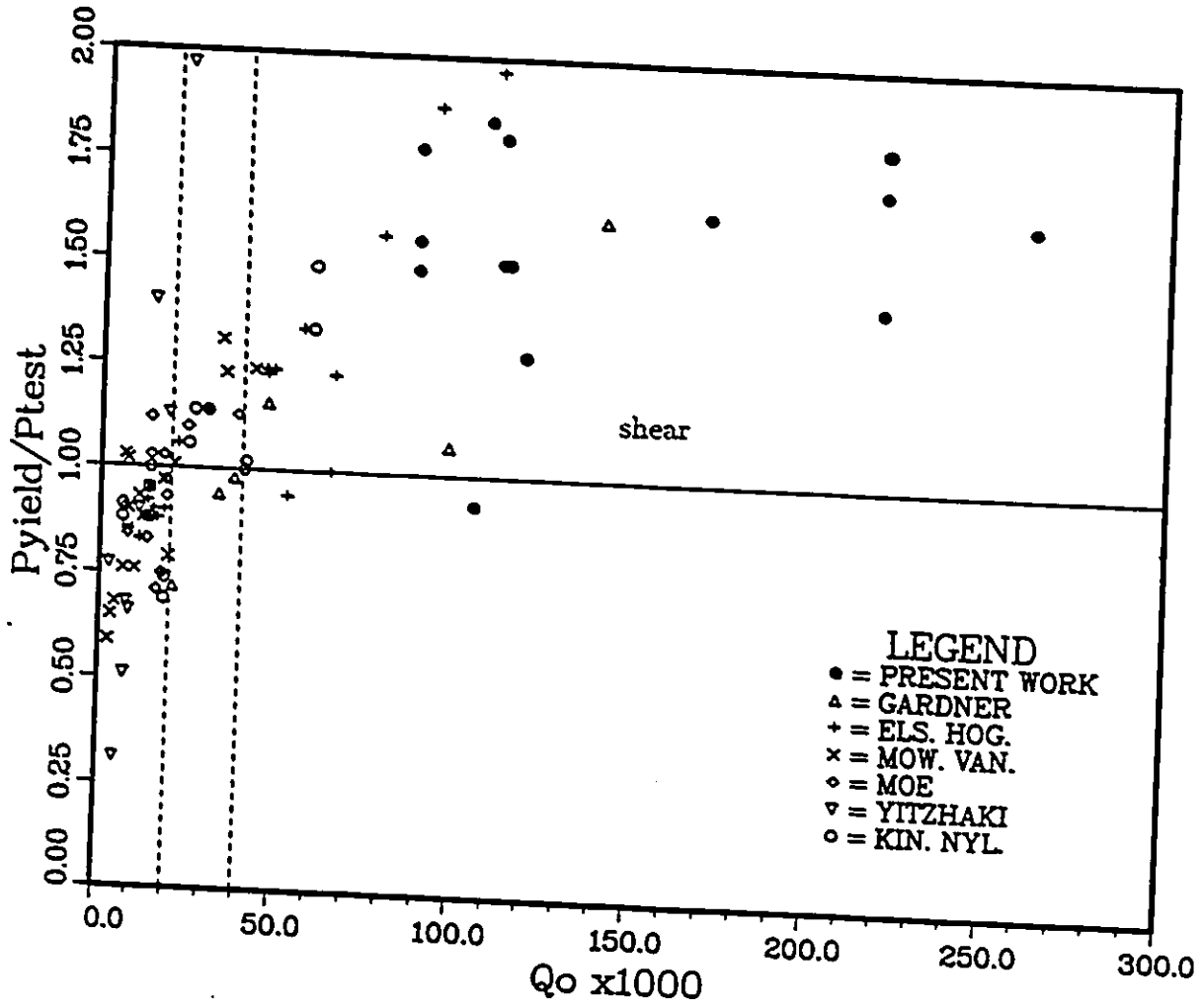

Figure 4.8: P_{yield}/P_{test} ratio versus Q_0 (equation 4.13)

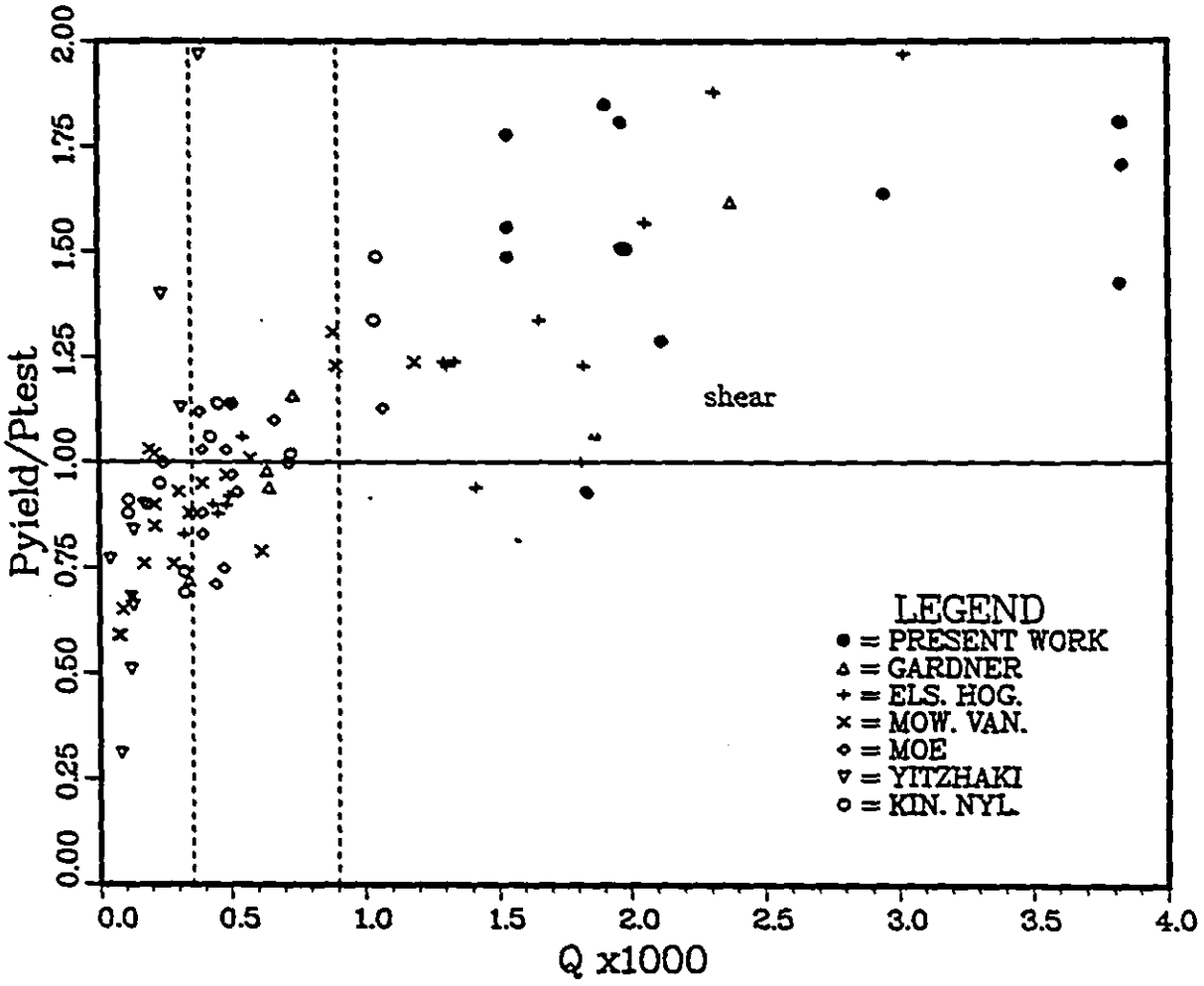

Figure 4.9: P_{yield}/P_{test} ratio versus Q (equation 4.14)

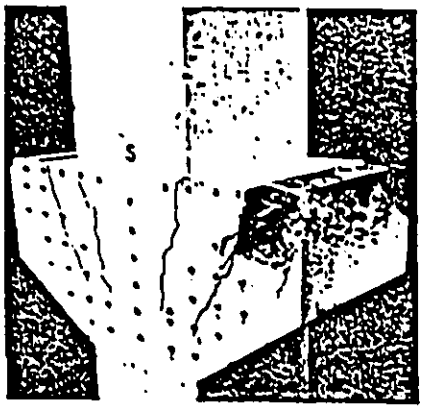

Figure 4.10: Reinforced concrete corbel after failure (after Cook)

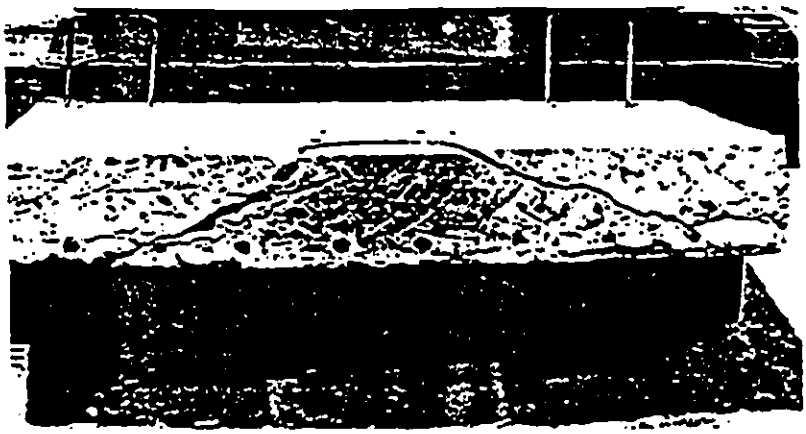

Figure 4.11: Cross-sectional view of slab C1 after failure

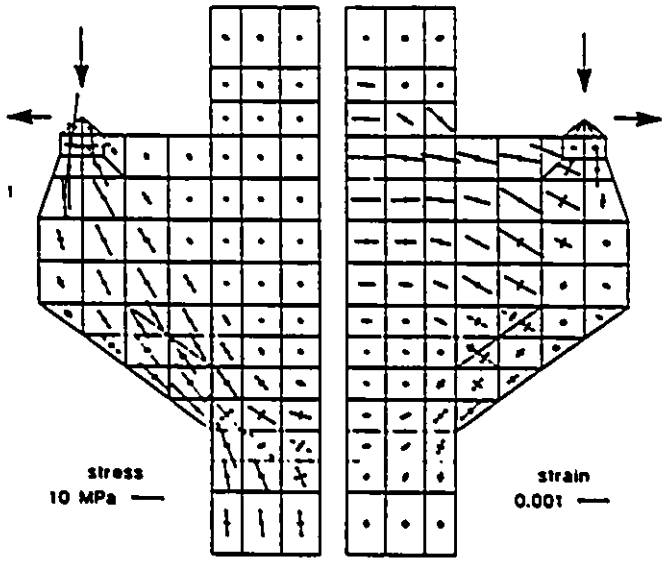

Figure 4.12: Predicted principal stresses and strains of a concrete corbel by non-linear finite element analysis

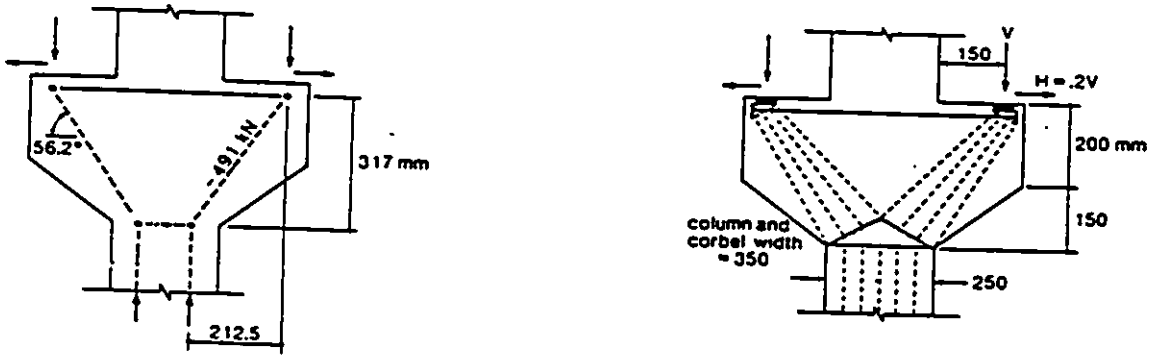

Figure 4.13: a) Strut and tie model b) Truss idealization

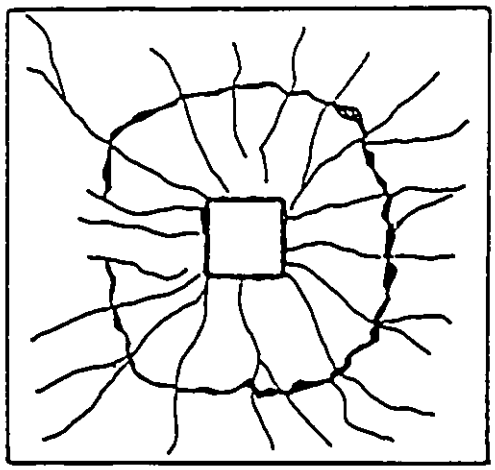

Figure 4.14: Typical punching failure of interior columns (after Van Dusen)

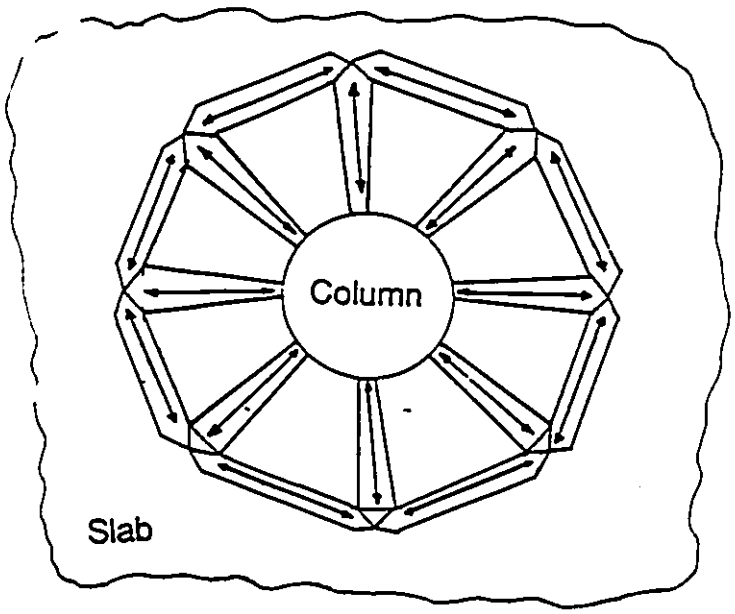

Figure 4.15: In-plane struts in an interior column-slab connection

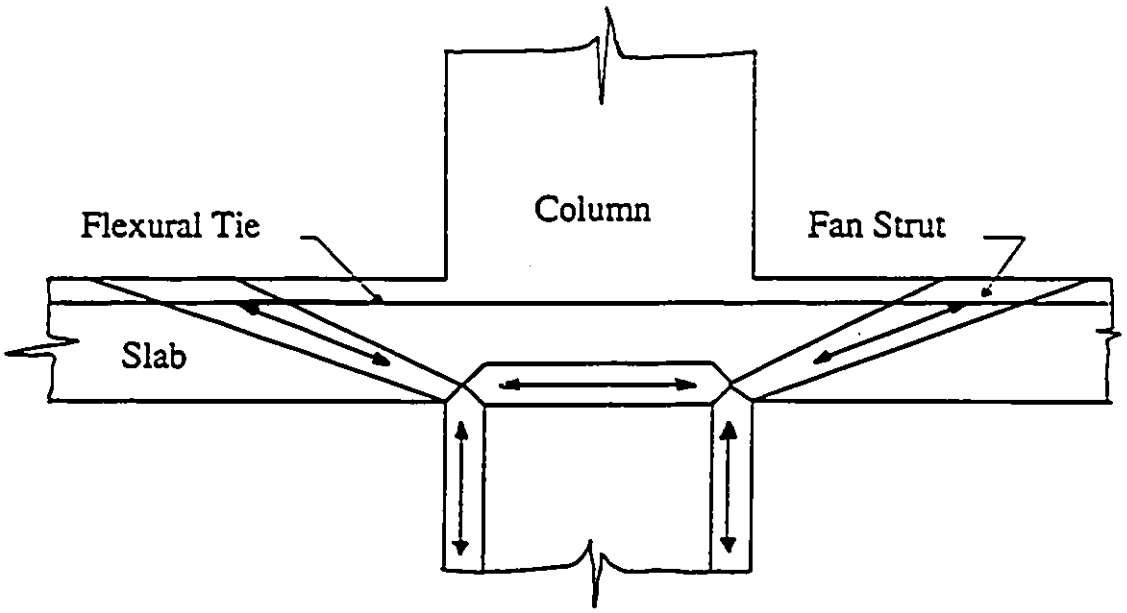

Figure 4.16: Out-of-plane struts in an interior column-slab connection

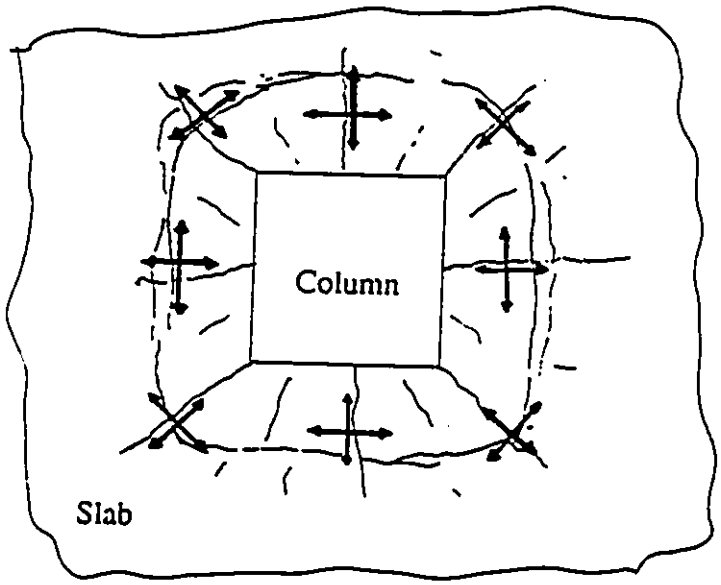

Figure 4.17: Plan view of the distribution of the forces in a square column connection

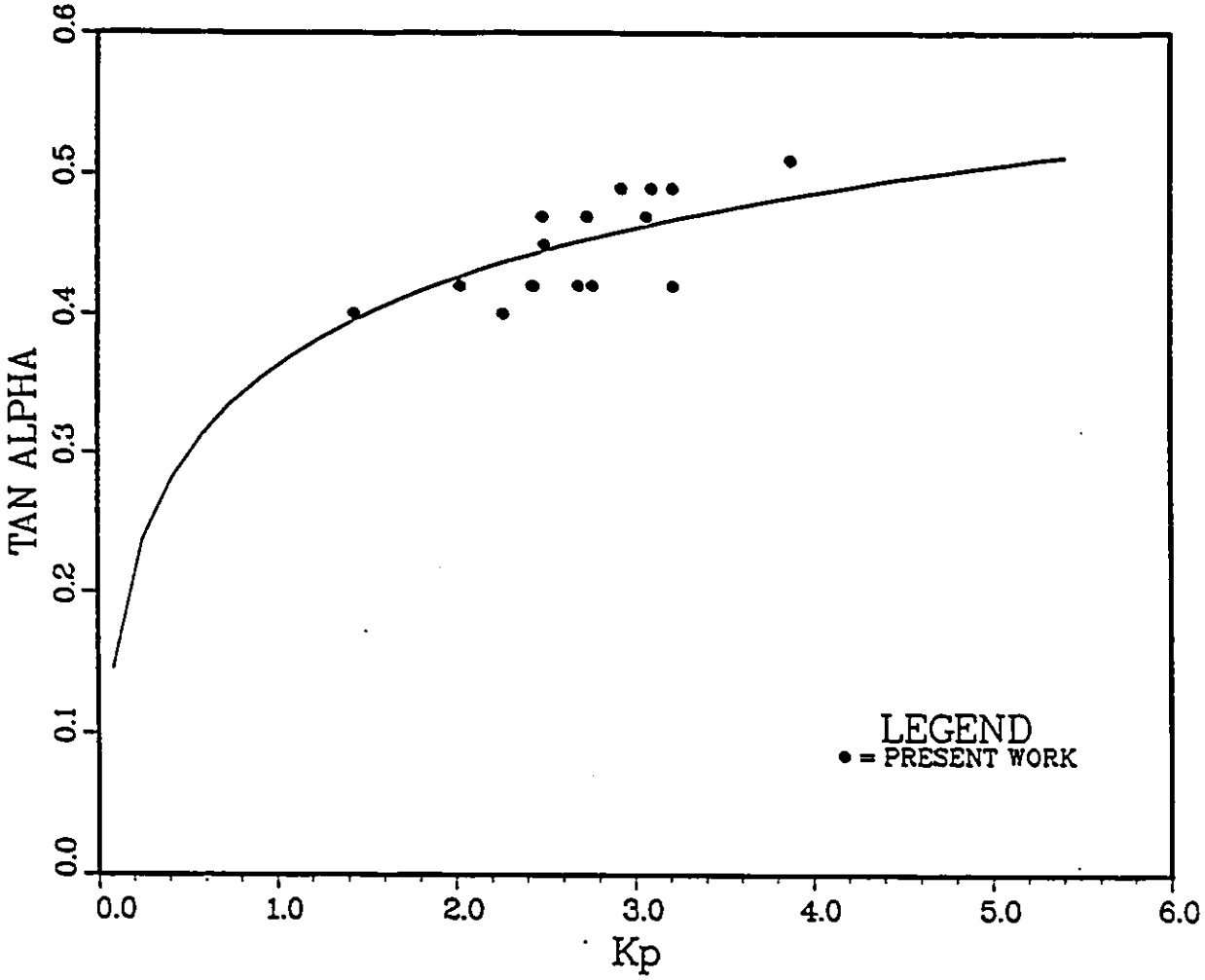

Figure 4.18: Tan α verus K_p

Chapter 5

Parametric Study

5.1 Introduction

Because of the lack of understanding of the punching shear failure mechanism, most researchers had difficulties in rationally modelling the phenomenon. In fact, many empirical procedures have been developed for the prediction of the ultimate punching resistance load of a slab-column connection. These procedures were based on assumptions which are reliable only over the limited range of data for which they were calibrated. However, most current codes uses empirical equations for punching shear design because of their simplicity. But these empirical equations do not explain the failure mechanism and sometimes are very conservative in their predictions. In this chapter, the behavior of slabs at cracking under punching load is explained and a consistent empirical study taking consideration of the effect of all the parameters of a column-slab connection is proposed to help the designer to visualize the failure mechanism. A comparison of the proposed equation with four codes with respect to critical parameter is presented.

5.2 Failure Mechanism

Before studying the effect of each parameter of a slab column connection on punching shear resistance, a theoretical explanation of the failure mechanism is needed. The description of this phenomenon is based on the observations during the tests carried out in the structural laboratory at the University of Ottawa and on the reports in the literature by previous investigators.

When a simply supported slab is loaded in the center through a bearing plate, it may behave in two different ways: ductile or brittle behavior. The first type of behavior is characterized by large deflections and excessive longitudinal cracks on the tension face of the slab. All the reinforcement crossing the column-slab connection reaches the yield stress point near the column faces. The second type of behaviour is characterized by less deformation prior to failure than in flexural failures, by the violence of the failure and by the sudden drop in resistance from the peak load. This type of failure is referred to as punching shear; the mechanism of which will be described in detail hereafter.

When the load is applied on the top of a simply supported slab, the center deflection of the slab underneath the loaded area increases linearly with the load. At about 50 to 60 % of the ultimate load, tangential flexural cracks occur at a distance from the slab center approximately equal to the radius of loaded area. Then radial cracks develop starting at the tangential crack along the circumference of the loaded area. These cracks spread, so that the slab is divided into radial segments. As they extend, more tangential cracks develop outside the circumference of the loaded area. As the load increases, a first flexural crack running in a tangential direction appears, at a distance from the circumference of the loaded area which may be greater than, or equal to, the thickness of the

slab. This crack may be regarded as the first shear crack as Kinnunen and Nylander [37] reported. Once the shear crack appears, more flexural cracks form around the periphery of the loaded area and the radial cracks extend as the center deflection of the slab increases with increasing load. The shear cracks (longitudinal direction) increase in depth vertically, but when they reach the flexural reinforcement, which will carry part of the shear forces thereafter, they deviate from their initial direction to be inclined along the steel reinforcement plane. Experimentally, it is not possible to determine a completely unique value of the shear cracking load; i.e., the load at which the shear cracks begin to open up. It is note worthy that, punching failure does not occur when an inclined crack is formed. However, under the load the compressive zone in the vicinity of the column faces undergoes variable compressive stress states. At locations very close to the load area peripheries the stress state is believed to be triaxial with the minor principal stress σ_3 being very small. At critical locations adjacent to the triaxial stress state locations, σ_3 disappears and a biaxial compressive stress state may occur. In most tested slabs, the compressive strain of the concrete close to the loaded area in a radial direction decreases as the applied load approaches the ultimate and even some can be converted into tensile strain [31]. Just before failure, a final shear crack in the tension side, coinciding with, or located outside the most distant (from the loaded area periphery) tangential crack will be formed. The slab portion outside this shear crack is practically a rigid body during deformation. As the last shear crack increases in depth, the thickness of the compression zone, in which the vertical component of the principal stresses is acting, decreases. The opening of the shear cracks indicates that the concrete has failed in splitting and part of the shearing forces in the tension side will be taken by the steel reinforcement. It is a well known feature of punching shear that failure occurs before the ultimate strength of the reinforcement is reached or even without occurrence of any yielding of the steel reinforcement. Hence it

is believed that failure may be attributed to the increase in depth of the shear crack which leads to decrease of thickness of the compression zone. In spite of such, the average thickness of the compression zone was measured by Kinnunen and Nylander [37] to be 0.3d. Once the principal stress reaches a certain values (greater than f_{cc}) a very small crack may initiate near the column faces. This will lead to the loss of the confinement of the triaxial compressive state which can no longer be sustained nor redistributed. All of a sudden, failure occurs and the resistance drops markedly as more load is applied. After the initial failure, the deflection increases dramatically and the concrete cover torn away along the plane of flexural steel at the outside of its intersection with the inclined failure surface.

5.3 Punching Shear Resistance Equation

In order to derive an empirical equation for punching shear resistance, it is of interest to study the parameters upon which interior column-slab connections depend.

It should be noted that after the author's experimental results described in Chapter 3 were completed, the data were added to the original data selected from the literature. The derivation of the equation (5.8) was based on the original data.

5.3.1 Critical Section and Failure surface

The critical section worried many researchers in the past, and it is still a key point to determine the ultimate punching load. The nominal punching shear stress is usually calculated by dividing the failure load by the cylindrical area of a chosen

control surface. In fact, the choice of a critical perimeter u differs from one design code to another. All the existing codes consider that the critical perimeter , upon which the nominal punching shear stress depends, is a function of the loaded area shape and the effective depth only. The British code (BSS110-S5) states that the critical perimeter should be at a distance 1.5 times the effective slab depth d outside the column. Its shape should be a square whether the load is circular or square. However the North American codes suggest a perimeter much closer to the loaded area. This perimeter u follows the shape of the loaded area at a distance (0.5d) from its peripheries.

Usually, the punching shear load is defined as the nominal shear stress multiplied by a projected area of the failure surface which has the shape of a cone. The angle α between the failure surface and the slab plane was not well studied by previous researchers. To have correlation with test results, Regan [52] choose α equal to 22 degrees ($\cot\alpha = 2.5$), and calculated the area of the failure surface A_c (See Figure 5-1) to be:

$$A_c = d\sqrt{1+\cot^2\alpha}(u_0 + \pi d\cot\alpha) \tag{5.1}$$

where u_0 is the perimeter of the column and d is the effective depth of the slab. The failure area surface given by the equation 5.1 differs from that of current codes of practices which consider it as the product of the slab depth and a nominal critical perimeter. The suggested change gives the designer a better picture of what is involved and should help to avoid some of the mistakes which can be made when the critical perimeter approach is used blindly. The new approach makes possible the rational treatment of various cases which can not be dealt with satisfactorily by present code methods. These include slabs of variable depth and slabs with shear reinforcement where failure may occur between a column and the inner most shear steel. However, it was observed during tests of simply supported slabs that the failure angle could go up to 30 degrees. Thus it is better to choose

an average angle α of 26 degrees ($22 < \alpha < 30$ degrees). Moreover, any shape of loaded area can be replaced by a circle having an area equal to the original one. Therefore equation 5.1 can be written in simple way:

$$A_c = 2.2\pi(c + 2d)d \tag{5.2}$$

where c is the diameter of the equivalent circle of the loaded area. A square column is replaced by circular one, having a diameter c equal to the side length of the original. This reduction in area is because square columns resist less load than circular ones as test results showed (Chapter 3). The choice of the above failure area surface is based on an assumption that the columns or loads are widely spaced. In the case of bridges, where edge bearings and intermediate supports are usually relatively close together, with respect to the slab depth, design punching surfaces can intersect. So the design perimeter should be modified and the failure surface A_c should be decreased by a factor ($\frac{1.8d}{a_v}$), where a_v is half distance between two supports ($a_v < 1.8d$).

5.3.2 Concrete Strength

In many countries, the basic concrete strength parameter is the uniaxial compression strength f_{cc}, determined from tests of standard $150mm \times 300mm$ cast cylinder after 28 days of moist curing. The cube strength f_{cu} is found from standard 150mm test cubes. To relate the compressive strength f_{cu} to f_{cc}, Hewitt and Batchelor (34) suggested the following equation:

$$f_{cu} = \frac{f_{cc}}{0.75 + 0.000025 f_{cc}} \qquad (psi) \tag{5.3}$$

Equation (5.3) is an approximation of a curve that relates f_{cu} and f_{cc} given by Evans. For general use, it is suggested to take $f_{cu} = 1.25 f_{cc}$.

The strength of concrete is affected by the cement water ratio, the bond between the aggregate and the cement paste, and by the moisture conditions during curing. Also, it depends on the shape and the density of aggregate. In fact as reported in the literature [41], beams and one way-slabs failing in shear showed decreases of strength of 20% for lightweight aggregates compared to normal density aggregates.

Many researchers believed that punching shear failure is caused by the failure of concrete in tension. However, knowledge of the relation between the tensile strength and the compression stress of concrete is still limited. The tensile strength of concrete varies between 8% and 15% of the compressive strength. Although the tensile strength of concrete increases with an increase in the compressive strength, the ratio of tensile strength to the compressive strength decreases as the compression strength increases (See Figure 5.3). Thus, some researchers suggested that the tensile strength is approximately proportional to the square root of the compressive strength. However, recent research shows that the tensile strength depends on a power of f_{cc} greater than 0.5. Zhao [69] found this power to be equal approximately to $\frac{2}{3}$, which used by most of the European codes.

To derive his punching resistance equation, Moe [44] used the square root relationship because he believed that shear failure is to be controlled by the tensile strength which was generally assumed to be proportional to $\sqrt{f_{cc}}$. To check the relationship between the punching resistance of reinforced concrete flat slabs and the concrete strength, slabs having constant effective depth and constant side length of loaded area (b for square and c for circular) were analyzed. Assuming that the ultimate shear stress is proportional to the fourth root of the ratio of flexural reinforcement ($v_u \propto \rho^{\frac{1}{4}}$), a relationship between the compressive strength of concrete and the punching shear resistance of a column slab joint

can be established. This relationship is shown in Figure 5.4 and 5.5 where the least square fitting curves were drawn. From these Figures, it can be seen that there is not much difference between the two relationship. However, the cube root relationship shows a reasonable overall agreement.

5.3.3 Flexural Reinforcement

While it is generally agreed that flexural reinforcement has an effect on the shear strength of slab-column connection, some analytical procedures neglect it. Investigators such as Yitzhaki [66] suggested that the ultimate shear stress of slabs v_u should be calculated by flexural analysis. In these equations, v_u is primarily a function of the ratio of flexural reinforcement times its yield strength ($v_u \propto \rho f_y$). However Moe [44] suggested a design equation that depends only on the square root of the concrete compression strength ($\sqrt{f_{cc}}$) and the ratio of the side length of loaded area to slab thickness ($\frac{c}{d}$). His idea was based on the fact that the concentration of reinforcement within a band approximately 0.5d either side of the column did not increase the punching strength. In fact, strength decreases by roughly 6% compared with those for slabs with uniform steel. This does not mean that the shear is effectively independent of ρ within the column area. Moe's findings could be attributed to the large quantity of reinforcement present. The lowest reinforcement ratio of 1.06% and the highest of 3.45% used by Moe can be compared to the lower limit of 0.8% suggested by CEB-FIB code [12] or 0.5% by Gardner [25]. In fact, Gardner tested some specimens with zero steel and others with steel ratio less than 0.5%. These specimens failed in flexure indicating that punching shear is not critical for unreinforced slabs and it is affected by the flexural reinforcement. An appropriate layout of tensile reinforcement can improve the shear strength and optimize the flexural behavior of the slab in the service

load range. So an increase of tensile reinforcement would increase the depth of the compression zone of concrete and thus the area of non-cracked concrete available to resist the shear. It would reduce the width of cracks, thus improving the transfer of forces by aggregate interlock, and would also increase the dowel action. The high strains in the periphery of the loaded area may lead one to consider placing reinforcement in order to make full use of its ductility.

There is some difficulty in the definition of ρ, as the width of slab to be used in its calculation has to be specified. It is better to calculate ρ for the full width of the effective transverse slab strip, that is a width approximately equal to the slab breadth when there is a single central support. Even though there is a difference between ρ within the slab-column connection and ρ in the slab far away from the column, the difference in the values of the punching resistance load P_u will be very small because P_u is function of the forth root of ρ. This conclusion agrees with test results of two-way slabs done by Moe [44], and Elstner and Hognestad [20]. However Regan suggested it would be probably be appropriate to calculate steel ratios for column strips only and not full column-to-column widths.

Practically it is too hard to get a smooth distribution of reinforcement in x and y directions. In the case of an unequal orthogonal reinforcement, the expression of ρ can be obtained by the simple average and it would not give rise to any serious errors.

$$\rho = \frac{\rho_x + \rho_y}{2} \tag{5.4}$$

However, some researchers suggested the square root relationship.

$$\rho = \sqrt{\rho_x \rho_y} \tag{5.5}$$

The difference in formulations is insignificant.

Figure (5.6) shows $\left(\frac{P_{exp}}{(\frac{f_{cc}}{d})^{\frac{1}{3}} A_c}\right)$ plotted against the ratio of flexural reinforcement

for tests done by Elstner and Hognestad [20], Gardner [25] and Moe [44]. It can be seen that the use of forth root function is more convenient than the cubic root and it is consistent with test results.

The limit amount of reinforcement required for slab-column connection is based on the concept of balanced failure where the concrete crushes and the steel yields. When the reinforcement is in excess of this amount the failure is always governed by crushing of concrete, whereas in the opposite case the failure is governed by the yielding of the steel which results in a more ductile connection.

The influence of the provision of compression reinforcement has not been clearly dealt with by researchers. Elstner and Hognestad [20] believed that compression reinforcement has a negligible effect. However, Neth, de Paive and Long [49], observed significant strain jumps in compression reinforcement upon yielding of the tension reinforcement, which may indicate that this reinforcement does play a significant role in preventing crushing of the concrete. In fact when compression steel is properly detailed, it could act as a suspension net, supplying an alternative load path that hold the slab together even after a punching failure as recommended by the Canadian code CSA A23-3M [11]. Since the width of the punching area at the compression side of the slab is much smaller than the tension side, it is likely that the effective number of compression bars are less than the tension ones. So, the compression steel is less effective than the tension steel. The ratios of compression steel vary usually from 0.3 to 1 times the ratios of tension steel and the maximum increase of punching resistance is only 12% as reported by Regan [51].

The yield strength of flexural reinforcement f_y was used by many researchers as a parameter defining the punching resistance. It can be expected to have some influence at least where some of the steel yields before failure. In practice the

influence of f_y can be neglected. The evidence is that Moe [44] tested similar slabs having steel with a yield strength of 330 MPa in one set and 480 MPa in the other, and there was no difference between the punching strengths obtained.

5.3.4 Scale Effect

It is well known that in beams and one way slabs without shear reinforcement, the ultimate nominal shear stress ($\frac{P_u}{bd}$) decreases with increasing depth, if other parameters are kept constant. The same phenomenon has been shown for two way slabs. In Figure (5.7), values $\left(\frac{P_{test}}{A_c \rho^{\frac{1}{4}} f_{cc}^{\frac{1}{3}}}\right)$ are plotted against d. Both cube and fourth root functions give a reasonable overall correlation. The fourth root is preferred to be used by Regan [51]. Some empirical equations for the ultimate punching shear resistance include the column size-slab depth ratio ($\frac{c}{d}$). The relation between $\left(\frac{P_{test}}{A_c \rho^{\frac{1}{4}} f_{cc}^{\frac{1}{3}}}\right)$ and ($\frac{c}{d}$) is shown in Figure(5.8). The solid line drawn represents $v_u \propto (\frac{c}{d})^{\frac{1}{3}}$ and fits the data well. However, other researchers used the fourth root function. Simmonds and Alexander (4) got the relation ($P_u \propto (\frac{c}{d})^{\frac{1}{4}}$) by trial and error.

5.3.5 Equation

As described previously, the punching shear resistance of reinforced concrete flat slab-column connection depends mainly on the concrete strength, flexural reinforcement and geometry of the connection. Therefore a general equation can be written in terms of the simplest possible parameters.

$$\frac{P_u}{A_c} = v_u = k\rho^l {f_{cc}}^m d^n \tag{5.6}$$

where A_c is the failure surface determined by equation (5.2). The $(\frac{c}{d})$ fraction was not considered in the equation, because it is believed that when $(\frac{c}{d}) > 1$, it will not have an effect on the punching shear resistance (see Figure 5.8). However, when $(\frac{c}{d}) < 1$, which is not the case in practice, errors that may anticipated will be in the conservative side.

Applying the logarithmic function, equation (5.6) becomes:

$$\ln v_u = \ln k + l \ln \rho + m \ln f_{cc} + n \ln d \tag{5.7}$$

77 reinforced concrete flat slabs, tested by previous investigators were selected for the analysis. By statistical analysis, the values of the parameters in the equation 5.7 were found to be: $k = 5.21$, $l = 0.26$, $m = 0.33$, $n = -0.29$. To make these parameters more convenient in practice, it is better to modify them in form of fractions; that is : $l = \frac{1}{4}$, $m = \frac{1}{3}$, $n = \frac{-1}{3}$. Thus a general equation can be written as follows:

$$P_u = k A_c \rho^{\frac{1}{4}} f_{cc}^{\frac{1}{3}} d^{\frac{-1}{3}} \tag{5.8}$$

Considering the new parameters, k can be determined using this average equation:

$$k = \frac{1}{n} \sum \frac{P_u}{A_c \rho^{\frac{1}{4}} f_{cc}^{\frac{1}{3}} d^{\frac{-1}{3}}} \tag{5.9}$$

where n is the number of specimens.

The constant k depends on the kind of concrete, and the arrangement of reinforcement. To determine k for isotropic flexural reinforcement, 77 slabs were chosen for normal weight concrete and 13 slabs for lightweight aggregate concrete. The values of k were found to be 4.61 and 3.69 respectively. For slabs with radial and circular reinforcement arrangement, the value of k was found to be 4.00 about 13% less than the isotropic reinforcement. However, when the slab is circularly reinforced, its resistance to punching shear reduced by 30% compared

to the two way reinforced slabs. The value of k was found to be equal to 3.14. The different calculated values of k from different tests, the mean, the standard deviation, and the coefficient of variation values of the ratio of the experimental failure load to the calculated punching resistance load using equation (5.8) are shown in Table 5.1.

5.3.6 Calculations

The calculated and the test result values of the punching shear loads for the present experimental investigation are shown in Table 3.2. The calculation of the ultimate punching load is based on the equation (5.8). The ratio of the test failure load to the calculated ultimate load is 0.94 for slab B2 which was not expected. This can be explained by the fact that the equation takes the effect of the reinforcement on the tension side only. Since B3 had failed in flexure, it is obvious that the punching failure load is greater than the predicted one due to the greater gross thickness.

In the calculation, the effect of load area shape was considered by replacing any area shape by a circle having the same area as the original. For slab C5, the calculation showed that the cycling effect reduced the punching shear capacity of a slab by about 20 percent. However when the reinforcement ratio decreased by half in slab C7, the failure load is low compared to the predicted one. This can be explained by the fact that the spacing between the steel is greater than the diameter of the loaded area. Hence the calculated value of the reinforcement ratio is not precise since it is hard to calculate how many bars cross the critical section. Based on the theoretical calculation, the different cross-section shapes of the reinforcing steel used in slabs C7 and C8, had no effect on the punching

shear capacity which contradicts the experimental work. The average ratio of the predicted to test load is about 0.96 for the tested slabs.

Figure 5.9 shows the ratios of the failure test load P_{test} of 90 slabs to the predicted ultimate punching failure load P_u using the equation (5.8) plotted against P_{test}. Two horizontal dotted lines were drawn at values of P_{test}/P_u ratio equal to 0.85 and 1.15 to limit the interval of "goodness" of the results. It can be seen from the Figure that distribution of the points is random. Also, only few points are outside of the tolerance which endorse the precision of the suggested equation.

5.4 Codes of Practice

5.4.1 General

The mechanics of shear failure in reinforced concrete slabs were not well understood in the past. Around the mid of the twentieth century, the calculation of the punching shear resistance was based on one of the two theories: The first one is to consider the zone around the column as a circular simply supported slab, concentrically loaded on the middle. A punching failure occurs when the shear stress in a determined critical section reaches a limited value fixed based on the observation done during experimental tests. The second theory is to transform the punching shear problem of flat slabs to the shear of reinforced concrete beams. Therefore, the method of equivalent frame was used. The frame is formed by columns and a strip of slab in which the effective width is determined empirically.

Until 1960, most of the existent codes were based on the first theory, but the

second one was used by a few codes such the German one (DIN 1045). At that time, the punching shear test results reported by Moe, Kinnunen and Nylander forced many countries to revise their codes and to consider the punching as a specific problem for flat slabs.

5.4.2 Equations

In view of the complexities and many parameters involved, codes of practice express shear capacities in terms of nominal average shear stress acting over nominal cross-sectional areas. All the codes, currently consider shear in reinforced concrete slab at the ultimate limit state. For the following code equations, the notation used is as follows:

c : Diameter of a circular column or loaded area (mm).

b : Side dimension of a square column or loaded area (mm).

d : Mean effective depth of slab (average of effective depths in orthogonal directions) (mm).

f_{cc} : Cylinder crushing strength of concrete.

f_{cu} : Cube crushing strength of concrete.

h : Overall thickness of slab (mm).

u : Length of control perimeter (mm).

u_0 : Length of periphery of loaded area (mm).

P_u : Punching resistance load (N).

v_u : Punching shear resistance (stress) (MPa).

γ_m : Partial safety factor for resistances or materials.

Φ : Partial safety factor for resistances.

ξ_s : Size or depth effect factor.

ρ : Ratio of flexural reinforcement.

BS 8110-85

$\rho = \frac{\rho_x + \rho_y}{2}$, $\gamma_m = 1.25$

$v_u = \frac{0.79}{\gamma_m}(100\rho)^{\frac{1}{3}}(\frac{f_{cu}}{25})^{\frac{1}{3}}(\frac{400}{d})^{\frac{1}{4}}$

$u = 4(c + 3d)$ for circular loaded areas.

$u = 4(b + 3d)$ for square loaded areas.

$P_u = v_u ud < 1.2\sqrt{f_{cu}} u_0 d$

ρ is calculated for a width equal to(c+3d) or (b+3d).

CP 110-77

$\rho = \frac{\rho_x + \rho_y}{2} < 0.03$

$v_u = 0.27(100\rho f_{cu})^{\frac{1}{3}}$

$\xi_s = 1.6 - 0.0021h > 1.0$

$u = \pi(c + 3h)$ for circular loaded areas.

$u = 4b + 3\pi h$ for square loaded areas.

$P_u = \xi_s v_u ud$

ρ is calculated for a width equal to(c+6h) or (b+6h).

ACI 318-89

$v_u = \Phi(0.083\beta)\sqrt{f_{cc}}$, $\Phi = 0.7$

$\beta = 2 + \frac{4}{\beta_c}$ β_c is the ratio of longer to shorter dimension of the loaded area.

$u = \pi(c + d)$ for circular loaded areas.

$u = 4(c + d)$ for square loaded areas.

$P_u = v_u ud$

CEB-FIP-78

The model is prepared by the Comite Euro-International du Beton(CEB) and the Federation International de la Precontrainte (FIP). The ratio of flexural reinforcement is calculated for a width of (c+5d) or (b+5d).

$\rho = \sqrt{\rho_x \rho_y}$, $\gamma_m = 1.5$

$v_u = \frac{0.084}{\gamma_m}((1 + 50\rho) f_{cc})^{\frac{2}{3}}$

$\xi_s = 1.6 - 0.001d$

$u = \pi(c + d)$ for circular loaded areas.

$u = 4b + \pi d$ for square loaded areas.

$P_u = \xi_s v_u u d$

5.4.3 Comparison Between the Code Provisions

Looking at the codes formulas, one can notice that the control perimeters used by both British codes are larger compared to the ACI and CEB codes. The latter have perimeters much closer to the loaded area (see Figure 5.10). The significant difference between these documents are:

• In BS8110 the control perimeter has square corners whether the loaded area is square or circular, whereas the CP 110 and CEB perimeters have rounded corners in all cases. In ACI code, the control perimeter is taken to have the same shape as the loaded area.

• In BS 8110, the ratio of flexural reinforcement is calculated for a width of slab equal to that of the loaded area plus 1.5d to either side of it, while in CP 110 the width is that of the loaded area plus 3h each side. In CEB code, this width is equal to (B+5d) or (b+5d) breadth of the slab. For the ACI code, the limiting

shear stress depends only on the concrete strength.

• The range of slab depths over which a size effect is considered on punching resistance in BS S110 is $100mm < d < 400mm$ while in CP 110 the corresponding limits are $150mm < h < 300mm$.

For the calculation of shear, all codes assume that it is uniformly distributed over the slab depth and all along the critical perimeter. The function for the calculation of the ultimate nominal punching stress depends on parameters that differ from code equation to another. Test results showed that certain parameters, such as the compression strength of concrete, the geometry of a slab column connection and sometimes the flexural reinforcement, have an effect on the punching shear resistance. Based on some theoretical considerations that essentially support the equilibrium condition in the vertical direction (for example $\sum V = 0$) and observations made during tests, empirical formulas were derived. The results obtained are adjusted to those of tests by statistical methods. This way of proceeding has the advantage of being simple and rapid and gives the numerical values that corresponds very well to those measured during the tests. However this method does not contribute to the understanding of the punching shear phenomenon and can lead to a wrong interpretation of the behavior of a slab-column connection.

5.4.4 Comparison with Test Results

To compare with the predictions by the code equations, 77 slabs tested by previous investigators and 12 slabs tested by the author were selected. For the purposes of making comparisons with test results, safety factors Φ and γ_m have been removed from the code equations to give expressions for characteristic resistances.

Tables 5.2 to 5.5 show the values of the mean, standard deviation and the coefficient of variation of the ratio (P_{test}/P_u) for different test results using the four code equations. The lowest overall mean was found to be 1.0 for the BS S110 code, whereas the highest is 1.51 for the ACI code. The highest coefficient of variation was found to be 0.22S for the ACI code also. The BSS110 code has the lowest coefficient of variation (0.123)

The residual values (P_{test}/P_u) were plotted versus the test load P_{test} to check the "goodness" of each code model. Two horizontal dotted lines were drawn at values of (P_{test}/P_u) ratio equal to 0.S5 and 1.15 to limit the interval of "goodness" of the results. The difference of the distribution of the points around the horizontal unity line can be seen in Figures 5.11 to 5.14. The best random distribution can be noted in the case of the BS S110 code. In fact most points are between the two dotted lines. For the case of CP 110, most points are also in the zone of tolerance, but its predictions are not as good as BS S110. Most of the predicted points for the ACI and CEB-FIP codes are above the horizontal line. The variations in the CEB-FIP code predictions are larger compared to the ACI code. The big difference between the predicted values and the tests values is due to the use of a control perimeter too close to the loaded area by both codes. The difference is also increased by neglecting the size and the scale effects in the case of the ACI code, while the use of $(f_{cc}^{\frac{2}{3}})$ by the CEB-FIP code contributes to the scatter.

5.4.5 Comparison of Code Equations with Equation (5.8)

As mentioned previously, the derivation of equation 5.8 was based on data from the literature. The test results of the slabs tested by the author were added and analyzed using different codes equations and the proposed equation. Equation

(5.8) predictions of the failure load of all tested specimens were compared to the code provisions. The comparison is shown in Table 5.6, where the ratio of the failure test loads and the predicted loads is computed. From this Table, it can be seen that almost no difference between the equation (5.8) and the BS 8110 code predictions of the ultimate load of each specimen. Also, a comparison between the mean, the standard deviation and the coefficient of variation of the ratio (P_{test}/P_u values for all the analyzed slabs (90 specimens), is shown in Table 5.7. From this Table it can be seen that equation (5.8) has the lowest coefficient of variation (0.108)and a mean of (0.98).

To make a better comparison of the code equations, and to study the effect of variation of slab parameters on punching resistance, 12 hypothetical slabs of typical dimensions shown in Table 5.8 were analyzed. The slabs are circular, simply supported, isotropically reinforced, and normally loaded with a single central load. For all the slabs, the reinforcing steel has these parameters: $A_b = 100mm^2$, $E_s = 200000MPa$, $f_y = 400MPa$.

Figure 5.15 shows the effect of variation of the concrete compressive strength on the ultimate load predictions by the codes and equation 5.8. The ACI code predicts the lower values of P_u since it neglects the effect of the flexural reinforcement and consider a critical section much closer to the column peripheries. Even though the CEB-FIP code uses the highest power for the compressive strength ($f_{cc}^{\frac{2}{3}}$) and considered the effect of the reinforcement, it still predicts P_u values less than the British codes and the proposed equation (5.8). If the critical perimeter suggested by the CEB-FIP code is replaced by that suggested by one of the British codes, the ultimate load predictions will be over estimated because the power of f_{cc} is high (2/3). This can be seen in Figure 5.15 where the slope of the curve representing the CEB-FIP code is high compared to the others. Curves

representing the equation (5.8) and the BS 8110 code are close and parallel which indicates that a prediction similarity between the two.

Figure 5.16 shows the effect of variation of the amount of the flexural reinforcement on the ultimate punching shear load predicted by the equation 5.8 and the four codes. The ACI code was represented by a horizontal line because it neglects the effect of steel, whereas the CEB-FIP code was represented by an inclined straight line because the punching resistance load P_u is assumed proportional to ρ. The ACI and CEB-FIP codes predict P_u values less than those predicted by British codes. The curve representing equation (5.8) runs between the CP 110 and BS 8110 curves.

Figure 5.17 shows the effect of the slab effective depth (d) on the punching capacity of an interior column-slab connection. From this Figure (5.17), it can be seen that all the curves have almost the same trend. The ACI and the CEB-FIP codes still predict the lower values of P_u than the British Codes. The curve representing the equation is also between the BS 8110 and CP 110 Code curves.

The relationship between the ratio c/d and P_u using the four code provisions and equation (5.8) is shown in Figure 5.17. All the curves have the same trend, but the ACI and CEB-FIP codes still predict the lowest values of P_u compared to the British codes. The closest curve to the equation (5.8) one is that of the BS 8110 code.

5.4.6 Summary

The general expression of the failure surface A_c in equation (5.1) gives the designer a better picture of the failure mechanism of various punching situations.

The change is motivated by the possibilities which it opens up of future semi-rational treatments of a range of phenomenon which can not be dealt with satisfactory on the basis of "critical perimeter". The proposed equation (5.8) provides information on the effect of different parameters on the punching shear resistance of an interior column-slab connection.

While North American codes neglect the effect of the flexural reinforcement in the punching shear resistance, they require that it must be provided within 1.5h either side of the column to carry moments. Information such as how ductile the failure will be, or how much transverse reinforcement required is not given by the codes. The neglect of ρ also introduces a systematic trend for the ratio of experimental to calculated strength to increase with increasing reinforcement. The use of $P_u \propto \sqrt{f_{cc}}$ does not seem to cause any safety problem, but the lack of a size factor does mean that calculated P_u tends to be lower than the test value P_{test} for thicker slabs and higher for thinner slabs.

The European codes include the reinforcement ratio in the expression for ultimate shear stress and hence provide some information on the influence of the reinforcement steel, but the knowledge on the failure mechanism and ductility is still lacking. For the British codes, there appears to be no systematic error with respect to any of the parameters considered although conservative errors may well be anticipated for $\frac{c}{d} < 1.0$

Comparison between the proposed equation (5.8) and the code provisions showed that the equation can be used with confident. In fact its predictions are similar to the British code provisions.

Table 5.1: Predictions by equation (5.8)

Investigator	No. of Samples	k	P_{test}/P_u		
			Mean	St. Deviation	Coef. of Variation
Isotropic Reinforcement- Normal weight Concrete					
Present work	12	4.99	1.05	0.067	0.063
Gardner	18	4.04	0.88	0.101	0.115
Els. Hogn.	17	4.46	0.97	0.058	0.060
Moe	12	4.99	1.09	0.100	0.091
Yitzhaki	8	4.54	0.99	0.131	0.132
Kin. Nylan.	10	4.65	1.01	0.080	0.079
Isotropic Reinforcement- Lightweight Concrete					
Mow. Vand.	13	3.69	1.00	0.100	0.10
Circular Reinforcement- Normal weight Concrete					
Kin. Nylan.	11	3.14	1.00	0.076	0.076
Circular and Radial Reinforcement- Normal weight Concrete					
Kin. Nylan.	8	4.00	1.00	0.080	0.080
Average		-	0.98	0.106	0.108

Table 5.2: Predictions by the BSS110 code model

Investigator	No. of Samples	P_{test}/P_u		
		Mean	St. Deviation	Coef. of Variation
Present work	12	1.0S	0.0S0	0.074
Gardner	1S	0.SS	0.107	0.122
Els. Hogn.	17	0.9S	0.06S	0.069
Mow. Vand.	13	0.94	0.069	0.073
Moe	12	1.12	0.100	0.0S9
Yitzhaki	S	1.09	0.130	0.119
Kin. Nylan.	10	1.04	0.06S	0.066
Average		1.00	0.091	0.091

Table 5.3: Predictions by the CP 110 code model

Investigator	No. of Samples	P_{test}/P_u		
		Mean	St. Deviation	Coef. of Variation
Present work	12	1.17	0.0S9	0.076
Gardner	18	1.02	0.120	0.118
Els. Hogn.	17	1.00	0.072	0.072
Mow. Vand.	13	1.03	0.067	0.065
Moe	12	1.16	0.102	0.088
Yitzhaki	8	1.31	0.155	0.118
Kin. Nylan.	10	1.20	0.086	0.072
Average		1.10	0.145	0.132

Table 5.4: Predictions by the ACI code model

Investigator	No. of Samples	P_{test}/P_u		
		Mean	St. Deviation	Coef. of Variation
Present work	12	1.66	0.182	0.110
Gardner	18	1.80	0.400	0.223
Els. Hogn.	17	1.39	0.204	0.147
Mow. Vand.	13	1.27	0.232	0.183
Moe	12	1.36	0.139	0.102
Yitzhaki	8	1.68	0.283	0.168
Kin. Nylan.	10	1.53	0.206	0.135
Average		1.51	0.345	0.228

Table 5.5: Predictions by the CEB-FIP model

Investigator	No. of Samples	P_{test}/P_u		
		Mean	St. Deviation	Coef. of Variation
Present work	12			
Gardner	18	1.36	0.276	0.203
Els. Hogn.	17	1.14	0.209	0.183
Mow. Vand.	13	1.12	0.208	0.186
Moe	12	1.46	0.191	0.131
Yitzhaki	8	1.84	0.311	0.169
Kin. Nylan.	10	1.54	0.136	0.088
Average		1.23	0.401	0.326

Table 5.6: Predictions of ultimate punching shear loads of the tested slab using equation (5.8) and different codes

Slab Num.	P_{test} (kN)	P_{test}/P_u				
		Eq.(5.8)	BS 8110	CP 110	ACI	CEB-FIB
A1	176.8	1.23	1.23	1.40	2.63	2.38
B1	160.6	1.00	1.00	1.13	2.04	1.72
B2	150.4	0.93	0.93	1.07	1.89	1.61
B3	203.2	1.26	1.26	1.14	2.56	2.17
C1	200.0	1.04	1.09	1.26	2.00	1.69
C2	221.2	1.15	1.14	1.33	1.79	1.56
C3	211.5	1.03	1.20	1.23	1.64	1.51
C4	185.1	1.02	1.04	1.22	1.96	1.67
C5	163.5	0.91	0.93	1.06	1.75	1.47
C6	227.5	1.14	1.19	1.39	2.13	1.78
C7	133.4	0.83	0.91	1.06	1.31	1.43
C8	167.0	0.86	0.89	1.04	1.64	1.37
C9	200.4	1.03	1.03	1.25	1.96	1.67
C10	220.8	1.01	1.00	1.14	2.27	1.32
C11	170.0	1.06	1.06	1.20	2.17	1.85
C12	160.0	1.11	1.07	1.22	2.00	1.96
C13	190.0	1.12	1.14	1.26	1.89	1.79

Table 5.7: comparison between the equation 5.8 and codes predictions for the 90 slabs

	P_{test}/P_u				
	Eq.(5.8)	BS110	CP 110	ACI	CEB-FIP
Mean	0.98	1.00	1.10	1.51	1.23
Stand. dev.%	10.6	12.3	14.5	34.5	40.1
Coef.of var.%	10.8	12.3	13.2	22.8	32.6

Table 5.8: Hypothetical slabs selected for the analysis

Slab#	d (mm)	c (mm)	f_{cc} (MPa)	ρ	S (mm)
1	120	150	10	0.015	56
2	120	150	20	0.015	56
3	120	150	30	0.015	56
4	120	150	40	0.015	56
5	120	150	30	0.005	167
6	120	150	30	0.030	28
7	120	150	30	0.050	17
8	80	150	30	0.015	83
9	200	150	30	0.015	33
10	360	150	30	0.015	19
11	120	100	30	0.015	56
12	120	200	30	0.015	56
13	120	250	30	0.015	56

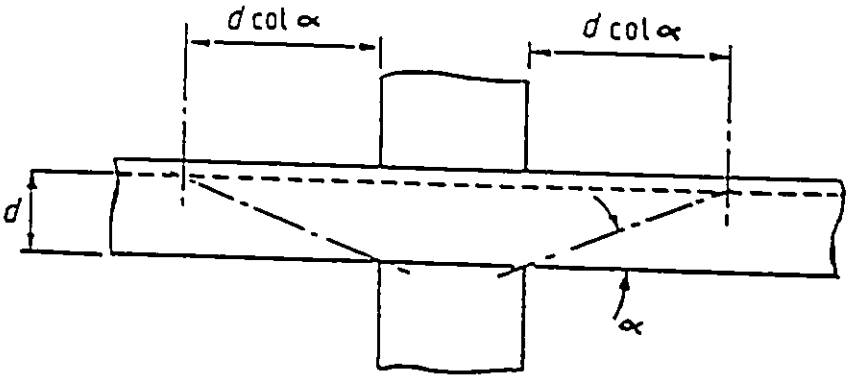

Figure 5.1: Failure surface used by Regan

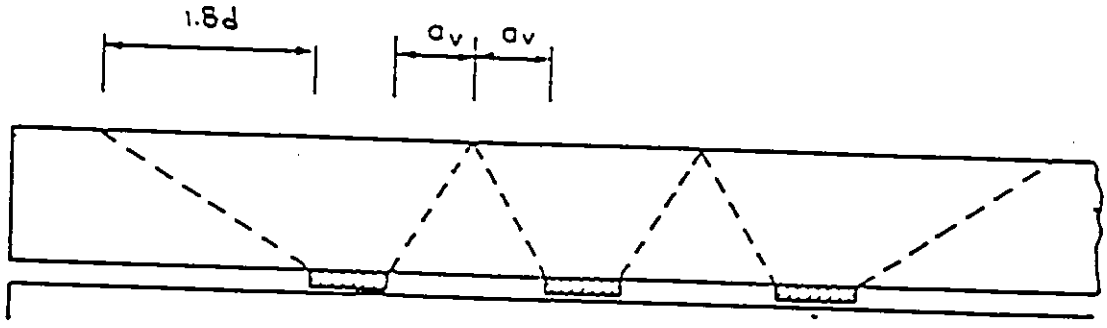

Figure 5.2: Overlap of punching perimeters

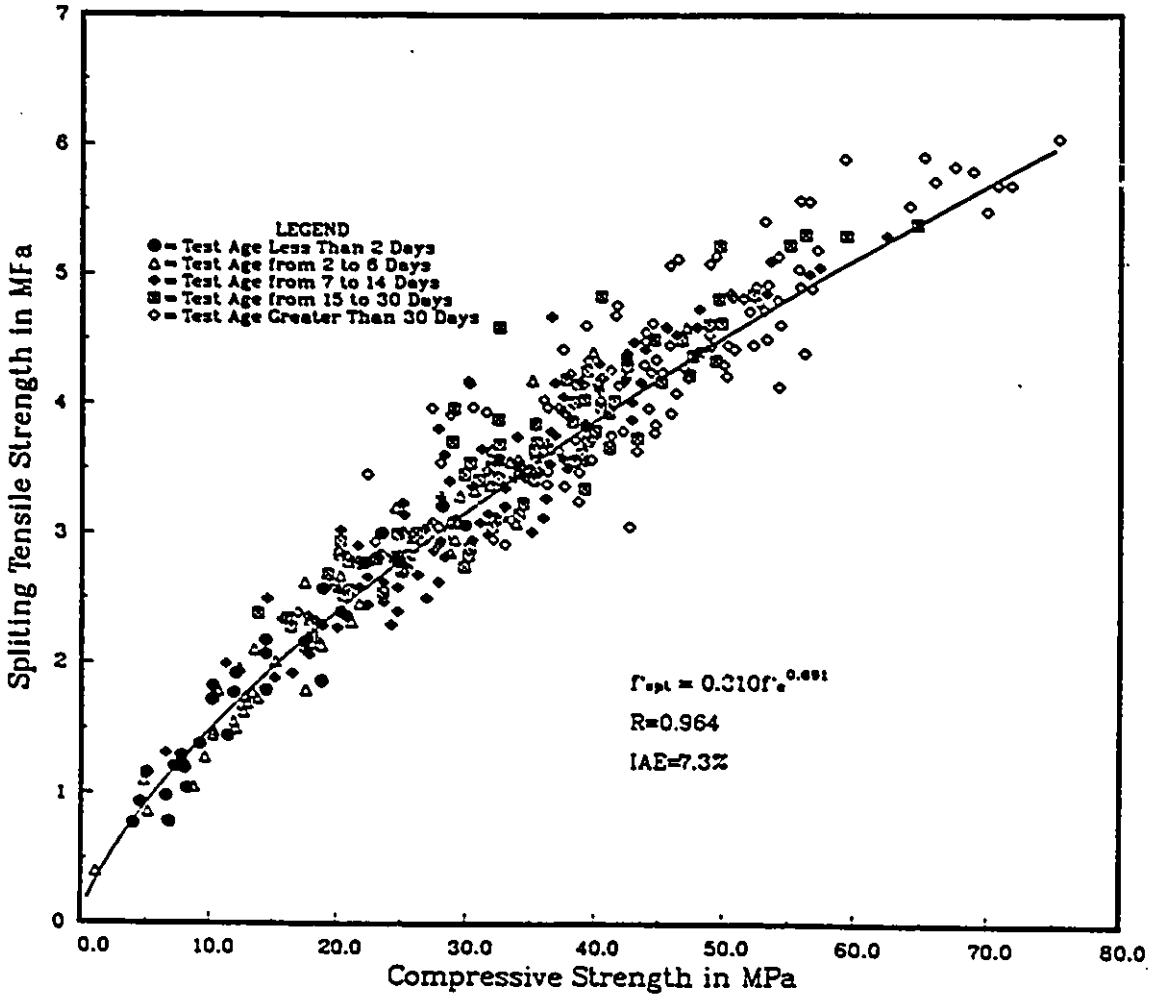

Figure 5.3: Relationship between the splitting tensile strength and compressive strength of concrete (After Zhao 1990)

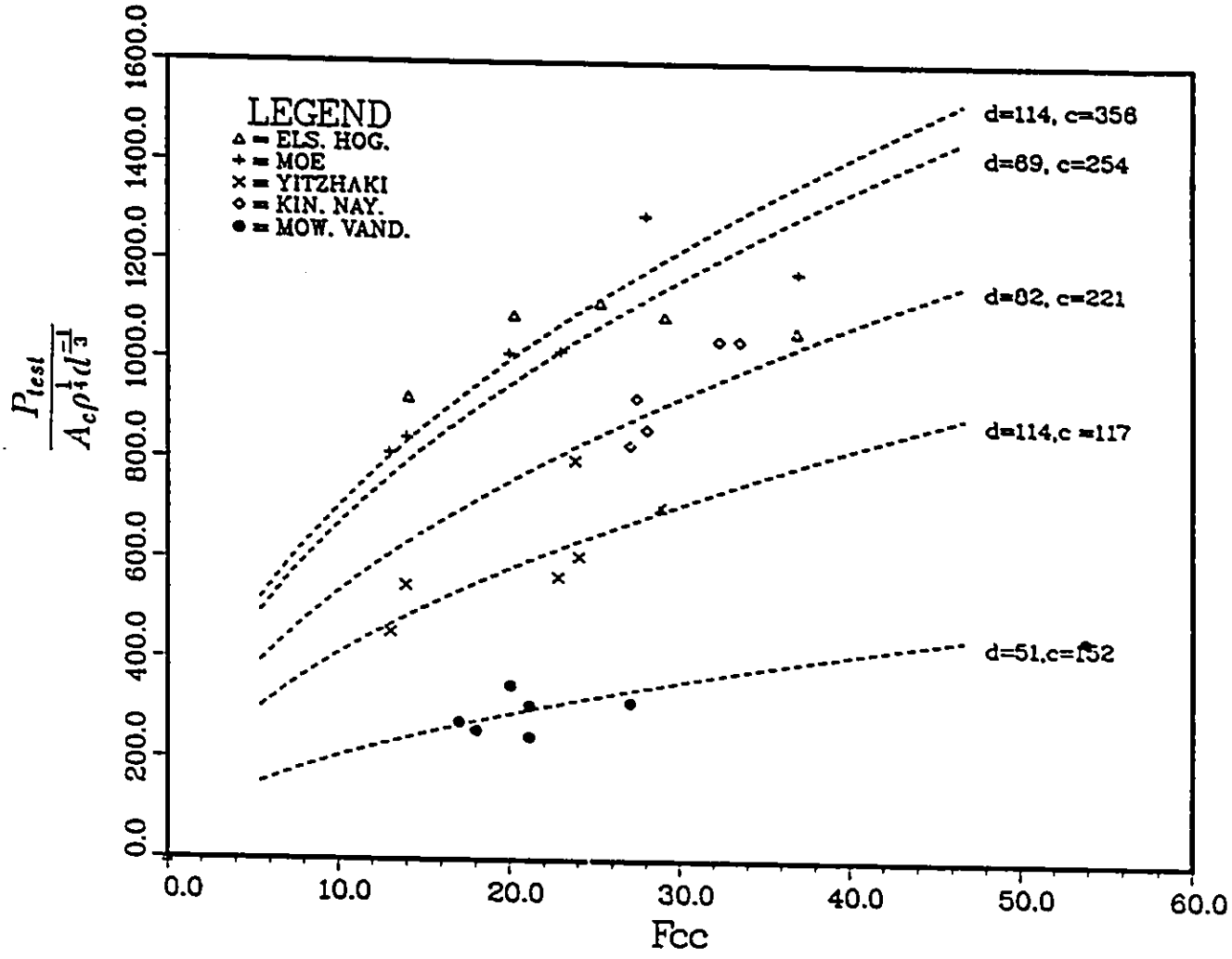

Figure 5.4: Relationship between the punching shear stress and the square root of the compressive strength of reinforced concrete flat slabs

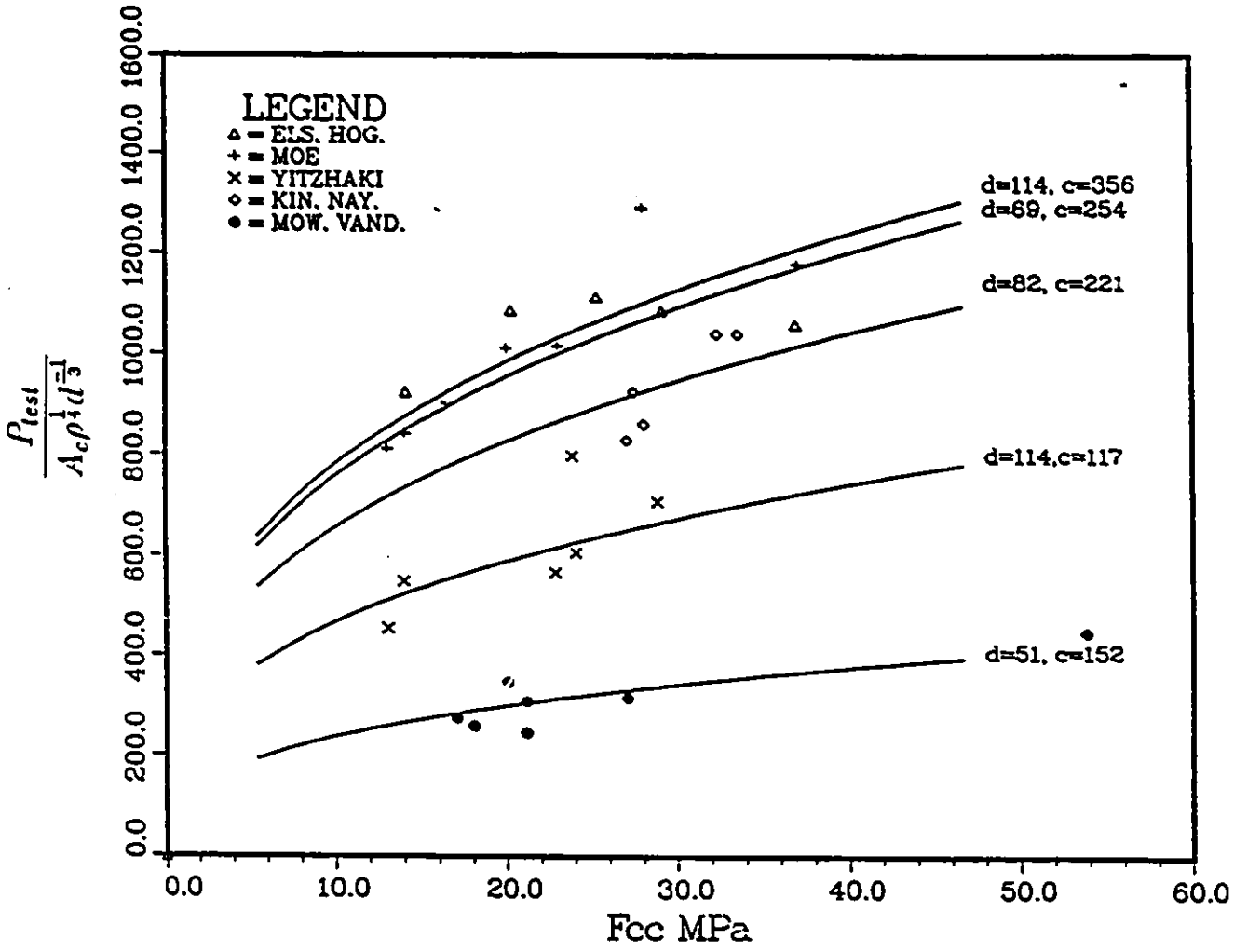

Figure 5.5: Relationship between the punching shear stress and the cubic root of the compressive strength of reinforced concrete flat slabs

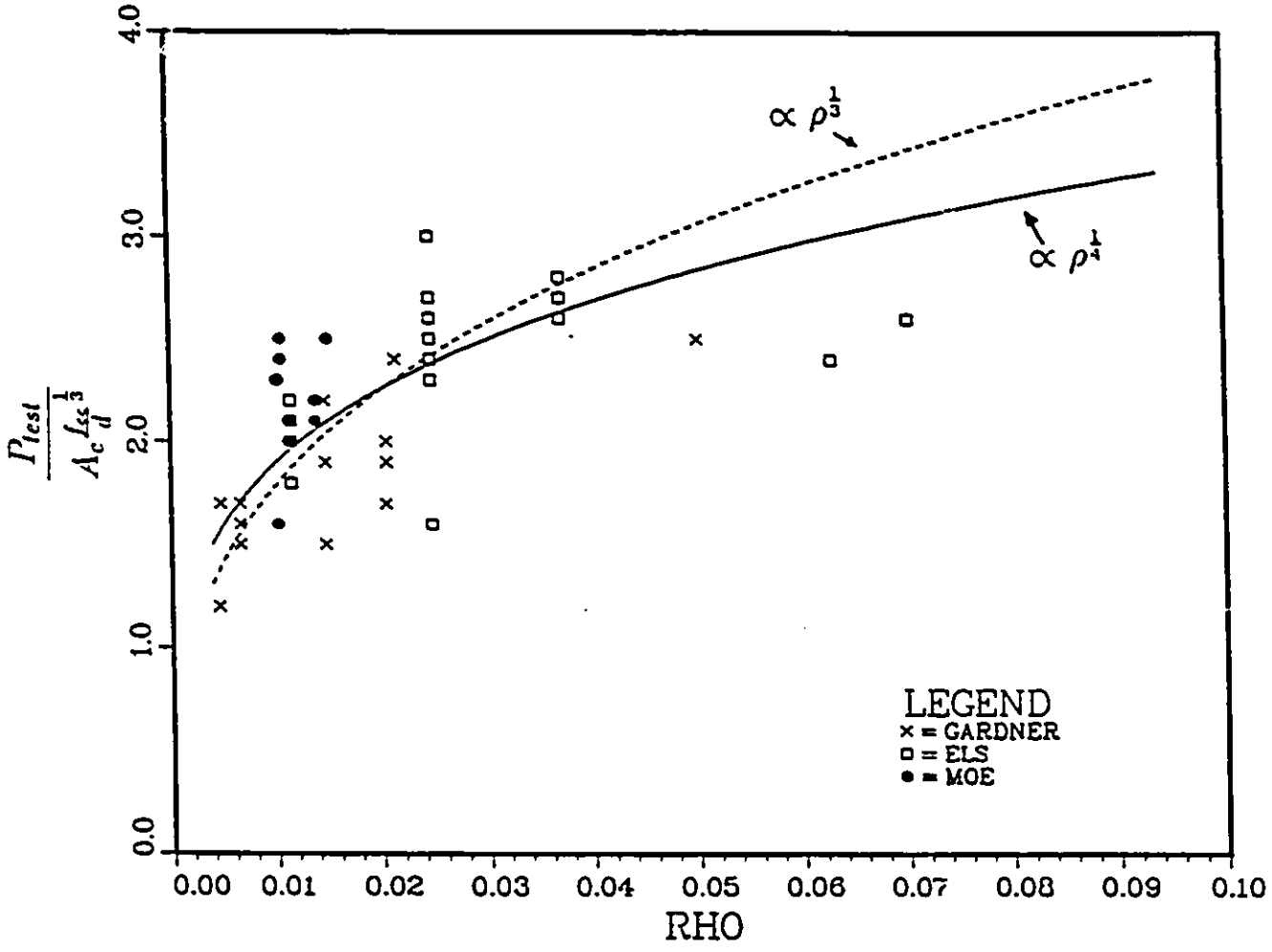

Figure 5.6: Influence of ratio of reinforcement on punching resistance

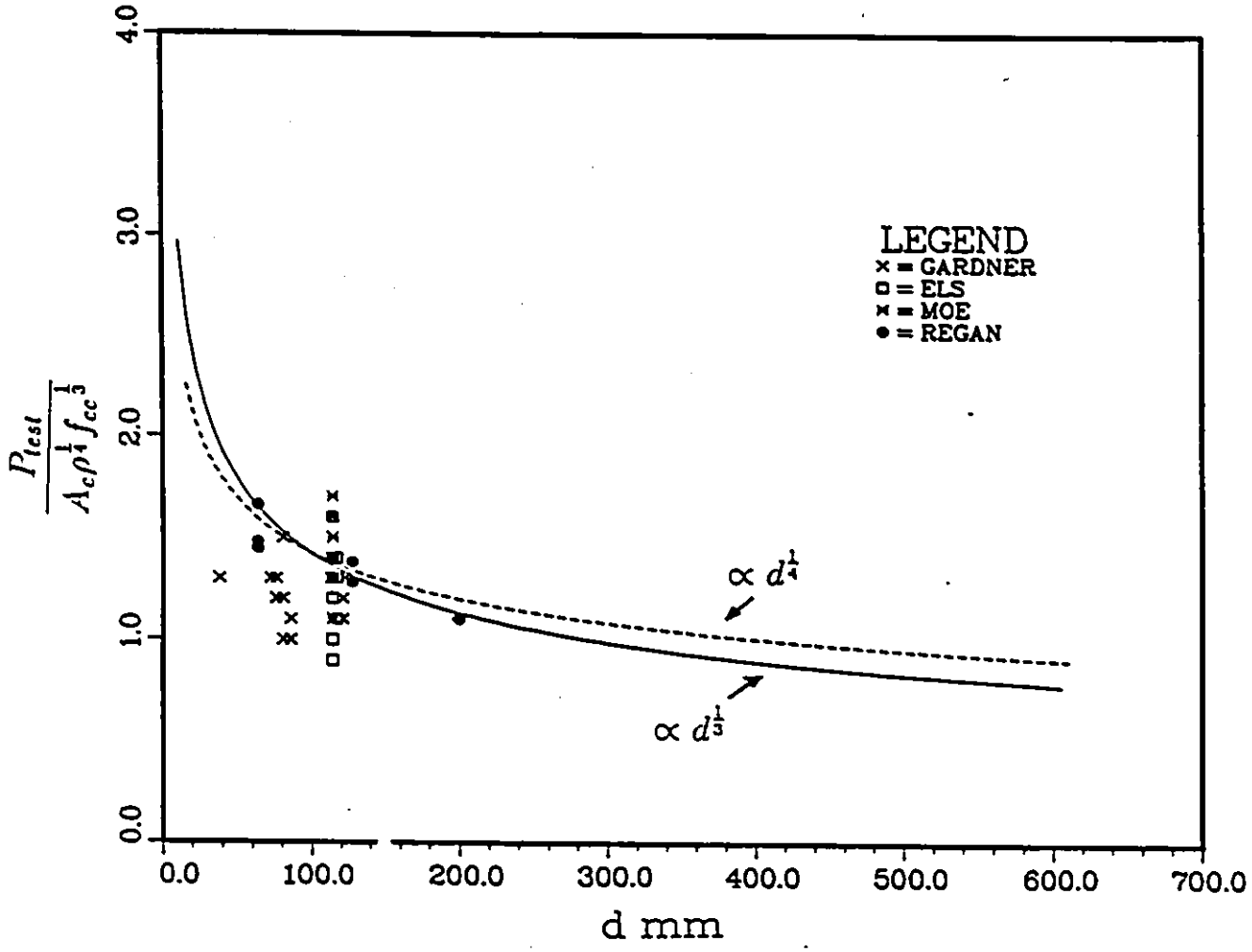

Figure 5.7: Influence of the effective depth of a slab on punching resistance

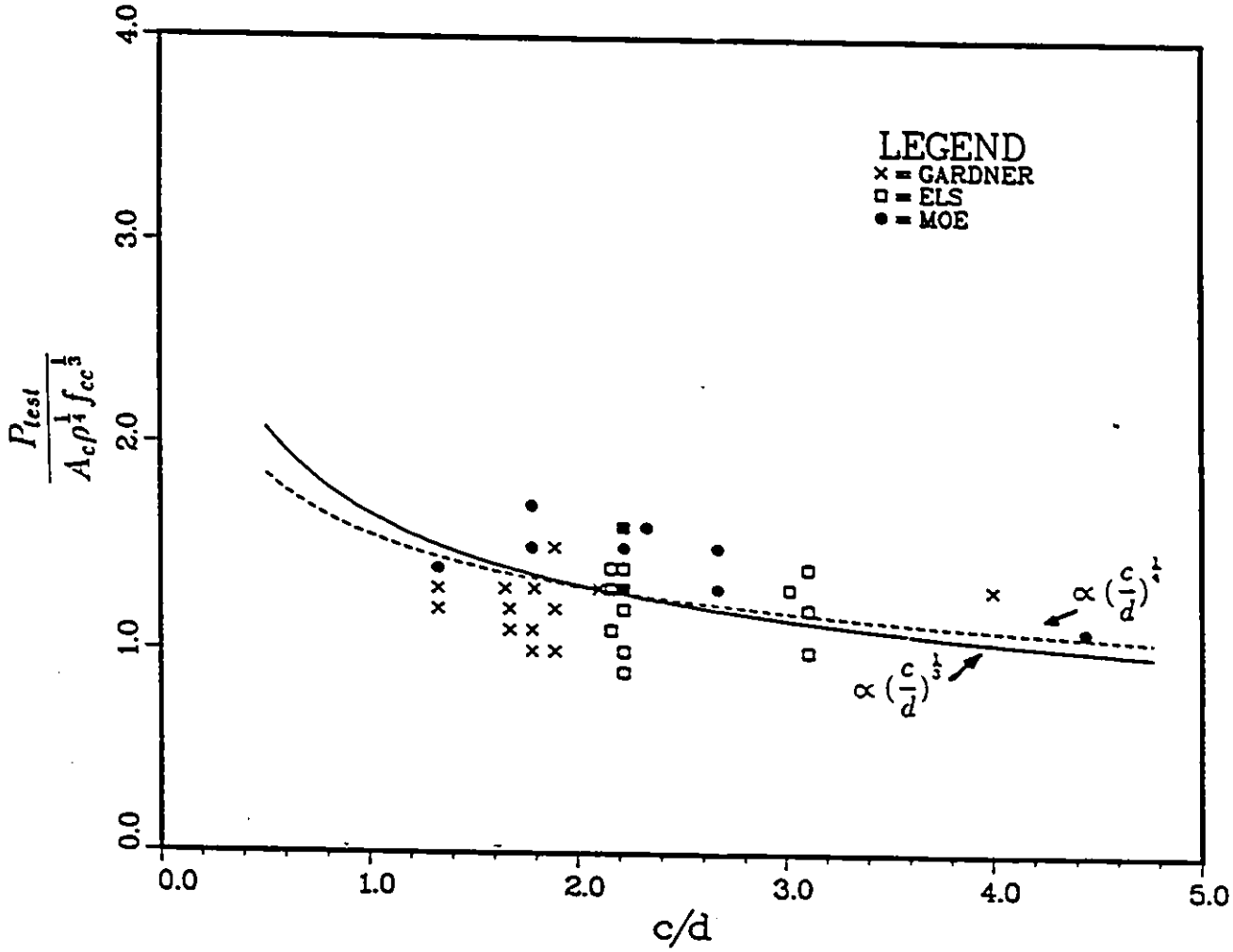

Figure 5.8: Size effect on punching resistance

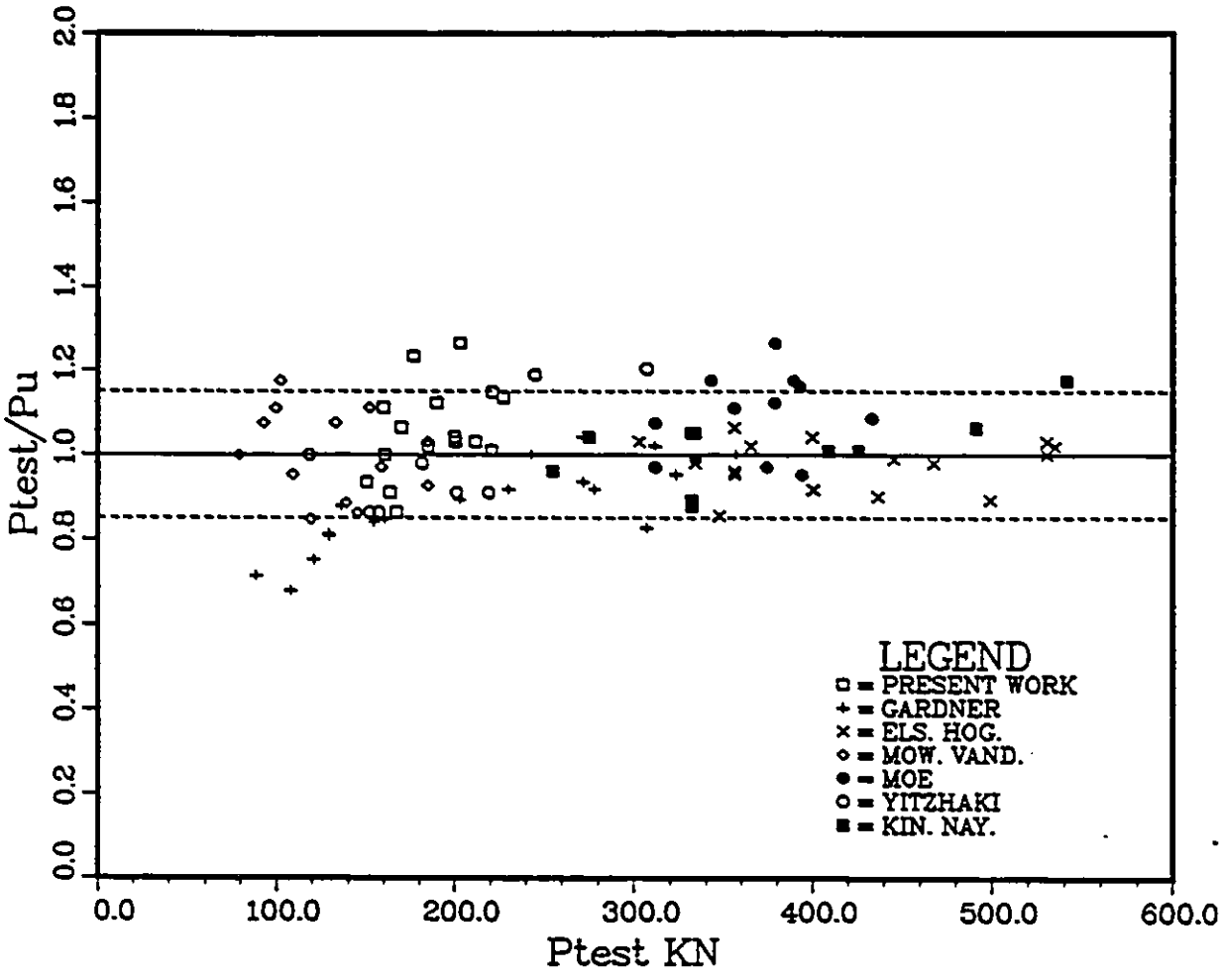

Figure 5.9: Correlation between the predicted values P_u and the tests using equation (5.8)

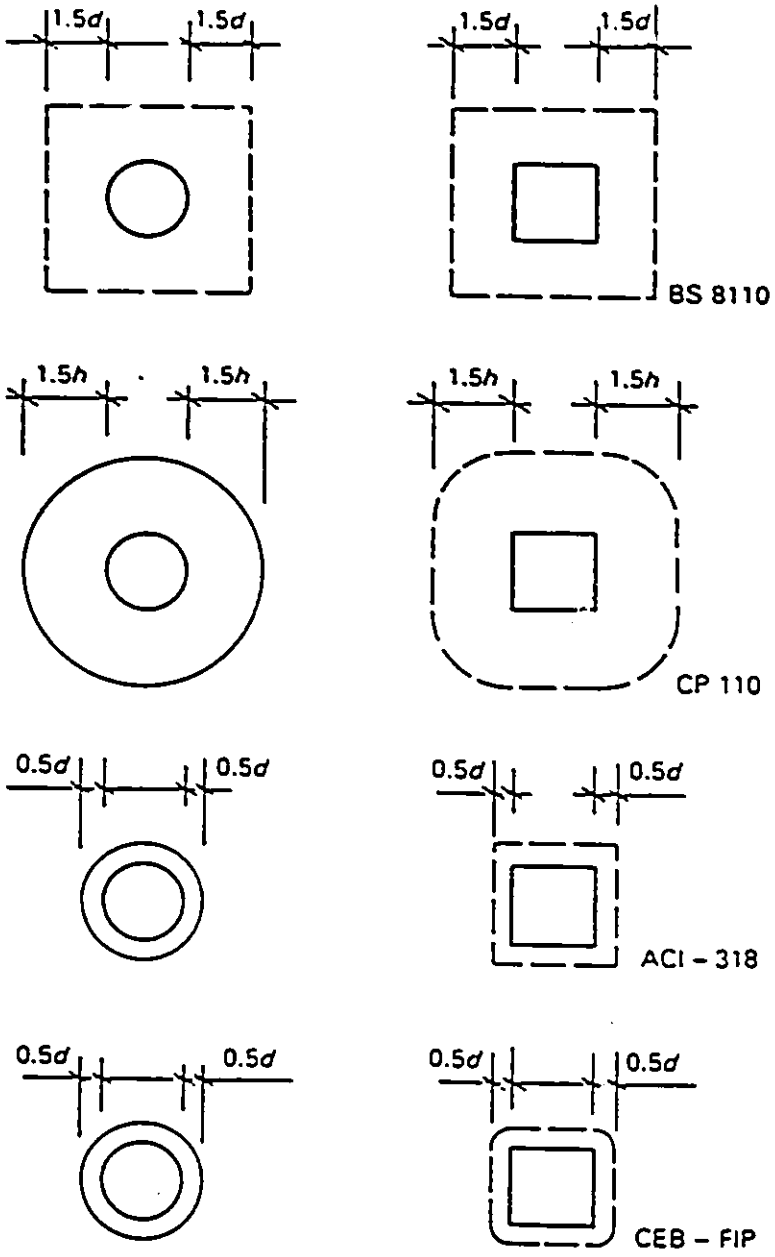

Figure 5.10: Control perimeters for different codes

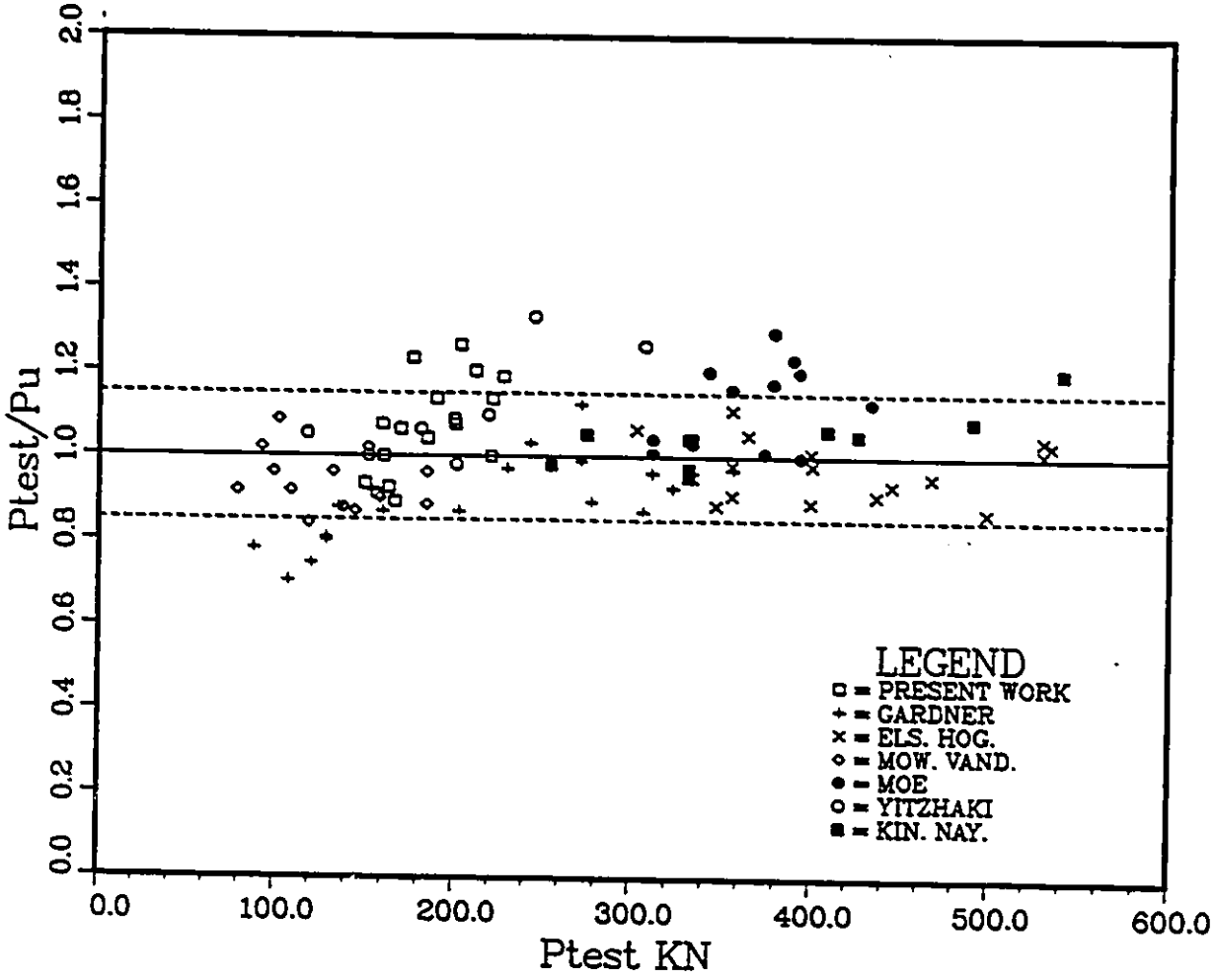

Figure 5.11: Correlation between the predicted values P_u and the tests using BS8110 code model

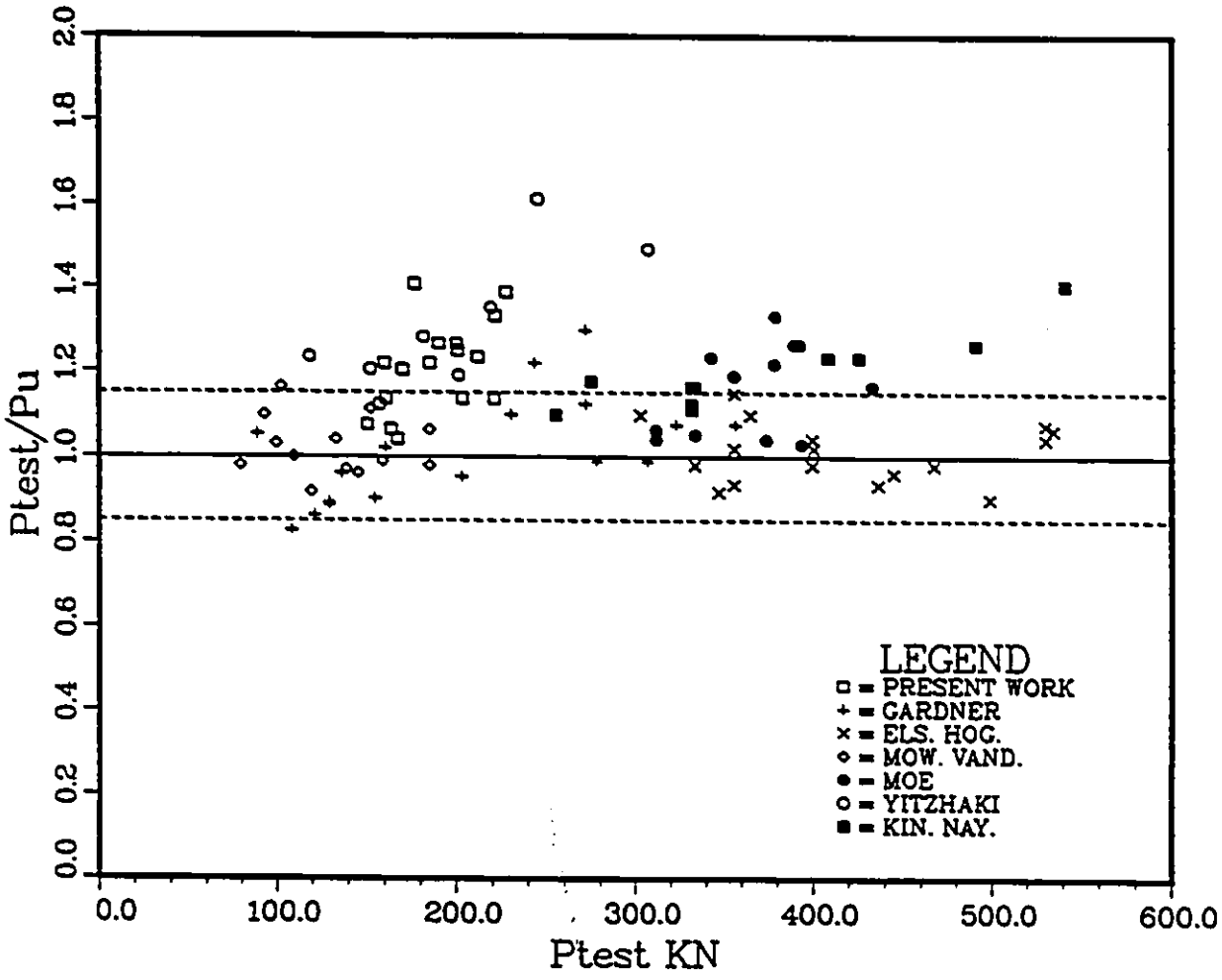

Figure 5.12: Correlation between the predicted values P_u and the tests using CP110 code model

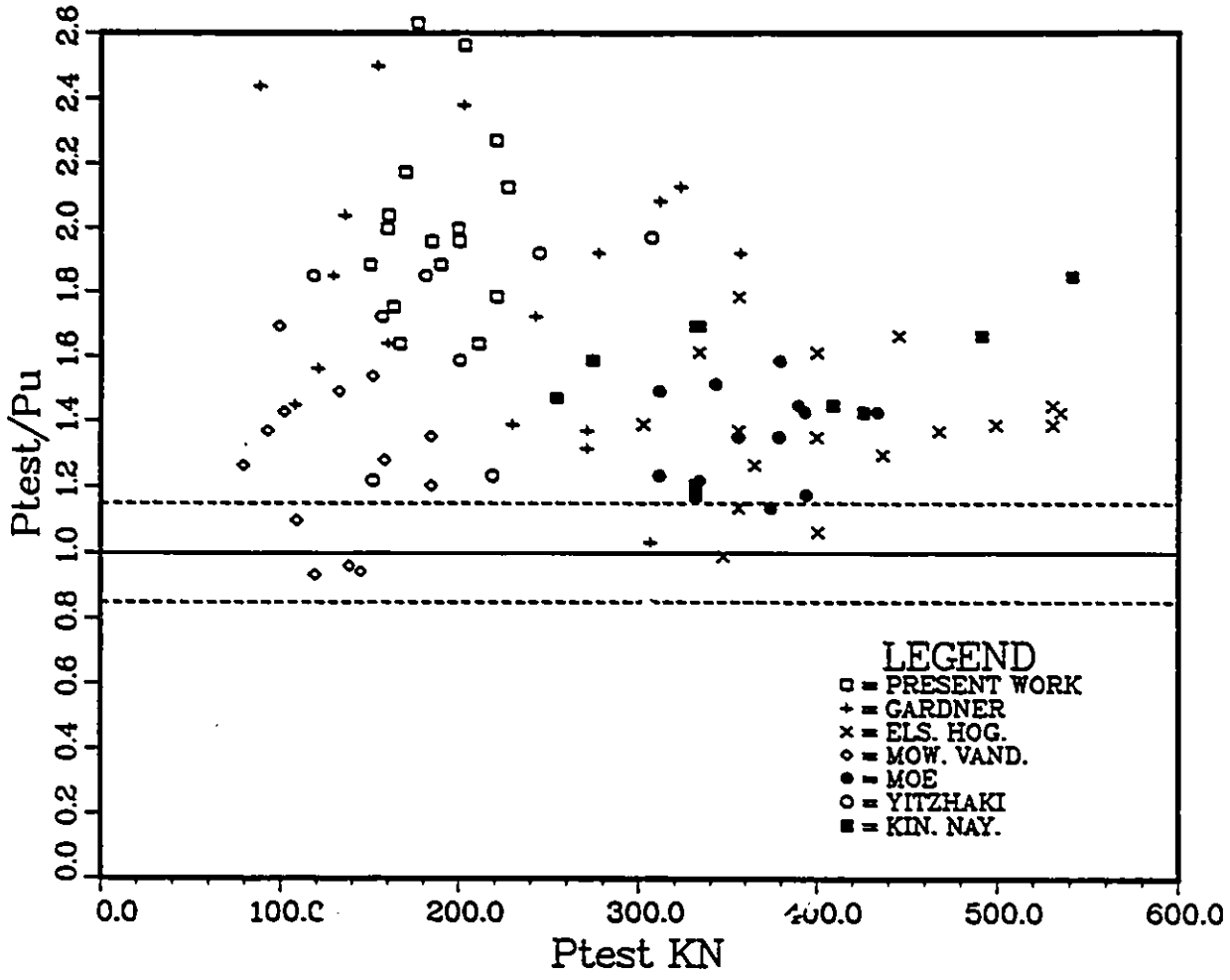

Figure 5.13: Correlation between the predicted values P_u and the tests using ACI code model

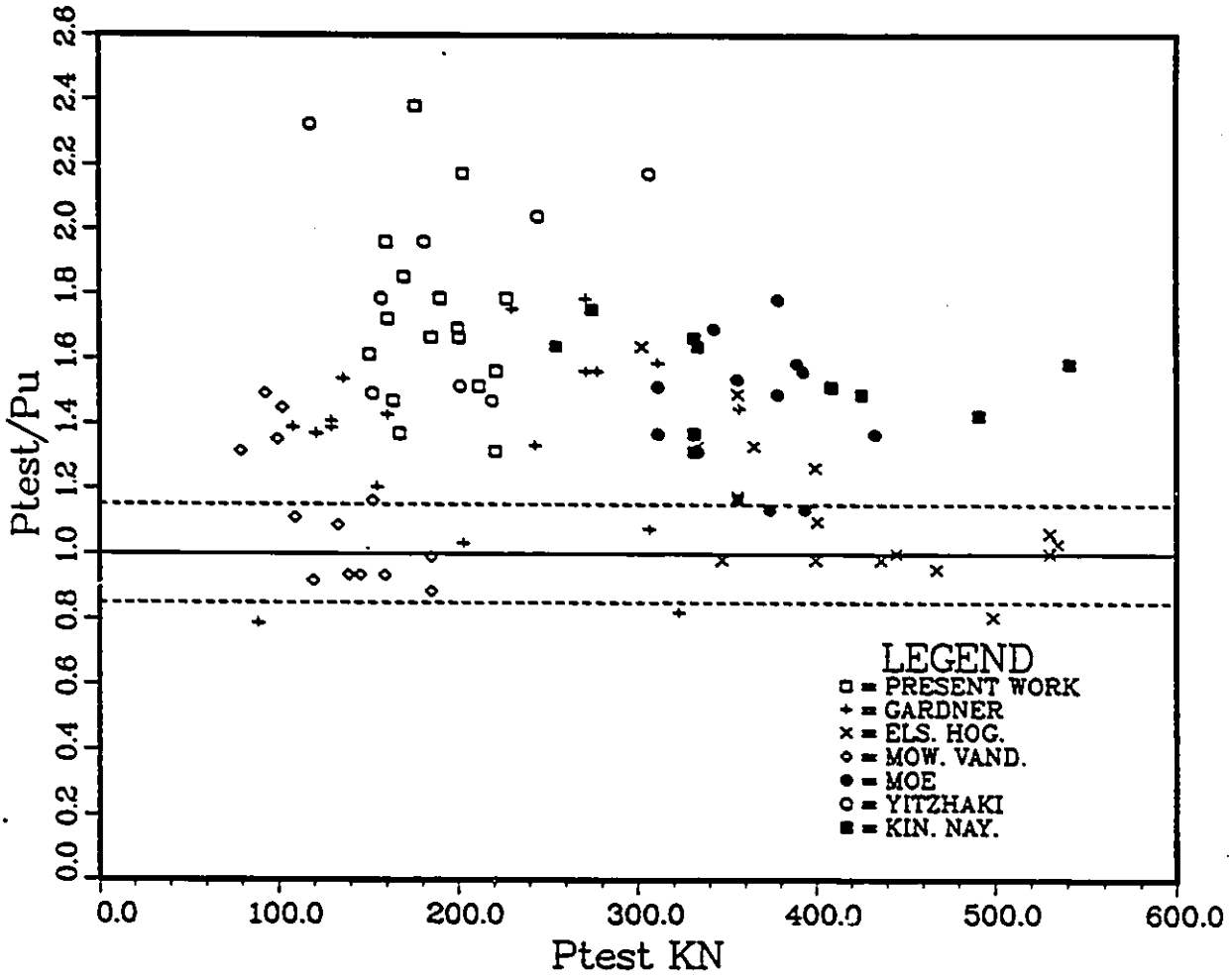

Figure 5.14: Correlation between the predicted values P_u and the tests using CEB-FIP code model

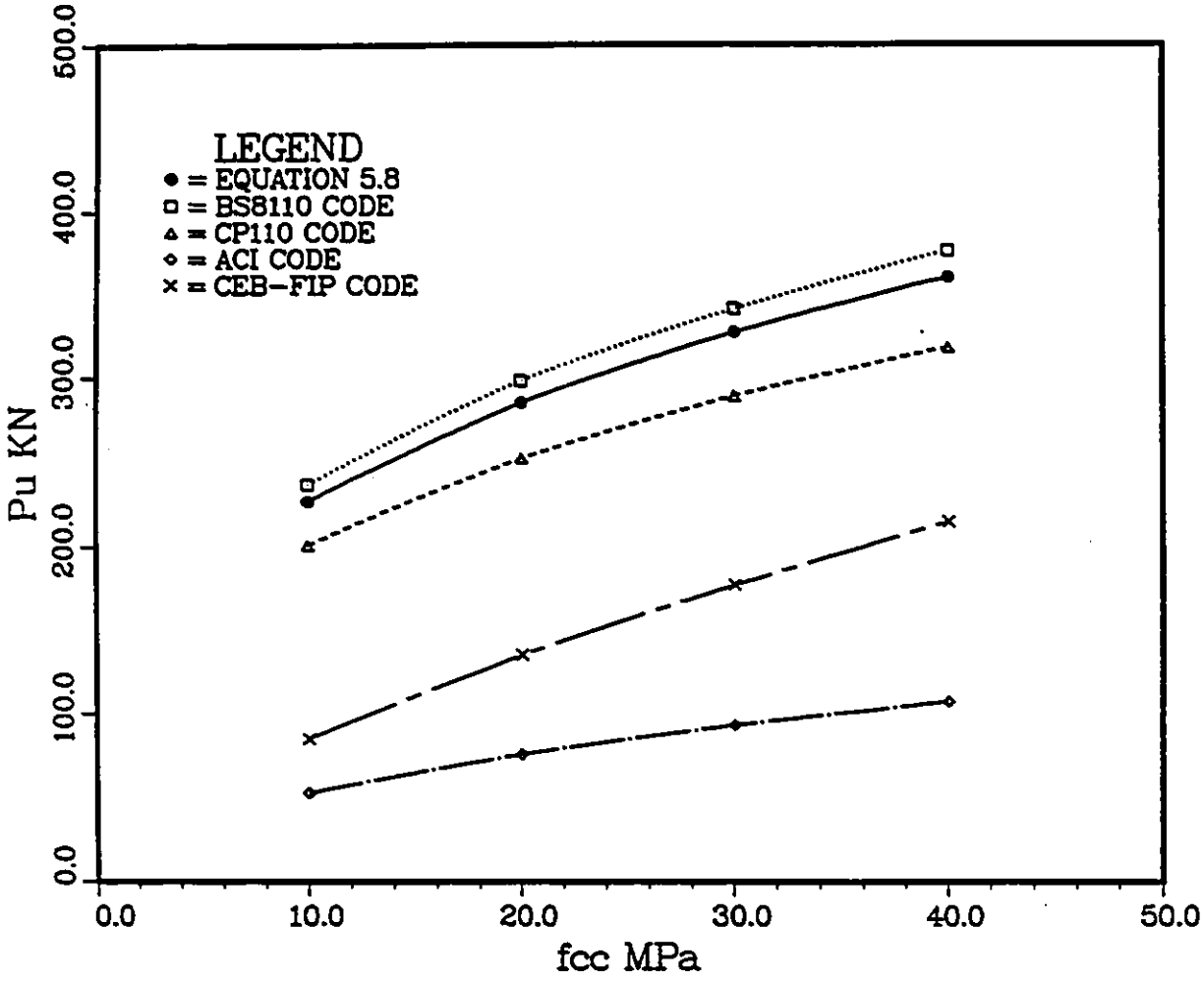

Figure 5.15: Comparison between the codes and equation (5.8) with respect to the compressive strength of concrete

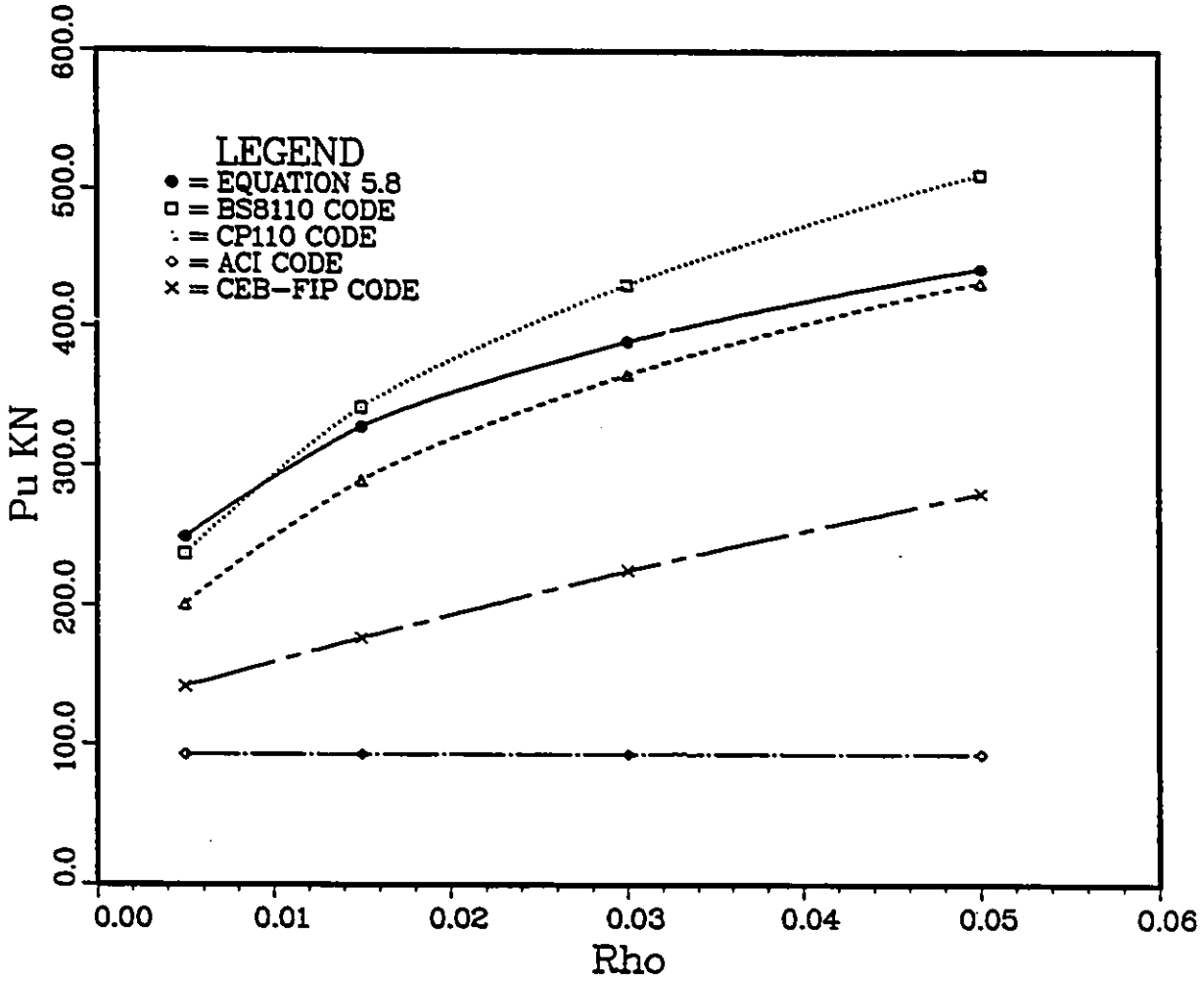

Figure 5.16: Comparison between the codes and equation (5.8) with respect to the reinforcement ratio

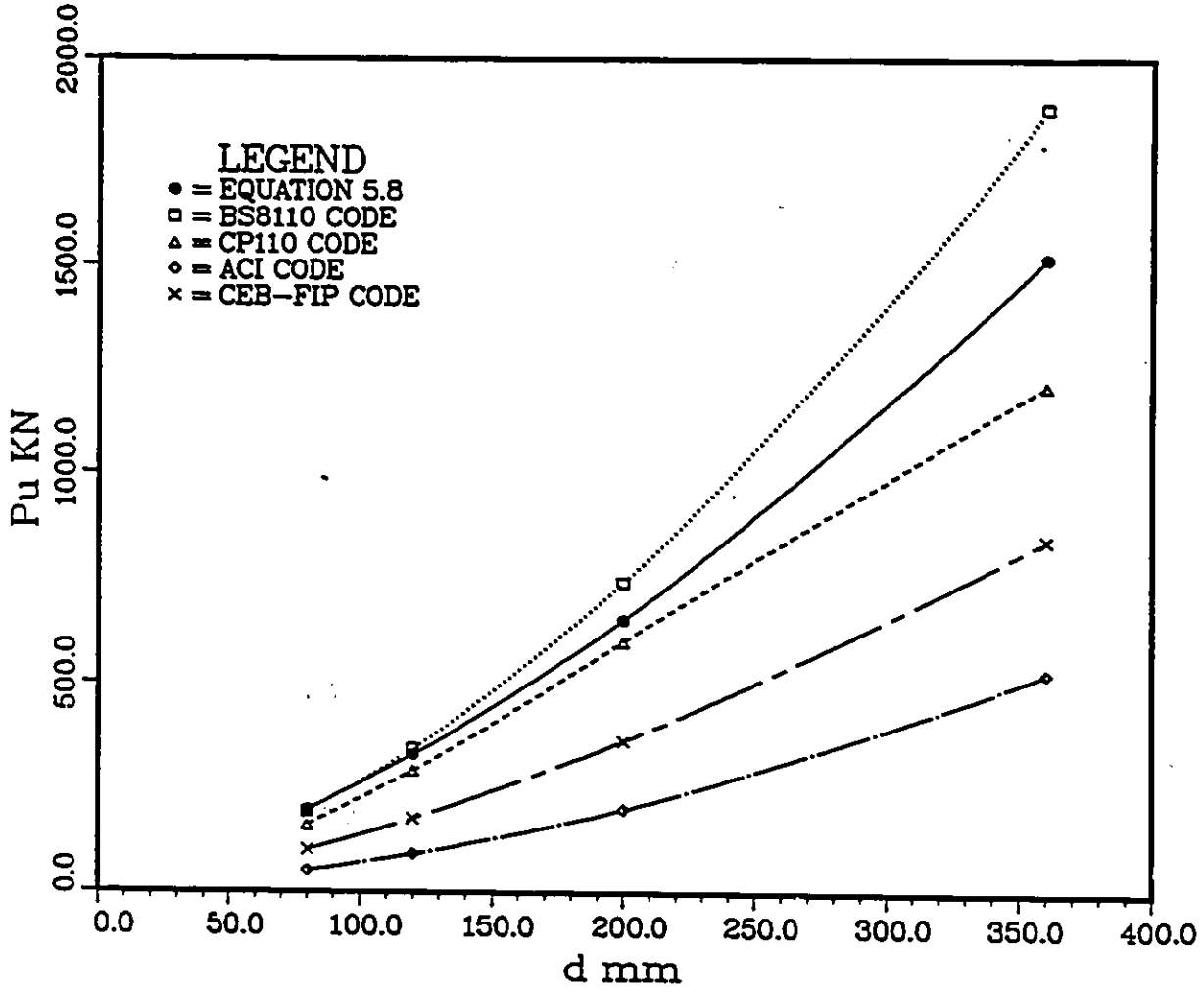

Figure 5.17: Comparison between the codes and equation (5.8) with respect to the effective depth of a slab

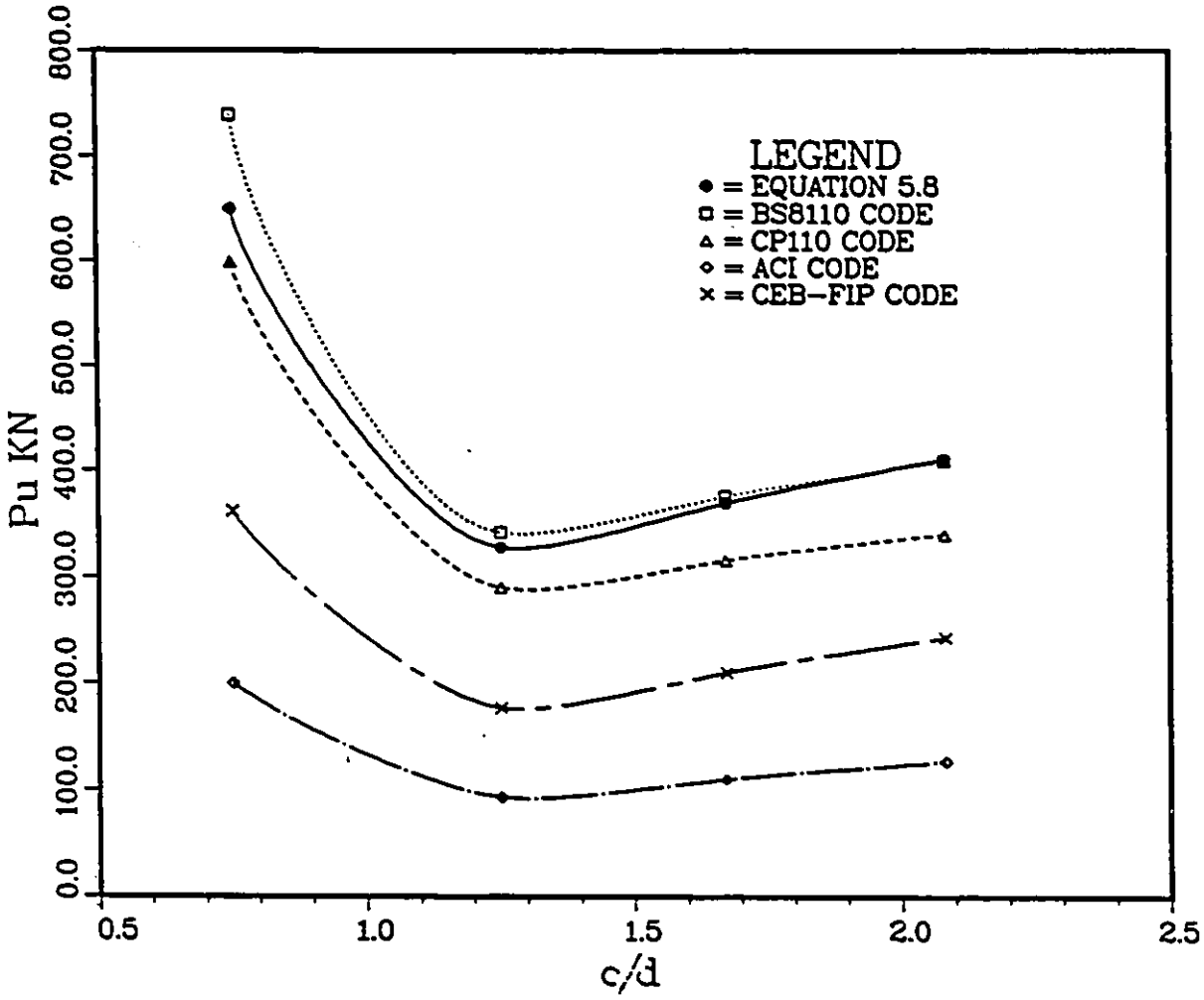

Figure 5.18: Comparison between the codes and equation (5.8) with respect to the ratio c/d

Chapter 6

Rational Models

6.1 Introduction

While the North American design approach is usually to develop empirical equations suitable for codification to explain the punching shear phenomenon, the European approach is often to develop rational models providing reasonable description of the actual behavior of slab-column connections. These models have the advantage over the empirical methods in helping the designer to visualize the behavior of reinforced concrete column-slab connections, and give a clear indication of the effects of each parameter. Unfortunately, only few rational models were developed in the past two decades, and none of them was convincing or widely accepted by design engineers. The development of these models was involved either some unrealistic assumptions or too many equations and iterations. In this project, four different rational models proposed during the last two decades, will be presented and discussed.

6.2 Upper Bound Solution

6.2.1 Description of the Model

In 1986, a theoretical model for the punching shear strength of concrete slabs was presented by Jiang and Shen [34]. Their solution is similar to that of Beastrup-Nielson solution published in 1976. The failure mechanism is shown in Figure 6.1. The Upper Bound Solution for the ultimate punching load P_u is derived by equating the rate of external work done by the applied load with the rate of internal work dissipated in the failure surface. This model is based on three principal concrete parameters, tensile strength f_{ct}, compressive strength f_{cc} and the angle of internal friction ϕ which determines the parameter m as the ratio of the effective compressive strength to the effective tensile strength. The authors defined the failure as a three dimensional state of stress, primarily in the region of tension-compression-compression or compression-compression-compression, in which compression plays a dominant role.

6.2.2 Basic Assumptions

- The shape of the slab and the load area is circular.
- Deformations are normal to the slab. No deformations in the tangential direction.
- Dowel action due to the flexural reinforcing bars is neglected.
- The flexural reinforcement does not contribute to the punching strength.
- The concrete slab is rigid

- The punched out cone is connected to the rest of the slab by perfectly plastic shell.
- The internal friction angle of concrete is 37 degrees.
- The yield line for the failure cone is straight.

6.2.3 Equations

The work equation for the failure of Figure 6.2 yields to determine the ultimate punching load as:

$$P_u = f'_{ct} \int_A (1 + k\cot^2\alpha) \sin\alpha dA \tag{6.1}$$

where f'_{ct} is the effective tensile strength of concrete, k is parameter depending upon m which is the ratio between effective compressive strength (f'_{cc})to effective tensile strength of concrete and the punch angle α.

If the yield line is represented by the function $r = r(x)$, the thickness of the slab by h and the diameter of the loaded area by c, then the above equation can be written as:

$$P_u = 2\pi f'_{ct} \int_0^h (\tan\alpha + k\cot\alpha) r dx \tag{6.2}$$

Knowing that $\tan\alpha = \frac{dr}{dx}$ and $r = \frac{d}{2} + x\tan\alpha$, and substituting these values in the equation(6.2), the collapse load is:

$$P_u = \pi f'_{ct} (\tan\alpha + k\cot\alpha)(\frac{c}{h} + \tan\alpha) h^2 \tag{6.3}$$

The critical angle of the punching is determined by taking $\frac{\partial P}{\partial \alpha} = 0$. then:

$$\frac{1}{\tan\alpha} = \left(\frac{h}{kc}\left(1 + \sqrt{1 - \frac{c^2}{27kh^2}}\right)\right)^{\frac{1}{3}} + \left(\frac{h}{kd}\left(1 - \sqrt{1 - \frac{c^2}{27kh^2}}\right)\right)^{\frac{1}{3}} \tag{6.4}$$

The authors simplified the problem by chosing $\alpha = 45$. Then the equation (6.3) becomes:

$$P_u = (k+1)f'_{cc}A_c \tag{6.5}$$

in which $A_c = \pi(B+h)h$.

After they studied the effect of the parameter m, the authors suggested that $f'_{cc} = 0.35f_{cc}$, and proposed the following design equation for the ultimate punching load.

$$P_u = 0.074f_{cc}A_c \tag{6.6}$$

6.2.4 Discussion

A selected series of test results were used to check the validity of this model. Figure 6.3 shows no smooth distribution of points around the horizontal line, which indicates how bad the model predicts the values of the punching resistance load of flat reinforced concrete slabs. In fact the highest coefficient of variation for the different selected sets of tests is 32.3% and the lowest is 10.2%. (see Table 6.1). In addition to the complexity of the theoretical development of the model, some unrealistic assumptions were made to simplify the final equation. Namely, the authors assumed that the angle of failure is 45 degrees which is too high and experimentally, no investigator has reported that a failure surface had reached this angle during tests. Using the theoretical equation deveioped by the authors to determine the failure surface angle to the horizontal, it can be seen that the formula predicted quite high values. The minimum values for the analyzed slabs was found to be equal to 37 degrees. Another unrealistic assumption is that the authors neglected completely the effect of the flexural reinforcement in the slab. Even though the idea is the same as the ACI code which was shown to

be conservative, this model relates the ultimate punching resistance load directly proportional to the compressive strength of concrete. That means, no matter how much one places reinforcement steel in the slab, the punching resistance of the slab is constant and the only way to increase this resistance is to increase the thickness of the slab or the compressive strength of concrete. However, during early stages of construction, the concrete compressive strength will not go beyond 30 MPa and that means only one choice left is to increase the thickness of the slab if the column dimensions wanted to be kept constant. The design formula (6.6) that was suggested by the authors differs completely from the conventional formulas by the fact that they related the ultimate resistance punching load directly to the compressive strength of concrete rather than a power of it.

6.2.5 Summary

The problem with the plastic theory when is applied to reinforced concrete material, is that so many assumptions should be made, notably the neglect of the contribution of the flexural reinforcement and the radial or the tangential deformation. Beside the complexity of the development of the theoretical equations, the simplified final design equation of the model does not give a good prediction of the ultimate punching load resistance of reinforced concrete slabs.

6.3 Pralong's Model

6.3.1 Description of the Model

In 1982, Pralong [52] used a lower bound approach involving the tensile strength of concrete to develop a new model for the symmetric punching shear resistance. Pralong modelled the shear resistance of an isotropically reinforced concrete slab subjected to concentric load by that of a series of beams radiating from the center and making a star with a slab having a hole in the middle (See Figure 6.4). The author relates the problem to simply supported circular slabs and loaded in the centre by a concentric load. The concentric load could be uniformly distributed on a circular area or linearly concentrated along a circle.

Pralong studied two cases of slabs: first, an annular circular slab loaded along the periphery of the hole; second, a circular slab loaded uniformly on a circular area in the middle. Then he extend his work to the slabs with shear reinforcement and slabs under rectangular loaded area

6.3.2 Basic Assumptions

- The slab is circular and simply supported.
- The punching failure is due to failure of concrete in tension.
- The depth of the compression zone calculated to be a fraction of the effective depth ωd. The compression stress is uniformly distributed.
- The shear stress is uniformly distributed over the depth $d(1 - \frac{\omega}{2})$, and decreases linearly to zero at the compression zone. (See Figure 6.5).

- The limit value of tension of concrete is estimated to be $f_t = 0.3 f_{cc}^{\frac{2}{3}}$
- For annular circular slabs loaded around the peripheries of the hole, the effect of the reinforcement was neglected.
- For circular slabs, the steel in the interior zone of punching reaches yield point.
- The minimum reinforcement ratio is 0.5% for annular circular slabs.

6.3.3 Equations

Annular Circular Slabs

The equation for punching shear resistance of a circular slabs having a hole of radius $r = c/2$ in the middle was derived to be representative of the lower bound of the ultimate load. If the punching failure takes place and the steel did not reach the yield point, than this failure is mainly caused by the failure of concrete in tension. Therefore the effect of flexural reinforcement can be neglected and the maximum shear resistance τ_{max} is equal to the tensile strength of concrete f_{ct}. The minimum ratio of steel is :

$$\rho_{min} = \frac{f_{ct} c}{2 f_y d} \tag{6.7}$$

where f_y is the yield stress of flexural reinforcement and d is the effective depth of the slab. Pralong suggested that the minimum flexural reinforcement ratio for the above type of slabs is 0.5%. If ρ exceeds this value, then the steel will not reach the yield point.

The compression and tension stresses are assumed to be uniformly distributed

(See Figure 6.6) The limit of compression zone ωd is given by:

$$\omega d = \frac{c}{2(\frac{f_{cc}}{f_{ct}} - 1)} \tag{6.8}$$

The ultimate punching resistance load can be expressed as:

$$P_u = \pi c f_{ct} d(1 - \frac{\omega}{2}) \tag{6.9}$$

Circular Slabs

For a simply supported circular slab subjected to a circular area load in the middle, the ultimate punching resistance load is expressed as :

$$P_u = \pi c f_{co} \sqrt{\omega \omega_w} d(1 - \frac{\omega}{2}) \tag{6.10}$$

where:

f_{co} is the maximum compressive stress of concrete.

$\omega = \rho \frac{f_y}{f_{co}}$

$\omega_w = \frac{f_{ct}}{f_{co}}$

The compression stress f_{co} was derived from the modified Coulomb failure criterion applied to the co-acting shear (τ) and the compression (f_{co}) at the bottom of the compression zone.

$$f_{co} = f_{cc} \frac{3 + 5\sqrt{1 - 16(\frac{\tau}{f_{cc}})^2}}{8} \tag{6.11}$$

$$\tau = \sqrt{\rho f_y f_{ct}} \tag{6.12}$$

In the absence of shear reinforcement, the vertical tension must be provided by the concrete and its limit value is estimated by Kupfer and Gerstle as:

$$f_{ct} = 0.3 f_{cc}^{\frac{2}{3}} \tag{6.13}$$

(This equation is the same as the one recommended by the CEB-FIP code.)

It was demonstrated that the stresses in the remainder of the slab do not exceed yield or limit values in slabs without shear reinforcement so long as:

$$\omega_w + \omega \leq 1 \tag{6.14}$$

The maximum value of ω is 0.5. Once ω exceeds this value, the slab will be over reinforced.

The inclination angle α of the failure surface with respect to the horizontal is given by the relation:

$$\tan\alpha = \sqrt{\frac{\omega_w}{\omega}} \tag{6.15}$$

For a slab with ring reinforcement ($\omega = \omega_w$), the radial tensile stress is resisted by the concrete only, and the slab can be considered as a slab with a circular hole in the middle loaded with concentric loads along the periphery of the hole. So the ultimate punching resistance load P_{ul} is given by the equation(6.9). Regan demonstrated that for the case of a slab with isotropic reinforcement, its strength can be expressed as :

$$P_u = P_{ul}\cot\alpha \tag{6.16}$$

For the case of slab with shear reinforcement, the parameter ω_w will be replaced by ω_{ws}, which is function of the shear reinforcement ratio ρ_{ws}, f_y and f_{co}.

$$\omega_{ws} = \rho_{ws}\frac{f_y}{f_{co}} \tag{6.17}$$

Then, the ultimate punching shear resistance load and the inclination angle of the failure surface are expressed as:

$$P_u = \pi c f_{co}\sqrt{\omega\omega_{ws}}d(1-\frac{\omega}{2}) \tag{6.18}$$

$$\tan\alpha = \sqrt{\frac{\omega}{\omega_{ws}}} \tag{6.19}$$

The maximum distance r_3 from which the shear reinforcement should be placed is given by :

$$r_3 = \frac{1}{2}\left(\frac{C}{2} + 2\sqrt{C^2 - \frac{\omega_{ws}}{\omega_w}c(C-c)}\right) \tag{6.20}$$

where C is the diameter of the circular slab.

Two conditions should be checked:

$$C^2 - \frac{\omega_{ws}}{\omega_w}c(C-c) > 0 \tag{6.21}$$

and

$$\omega_{ws} + \omega < 1 \tag{6.22}$$

For the case where the loaded area is a rectangle having a side (b_2) longer than the side(b_1), the punching analysis is applied around the short ends while the remaining slab strips spanning onto the longer sides are treated as one-way members like wide beams. The ultimate resistance punching shear for circular slabs without shear reinforcement is expressed as:

$$P_u = \left[2(b_2 - b_1)\omega d\frac{2}{C - b_1} + \pi b_1\sqrt{\omega\omega_w}\right] f_{co}(1 - \frac{\omega}{2}) \tag{6.23}$$

6.3.4 Discussion

The given model equations were applied to selected test data for circular and square slabs of previous investigators. The residual values are plotted against the measured load test values in Figure (6.8). As it can be seen in this graph, the results predicted by the model are overestimated. The average of the ratio (P_{test}/P_u) for the selected tested slabs is 0.70 and the overall coefficient of variation is 35.4%.

The punching failure was assumed to take place when the applied forces exceed the tensile resistance of concrete. The main problem here is how to calculate the resistance of concrete in tension. The author used the formula (6.13) given by Kupfer and Gerstle to relate the tension stress of concrete to compression stress.

For annular circular slabs, and loaded along the periphery of the hole, Pralong assumed that the minimum ratio of reinforcement is 0.5%. This assumption is in accordance with what Gardner [26] suggested. However looking back to equation (6.7), the author relates the reinforcement ratio to the concrete and steel parameters, and to the geometry of the slab. Assume that $\rho_{min} = 0.005$, $f_y = 400$ and $f_{cc} = 30MPa$, the minimum radius of the hole will be equal to about 0.7d. The equation (6.9) expresses the ultimate punching load as a function of concrete parameters and neglects the effect of the flexural reinforcement. This assumption is a favorable limit for lower bound solution and could result in a very conservative results.

For circular slabs, the author assumed that reinforcement inside the punching load area reaches the yield point. However, the assumption is valid only for slabs which verify the limitation given by equation (6.14). Therefore the model is not general and is limited to only specified kind of slabs. The author also neglected the contribution of the steel outside the punching load area. In addition to the difficulty of expressing the tensile stress as functior. of the compressive stress of concrete, the calculation of the maximum compressive strength of concrete presents an other difficulty. The expression for f_{co} was derived based on a modified Coulomb Envelope Failure having an angle of 37 degrees. The expression under the square root in the equation (6.11) should be positive that requires a condition on the reinforcement ratio. Pralong suggested that ω, which function of ρ, should have a maximum value of 0.5. This indicates that the model is not

able to predict the punching shear load for heavy reinforced slabs.

Substitution of equation (6.9) and (6.15) into equation (6.16) results on the following equation:

$$P_u = \pi c f_{ct} d \left(1 - \frac{c}{4d(\frac{f_{cc}}{f_{ct}} - 4)}\right) \sqrt{\frac{\rho f_y}{f_{ct}}} \tag{6.24}$$

Thus the predicted resistance of a slab with isotropic reinforcement is predicted to be approximately proportional to the square root of ρf_y and the square root of f_{ct} (or the cube root of f_{cc}). The use of the parameter ρf_y in the model is unique and was not considered in other rational models. It should be noted that Kinnunen and Nylander used ρf_s where f_s is the stress in the reinforcement steel and it could be less than f_y. For small values of c, P_u is approximately proportional to the perimeter of the loaded area. However as c increases the rate of increase of predicted ultimate load decreases. In regard to the influence of c, Pralong's theory differs from all others as P_u tends to zero for a theoretical concentrated point load.

The author's attempt to give expressions for punching resistance load of circular slabs with shear reinforcement, and for slabs subjected to a rectangular loaded area was quite successful. However he was dealing only with simply supported circular slabs. In reality, most slabs are rectangular or square, and can be subjected to lateral restraint.

6.3.5 Summary

In this model the punching failure was assumed to take place when the tensile resistance of concrete reach its limit. The ultimate punching load is proportional to the square root of ρf_y and the cubic root of f_{cc}. The model can not predict the

punching shear load of under-reinforced or heavy reinforced slabs. It is limited to only the normal slabs and it can not distinguish between punching and flexural failure.

6.4 Truss Model

6.4.1 Description of the Model

The idea of modeling the flow of forces between the slab and columns was first proposed by Van Dusen [62]. He proposed the truss model for an edge column as illustrated in Figure 6.9. He did not develop the model beyond the conceptual stage. He noted that the configuration of concrete compression struts is in good agreement with observed crack patterns. Shear is carried by the vertical components of the inclined concrete struts.

Alexander and Simmonds [4] developed this model to a three dimensional space truss composed of concrete compressive struts and steel tension ties. They classified the compression struts into two types:

- Those parallel to the plane of the slab (Anchoring struts).
- Those at some angle α to the plane of the slab(Shear struts).

Both anchoring and shear struts are tied to the column by means of strut steel. Figure 6.10 shows the first type of struts. The compression strut meets the column face at the front at point A, the front corner of the column. Equilibrium of the entire bar-strut assembly is satisfied by summing moments of the bar forces

about this point. The second type can be compared to a case of corbel (Figure 6.11). The geometry of the force triangle is determined by the strut angle α, the magnitude of the compression force in the concrete strut and the magnitude of the tensile force in steel. These three quantities depend on each other.

6.4.2 Basic Assumptions

The development of this model was based on many assumptions:

- The strut steel that ties the anchoring and shear struts to the column includes all steel passing through the column.
- The steel within a distance, equal to the effective depth of the slab (d), of the column is partly effective in developing a compression strut. Its contribution is reduced linearly with the distance from the column, vanishing at a distance equal to d. (No reason for this was given).
- At punching failure the strut steel will always yield.
- Compression failure of concrete strut will never govern.
- The ultimate capacity is reached with the steel bar at yield and the angle of inclination of the compression strut α at some critical value.
- The tensile strength of concrete is proportional to $\sqrt{f_{cc}}$

6.4.3 Equations

The angle α is measured experimentally by taking $\tan\alpha$ equal to the ratio of the failure load to the total area of top mat steel times its yield strength.

$$\tan\alpha = \frac{P_u}{A_s f_y} \tag{6.25}$$

A non-dimensional factor K was defined as follows:

$$K = \frac{Sd'\sqrt{f_{cc}}}{A_b f_y (\frac{b}{d})^{0.25}} \tag{6.26}$$

where:

S : Effective tributary width of reinforcing bars

d' : Cover of reinforcing mat measured from center of mat to near surface of the slab

f_{cc} : Compressive cylinder strength of concrete

A_b : Area of single reinforcing bar

f_y : Steel yield stress

b : Dimension of column face perpendicular to bar being considered

d : Effective depth of slab

A design equation that relates α to K was proposed:

$$\tan\alpha = 1 - e^{-2.25K} \qquad (SI) \tag{6.27}$$

or

$$\tan\alpha = 1 - e^{-0.85K} \qquad (Imperial) \tag{6.28}$$

where stresses are in MPa for SI units and ksi for imperial units.

6.4.4 Discussion

The authors' approach has been developed for edge columns, but they claimed the model has general validity and it was calibrated by tests on internal columns.

The author's test results and those selected from the literature were analyzed using this model. the test data considered are given in the appendix. These slabs and the column have either circular or square shape. To apply the model each face should be treated independently to take the effect the column shape. To simplify the procedure, circular column were replaced by square column of the same area as the original one. The load is either applied on the middle of the slabs which are simply supported along their peripheries, or it is applied around the edges for the case of slabs supported at the middle by a strut column. Figure 6.12 shows the comparison of the test results with the values predicted by the model. It can be seen that most of the points are below the horizontal unity line. That does not mean that the model is safe, but when the non-random distribution of the points of residual values around the horizontal line can be noted. This proves that this model has trouble predicting the ultimate punching resistance of a reinforced concrete flat slab at interior columns.

The beauty of truss models is that they allow the designer to detail the reinforcement in the way that is most beneficial for the structure. However, this can not be done based on unrealistic assumptions which could lead to absurd results, and leave the designer in real trouble. The principal difficulties that Alexander and Simmonds faced in developing their model are the geometric arrangement of the concrete struts and the evaluation of the strength measure to associate with compressive strut failure. The authors circumvent these problems by assuming that the compression failure of concrete strut will never govern and is always associated with yielding of the reinforcing steel. They justified this unrealistic assumption by the fact that most test slabs in the laboratory show steel yielding at failure. Therefore, the model predicted the punching failure resistance of the slab-column connection in the similar way as the yield line theory. Hence, this model will not make any difference between the flexural and the punching failure

modes.

Beastrup [53] noted that yielding of flexural steel is observed in the majority of slab tests might reflect the inability of the test specimens to correctly model the conditions in prototype structures. Regan [56] measured strains around the columns during tests, and noted that not all the reinforcement yielded. Also the above assumption is unrealistic for the case of heavy reinforced slab-column connection. Based on that assumption the punching resistance exclusively depends on the reinforcement, the punching capacity will vanishes in the absence of flexural reinforcement. This means that the lateral restraint provided to the slab by means other than slab reinforcement has no effect. Moreover, it means there will be no assignment of shear strength when the reinforcement is placed more than one slab depth (d) away from the column.

The assumption of that the contribution of steel within a distance d from the column faces, was not justified by the authors. In addition, it appears that the authors assumed the failure surface takes place around the column peripheries which is not the case and contradict what they suggested in equation 6.25. In another way, knowing the angle α defined by the equation (6.25), the position of the shear crack can be determined. It is generally agreed that the stress in steel is high in the shear crack compared to other regions. Thus their assumption is not realistic.

The assumption that the tensile strength of concrete is proportional to the square root of the compressive strength seems to be reasonable assumption as it was discussed in the Chapter 5. However most of the European researchers and design codes favor the use of the cubic relationship ($P_u \propto (f_{cc})^{\frac{1}{3}}$). In fact Regan and Beastrup [53] showed that the use of the square root relationship does not seem to cause any marked error but the lack of size factor does mean that the

ratio of test to calculated punching shear load tend to be low for thicker and high for thinner slabs. Figure 6.13 shows no considerable effect when $f_{cc}^{\frac{1}{3}}$ is used.

The design formula suggested by the authors differs from conventional formulas by the fact that the strength of the reinforcement f_y that enters, rather than the ratio ρ. But, as discussed in the previous Chapter, tests by Moe [44] showed that the yield stress of the reinforcement has no influence on the punching resistance. If one focuses on the relation between $\tan\alpha$ and K, it can be noted that an increase in reinforcement will not vary the strength of a slab-column connection too much, because both variables depend on $A_s f_y$, and so the increased contribution is cancelled out. This can be explained mathematically in another way: Using the SI units, the maximum value of K was found to be 0.62. The design equation was drawn and it is shown in Figure 6.14. Looking to the distribution of the points, the equation line can be replaced by a straight line. A least square fitting gives the following line equation:

$$\tan\alpha = 1.6K \tag{6.29}$$

Replacing each variable by its expression in the above equation results in the following expression:

$$\frac{P_u}{A_s f_y} = 1.6\frac{Sd'\sqrt{f_{cc}}}{A_b f_y (\frac{b}{d})^{0.25}} \tag{6.30}$$

Knowing that the number of steel bars contributing to the punching strength of the connection n is the ratio of the total area of steel A_s to the area of a single bar:

$$n = \frac{A_s}{A_b} \tag{6.31}$$

Also, n can be expressed as the ratio of a width of the slab area contributing to the punching strength B' to the effective spacing between the bars. Thus the relationship can be written as follows:

$$B' = nS \tag{6.32}$$

Simplifying the equation (6.30) implies:

$$P_u = \frac{1.6B'd'\sqrt{f_{cc}}}{(\frac{b}{d})^{0.25}} \tag{6.33}$$

Although, the whole theory for the developed truss model depend on steel reinforcement, equation (6.33) proves the opposite. In fact, equation (6.33) is close to that suggested by the ACI code, but it has d' instead of d. That means the authors believed that the failure of the slab column connection in punching shear is caused by the failure of the concrete cover to resist the whole applied load. This does not explain the mode of failure because experimentally it was seen that the cracks starts from the tension side and propagate to the compression side. The cover concrete usually fails in tension at low load compared to the ultimate punching load. This phenomenon is better explained in the Kinnunen and Nylander model in the next section. Moreover most researchers agreed that the parameter d' has nothing to do with the punching shear resistance, and if it has an effect, it is negligible. Windisch [53] reported that an increase or reduction of the cover will not have any significant effect on the shear strength. For this reason, in most of punching theories, the effect of the dowel action is neglected, or is just considered to be only a fraction of the punching shear resistance. Kinnunen and Nylander [36] suggested that the dowel effect on a column-slab connection capacity is only 10 percent.

6.4.5 Summary

The approach of applying a truss models to the punching of slab offers the brightest prospects of providing a rational and generally applicable description of the phenomenon. Truss models have been successively applied to beams, but not for the case of slabs. The suggested model by Alexander and Simmonds needs to

be examined again to be more realistic and generally applicable for most cases. The compressive concrete struts need more description and should be taken into account in the model. Cases where, shear reinforcement, holes in slabs or pre-stressing ties are present should be also considered in the model.

6.5 Kinnunen and Nylander's Model

6.5.1 Description of the Model

In 1960, Kinnunen and Nylander [36] proposed a rational mechanical model for the punching failure of slabs. Based upon observations of tests on circular slabs, centrally supported on circular columns affixed to the slabs and loaded the free edges, they considered an idealized structural system shown in Figure 6.15. It consists of central truncated cone confined by the shear crack and segmental slab parts, separated by radial cracks. The segments are regarded as rigid bodies so far as the deformation in a radial plane is concerned and are supposed to be carried by an imaginary compressed conical shell between the column and the root of the shear crack.

The criteria of failure is defined as the collapse of the conical shell. Failure is assumed to occur when the tangential strain reaches an empirical critical value. This proposed model was adopted by the Swedish State Concrete Committee in 1966 in their standard specifications for the design of concrete slabs supported on columns. In 1972, Hewitt [33] extended the model to include effects of horizontal restraint.

6.5.2 Basic Assumptions

- The slab portion outside the shear crack, which is bounded by this crack and by radial cracks, can be regarded as a rigid body so far so the deformation in a radial vertical plane is concerned.
- The slab portion outside the shear crack is assumed to be carried by a compressed conical shell that develops from the column to the root of the shear crack.
- The thickness of the conical shell is assumed to vary in such a manner that the compressive stresses at the intersection with the column and at the root of the shear crack are approximately equal.
- Under load, the rigid slab portion outside the shear crack is assumed to turn around the root of the shear crack: that is the center of rotation C.R.
- The slab portion inside the shear crack, that is the slab portion over the column, is assumed not to undergo any deformation in a radial vertical plane.
- The tensile strain in the reinforcement and the compressive strain in the concrete in compression are assumed to be directly proportional to the angle of rotation ψ of the rigid outer slab portion in a radial vertical plane.

6.5.3 Equations

The expressions given below are slightly modified compared to the original ones, and are valid only for two-way reinforcement with equal spacing. The derivation of these expressions will not be given. For more detail, the reader is advised to

refer to the original document. The units used here are (MPa) for stresses and (mm) for dimensions.

The stress σ_t in the conical shell depends on the side length of the loaded area (c), the effective depth of slab (d), and the compressive strength of concrete (f_{cu}). The relationship between the cube compressive strength of concrete to the cylindrical one is given by the formula (5.3)

For $0 \leq \frac{c}{d} \leq 2$

$$\sigma_t = 31.0(0.35 + \frac{f_{cu}}{49.1})(1 - 0.22\frac{c}{d}) \tag{6.34}$$

For $\frac{c}{d} \geq 2$

$$\sigma_t = 45.2(0.35 + \frac{f_{cu}}{49.1}) \tag{6.35}$$

The inclination angle θ of the conical shell with respect to the horizontal depends on geometry of the slab-column connection. It is a function of c, d, C, and y. The parameters C and y are the diameter of the slab and the distance from the bottom surface of the slab to the root of the shear crack at failure respectively. Thus α can be determined using the equation:

$$(K_y \tan\theta - 1)(\frac{1 - \tan\theta}{1 + \tan^2\theta}) = \frac{1}{4.7}(1 + \frac{y}{b})\ln\frac{C}{b + 2y} \tag{6.36}$$

where $K_y = 1.5(\frac{C-c}{3d-y})$

The resistance load P_u which is transmitted through the conical shell is given by the following equation:

$$P_u = \pi cy\frac{c + 2y}{c + y}\sigma_t f(\theta) \tag{6.37}$$

where $f(\theta) = \sin\theta\cos\theta(1 - \tan\theta)$ and it has a maximum value of 0.207 for $\theta = 22.5$ degrees. To take account of the dowel effect, the authors suggested that P_u should be increased by 10 percent.

Also the resistance load P_u can be expressed as a function of forces in reinforcement R_1 and R_2. (see notations in Figure 6.15). At failure the angle of rotation is expressed as:

$$\psi = \epsilon_{ctr}(1 + \frac{c}{2y}) \tag{6.38}$$

where ϵ_{ctr} is a characteristic value of the circumferential concrete strain at failure and it is dependent on the ratio $\frac{c}{d}$. The following expressions were derived empirically from test results. They were derived on the basis of measurements of the concrete strain in a radial direction on the top surfaces of slabs with ring reinforcement.

For $0 \leq \frac{c}{d} \leq 2$

$$\epsilon_{ctr} = 0.0033(1 - 0.22\frac{c}{d}) \tag{6.39}$$

For $\frac{c}{d} \geq 2$

$$\epsilon_{ctr} = 0.0019 \tag{6.40}$$

Kinnunen [37] later proposed that for slabs with two way reinforcement, $\epsilon_{ctr} = 0.00195$ should be used in equation (6.40)

The distance $C_o/2$ in the plane of reinforcement from the column center to the concentric shear crack at failure, was determined experimentally to be:

$$\frac{C_o}{2} = \frac{c}{2} + 1.8d \tag{6.41}$$

The angle α of failure surface can be calculated as :

$$\alpha = \tan^{-1}\left(\frac{2d}{C_o}\right) \tag{6.42}$$

The yield stress f_y is reached in the reinforcement within a slab area of radius r_s

where:

$$r_s = \psi(d-y)\frac{E_s}{f_y} \tag{6.43}$$

Outside this area, the state of stress in the reinforcement is elastic. (See Figure 6.16)

If the reinforcement ratio, ρ, is low then $r_s > \frac{C_o}{2}$ at failure, which means f_y is reached in all reinforcement. In the alternate case $r_s \leq \frac{C_o}{2}$ and the state of stress is elasto-plastic.

The resultant R_1 of the forces in reinforcement depends on c_o, r_s, d, ρ, f_y and the diameter of the circular slab C_s

For $r_s \geq \frac{C_o}{2}$

$$R_1 = \rho f_y d((r_s - \frac{C_o}{2}) + r_s \ln \frac{C}{r_s}) \tag{6.44}$$

For $r_s \leq \frac{C_o}{2}$

$$R_1 = \rho f_y d(r_s \ln \frac{C}{C_o}) \tag{6.45}$$

For determining the force R_2, which acts at the section $r = C_o/2$ in a radial direction, the two way reinforcement inside the shear crack is regarded as a circular mat loaded by a uniformly distributed tensile force $\frac{R_2}{\frac{C_o}{2}\Delta\varphi}$ per unit length, which acts in an outward radial direction and which produces a constant tension in all directions. ($\Delta\varphi$ is the angle of a sector element of the slab over a column)

For $r_s \leq \frac{C_o}{2}$

$$\frac{R_2}{\Delta\varphi} = \rho f_y dr_s \tag{6.46}$$

For $r_s \geq \frac{C_o}{2}$

$$\frac{R_2}{\Delta\varphi} = \frac{\rho f_y d C_o}{2} \tag{6.47}$$

From equilibrium, the load P_u can be expressed as:

$$P_u = \frac{2\pi}{K_y}(R_1 + \frac{R_2}{\Delta\varphi}) \tag{6.48}$$

The only unknowns in all the above equations are y, and P_u. So, this two equations system can be solved by trial and error. That is the ultimate load P_u can be determined by successive calculations. It is convenient to assume a certain value of y and calculate P_u using both equations. If the values of P are different adjust y until they become equal.

6.5.4 Discussion

This rational model was developed by Kinnunen and Nylander based on their experimental work done on different slabs with the same dimensions and with different kind of arrangement of reinforcement. To study this model, 90 two-way reinforced concrete slabs tested for punching shear by previous investigators were chosen to check its validity. It was found that the theory is useful for the determination of the punching shear strength of simply supported isotropically reinforced, circular or square flat concrete slabs, of uniform thickness and loaded with a single central load applied normally to the slab. The equivalent diameter of a non-circular slab or loaded area is taken to be the diameter of a circle having the same area as the original one. The problem with this model is that too much calculation and iteration processes are involved and it is suitable only for computer use. The calculation of the ultimate load P_u proceeds in the following steps suggested by Kinnunen and Nylander.

1. Select a value for y (it is convenient to start with y = 0.3d)

2. Calculate:

   (a) σ_t from equation (6.34) or (6.35)

   (b) tan(θ) for f(θ) from equation (6.36).

   (c) P_1 from equation (6.37)

3. calculate:

   (a) ψ from equation(6.38)

   (b) C_o from equation (6.41)

   (c) r_s from equation (6.43)

   (d) R_1 from equation (6.44) or (6.45)

   (e) R_2 from equation (6.46) or (6.47)

   (f) P_2 from equation (6.48)

4. If the values of P_1 and P_2 differ significantly, select a new value for y and repeat the calculation at step 3 until the two values of P are sufficiently similar.

The theory appears to be equally useful when the load is applied through a column affixed to the slab and when it is applied through a loading plate.

A small program has been developed to calculate the ultimate punching resistance of flat slabs following the above steps. If the two values of P were found to be sufficiently different, the value of y will be changed to $\frac{y}{2}(1+\frac{P_2}{P_1})$ and the iterative calculation of P_1 and P_2 will be continued until the difference between P_1 and P_2 is less than 1% of P_2. If the solution diverges or y gets greater than d, a

simple progressive search for y is entered. When the solution has closed, the theoretical punching shear load P_u will be the average of P_1 and P_2. A flow chart of the program is shown in Figure 6.17. The program first was checked with tests and the results reported by Kinnunen and Nylander. With this program, the solution closes within 3 to 10 iterations only. Looking to Table 6.4, the coefficient of variation of the test load to the predicted load ratio is 17.6%. It is also apparent that during the analysis of the 90 slabs selected previously, that the theory of Kinnunen and Nylander was unreliable for estimating the ultimate punching load of some slabs. Therefore there should be some limitations to the application of this model. Hewitt and Batchelor (36) showed that the theory is applicable only to slabs with parameters within the following limits.

- $4 \leq C/d \leq 17$
- 186000 MPa $\leq E_s \leq$ 228000 MPa
- $0.05 \leq \frac{\rho f_y}{f_{cc}} \leq 0.45$
- $\frac{c}{d} \leq 6$

In the case of the fourth limitation the Swedish State Concrete Committee suggested that the theory of Kinnunen and Nylander should be restricted to the analysis of slabs with values of $\frac{c}{d}$ less than or equal to 3.5, but Hewitt and Batchelor showed that $\frac{c}{d}$ can go up to 6 and the model still gives a safe estimation of the punching load. Among other limitation that should be considered in any model, is the restriction on the support length. That is where the failure surface intersects with the support line, the mode of failure will change. Most researchers agree that the experimentally observed angle of failure surface to the horizontal varies between 22 to 30 degrees. Taking the extreme case, the minimum support

length required is (5d+ c). Among the 90 slabs selected for the analysis, only 37 of them have the parameters within the limits imposed previously. For these 37 slabs, the mean value of the ratio of the test load to the calculated ultimate load is 0.82, 1.12 and 1.07 for the slab tested by the author,Gardner and Kinnunen and Nylander respectively. The low calculated values for some specimens can be attributed to dowel and membrane effects as Hewitt and Batchelor reported. Kinnunen and Nylander found that their theory gave values for the punching shear load which were in satisfactory agreement with results of their own tests as well as those of Elstner and Hognestand. They attributed low calculated values in the case of two way reinforcement, to dowel and membrane effects and suggested that they should be taken into account by multiplying the calculated ultimate load by 1.1.

Hewitt and Batchelor applied this model to the 93 footings tested by Richart and to 41 slabs tested by different investigators. They suggested that the theoretical ultimate punching load should be multiplied by a "dowel factor" , which includes the effects of both dowel and tensile membrane action, of 1.2. The analysis of the 34 slabs chosen above, showed that neither a factor of 1.1 or 1.2 is a proper value to choose and it should not be constant. In fact it depends on many factors notably, as Kinnunen reported in his second publication, such as: the strength properties of concrete, the strength properties of the reinforcing steel, the bond between the steel and the concrete, the amount of reinforcement, the diameter of the reinforcing bars, the anchorage, the embedment of the reinforcement in concrete, the thickness of the concrete cover, the direction of the reinforcing bars with reference to the shear crack and the slope of the shear crack. However almost all the theoretical values of the ultimate punching load determined using this model can be considered safe.

The assumption that the compressive stresses in the conical shell were approximately constant throughout, was made in neglect of probable shearing stresses on the shell surfaces. This assumption was not explained by the authors, but just justified , along with their criterion of failure by showing consistent satisfactory agreement between the calculated and test punching loads.

Lightweight aggregate concrete slabs tested by Mower and Vanderbilt were analyzed and the theory was found to give inaccurate estimates of the punching loads. A mean value of the test to the predicted load ratio was found to be 1.03 with a coefficient of variation of 19.9 percent. This is not surprising considering that Mower and Vanderbilt concluded that the empirical equations of Moe which have been proved useful for normal concrete slabs were not adequate for lightweight aggregate concrete slabs. Also the ratio of $\frac{c}{d}$ of the slabs tested by Mower and Vanderbilt were greater than the maximum limit suggested here for the Kinnunen and Nylander model which may have a considerable effect on the predicted loads.

3.5.5 Summary

This rational model for slab-column connections can be considered as the best of all the recently proposed ones. The model is able to predict the ultimate load irrespective of whether the type of failure is flexural failure or punching failure. It gives a continuous transition between these two types of failures. Moreover, contrary to other methods, it also predicts the deformations of the slabs at failure. Assumptions made in calculations were the elastic property of concrete in compression, and the limiting compressive stress taken as that for uniaxial compression. The validity of these assumptions were justified by the good agreement

the theoretical and the test results. The calculation procedures and the numerical constants obtained were based on tests of slabs of fixed dimensions. That is the reason why the model has some trouble to predict the punching shear load of slabs with slightly different configurations and dimensions. In addition, the procedure, which is an iterative process, and which consists of solution of large number of equations, and use of design charts, is too lengthy and is unsuitable for general use.

6.6 Comparison of the Models with Equation(5.8)

Hypothetical slabs (#1 to 12) of typical dimensions and material properties were analyzed in order to compare the models to equation (5.8) with respect to the slab parameters. Parameters of the hypothetical slabs are given in Table 5.8.

Figure 6.19 shows the effect of variation of the concrete compressive strength on the ultimate load predictions by the models and equation (5.8). The linear relationship between P_u and f_{cc} can be clearly seen in the case of the Upper Bound Solution model. The truss model, which uses the square root relationship, predicts the lowest values of P_u. However the Kinnunen and Nylander's and Pralong's Models predict P_u values higher than that predicted by equation (5.8), but the Kinnunen and Nylander model curve runs parallel to the equation curve with a interval of about 30 kN. This means that a cubic root relationship used in equation (5.8) is a good assumption. Also it can be seen that P_u is proportional to twice the cubic root of the concrete strength ($f_{cc}^{\frac{2}{3}}$) in the Pralong's model.

Figure 6.20, shows the effect of variation of the flexural steel reinforcement ratio on the ultimate punching shear load predicted by the four models and equa-

tions(5.8). The Upper Bound Solution model is presented by a horizontal line because it neglects the effect of steel in punching shear resistance of slabs. The lowest values of Pu are predicted again by the truss model. The closest Model curve to the equation is that of the Kinnunen and Nylander Model. The model and empirical equation curves intersect at ρ= 0.01 , then they diverge from each other. However the curve representing the Pralong's model runs almost parallel to the equation curve.

Figure 6.21 shows the effect of the slab effective depth d on the punching capacity of a slab-column connection. the Upper Bound Solution looks to unreasonable in estimating the ultimate punching load of thick slabs. Also, it can be seen that in Pralong's and the truss model, the punching shear load P_u is linearly dependent of the effective depth of a slab. However, the later model still gives the lowest value of P_u compared to the other models. The closest model prediction to the equation (5.8) is that of Kinnunen and Nylander model.

The relationship between the ratio $\frac{c}{d}$ and the ultimate punching resistance load prediction by the four models and equation (5.8) is shown in Figure 6.22. It can be seen that the Upper Bound Solution and the truss models predict the highest and lowest values of P_u respectively. The Pralong's model curve diverge from the equation curve as $\frac{c}{d}$ increases. The closest curve to the equation (5.8) one is that of Kinnunen and Nylander Model.

6.7 Summary

Among the four rational models studied above, the Kinnunen and Nylander's model can be considered the most complete one. A good predictions similar to those of Kinnunen and Nylander's model may be obtained using the proposed empirical equation (5.8).

Table 6.1: Predictions using Upper Bound Solution model

Investigator	No. of Samples	P_{test}/P_u		
		Mean	St. Deviation	Coef. of Variation
Present work	12	1.26	0.179	0.142
Gardner	18	1.13	0.306	0.271
Els. Hogn.	17	1.17	0.320	0.221
Mow. Vand.	13	0.90	0.199	0.221
Moe	12	1.07	0.139	0.130
Yitzhaki	8	1.36	0.346	0.323
Kin. Nylan.	10	0.92	0.094	0.102
Average		1.14	0.294	0.258

Table 6.2: Predictions using Pralong's model

Investigator	No. of Samples	P_{test}/P_u		
		Mean	St. Deviation	Coef. of Variation
Present work	12	0.82	0.160	0.195
Gardner	18	0.72	0.083	0.115
Els. Hogn.	17	0.616	0.100	0.162
Mow. Vand.	13	0.51	0.130	0.255
Moe	12	0.70	0.110	0.157
Yitzhaki	8	1.12	0.410	0.366
Kin. Nylan.	10	0.71	0.205	0.286
Average		0.70	0.248	0.354

Table 6.3: Predictions using Truss model

Investigator	No. of Samples	P_{test}/P_u		
		Mean	St. Deviation	Coef. of Variation
Present work	12	1.19	1.83	0.086
Gardner	18	0.96	0.126	0.131
Els. Hogn.	17	0.99	0.067	0.068
Mow. Vand.	13	1.31	0.140	0.107
Moe	12	1.00	0.091	0.091
Yitzhaki	8	2.11	0.620	0.294
Kin. Nylan.	10	1.13	0.097	0.086
Average		1.17	0.381	0.326

Table 6.4: Predictions using Kinnunen and Nylander's model

Investigator	No. of Samples	C/d		P_{test}/P_u		
		Min.	Max.	Mean	St. Dev.	Coef. of Var.
Present work	12	4.5	5.25	0.99	0.057	0.057
Gardner	18	4.4	18.0	0.86	0.150	0.174
Els. Hogn.	17	17.6	18.0	1.02	0.099	0.097
Mow. Vand.	13	27.1	27.1	1.03	0.205	0.199
Moe	12	18.1	18.1	1.24	0.162	0.131
Yitzhaki	8	10.7	21.3	1.20	0.118	0.098
Kin. Nylan.	10	13.4	14.6	1.07	0.086	0.080
Average				1.04	0.183	0.176

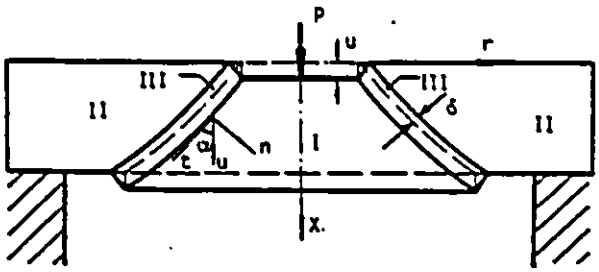

Figure 6.1: Collapse mechanism for the Upper Bound Solution

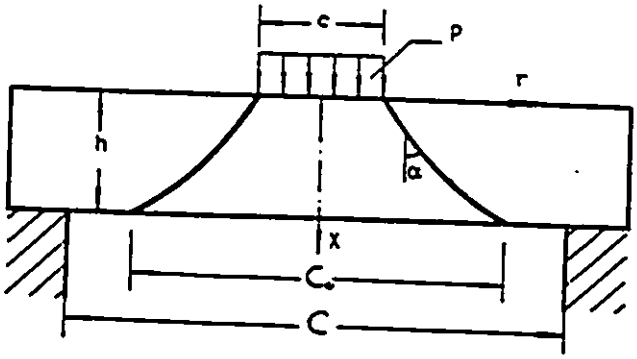

Figure 6.2: Failure mechanism (generatix) for the Upper Bound Solution

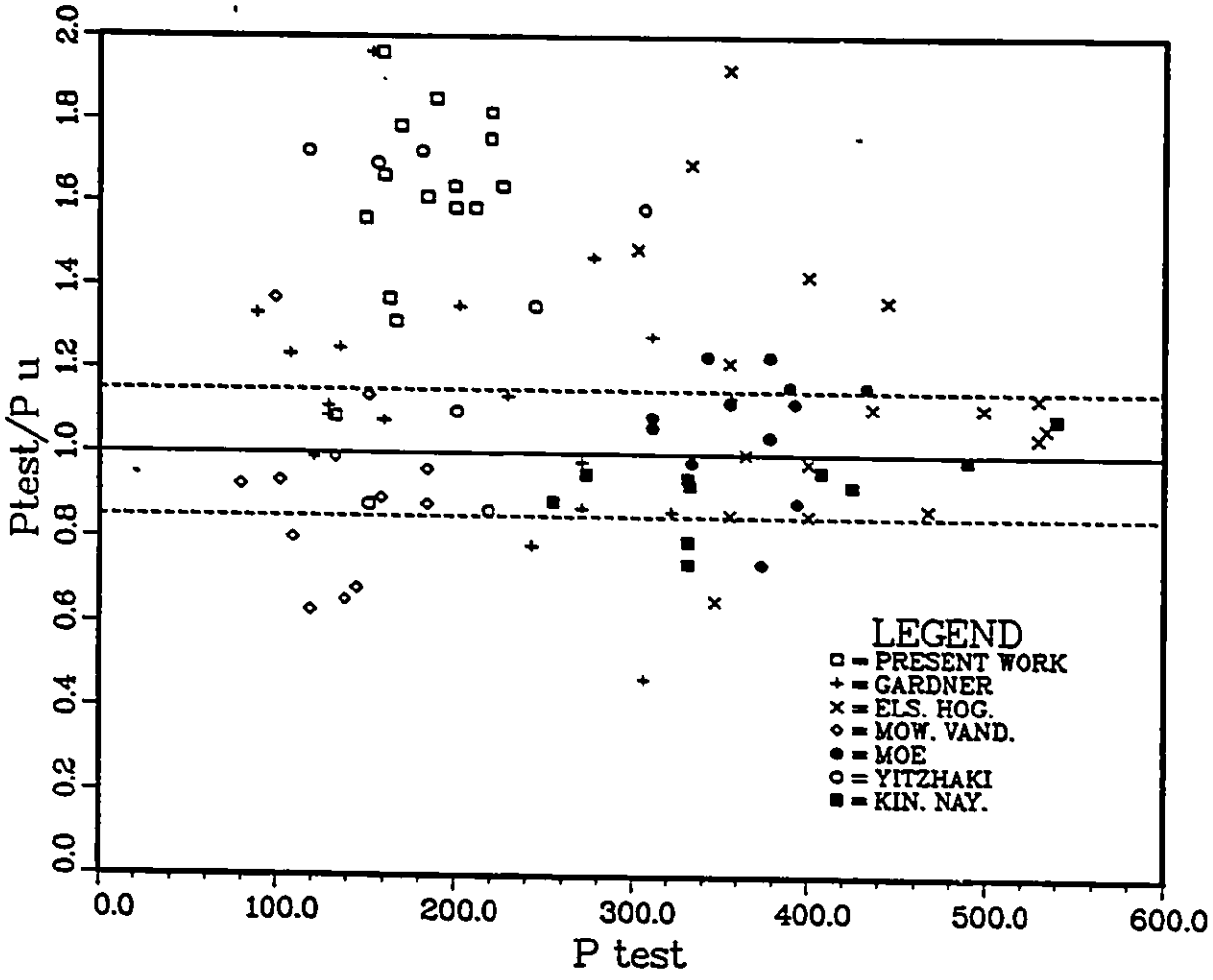

Figure 6.3: Correlation between Upper Bound solution model and tests

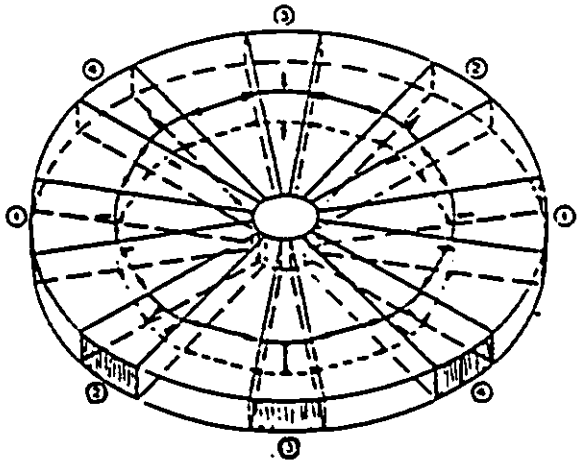

Figure 6.4: Pralong's model: Beams radiating from the center of the slab

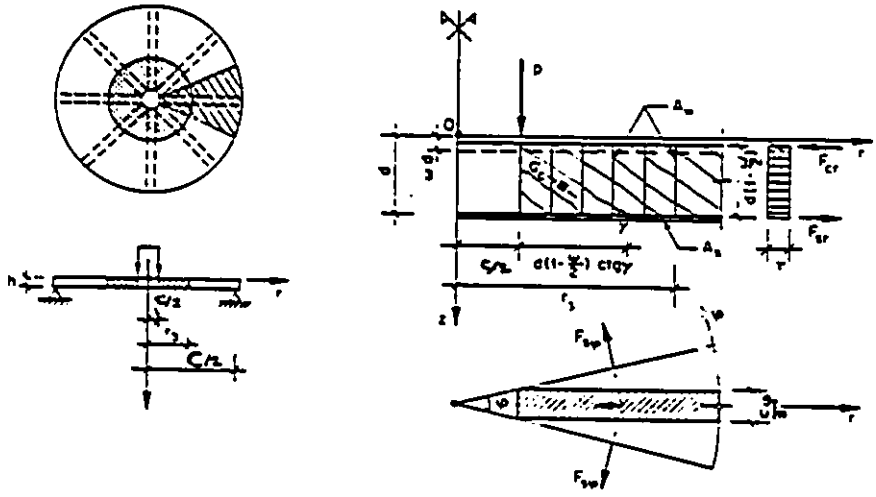

Figure 6.5: Pralong's model: Slabs with shear reinforcement

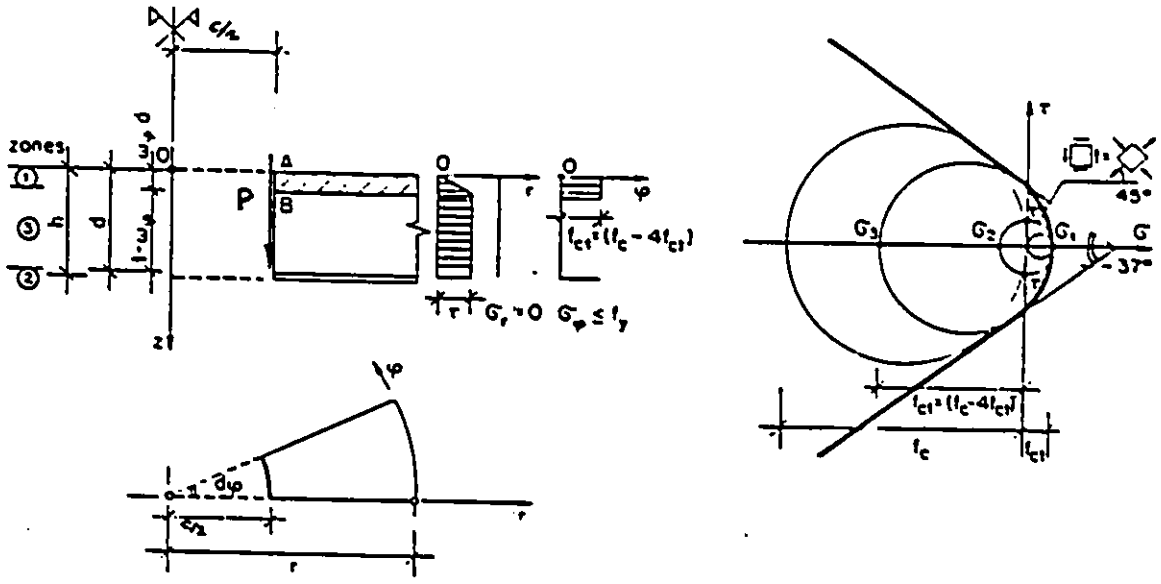

Figure 6.6: Stress distribution of a circular slab with a hole in the middle

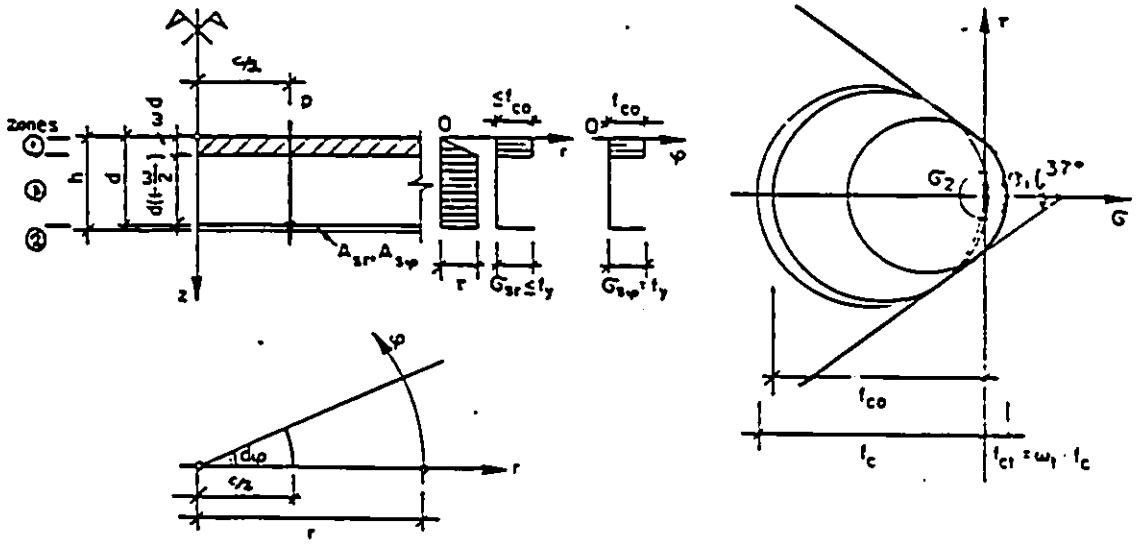

Figure 6.7: Stress distribution for a circular slab

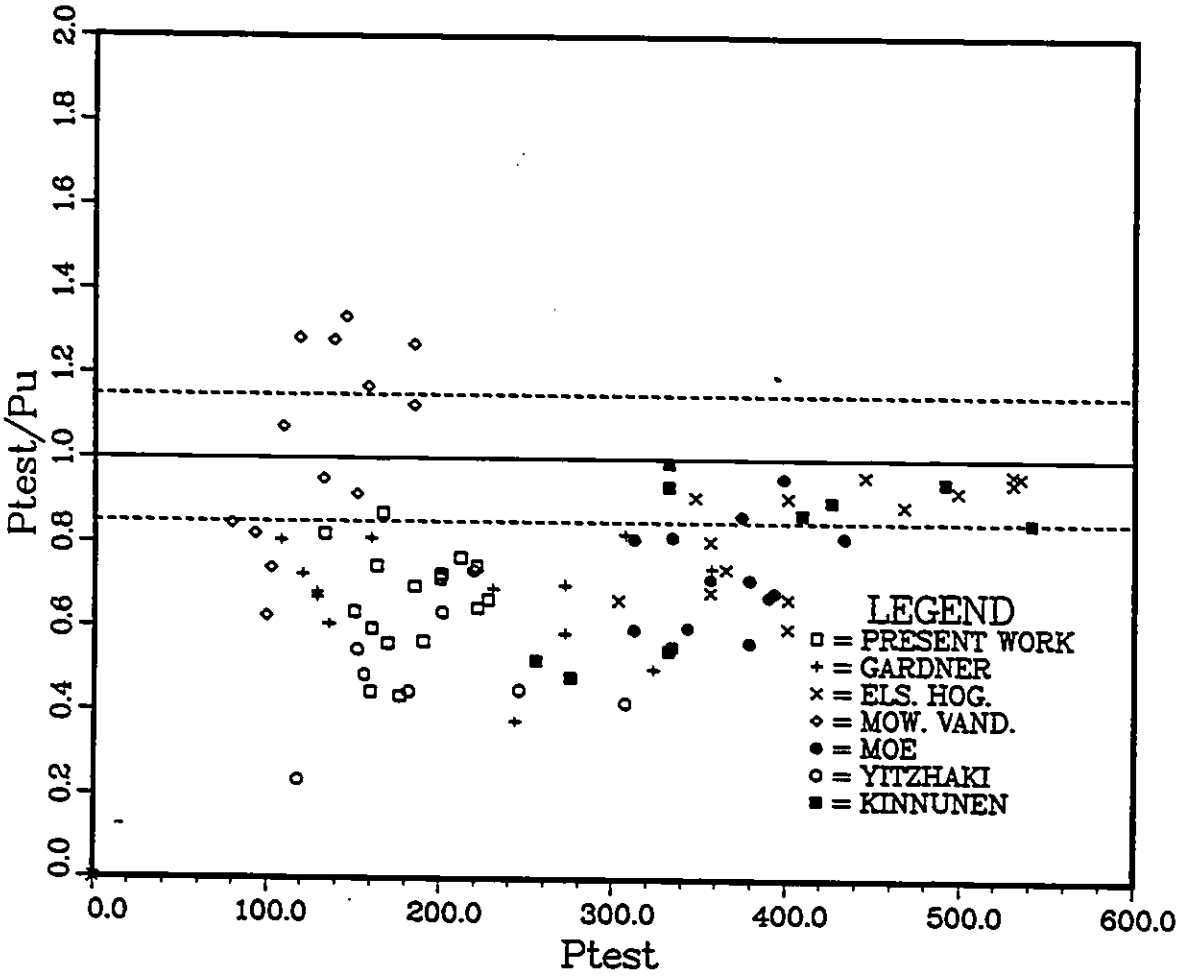

Figure 6.8: Correlation between Pralong's model and tests

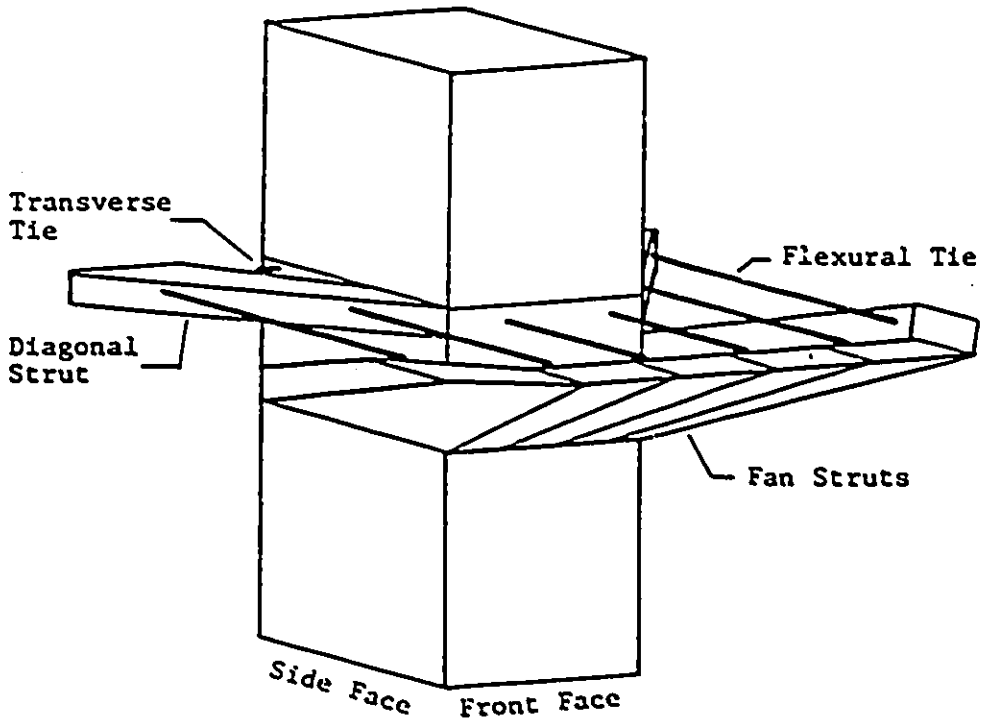

(after Van Dusen)

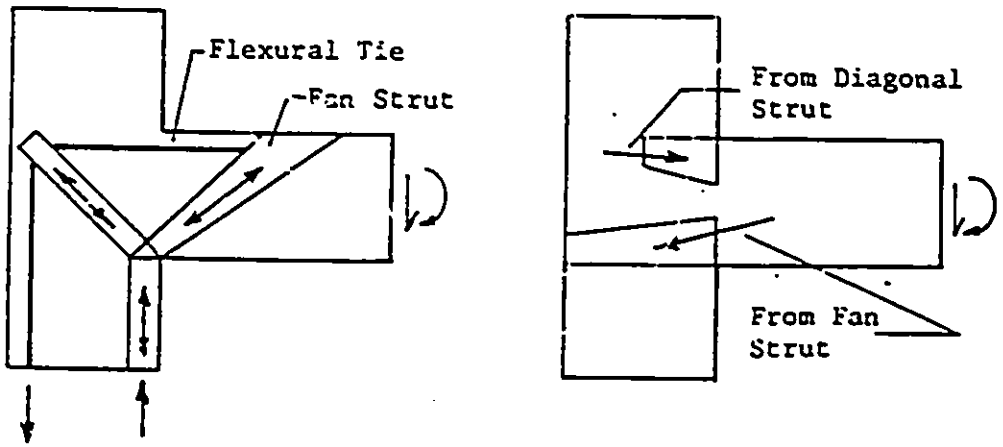

(a) Section Through Front Face

(b) Forces on Side Face

Figure 6.9: Van Dusen's truss model for an edge column

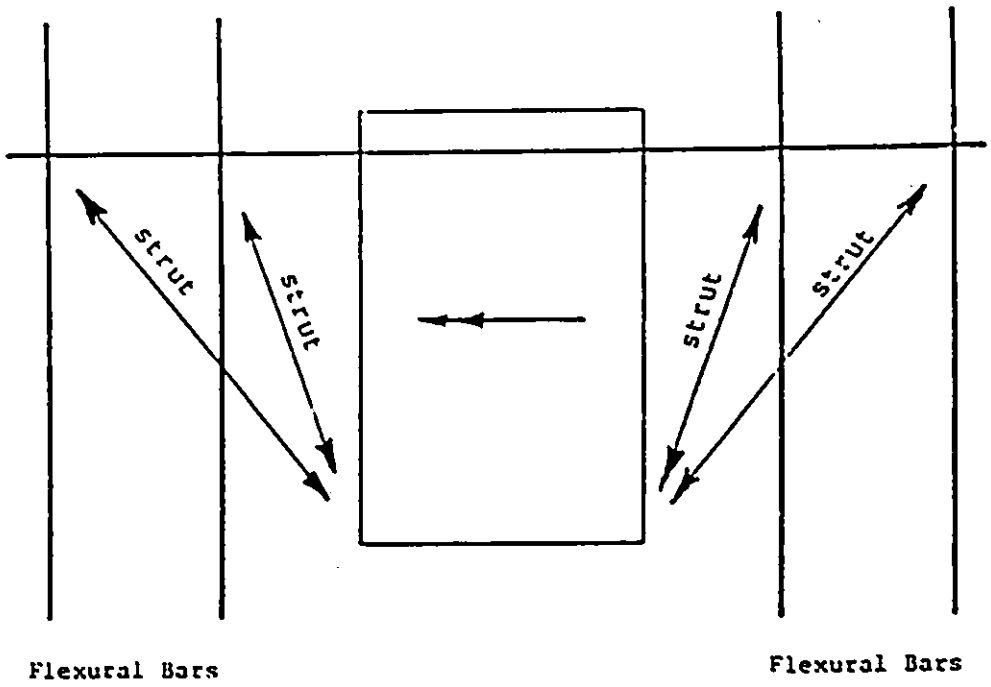

Figure 6.10: Anchoring struts

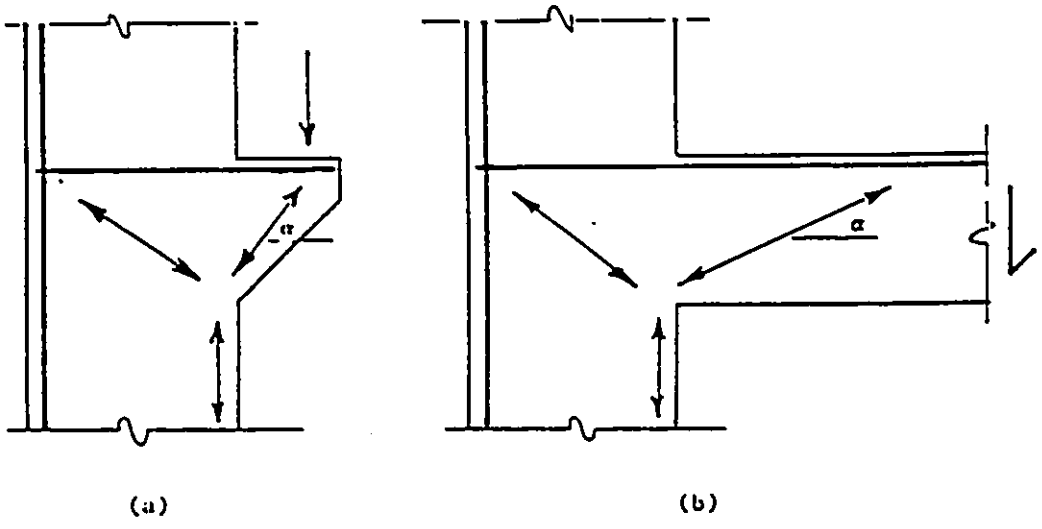

Figure 6.11: Comparison of corbal with out of plane struts

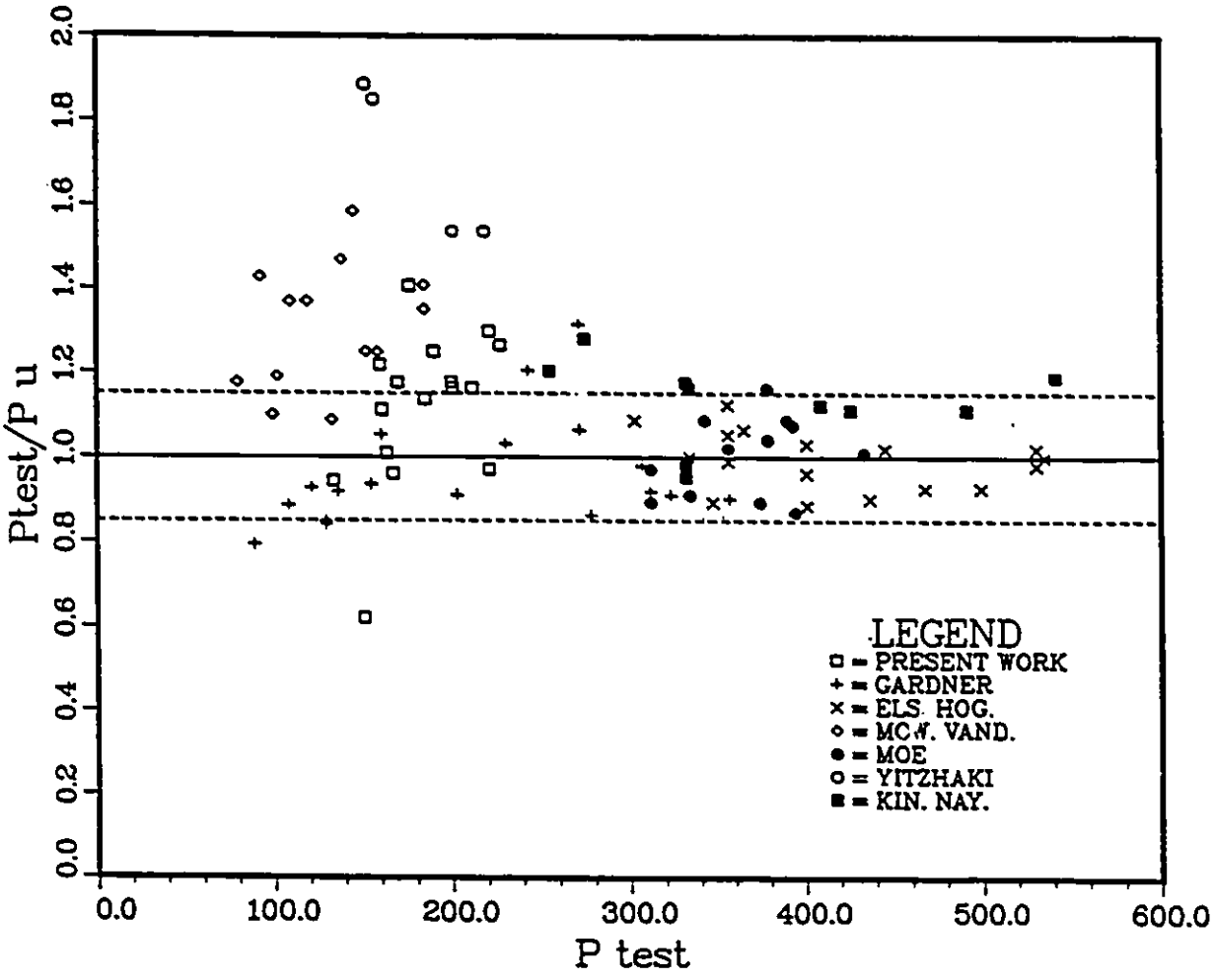

Figure 6.12: Correlation between truss model predictions and tests

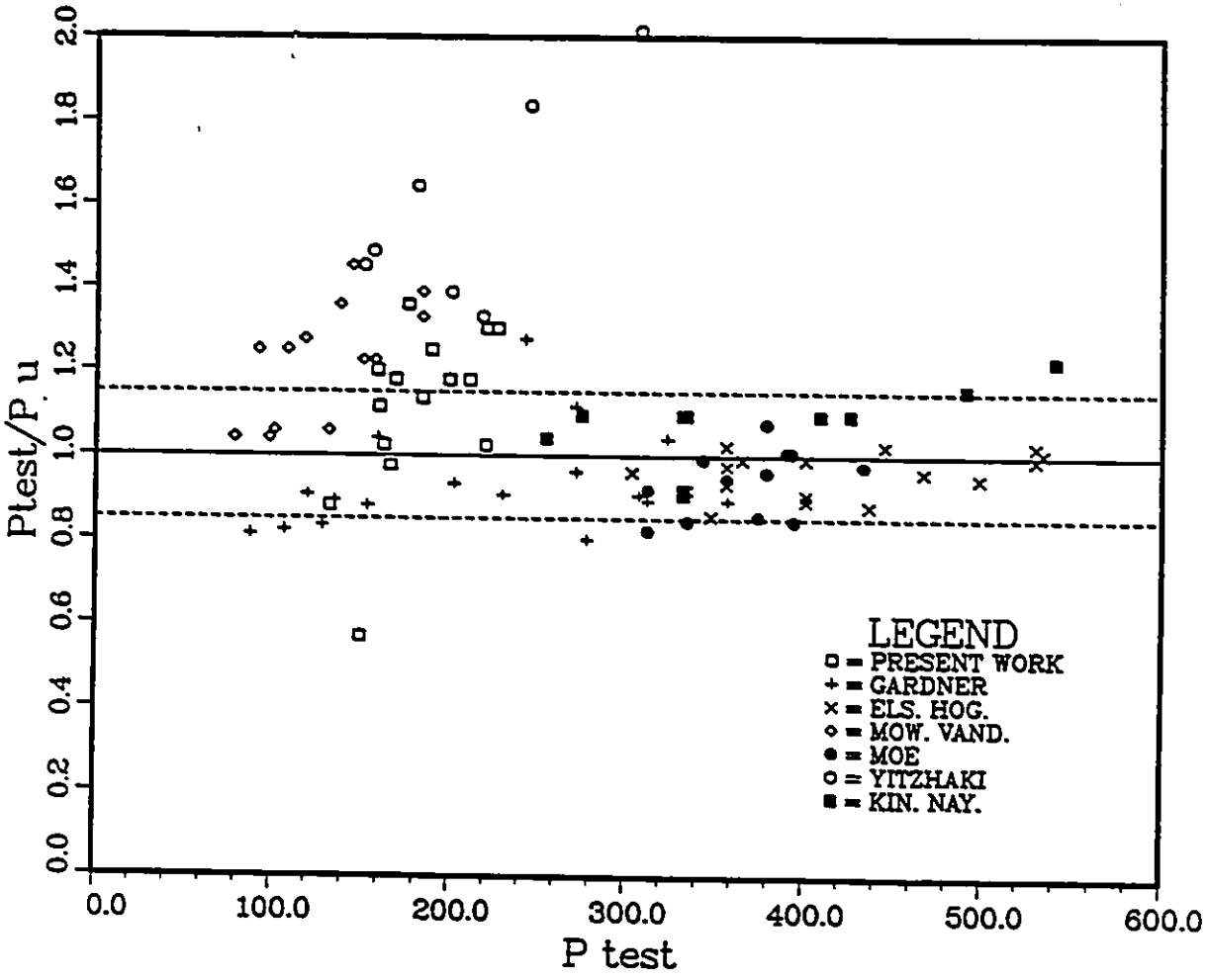

Figure 6.13: Correlation between truss model predictios and tests using cubic root of f_{cc}

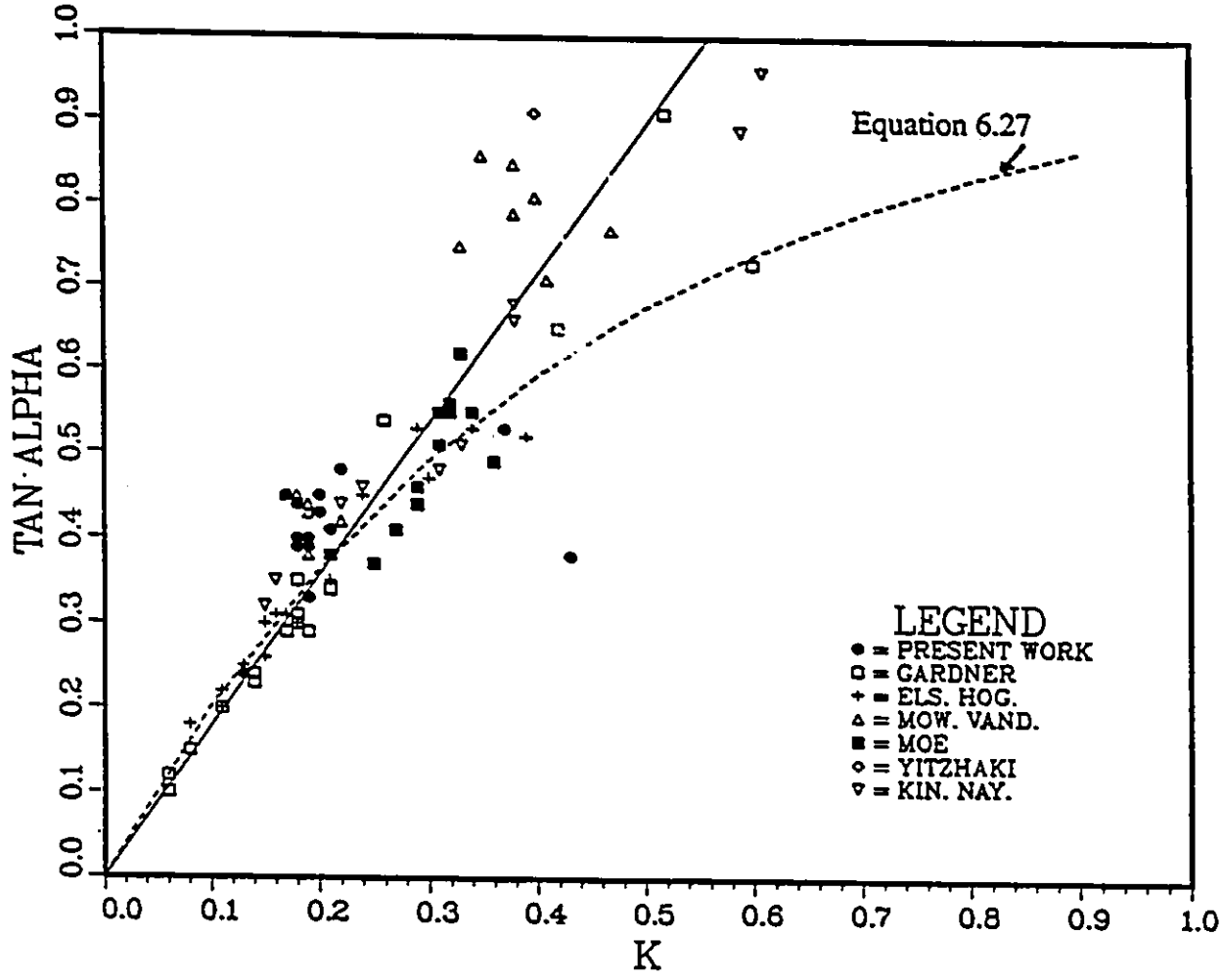

Figure 6.14: Relation between tanα and K for truss model

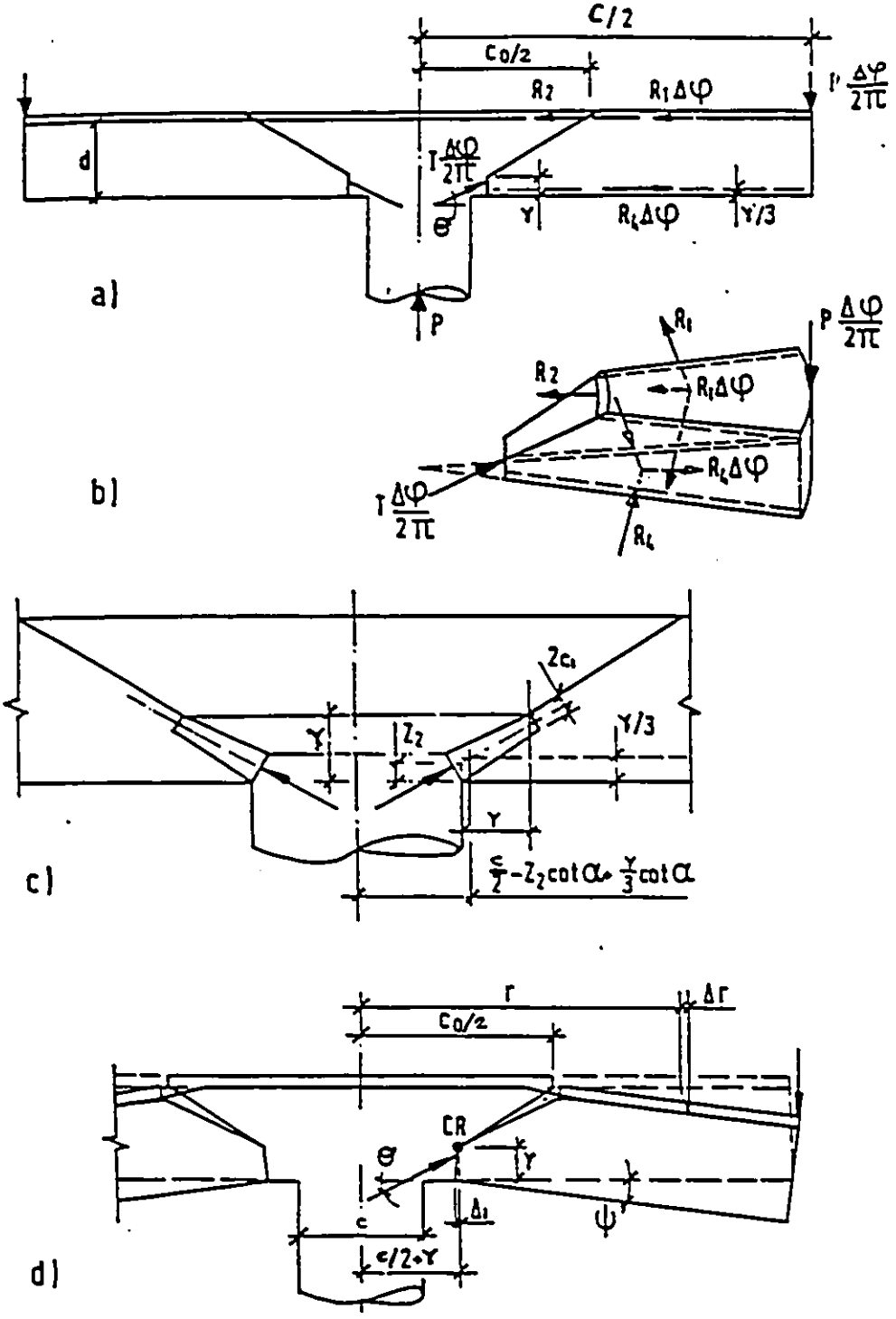

Figure 6.15: Kinnunen and Nylander's model

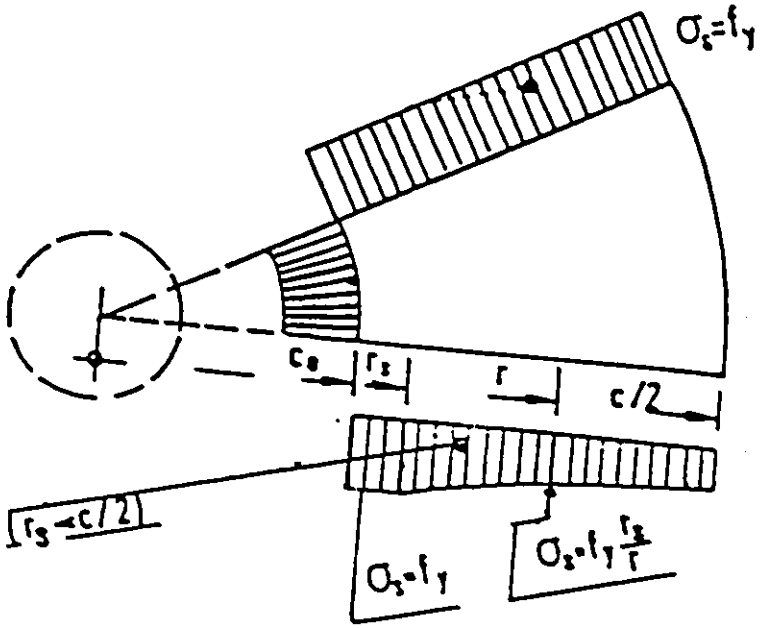

Figure 6.16: Stress distribution in the tangential direction in the flexural reinforcement for Kinnunen and Nylander model

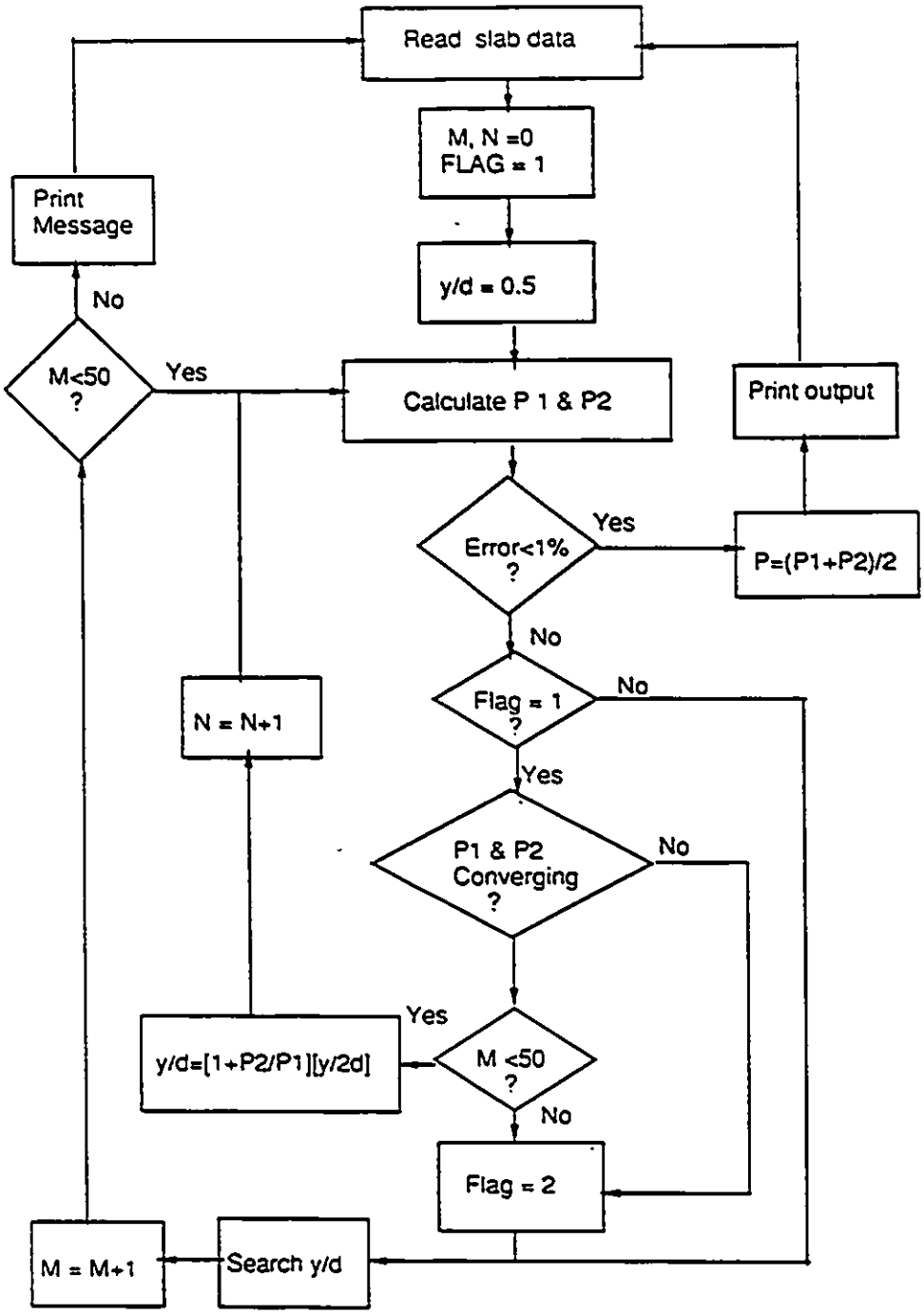

Figure 6.17: Flow chart of the program used for Kinnunen and Nylander' model

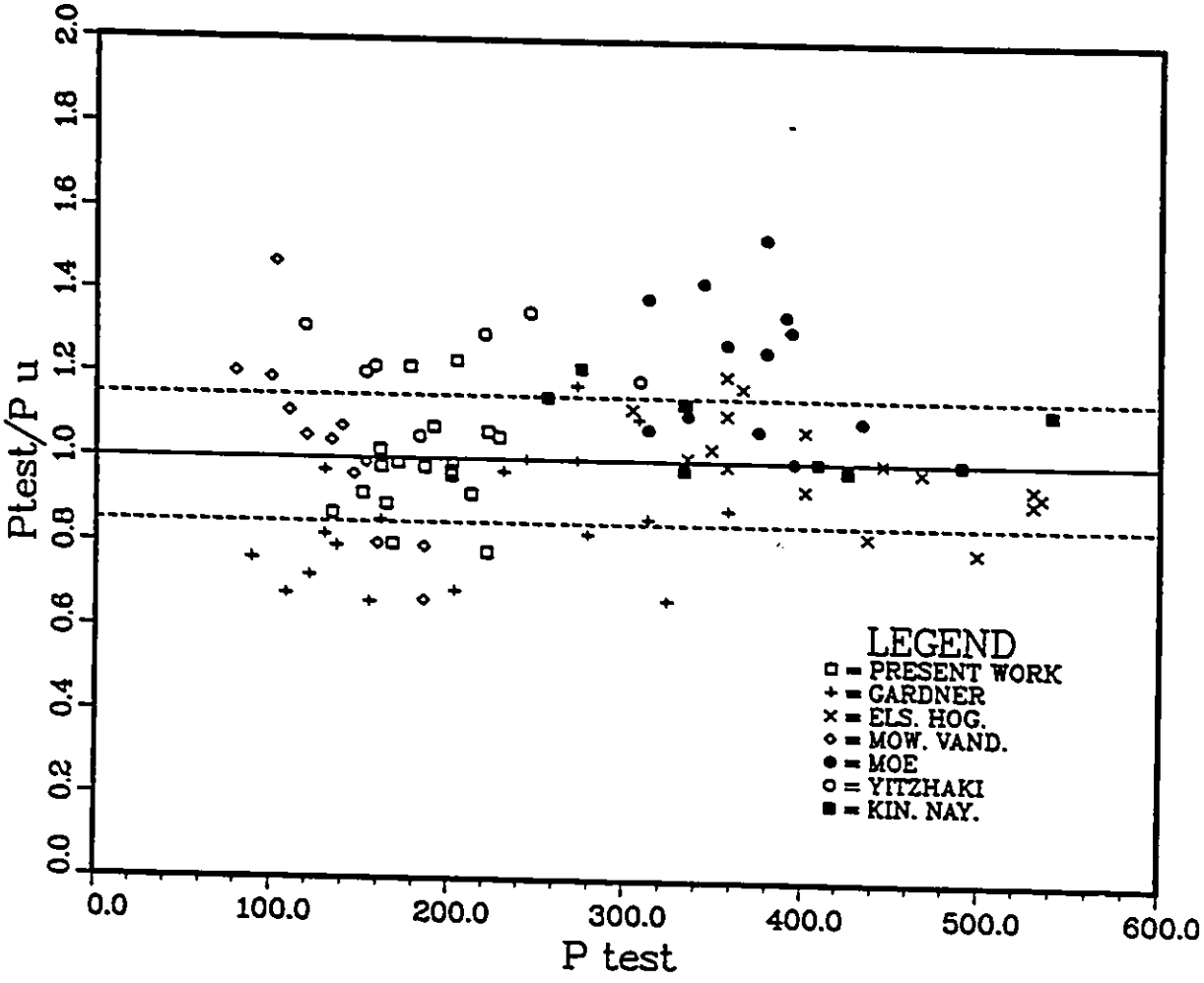

Figure 6.18: Correlation between Kinnunen and Nylander model and tests

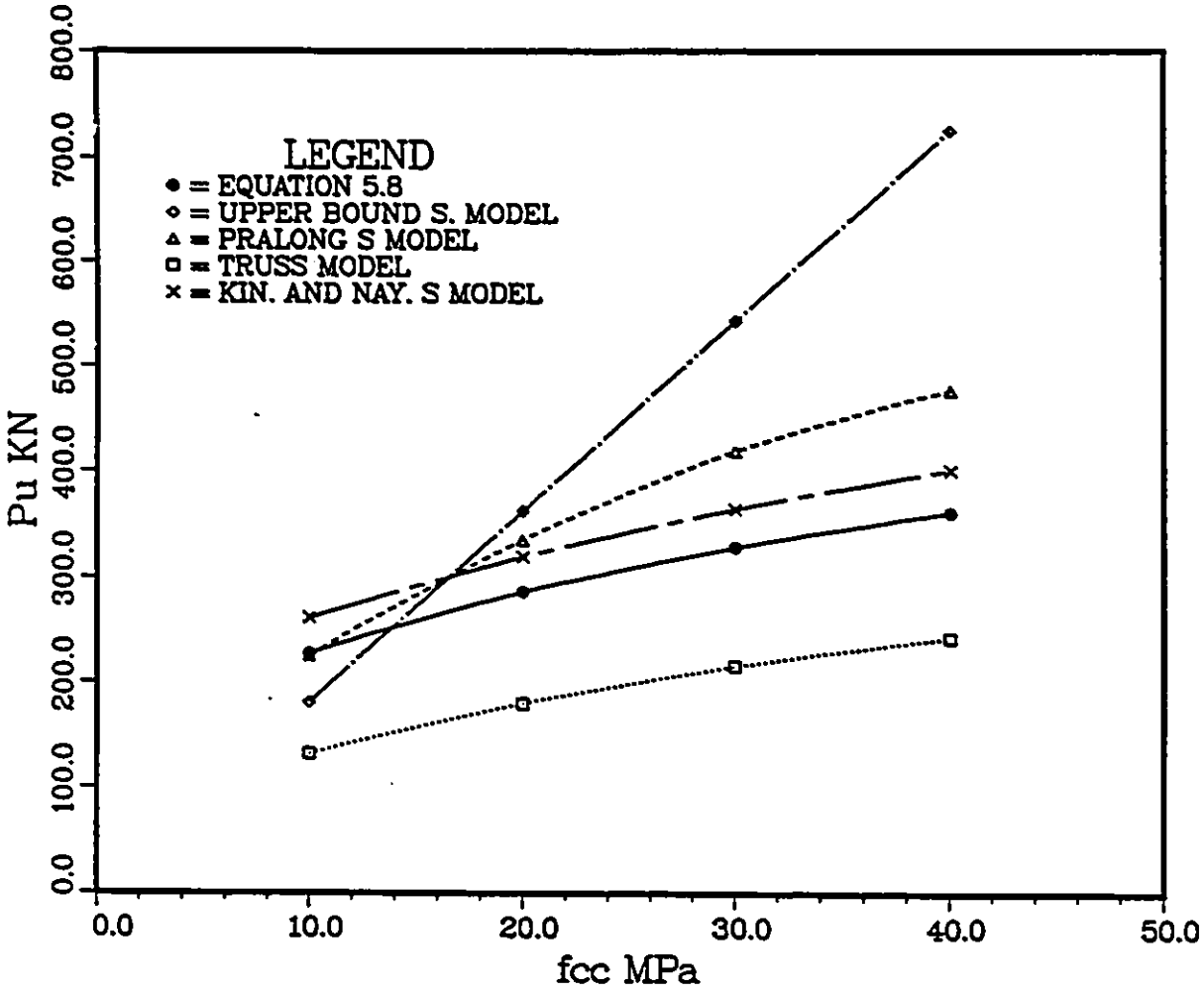

Figure 6.19: Comparison of equation 5.8 with the models with respect to f_{cc}

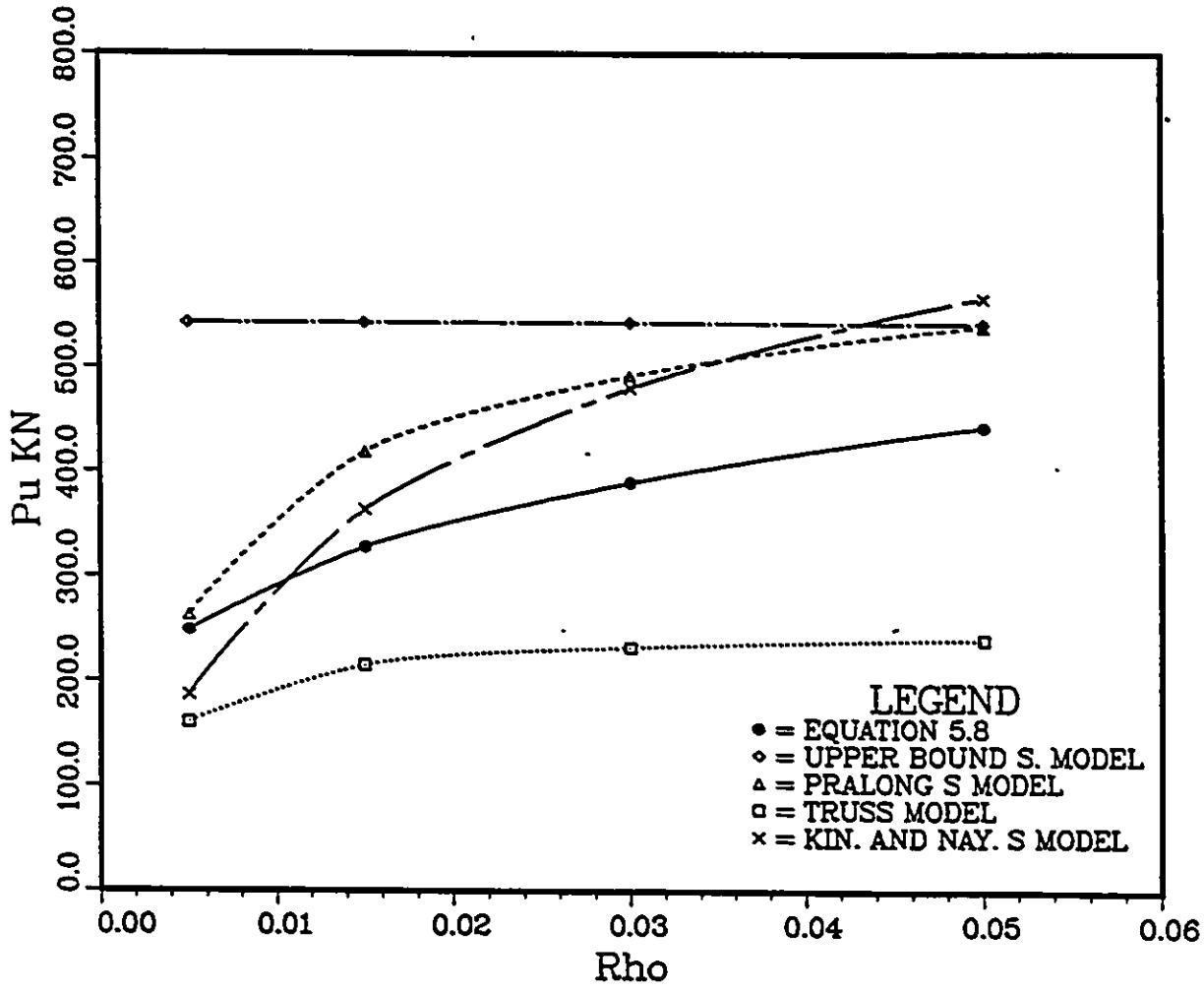

Figure 6.20: Comparison of equation 5.8 with the models with respect to ρ

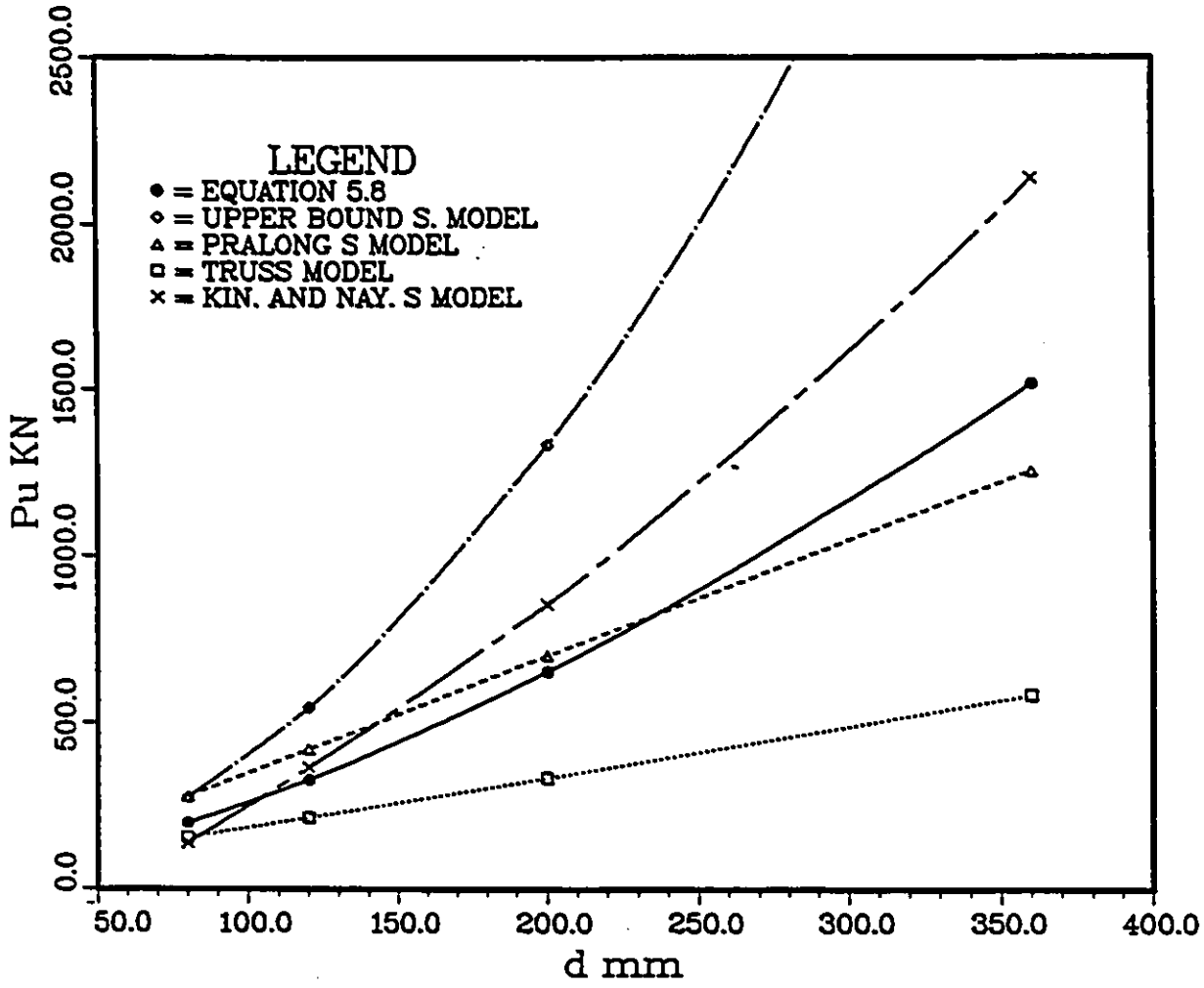

Figure 6.21: Comparison of equation 5.8 with the models with respect to d

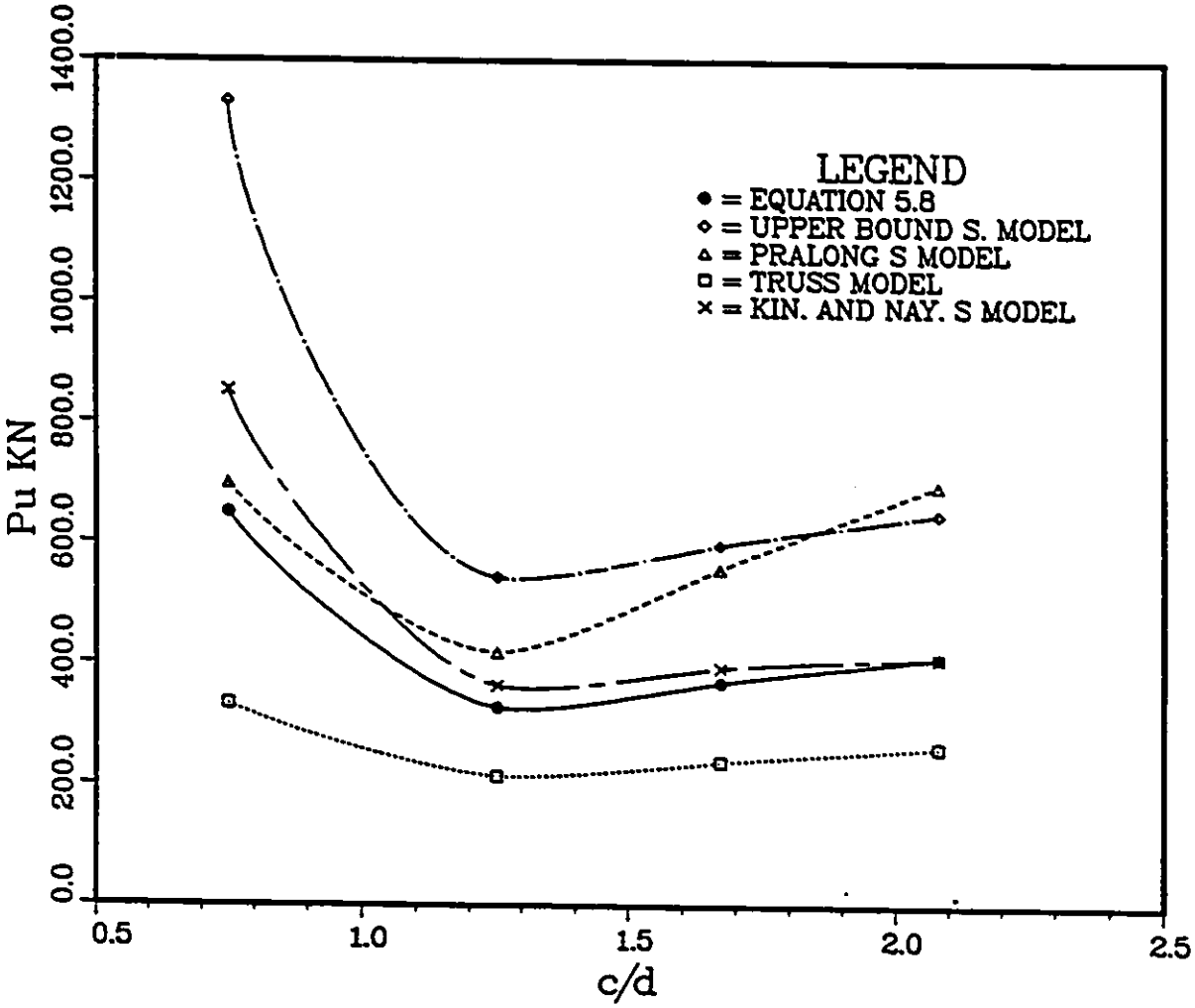

Figure 6.22: Comparison of equation 5.8 with the models with respect to $\frac{c}{d}$

Chapter 7

Conclusions and Recommendations

7.1 Conclusions

Within the scope of the literature review, the experimental work and the theoretical investigation reported in this thesis on symmetric punching shear of reinforced concrete slabs, the following conclusions may be drawn:

- In respect of symmetric punching shear of slab without shear reinforcement, there is a major agreement between most researchers about behaviour. Longitudinal and radial flexural cracks in tension side may appear at about 60 % of the ultimate load. At the periphery of the column, the compression zone resists transverse load by inclined radial compression. Additional load is carried by interface forces across the cracks and by dowel action of the flexural reinforcement.

- Even though compression reinforcement theoretically increases the flexural strength of the slabs, it does not increase significantly its punching resistance. Furthermore, placement of compression reinforcement may be harmful some times.

- Strengths for loading through circular areas are greater than for loading through square areas. More realistic capacities for square columns can be determined by using a circular one having the same area as the original.

- Concrete cover has no effect on punching shear as long as it is designed with respect to the codes specification. Thick cover may result in high dowel effect of the flexural reinforcement on punching resistance.

- The punching shear resistance of a slab decreases under the effect of cyclic load.

- The punching shear resistance of a slab depends mainly on the ratio of the flexural reinforcement, the effective depth and the compressive strength of concrete and the punch size.

- In addition to their role in carrying vertical loading, bridge girders and diaphragms contribute substantially to lateral confinement which may increase the punching resistance of a bridge deck slab.

- The use of the yield line theory to predict the punching shear resistance of a slab is not recommendable because of the violent and non ductile nature of punching shear failure.

- Strut and tie models could be applied to the punching shear phenomenon if the value of the critical crushing stress of concrete has been determined experimentally.

- The suggested expression of the failure surface A_c in equation (5.1) makes possible the rational treatment of various cases which can not be dealt with satisfactorily by present code methods; namely slabs of various depths, slabs with shear reinforcement and bridge decks.

- The proposed empirical equation (5.8) is simple and give a good predictions similar to those of Kinnunen and Nylander model.

- In principal, British codes are right to take account for flexural and depth effects over a relatively large range of slab depths and the failure of the North American codes to include these effects leads to errors.

- The mathematical solution of the plastic theory is complex and is limited to symmetric punching. Simplified results are not suitable and gives very conservative results.

- Pralong's model is based on a truss model and employs the concrete in tension as the vertical component of a web lattice. This does not seem altogether realistic. Also the model is not adequate for heavy or under-reinforced slabs.

- The proposed truss model by Simmonds and Alexander has trouble predicting the punching shear strength of slabs because of unrealistic assumptions.

- The most complete rational model currently available is that proposed by Kinnunen and Nylander. Using this model, the punching strength of a slab of usual dimensional and material properties can be calculated rapidly and accurately assuming that punching load is enhanced by 10% due to dowel effect.

7.2 Recommendations

In order to arrive at a better understanding of the shear strength of both reinforced and prestressed concrete flat plates it will be necessary to test large scale models which simulate real structures rather than the simply supported plates of past investigations. The descriptions of behaviour and available test results are inedequate for the case of footings or slabs lacking symmetry. 1 It would be desirable to determine the influences of force transfer across cracks and of dowel action. One is to encourage studies aimed at the satisfactory modelling of the phenomenon of punching shear failure of different kind of slab-column joints, because there is a strong foundation to be built upon. To the knowledge of the author, fatigue life of concrete slabs, seismic punching resistance and impact has not been investigated and the codes provisions do not consider these facts. Hence, in view of the potential using of the limit state design, it is felt that the problem require more attention.

Bibliography

[1] ACI Committee 318, *Building Code Requirements for Reinforced Concrete (ACI 318-89) and Commentary-ACI 318R-89*, American Concrete Institution, 1989, 353 pp.

[2] Adebar P., Kuchma D., and Collins M.P., *Strut and Tie Models for the Design of Pile Caps: An Experimental Study*, ACI Structural Journal, Jan.-Feb. 1990, pp. 81-92.

[3] Andersson J.L. *Punching of Concrete Slabs With Shear Reinforcement*, Transactions of the Royal Institute of Technology, Stockholm, Sweden, 1963.

[4] Alexander S.D.B., and Simmonds S.H., *Ultimate Strength of Slab-Column Connections*, ACI Structural Journal, May-Jun. 1989, pp. 255-261.

[5] Aoki Y., and Seki H., *Shearing Strength and Cracking in Two-Way Slabs Subjected to Concentrated Load*, SP-30, ACI, 1971.

[6] Batchelor B.deV., and Hewitt B.E., *Tests of Model Composite Bridge Decks*, ACI Journal, June 1976, pp. 340-343.

[7] Batchelor B.deV., and Tong P.Y., *An Investigation of the Ultimate Shear Strength of Two-way Continuous Bridge Slabs Subjected to Concentrated*

Loads, D.H.O. Report No. RR 107. Sept. 1970.

[8] Bazant Z.P., and Zhiping C., *Size Effect in Punching Shear Failure of Slabs*, ACI Structural Journal, Jan.- Feb. 1987, pp. 44-53.

[9] Bhide S.B., and Collins M.P., *Influence of Axial Tension On the Shear Capacity of Reinforced Concrete Members*, ACI Structural Journal, Sept.-Oct. 1989, pp. 570-581.

[10] British Standard Institution, *Structural Use of Concrete: Part 1, Code of Practice for Design and Construction*, (BS8110: Part 1: 1985), London, 1985, 126 pp.

[11] Canadian Standards Associations, *Code for the Design of Concrete Structures for Buildings*, (CSA.A23.3-84), Rexdale, 1984, 281 pp.

[12] Collins M.P. and Mitchell D., *Rational Approach to Shear Design - 1984 Canadian Code Provisions*, ACI Journal, Nov.-Dec. 1986, pp. 925-933.

[13] Collins M.P. and Mitchell D., *Prestressed Concrete Basics*, Canadian Prestressed Concrete Institute, Ottawa, 1987, 614 pp.

[14] CEB-FIP *Model Code for Concrete*, 3rd edition, Comite Euro-International du Beton/Federation International de la Precontrainte, Paris, 1978, 348 pp.

[15] Cope R.J., *Concrete Bridge Engineering Performance and Advances*, Elsvier Publishing Ltd, 1987, pp. 189-213.

[16] Corly G., and Hawkins N.M., *Shear Head Reinforcement for Slabs*, ACI Journal, October 1968, pp. 811-824.

[17] Csagoly P.F.,and Lybas J.M., *Advanced Design Method for Concrete Bridge Deck Slabs*, Concrete International , May 1989, pp. 53-63.

[18] Dei Poli S., di Prisco M., and Cambarova e.P., *In Tema Di Trasmissione del Taglio Negli Element Di C.A.*, Studi E Ricerche - Vol.10, 1988 Corso di Perfezionamento per le Costruzioni in Cemento Armato Fratelli Pesenti, Politecnico di Milano, Italia.

[19] Dilger W.H., and Ghali A., *Shear Reinforcement for Concrete Slabs*, proceeding ASCE, Vol. 107, No. St.12, Dec. 1981, pp. 2403-2420.

[20] Elgabry A.A, and Ghali A., *Tests on Concrete Slab- Column Connections With Stud-Shear Reinforcement Subjected to Shear-Moment Transfer*, ACI Structural Journal, Sept.-Oct. 1987, pp. 433-442.

[21] Elstner R.C., and Hognestad E., *Shearing Strength of Reinforced Concrete Slabs*, ACI Journal, July 1956, pp. 29-58.

[22] Fenwick R.C., and Dickson A.R., *Slabs Subjected to Concentrated Loading*, ACI Structural Journal, Nov.-Dec. 1989, pp. 672-678.

[23] Fialkow M.N., *Strength Design of Shell Membrane Reinforcement*, Journal of Structural Engineering, ASCE, V. 109, No. 4, Apr. 1983, pp. 891-891.

[24] Fialkow M.N., *Design and Capacity Evaluation of Reinforced Concrete Shell Membranes*, ACI Journal Proceedings V. 82, No. 78, Nov.-Dec. 1985, pp. 844-852

[25] Franklin S.O. and Long A.E., *The Punching Behaviour of Unbounded Post-Tensioned Flat Plates*, Institution of Civil Engineers, Proceedings Part 2, No.73, Sept. 1982,pp. 609-631.

[26] Gardner N.J., *Relationship of the Punshing Shear Capacity of Reinforced Concrete Slabs with Concrete Strength*, ACI Structural Journal, Jan.-Feb. 1990, pp. 66-71.

[27] Gesund H., and Dikshit O.P., *Yield Analysis of the Punching Problem at Slab/Column Intersections*, SP-30, ACI, Detroit, 1971

[28] Gesund H., and Kaushik Y.P., *Yield Line Analysis of Punching Failures in Slabs*, International Association for Bridge and Structural Engineering, Zurich, V.30- I, 1970, pp. 41-60

[29] Gesund H., *Design for Punching Strength of Slabs at Interior Columns*, Proceeding of the International Conference on Concrete Slabs, Dundee University, 3-6 April 1979.

[30] Ghali A. and Neville A.M., *Structural Analysis: A Unified Classical and Matrix Approach*, John Wiley & Sons, New York, 1977, 779 pp.

[31] Gonzalez-Vidosa F., Kotsovos M.D., and Pavlovic, *Symmetrical Punching of reinforced Concrete Slabs*, ACI Structural Journal, May-June 1988, pp. 241-250.

[32] Grow J.B. and Vanderbilt M.D., *Shear Strength of Prestressed Lightweight Aggregate Concrete Flat Plates*, PCI Journal, August 1967, pp. 19-29.

[33] Hawkins N.M., Bao A., and Yamazaki J., *Moment Transfer form Concrete Slabs to Columns*, ACI Structural Journal, Nov.- Dec. 1989, pp. 705-716.

[34] Hewitt B.E., and Batchelor deV.B., *Punching Shear Strentgh of Restrained Slabs*, ASCE Struct. Div. Journal, Sept. 1975, pp. 1837-1852.

[35] Jiang D.H., and Shen J.H., *Strength of Concrete Slabs in Punching Shear*, Journal of Structural Eng. V.112, No.12, Dec. 1986.

[36] Kani M.W., Huggins M.W., and Wittkopp R.R., *Kani on Shear in Reinforced Concrete*, Departement of Civil Engineering, University of Toronto, 1979, 225 pp.

[37] Kinnunen S., and Nylander H., *Punching of Concrete Slabs Without Shear Reinforcement*, Transactions of the royal institute of technology ,Stockholm, Sweden, 1960.

[38] Kinnunen S., *Punching of Concrete Slabs with Two- Way Reinforcement*, Transactions of the Royal Institue of technolgy, Stockholm, Sweden, 1963.

[39] Langohr P.H., Ghali A., and Dilger H.D., *Special Shear Reinforcement for Concrete Flat Plates*, ACI journal, March 1976, pp. 141-146.

[40] Long A.E. and Bond D., *Punching Failure of Reinforced Concrete Slabs* Proc. Vol 37, Inst. of Civ. Eng., London, 1967, pp. 109-135.

[41] Long A.E., *Two Phase Approach to the Prediction of the Punching Strength*, ACI Journal, Feb. 1975 , pp. 37- 45.

[42] MacGregor J.G., *Reinforced Concrete: Mechanics and Design*, Prentice Hall, Englewood Cliffs, New Jersey, 1988, 799 pp.

[43] Marti P., *Basic Tools of Reinforced Concrete Beam Design*, ACI Journal, Jan. -Feb. 1985, p.46-56.

[44] Masterson D.M. and Long A.E., *Improved Experimental procedure For Determining the Punching Strength of R/C Flat Slab Structures*, ACI, SP-42, Detroit, Michigan, 1974.

[45] Moe J., *Shearing Strength of Reinforced Concrete Slabs and Footings Under Concentrated Loads*, Development Department Bulletin No. D47, Portland Cement Association, Skokie, April 1961, pp. 130.

[46] Moehle J.P., *Strength of Slab-Column Edge Connections*, ACI Structural Journal, Jan.-Feb. 1988, pp. 89-98.

[47] Moehle J.P., Kreger M.E., and Leon R., *Background to Recommendations for Design of Reinforced Concrete Slab-Column Connections*. ACI Structural Journal, Nov.- Dec. 1988, pp. 636-644

[48] Mower R.D., and Vanderbilt M.D., *Shear Strength of Lightweight Aggregate Reinforced Concrete Flat Plates*. ACI Journal, Nov. 1967, pp. 722-729.

[49] Narayanan R., and Darwish I.Y.S., *Punching Shear Tests on Steel Fibre Feinforced Micro-Concrete Slabs*. Magazine of Concrete Research, Vol.39, No.138, March 1987, pp. 42-50.

[50] Neth V.W., de Paiva H.A.R. and Long A.E., *Behavior of Models of a Reinforced Concrete Flat Plate Edge-Column Connection*. ACI Journal Jul.-Aug. 1981, Detroit, Michigan.

[51] Ong K.C.G., and Mansur M.A., *Punching Shear of Steel -Concrete Open Sandwich Slabs*, Magazine of Concrete Research, Vol.37, No.133, Dec. 1985, pp. 216-226.

[52] Pralong J., *Poiconnement Symmetrique des Planchers-Dalles*. Institut fur Bustatik und Konstruktion, Eidgenossische Technische Hochscule, Zurich, June 1982. (French).

[53] Regan P.E. *Behavior of Reinforced Concrete Slabs*, CIRIA Report 89, 1981.

[54] Regan P.E., *Punching Shear in Prestressed Concrete Slab Bridges*. Structure Research Group, Polytechnic of Central London, Jan. 1983.

[55] Regan P.E., and Breastrup,M.W., *Punching shear in Reinforced Concrete - A-State-of-Art Report*, Bulletin d'Information No 168, Comite Euro-International du Beton, Lausanne, 1985, 232 pp.

[56] Regan P.E., *The Punching Resistance of Prestressed Concrete Slabs*, Proc. Inst. Civ. Engrs., Part2, 1985, 79, Dec., pp. 657-680.

[57] Regan P.E., *Symmetric Punching of Reinforced Concrete Slabs*, Magazine of Concrete Reseach: Vol.38, No.136, Sept.1986, pp. 115-128.

[58] Shukry M.E.S. and Goode C.D., *Punching shear strength of Composite Construction*, ACI Structural Journal, Jan.-Feb. 1990, pp. 12-22.

[59] Simmonds H.S., and Alexander S.D.B., *Truss Model For Edge Column-Slab Connections*, ACI Structural Journal, Jul.- Aug. 1987, pp. 296-303.

[60] Smith W.S., and Burns N.H., *Post-Tensioned Flat Plate To Column Connection Behavior*, PCI Journal, May- Jun. 1974, pp. 74-91.

[61] Symko Y.B., *Transient Heat Conduction and Thermoelastic Analysis of Three-Span Composite Highway Bridge*. Ph.D. Thesis, University of Ottawa, 1980, 140 pp.

[62] Taylor R., and Hayes B., *Some Tests on the Effect of Edge Restraint on Punching Shear in Reinforced Concrete Slabs*, Magazine of Concrete Reseach, Vol.17, No.50, March 1965, pp. 39-44.

[63] Van Dusen M.H., *Unbalanced Moment and Shear Transfer at Slab-Column Connections: A Literature Review*, Master Thesis, University of Toronto, Sept.1985.

[64] Vecchio F.J., and Collins M.P., *The Modified Compression-Fiekd Theory for Reinforced Concrete Elements Subjected to Shear*, ACI journal, Mar.-Apr. 1986, pp. 219-231.

[65] Walker P.R., and Regan P.E., *Corner Column-Slab Connections in Concrete Flat Plates*, Journal of Structural Engineering, Vol.113, No4,

April,1987, pp. 704- 721.

[66] Wilby C.B., *Structural Concrete* . Butterworth & Co. (Publishers) Ltd. 1983, 256 pp.

[67] Yitzhaki R., *Punching Strength of Reinforced Concrete Slabs*, ACI Journal. Vol.63, No 5, May 1966, pp. 527-542.

[68] Zaghlool E.R.F., and Rawdon dePaiva H.A., and Glockner P.G., *Tests of Reinforced Concrete Flat Plate Floors* , S.D. Journal, March 1970, pp. 487-507.

[69] Zaghlool E.R.F., and Rawdon dePaiva H.A., *Strength Analysis of Corner Column-Slab Connections*, S.D. Journal, Jan.1973, pp. 53-70.

[70] Zhao F., *Early-Age Mechanical Properties of Concrete*, Master Thesis, University of Ottawa, November 1990. 120 pp.

Appendix A

Test Data from the Literature

Table A.1: Slabs tested by Gardner

Slab #	H (mm)	d (mm)	ρ	f_{cc} (Mpa)	f_y (Mpa)	c (mm)	C (mm)	P_{test} (kN)
8	101.6	76.2	0.0205	24.1	400.0	101.6	1117.6	129.2
9	101.6	76.2	0.0205	22.6	400.0	101.6	685.8	135.8
10	101.6	76.2	0.0205	24.6	400.0	101.6	381.0	129.2
11	152.4	113.3	0.0214	22.6	400.0	152.4	685.8	311.8
12	152.4	113.3	0.0214	24.8	400.0	203.2	685.8	357.0
13	152.4	121.7	0.0066	24.8	400.0	203.2	685.8	271.7
14	101.6	72.6	0.0502	25.0	400.0	152.4	533.4	202.6
15	101.6	80.8	0.0147	25.0	400.0	152.4	533.4	160.3
17	101.6	80.8	0.0147	25.5	400.0	101.6	533.4	120.8
18	50.8	31.8	0.0731	22.1	400.0	203.2	533.4	88.6
19	152.4	123.4	0.0047	22.1	400.0	203.2	685.8	271.7
20	152.4	113.3	0.0214	15.1	400.0	203.2	685.8	277.9
21	152.4	121.7	0.0066	16.1	400.0	203.2	685.8	230.3
22	101.6	72.6	0.0501	13.2	400.0	152.4	533.4	154.5
23	101.6	80.8	0.0147	14.5	400.0	152.4	533.4	107.8
25	152.4	121.7	0.0066	52.1	400.0	203.2	685.8	306.9
26	101.6	72.6	0.0501	52.1	400.0	203.2	685.8	323.3
27	101.6	80.8	0.0147	52.1	400.0	152.4	533.4	243.2

Table A.2: Slabs tested by Elster and Hognestad

Slab #	H (mm)	d (mm)	ρ	f_{cc} (Mpa)	f_y (Mpa)	b (mm)	B (mm)	P_{test} (kN)
A-1a	152.4	117.6	0.0115	14.1	332.6	254.0	2322.0	302.9
A-1b	152.4	117.6	0.0115	25.3	332.6	254.0	2322.0	365.2
A-1c	152.4	117.6	0.0115	29.0	332.6	254.0	2322.0	356.3
A-1d	152.4	117.6	0.0115	36.8	332.6	254.0	2322.0	347.4
A-1e	152.4	117.6	0.0115	20.3	332.6	254.0	2322.0	356.3
A-2a	152.4	114.3	0.0247	13.7	321.5	254.0	2322.0	334.0
A-2b	152.4	114.3	0.0247	19.5	321.5	254.0	2322.0	400.8
A-2c	152.4	114.3	0.0247	37.5	321.5	254.0	2322.0	467.6
A-3a	152.4	114.3	0.037	12.8	321.5	254.0	2322.0	356.3
A-3b	152.4	114.3	0.037	22.6	321.5	254.0	2322.0	445.4
A-4	152.4	117.6	0.0115	26.2	332.6	355.6	2322.0	400.8
A-5	152.4	114.3	0.0247	27.8	321.5	355.6	2322.0	534.5
A-6	152.4	114.3	0.037	25.0	321.5	355.6	2322.0	498.8
A-7	152.4	114.3	0.0247	28.5	321.5	254.0	2322.0	400.8
A-8	152.4	114.3	0.0247	21.9	321.5	355.6	2322.0	436.5
A-11	152.4	114.3	0.0247	25.9	321.5	355.6	2322.0	530.0
A-12	152.4	114.3	0.0247	28.4	321.5	355.6	2322.0	530.0

Table A.3: Slabs tested by Mowrer and Vandenbilt

Slab #	H (mm)	d (mm)	ρ	f_{cc} (Mpa)	f_y (Mpa)	b (mm)	B (mm)	P_{test} (kN)
M3-1-0	76.2	50.8	0.011	21.1	385.7	152.4	1164.0	79.3
M3-1-0a	76.2	50.8	0.022	18.0	385.7	152.4	1164.0	99.3
M-4-1-0	76.2	50.8	0.011	15.5	385.7	203.2	1164.0	92.6
M-4-2-0	76.2	50.8	0.022	27.2	385.7	203.2	1164.0	132.7
M-5-1-0	76.2	50.8	0.011	23.3	385.7	254.0	1164.0	109.1
M-5-2-0	76.2	50.8	0.022	22.9	385.7	254.0	1164.0	151.9
M-6-1-0	76.2	50.8	0.011	28.0	385.7	304.8	1164.0	118.9
M-6-2-0	76.2	50.8	0.022	26.4	385.7	304.8	1164.0	158.6
M-7-1-0	76.2	50.8	0.011	27.7	385.7	355.6	1164.0	138.5
M-7-2-0	76.2	50.8	0.022	25.0	385.7	355.6	1164.0	184.8
M-8-1-0	76.2	50.8	0.011	24.9	385.7	406.4	1164.0	145.2
M-8-2-0	76.2	50.8	0.022	24.6	385.7	406.4	1164.0	184.8
M-3-1-2	76.2	50.8	0.011	27.0	385.7	152.4	1164.0	102.0

Table A.4: Slabs tested by Moc

Slab #	H (mm)	d (mm)	ρ	f_{cc} (Mpa)	f_y (Mpa)	b (mm)	B (mm)	P_{test} (kN)
R-1	152.4	114.30	0.0138	27.5	400.0	304.8	2328.0	394.2
R-2	152.4	114.30	0.0138	26.5	400.0	152.4	2328.0	311.8
S1-60	152.4	114.30	0.0106	23.2	400.0	254.0	2328.0	389.7
S2-60	152.4	114.30	0.0103	22.0	400.0	254.0	2328.0	356.3
S3-60	152.4	114.30	0.0113	23.8	400.0	254.0	2328.0	334.1
S1-70	152.4	114.30	0.0106	24.4	400.0	254.0	2328.0	392.8
S2-70	152.4	114.30	0.0102	25.3	400.0	254.0	2328.0	378.6
S4-70	152.4	114.30	0.0113	35.1	400.0	254.0	2328.0	374.1
S4A-70	152.4	114.30	0.0113	20.4	400.0	254.0	2328.0	311.8
S5-60	152.4	114.30	0.0106	22.1	400.0	203.2	2328.0	343.0
S5-70	152.4	114.30	0.0106	24.2	400.0	203.2	2328.0	378.6
M1A	152.4	114.30	0.0150	23.0	400.0	304.8	2328.0	433.4

Table A.5: Slabs tested by Yitzhaki

Slab #	H (mm)	d (mm)	ρ	f_{cc} (Mpa)	f_y (Mpa)	c (mm)	C (mm)	P_{test} (kN)
II-1	101.34	82.3	0.0121	13.9	105.8	221.0	1163.0	181.5
II-4a	101.34	82.3	0.0089	23.8	180.7	221.0	1163.0	245.3
II-5	101.34	82.3	0.0053	22.8	173.4	221.0	1163.0	152.1
II-6	101.34	82.3	0.0133	12.3	93.2	221.0	1163.0	157.0
II-8	101.34	82.3	0.0059	24.8	253.9	332.7	1163.0	219.0
IIR20-2	127.50	108.5	0.0093	19.8	192.9	200.7	1707.0	307.3
III-3	101.34	82.3	0.0121	24.0	182.5	221.0	1163.0	201.1
7	101.34	82.3	0.0074	13.2	68.9	119.4	1163.0	117.7

Table A.6: Slabs tested by Kinnunen and Nylander(Orthogonal Arrangement)

Slab #	H (mm)	d (mm)	ρ	f_{cc} (Mpa)	f_y (Mpa)	c (mm)	C (mm)	P_{test} (kN)
5215	149	117.0	0.0079	27.9	441.5	150.0	1710.0	255.1
5224	151	118.0	0.0078	27.4	454.2	150.0	1710.0	274.7
5269	153	121.0	0.0107	33.5	436.1	150.0	1710.0	333.6
5270	154	122.0	0.0106	32.3	439.0	150.0	1710.0	332.3
5107	158	128.0	0.0096	27.5	455.7	300.0	1710.0	425.9
5117	154	124.0	0.0099	26.2	451.3	300.0	1710.0	408.5
5281	151	120.0	0.0153	31.3	434.6	300.0	1710.0	490.6
5290	151	119.0	0.0154	31.3	448.3	300.0	1710.0	540.6
5125	150	120.0	0.0077	28.6	460.6	300.0	1710.0	332.3
5134	153	122.0	0.0076	26.1	458.6	300.0	1710.0	332.3

Table A.7: Slabs tested by Kinnunen and Nylander(Circular Arrangement)

Slab #	H (mm)	d (mm)	ρ	f_{cc} (Mpa)	f_y (Mpa)	c (mm)	C (mm)	P_{test} (kN)
5057	156	132	0.0116	28.7	447.8	50	1710.0	204.0
5083	154	127	0.012	28.6	445.9	50	1710.0	189.0
3375	150	126	0.0075	28.1	436.1	150	1710.0	188.0
3651	153	127	0.0074	25.4	448.3	150	1710.0	208.0
3661	155	130	0.0073	25.9	448.3	150	1710.0	188.0
3467	153	128	0.0147	26.2	440.5	150	1710.0	216.0
3477	152	127	0.0149	26.2	440.5	150	1710.0	228.0
3390	152	127	0.012	26.4	429.2	300	1710.0	281.0
3395	153	128	0.0119	26.4	429.2	300	1710.0	277.0
3448	153	128	0.0239	28.1	434.1	300	1710.0	355.0
3448	154	128	0.0239	26.2	434.1	300	1710.0	355.0

Table A.8: Slabs tested by Kinnunen and Nylander(Circ. & Rad. Arrangement)

Slab #	H (mm)	d (mm)	ρ	f_{cc} (Mpa)	f_y (Mpa)	c (mm)	C (mm)	P_{test} (kN)
3415	150	125	0.0047	26.6	443.4	150	1710.0	203.0
3420	149	126	0.0047	27.9	443.4	150	1710.0	198.0
3443	152	127	0.0081	26.7	441.0	150	1710.0	267.0
3465	150	124	0.0083	26.5	441.0	150	1710.0	284.0
3401	153	128	0.006	24.1	433.1	300	1710.0	299.0
3408	152	125	0.006	25.9	433.1	300	1710.0	300.0
1029	153	125	0.0129	27.4	452.2	300	1710.0	380.0
3436	154	130	0.0124	26.9	452.2	300	1710.0	429.0